Title
Defining the Role of Trogocytosis in Complement Evasion by Entamoeba histolytica and Tools for Future Study

Author
Miller, Hannah

Publication Date
2021

Peer reviewed|Thesis/dissertation

Defining the Role of Trogocytosis in Complement Evasion by *Entamoeba histolytica* and Tools for Future Study

By

HANNAH WARKENTIN MILLER

DISSERTATION

Submitted in partial satisfaction of the requirements for the degree of

DOCTOR OF PHILOSOPHY

in

IMMUNOLOGY

in the

OFFICE OF GRADUATE STUDIES

of the

UNIVERSITY OF CALIFORNIA

DAVIS

Approved:

_____

Katherine S. Ralston, Chair

_____

Stephen J. McSorley

_____

Scott C. Dawson

Committee in Charge

2021

Dedication

To the mentors who encouraged me to pursue a career in science, guided me along the way and believed in my ability to succeed.

Acknowledgements

I would like to thank Dr. Katy Ralston, Akhila Bettadapur, Tammie Tam and Rene Suleiman for their contributions to this work. I would also like to thank the members of the Ralston laboratory, both past and present, for helpful discussions. Finally, I would like to acknowledge my dissertation committee members Dr. Stephen McSorley and Dr. Scott Dawson as well as Dr. Michael Paddy from the MCB Light Microscopy Imaging Facility for his technical assistance.

Table of Contents

Abstract

Trogocytosis is an endocytic process that is present in many eukaryotes including multicellular organisms and unicellular microbes. Paradoxically, it can be used as a benign form of cell-cell interaction, and it can also be used as a mechanism for cell-mediated killing. Trogocytosis is characterized by ingestion of small pieces of living cells. Additionally, in mammalian immune cells, and in the pathogen *Entamoeba histolytica*, trogocytosis results in the transfer of membrane proteins from one cell to another. Here, we give a broad overview of trogocytosis, its functions, and proposed molecular mechanisms in different cell types. These studies also reveal trogocytosis as a novel immune evasion mechanism employed by *E. histolytica,* the parasite responsible for the diarrheal disease amoebiasis. We demonstrate that *E. histolytica* displays human proteins after performing trogocytosis on human cells, and that this leads to protection from complement lysis. Trophozoites (amoebae) are protected from complement lysis following trogocytosis of live cells but not phagocytosis of dead cells. Amoebic trogocytosis leads to decreased deposition of the complement protein C3b. Furthermore, amoebae acquire and display human CD59 and CD46, which are known negative regulators of the complement pathway. While deletion of one or two complement regulatory proteins from human cells was not sufficient to alter conferred protection, amoebae mutants that exogenously expressed human CD46 or CD55 were protected from lysis. Thus, surface display of an individual negative regulator of complement is sufficient to protect amoebae from lysis. These findings indicate that amoebae likely acquire multiple redundant complement regulators from trogocytosis of

human cells which leads to robust protection from complement lysis. Finally, we developed an assay to quantify trogocytosis in mammalian immune cells and generated mutant amoebae trogocytosis and phagocytosis defects. These tools can be used for future study of this important eukaryotic process.

Chapter 1

Biting off What Can Be Chewed: Trogocytosis in Health, Infection and Disease

Akhila Bettadapur*, Hannah W. Miller* and Katherine S. Ralston

The content of this chapter is reprinted with permission from *Infection and Immunity*, Volume 88, Issue 7, 22 June 2020, https://doi.org/10.1128/IAI.00930-19.

*Akhila Bettadapur and Hannah W. Miller contributed equally to this work. Author order is alphabetical.

Abstract

Trogocytosis is part of an emerging, exciting theme of cell-cell interactions both within and between species, and it is relevant to host-pathogen interactions in many different contexts. Trogocytosis is a process in which one cell physically extracts and ingests “bites” of cellular material from another cell. It was first described in eukaryotic microbes, where it was uncovered as a mechanism by which amoebae kill cells. Trogocytosis is potentially a fundamental form of eukaryotic cell-cell interaction, since it also occurs in multicellular organisms, where it has functions in the immune system, in the central nervous system, and during development. There are numerous scenarios in which trogocytosis occurs, and an ever-evolving list of functions associated with this process. Many aspects of trogocytosis are relevant to microbial pathogenesis. It was recently discovered that immune cells perform trogocytosis to kill *Trichomonas vaginalis* parasites. Additionally, through trogocytosis, *Entamoeba histolytica* acquires and displays human cell membrane proteins, enabling immune evasion. Intracellular bacteria seem to exploit host cell trogocytosis, since they can use it to spread from cell-to-cell. Thus, a picture is emerging in which trogocytosis plays critical roles from normal physiology to infection and disease.

Introduction

Trogocytosis (*trogo-:* nibble) is an underappreciated theme in eukaryotic biology that is gaining ground **(Fig. 1.1)** (1, 2). In this process, one cell physically extracts and ingests “bites” of cellular material from another cell. Trogocytosis contrasts with phagocytosis (*phago-:* devour), where one cell ingests another cell in its entirety. Trogocytosis has been distinguished from other mechanisms for cell-cell exchange, such as nanotubes or exosomes, by its requirement for direct contact between living cells (3–5), its fast timeframe (3, 6), and its transfer of intact proteins (7, 8). Since the underlying molecular mechanism has not been fully defined, it is not clear if all examples of trogocytosis that have been described represent the same, conserved molecular process, or if they represent multiple distinct mechanisms. If trogocytosis is a unified molecular process, it is likely to be fundamental to eukaryotic biology, as it is seen in at least three supergroups.

Trogocytosis was first described in microbes in the late 1970s to mid 1980s, where microbes were seen using trogocytosis to attack and kill other cells (9–12). Later, trogocytosis was seen between mammalian immune cells. Since the early 2000s (3, 13, 14), trogocytosis by immune cells has been actively studied. In immune cells, trogocytosis has been characterized as a benign form of cell-cell interaction, without cell death (3, 15). Within the last five years, trogocytosis has expanded broadly. Trogocytosis has now been detected in many different cell types, including cells of the nervous system (16) and embryonic cells (17). Its functions have broadened to include remodeling of one cell by another (16, 17), cell-cell spread of intracellular bacteria (18),

and killing of microbes by immune cells (19). Trogocytosis can result in display of acquired membrane proteins by the nibbling cell, a process that can enable microbial immune evasion when acquired host proteins are displayed (20). In light of these recent paradigm changes, here we will discuss: the wide-ranging biology of trogocytosis, its underlying mechanism, the display of membrane proteins acquired through trogocytosis, and the major outstanding questions.

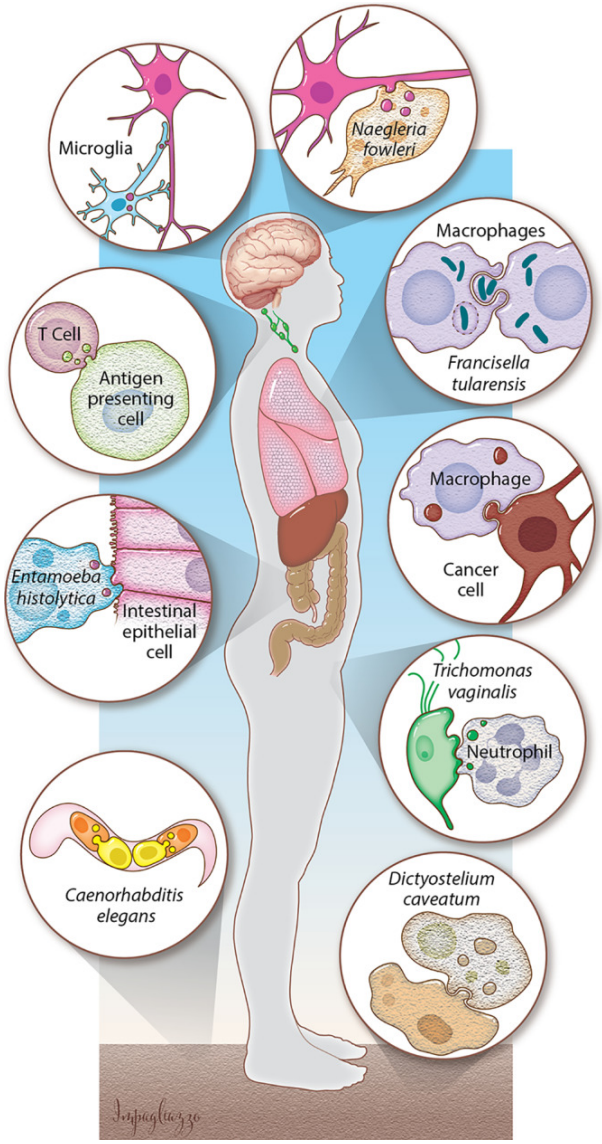

Fig. 1.1: Trogocytosis is a broad, developing concept.
In the central nervous system, microglia use trogocytosis to remodel neuronal synapses, and the parasite *N. fowleri* kills human cells through trogocytosis. Immune cells take bites out of other human cells. Bacteria such as *F. tularensis* exploit trogocytosis/merocytophagy to spread between cells. Macrophages can perform trogocytosis to kill antibody-opsonized cells. *E. histolytica* kills human cells by performing trogocytosis. Neutrophils kill *T. vaginalis* through trogocytosis. Primordial germ cells in *C. elegans* are nibbled by endodermal cells. *D. caveatum* kills other *Dictyostelium* species through trogocytosis.

Biology of Trogocytosis

Trogocytosis is used by microbes for cell killing

Trogocytosis was first described in eukaryotic microbes, where it was uncovered as a mechanism by which amoebae kill other eukaryotic cells. However, it has been studied in only a few microbes, and the molecular details are limited. The “brain-eating” amoeba *Naegleria fowleri* appears to kill mammalian cells by nibbling them (9). The term “trogocytosis” was coined for the first time to describe this process (9). It was later shown that the predatory soil amoeba *Dictyostelium caveatum* kills *D. discoideum* by “nibbling” (10). In addition to these studies, there are descriptions of pathogens including *Acanthamoeba* and *Hartmannella* that nibble on host cells (11, 12). More recently, it was shown that *Entamoeba histolytica* performs trogocytosis to kill human cells **(Fig. 1.2A)** (21)**.** Trogocytosis was required for invasion of explanted mouse intestinal tissue by *E. histolytica,* suggesting relevance to pathogenesis (21).

While all examples of trogocytosis by microbes involve amoebae, it is important to recognize that amoebae are not a phylogenetic group. “Amoeba” is a morphology that is found in many branches of the eukaryotic tree. The amoebae that perform trogocytosis belong to several eukaryotic supergroups, supporting the idea that trogocytosis may be fundamental to eukaryotes.

Trogocytosis is used for cell-cell communication and cell killing in the immune system

(i) Immune cells use trogocytosis for cell-cell communication and cell signaling

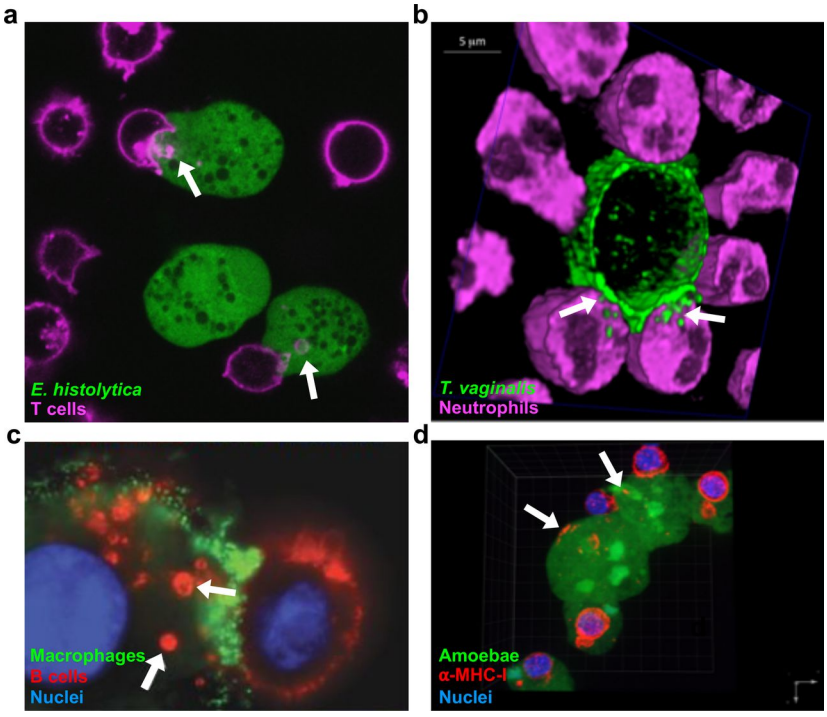

Fig. 1.2: Examples of trogocytosis within and between species. **(A)** *E. histolytica* kills human cells through trogocytosis. *E. histolytica* is stained with cell tracker green and human Jurkat T cell membranes are stained with DiD (pink). Arrows, ingested bites. **(B)** Neutrophils kill *T. vaginalis* through trogocytosis. *T. vaginalis* membranes are stained with streptavidin-488 (green) and neutrophils are stained with cell tracker deep red (pink). **(C)** Macrophages can perform trogocytosis to kill antibody-opsonized cells. Macrophages are stained with α-CD45 (green), Raji B cells are opsonized with Trastuzumab (red), and nuclei are stained with Hoechst (blue). Arrows, ingested bites. **(D)** E. histolytica acquires and displays human cell membrane proteins through trogocytosis. *E. histolytica* is stained with cell tracker green, human α-MHC-I is shown in red, and nuclei are stained with DAPI (blue). Arrows, acquired MHC-I. Reprinted from (20, 21, 41, 96) with permission.

In multicellular organisms, trogocytosis was first discovered in mammalian immune cells, where nibbling occurs at the immunological synapse (3). This was characterized by the transfer of cell membrane proteins from one cell to another (13). In the immune cell literature, the term “trogocytosis” has been used broadly, making it not entirely clear if different studies describe the same process. Some studies have simply defined trogocytosis as the acquisition of membrane and membrane proteins from another cell, without resolving the subcellular localization, while other studies have defined trogocytosis by the internalization of material acquired from another cell. Here we will refer to immune cell trogocytosis in both of these ways that it has been defined.

Instead of a cell-killing mechanism, immune cell trogocytosis has historically been described as a benign form of cell-cell communication (3, 15) that can serve to modulate the immune response (14). Protein transfer between immune cells was initially detected in studies that used MHC-mismatched mice (22, 23), and other studies suggested that antigen could be transferred from macrophages to lymphocytes (24, 25). Later, the transfer of MHC-I molecules from antigen-presenting cells to T cells was observed, and acquisition of MHC-I peptide complexes was linked to T cell fratricide, suggesting that trogocytosis could modulate the immune response (14). Many groups reported transfer of antigen and plasma membrane proteins from donor cells to T cells (6, 26–28). In the early 2000's, this process was named trogocytosis (13), making this the second time that trogocytosis was coined, following the original definition of the term in *N. fowleri* (9). Since then, trogocytosis has been seen in T cells, B cells (29), NK cells (30), dendritic cells (31), macrophages (32), neutrophils (5) and basophils (4), and the transfer of many different types of molecules has been reported.

It is not entirely clear which cellular components are transferred during immune cell trogocytosis. The accepted view is that only membrane and membrane proteins are transferred, without intracellular components. This is based on a few studies that used fluorescent cytoplasmic dyes and flow cytometry, and that did not detect cytoplasm transfer (6, 8). Microscopy would be a more sensitive assay, although, even with microscopy, cytoplasm transfer is more difficult to detect than membrane transfer (21). Thus, the use of sufficiently bright cytoplasmic markers, together with microscopy, would be the best way to resolve this. Supporting the idea that cytoplasm might be

transferred, recent microscopy data appear to show neutrophils acquiring cytoplasmic calcein dye during trogocytosis (33). Likewise, cytoplasmic bacteria spread between macrophages through a process that resembles trogocytosis, which results in transfer of bacteria together with cytoplasmic calcein dye and cell membrane (18). Finally, transfer of CFSE-labeled cytoplasmic proteins from HSV infected monocyte-derived dendritic cells to plasmacytoid dendritic cells has been observed (34). Membrane proteins were also transferred, consistent with trogocytosis (34). More studies are needed, but it appears likely that immune cell trogocytosis involves the transfer of intracellular components.

(ii) Neutrophils use trogocytosis to kill parasites

Although immune cell trogocytosis has historically been thought of as a benign form of cell-cell interaction, it has become clear that it can also be used for cell killing. A recent study revealed that neutrophils can perform trogocytosis to kill parasites **(Fig. 1.2B)** (19). Neutrophils killed *Trichomonas vaginalis* in a dose- and contact-dependent manner (19). Canonical mechanisms by which neutrophils kill microbes include phagocytosis, secretion of antimicrobial peptides, and release of extracellular traps known as NETs (35). Surprisingly, these mechanisms were not involved in the killing of *T. vaginalis* (19). Instead, neutrophils surrounded *T. vaginalis* parasites and killed them by taking bites. Interestingly, neutrophils performed trogocytosis to nibble live parasites, and performed phagocytosis to engulf dead parasites (19). This is similar to *E. histolytica,* which nibbles live human cells and performs phagocytosis to engulf dead

human cells (21). The discovery of neutrophil trogocytosis adds a new weapon to the arsenal of neutrophil cell killing mechanisms, and shows that trogocytosis is relevant to infection.

(iii) Macrophages and neutrophils use trogocytosis to kill cancer cells

Trogocytosis by macrophages and neutrophils has recently been linked to cell killing in the context of antibody therapy for cancer. The general principle of antibody therapy is that binding of antibodies to the surface of a cancer cell can directly downregulate growth factors, or lead to cancer cell death *via* several mechanisms: cell-mediated cytotoxicity, complement-dependent cytotoxicity, or phagocytosis (36). Trogocytosis has a known role in interfering with antibody therapy, since nibbling can remove both antigens and therapeutic antibodies such as anti-CD20 (*e.g.,* the leukemia treatment, Rituximab) from the cancer cell surface, allowing the cancer cell to evade therapy (37, 38). This has been called “shaving.” Dosing regimens have been developed to attempt to minimize the detrimental shaving effect of trogocytosis (39, 40).

In contrast to the detrimental effects of trogocytosis, in which therapeutic antibodies are removed, new studies have shown that trogocytosis can also result in cancer cell death. 3-D microscopy approaches revealed that macrophages kill Trastuzumab antibody-opsonized HER2-breast cancer cells through trogocytosis **(Fig. 1.2C)** (41). Increasing the IgG1 affinity for the FcγR caused higher levels of trogocytosis and cell death, supporting that cell killing was dependent on binding of the therapeutic antibody by the macrophage FcγR (41). In another key study, Kupffer cells, specialized

macrophages in the liver, killed invariant natural killer (iNKT) cells through trogocytosis (42). Kupffer cells grabbed and ripped the trailing edge of iNKT cells that moved over them, causing iNKT cell death (42). Further experimentation showed that iNKT opsonization with the antibody CXCR3-173 was necessary for cell killing, together with iNKT movement and Kupffer cell FcγR (42). This was described as antibody-dependent fragmentation since the cell fragments were potentially larger than most immune cell trogocytosis bites (42), but there is no clear size cut off that specifically defines trogocytosis. Together, these studies show that various kinds of macrophages can perform trogocytosis to kill cancer cells.

Neutrophils also engage trogocytosis to kill cancer cells (33). Killing of cancer cells by neutrophils required an antibody such as Trastuzumab, together with CD11b/CD18 interaction (33). Conjugate formation was independent of the CD47-SIRPα "don't eat me" signal that is overexpressed on cancer cells, and blocking the CD47-SIRPα interaction enhanced conjugate formation (33). The proportion and accumulation of trogocytosis events correlated with the lytic or necrotic cell death of antibody-opsonized cancer cells. This study used the term "trogoptosis" to refer to trogocytosis that results in cell death (33).

Trogocytosis is used to remodel cells in the nervous system

Trogocytosis has expanded beyond the immune system and the known functions of trogocytosis are also broadening. Moving beyond cell-cell communication and cell killing, new examples of trogocytosis in the nervous system and during embryonic

development have added cellular remodeling to the repertoire of trogocytosis.

(i) Microglia use trogocytosis to remodel synapses

In the nervous system, microglia shape and prune neuronal cells through trogocytosis (16). Microglia are motile glial cells that remodel neuronal synapses to create the mature synaptic connections (43). Microglia were previously thought to remodel synapses by using phagocytosis (43). In a study that used correlative light and electron microscopy (CLEM) techniques, microglia were seen directly contacting dendritic spines and ingesting presynaptic structures (16). Using this technique, the spine encapsulations that were previously thought to involve phagocytosis were recognized to be apposition events, rather than ingestion events (16). The small size of the ingested material was consistent with trogocytosis, rather than phagocytosis. Time lapse imaging further showed that trogocytosis occurred briefly, rapidly, and required contact with filopodia (dendritic membrane protrusions) (16).

(ii) Astrocytes use trogocytosis to remodel axons

Beyond microglia, there are examples of apparent cell nibbling by astrocytes, which are central nervous system glial cells (44). Astrocytes have been shown to nibble parts of neurons in the myelination transition zone (45). Astrocytes ingested bites containing mitochondria from retinal ganglion cell axon protrusions in the optic head nerve (46). These mitochondria were further digested in a mitophagy-independent manner within the Lamp1+ lysosome of the astrocyte, as seen through TUNEL and

MitoFISH (46). Interestingly, astrocytes capable of ingesting axon protrusions were seen throughout the central nervous system, hinting that cell nibbling might occur in other sites, beyond the myelination transition zone (46). Astrocytes are also crucial to shortening the myelinated axons of the *Xenopus laevis* optic nerve during late metamorphosis (47). The entrapment of myelin protrusions that have been seen are morphologically similar to trogocytosis, and expressing dominant negative forms of genes involved in astrocyte phagocytosis caused deficits in myelin clearance (47). Taking these examples together, astrocytes perform cell nibbling to remodel the size and organelle composition of neurons.

Trogocytosis is used to remodel cells during embryonic development

Trogocytosis has also been found to play a role in cellular remodeling during embryonic development in *Caenorhabditis elegans* and *X. laevis*. *C. elegans* primordial germ cells attach to intestinal precursor cells for proper gastrulation (48). These primordial germ cells then develop “lobes,” which later disappear in a manner that suggests they have been nibbled (49). Through confocal microscopy, the neighboring endodermal cells were found to nibble and ingest the lobes. Through the removal of these lobes/bites, the primordial germ cells became remodeled, since the number of mitochondria, cell body volume, and cellular composition were changed (17). Interestingly, the mitochondria removed from primordial germ cells were oxidant-rich (17). Thus, trogocytosis may allow primordial germ cells to dispense with organelles that are damaging or no longer needed.

During *X. laevis* gastrulation, endodermal cells were shown to move in an amoeboid like manner, and to elongate and have undulating membranes (50). Interestingly, the formation of double membraned vesicles also occurred, and culminated in the retraction, remodeling, and reabsorption of the trailing edge of the endodermal cell (50). This process involving ingestion of cellular material by another cell has been interchangeably called both macropinocytosis and trans-endocytosis, and it resembles trogocytosis morphologically. Together, the examples in *C. elegans* and *X. laevis* show that endodermal cells, a cell type previously not linked to ingestion, have an important role in performing trogocytosis for development of gastrulating cells.

Trogocytosis is exploited by intracellular pathogens

Fitting with its potentially fundamental role in eukaryotic biology, intracellular pathogens exploit trogocytosis. *Francisella tularensis* and *Salmonella typhimurium* reside in the macrophage cytoplasm and can transfer from one macrophage to another through trogocytosis (18, 51). In this scenario, plasma membrane, cytoplasm, and live bacteria from an initially infected cell were transferred to a new cell *via* a bite of ingested material (18). After trogocytosis occurred, bacteria resided in double-membraned vesicles that contained both donor and recipient cell membranes, and the bacterial type VI secretion system was required for escape from this compartment (51). The process was initially referred to as trogocytosis (18), and was subsequently renamed “merocytophagy” (51). The authors proposed that while trogocytosis might involve recycling of acquired material, merocytophagy involves trafficking of acquired material

for endocytic degradation. Since both *F. tularensis* and *S. typhimurium* can spread from cell to cell through merocytophagy/trogocytosis, it is possible that this may apply more broadly to other infections.

Eukaryotic intracellular pathogens also engage trogocytosis. Red blood cells infected with *Plasmodium falciparum* transferred membrane material and malaria antigens to endothelial cells in an actin-dependent manner (52). This increased the immune response to endothelial cells and opened endothelial cell intercellular junctions, both of which have potentially detrimental implications for cerebral malaria (52).

The Molecular Mechanism Underlying Trogocytosis

Despite its widespread occurrence, the molecular mechanism underlying trogocytosis has not yet been well-defined in any organism. Without an established molecular mechanism, it not clear if the wide variety of cell nibbling scenarios that have been described are all examples of the same, conserved molecular process. Since it is not clear if there is a single, unified, underlying trogocytosis molecular mechanism, here we will organize our discussion of the molecular mechanism by cell types and organisms.

The molecular mechanism underlying trogocytosis in multicellular organisms

(i) Trogocytosis vs. phagocytosis

It is presently unclear how much of the trogocytosis mechanism is distinct from the phagocytosis mechanism. It is possible that trogocytosis is essentially failed

phagocytosis, where a bite is ingested instead of an entire cell. However, when a macrophage fails to perform phagocytosis because the target is too large, it does not ingest bites. Rather, the macrophage attempts to surround the target in a futile process called “frustrated phagocytosis” (53, 54). Therefore, when phagocytosis fails due to the excessive size of a target cell, trogocytosis is not the outcome. If trogocytosis does represent a failure of phagocytosis in other scenarios, it would likely necessitate the use of scission machinery in order to physically extract a bite from a live target cell, an act that is likely to require mechanical force. Thus, even if trogocytosis does represent an outcome of failed phagocytosis, it is still likely to require a scission mechanism that is not a normal feature of phagocytosis. Fitting with this idea, and outlined in detail below, trogocytosis requires proteins involved in membrane bending and scission (17, 55) and a small GTPase (56), none of which normally have roles in engulfment and internalization of target cells during phagocytosis.

Trogocytosis does not represent a random failure of phagocytosis, as it occurs in specific situations. In some organisms, trogocytosis is performed to nibble live cell targets, while phagocytosis is performed to engulf dead cell targets (19, 21). As outlined below, expression of engineered receptors can induce macrophages to nibble on target cells that they would normally ingest through phagocytosis (57). Expression of these receptors in non-professional phagocytes can induce them to perform trogocytosis (57), further supporting that trogocytosis not simply a failure of a phagocyte to fully ingest a target. Potential distinctions between trogocytosis and phagocytosis are highlighted in more detail in the sections that follow.

(ii) The phagocytosis mechanism in immune cells

Phagocytosis by immune cells provides a general starting point for discussion of the mechanism of trogocytosis. The molecular mechanism of phagocytosis is the most well-studied in the case of Fc receptor-mediated phagocytosis (58). Once opsonized target cells are bound by Fc receptors, clustering of Fc receptors triggers their intracellular phosphorylation by Src kinases (59). The phosphorylated Fc receptors then recruit Syk kinase, leading to the activation of lipid-modifying enzymes (*e.g.,* PI3K and phospholipase C), kinases (*e.g.,* PKC), and small GTPases (*e.g.,* Rac and Cdc42), resulting in actin reorganization and pseudopod extension (59). The phagocytic cup extends to surround the target cell, and until the target is fully engulfed and ultimately contained within a phagosome (58). Finally, actin is depolymerized and the phagosome matures into a phagolysosome for degradation of its contents (60).

(iii) The trogocytosis mechanism in immune cells

In general, immune cell trogocytosis requires cell-cell contact mediated by receptor-ligand interactions, actin and PI3K. In specific cell types, roles for TC21, RhoG, Src, Syk intracellular calcium, and myosin light chain kinase have also been defined. All of these proteins are also involved in phagocytosis, with the exception of TC21.

Immune cell trogocytosis is initiated by either the formation of the immunological synapse or by engagement of Fcγ receptors **(Fig. 1.3A)**. Trogocytosis in T cells, B cells and natural killer cells occurs with formation of the immunological synapse (7, 61). Cytotoxic lymphocytes acquire antigenic peptides and plasma membrane fragments

from target cells through engagement of the T cell receptor (6), and the T cell receptor then becomes internalized after acquisition of antigen (14). Trogocytosis has also been described in models where phagocytes recognize antibody coated target cells through engagement of their Fcγ receptors (41, 62).

TC21 and RhoG appear to be required for T cell trogocytosis, and only RhoG has a known role in phagocytosis (56). This conclusion is based on a study that found that T cells were capable of phagocytosis of latex beads along with internalization of the T cell receptor. Ingestion of beads required actin, phosphatidylinositol-3-kinase (PI3K), TC21 and RhoG **(Fig. 1.3A)** (56). The molecules that were required for bead ingestion were inferred to be required for trogocytosis, and consistent with this, trogocytosis of membrane fragments and MHC-II molecules was dependent on PI3K, TC21 and RhoG (56). Actin along with Src, Syk, and PI3K have all been implicated in T cell trogocytosis (29). Similarly, actin, Src and Syk were involved in MHC-II transfer from dendritic cells to basophils (4).

There is potentially a role for receptor engagement in activating either trogocytosis or phagocytosis (57). A family of Chimeric Antigen Receptors were engineered to direct macrophages to perform phagocytosis (CAR-Ps). These CAR-Ps had an extracellular antibody fragment that recognized target cell antigens, and an intracellular signaling domain, such as the intracellular domain from Megf10 or FcRɣ that contained Immunoreceptor Tyrosine-based Activation Motifs (ITAMs) phosphorylated by Src family kinases (57). These CAR-Ps caused macrophages to primarily perform trogocytosis to ingest target cells, instead of phagocytosis. Enrichment

of phosphotyrosine at the synapse between cells increased trogocytosis of target cells. Expression of CAR-Ps in non-professional phagocytes, like fibroblasts, led them to nibble (57). These results suggest that specific ligand interactions are important for the initiation of either trogocytosis or phagocytosis (57).

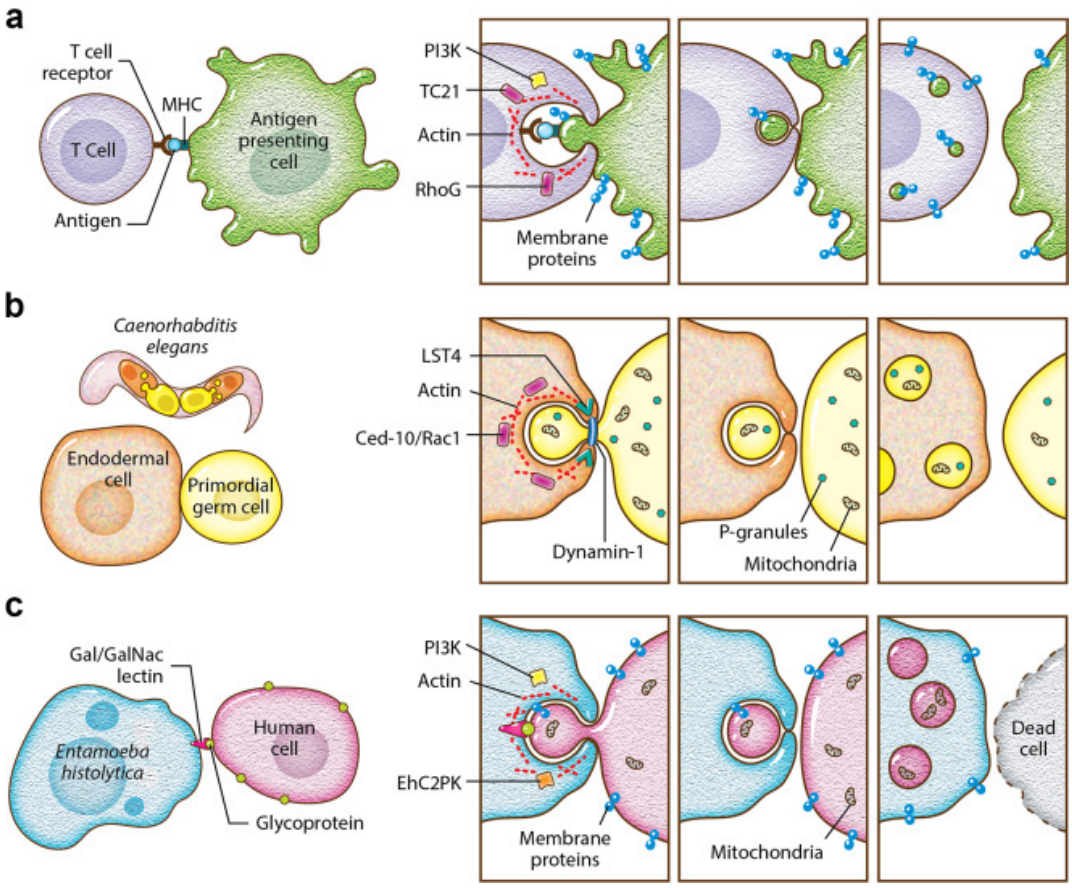

Fig. 1.3: The molecular mechanism underlying trogocytosis.
(A) T cell trogocytosis. T cell receptors engage with antigen bound by MHC. The small GTPases TC21 and RhoG play roles in trogocytosis, along with PI3K and actin. Membrane proteins from the antigen-presenting cell are ultimately displayed on the T cell. The cells separate and remain viable. **(B)** *C. elegans* endodermal cell trogocytosis. The small GTPase CED-10/Rac1 plays a role in trogocytosis, along with actin, Lst-4/SNX9 and dynamin-1. Lst-4/SNX9 has a role in membrane bending, and dynamin-1 has a role in membrane scission. Some P-granules and mitochondria are removed from the primordial germ cell. The cells separate without cell death, and after trogocytosis, the primordial germ cell is smaller in size and contains fewer P-granules and mitochondria. **(C)** *E. histolytica* trogocytosis. Glycoproteins on the human cell surface are engaged by the Gal/GalNAc lectin. The kinase EhC2PK plays a role in trogocytosis, together with PI3K and actin. Membrane proteins from the human cell are ultimately displayed on the amoeba. The cells separate once the human cell is killed.

When immune cells use trogocytosis as a cell killing mechanism, it appears to require the same machinery as benign immune cell trogocytosis. Neutrophil trogoptosis (killing of cancer cells *via* neutrophil trogocytosis) required a reduction in CD47-SIRPα interaction, together with CD11b/CD18 conjugate formation (33). Additionally, Syk, intracellular calcium, PI3K, and myosin light chain kinase were required (33). During neutrophil killing of *T. vaginalis*, neutrophil serine proteases were involved in trogocytosis but not phagocytosis, potentially working together with granules (19). Anti-human iC3b and anti-human immunoglobulin bound to parasites, indicating a role for human serum components such as antibodies and complement (19). Additionally, blocking the neutrophil Fc receptor inhibited killing of *T. vaginalis*, underscoring that killing was dependent on Fc receptor engagement (19).

(iv) The trogocytosis mechanism in embryonic development

As outlined below, there is new evidence for membrane bending and scission activities during embryonic trogocytosis. Dynamin and LST-4 (SNX9) can deform and pinch membranes (63, 64). They have roles during phagocytosis, after the target has been fully engulfed, where they aid in phagosome sealing and maturation (65, 66). In contrast, in newly defined roles in embryonic trogocytosis, these proteins localize to the site where a bite of material is being pinched (the “neck”), and they are required for excision and internalization of nibbled material (17, 55).

Aspects of the mechanism underlying Eph/ephrin trogocytosis have been defined. During development, cellular rearrangements such as repulsion (50, 67, 68)

can be mediated by the removal of adhesive receptor-ligand Eph/ephrin complexes. These complexes can be internalized and effectively removed through trogocytosis, which has also been called trans-endocytosis (50). Internalization of Eph/ephrin through trogocytosis required Src/Tyr signaling (69), Rac GTPases, and the guanine nucleotide exchange factor Tiam2 (70). More recently, it was shown that Gulp-1 (CED-6) regulates Eph/ephrin trogocytosis (55). Gulp-1 is involved in recognizing and engulfing apoptotic cells (71), a well-established phagocytosis pathway in *C. elegans*. Cells lacking Gulp1 directly contacted each other and did not disengage, which decreased trogocytosis (55). Gulp-1 was recruited to Eph/ephrin clusters by Tiam2, and it further recruited the GTPase dynamin-2 for membrane scission and extraction of bites (55).

It appears that trogocytosis during *C. elegans* embryonic development follows a similar model. During trogocytosis of *C. elegans* primordial germ cells, Rac1, dynamin-1 and LST-4 (SNX9), were required for removal and scission of bites **(Fig. 1.3B)** (17). Lst-4 is a sorting nexin, containing a lipid-binding PX domain and a BAR domain that functions in membrane bending (64). Thus, this fits with the model that includes membrane scission *via* dynamin that was established in the Eph/ephrin model, and adds membrane-bending activities to this model. Rac1 induces actin polymerization, and in *C. elegans*, Rac1 has a role in trogocytosis that is independent from its role in phagocytosis (17). Rac1 is one of the players in Eph/ephrin trogocytosis (55), further linking the *C. elegans* and Eph/ephrin models.

The same working model may also hold true in *X. laevis* embryonic trogocytosis. In *X. laevis,* trogocytosis was linked with the endocytosis-associated Rab5 GTPase

(72), as well as ephrin, which both accumulate in membrane clusters and localize to the trailing end of moving endodermal cells (50). Ephrin was also found in double-membraned vesicles, consistent with the Eph/ephrin model of trogocytosis (50). Additionally, injection of dominant negative Gulp-1 in the *X. laevis* gastrula significantly changed its normal developmental shape, pointing towards Gulp-1 regulation of endoderm migration and Eph/ephrin-dependent membrane uptake (50).

(v) The trogocytosis mechanism in the nervous system

Microglia use trogocytosis to remodel neuronal synapses. In this process, there is a hint of a mechanism distinct from phagocytosis. Complement signaling is known to promote ingestion by microglia (73). Interestingly, mice without the complement receptor CR3 had no deficit in microglial trogocytosis, indicating that this pathway may have a specific role in phagocytosis, and is not required for microglial trogocytosis (16).

Trogocytosis by astrocytes shares features with immune cells and embryonic cells. In order to perform trogocytosis of axonal protrusions with mitochondria, astrocytes upregulated the known phagocytic marker Mac2 (45), which requires stable γ-synuclein. Astrocytes involved in *X. laevis* myelination shortening during development expressed Rac1 to perform trogocytosis (47). Rac1 has a known role in phagocytosis, and as outlined above, is linked to trogocytosis during embryonic development. Astrocyte expression of Mfge8, a protein associated with immune cell phagocytosis (74), was also important in demyelination (47).

The molecular mechanism underlying trogocytosis in microbes

Distinctions between trogocytosis and phagocytosis in microbes have been proposed but are not yet fully clear. Trogocytosis in *N. fowleri* involves actin (9). Beyond this information from *N. fowleri,* essentially all of the mechanistic studies of microbial trogocytosis have been carried out in *E. histolytica.*

E. histolytica performs trogocytosis to nibble live human cells, and by contrast, performs phagocytosis to engulf dead human cells (21). Since *E. histolytica* is capable of performing both trogocytosis and phagocytosis, it presents a useful model to compare and contrast these processes. In *E. histolytica,* both processes require actin, signaling initiated by the Gal/GalNAc lectin, PI3K and the kinase EhC2PK **(Fig. 1.3C)** (21). It has been suggested that the kinase EhAGCK1 is specific to *E. histolytica* trogocytosis, while EhAGCK2 is involved in trogocytosis, phagocytosis and pinocytosis (75). However, this study did not directly test for a trogocytosis defect (75), and used a human cell-killing assay that is confounded by amoebic protease activity (76). The EhAGCK1 knockdown mutants in this study were generated using an approach that affects the expression of off-target genes (77). It has been suggested that *E. histolytica* PI3P membrane glycerophospholipid-binding proteins such as Vsps and SNXs might be involved in trogocytosis and phagocytosis (78). Further work is still needed to determine which mechanisms are specific to *E. histolytica* trogocytosis.

Inhibition of *E. histolytica* lysosome acidification led to a reduction in trogocytosis, which was consistent with an impairment in continued ingestion of human cell material (79). Phagocytosis was also inhibited, suggesting that lysosomes play a general role in

both processes. Inhibition of amoebic cysteine proteases with E-64 resulted in a specific defect in trogocytosis, and not phagocytosis (80). This fits with the finding that E-64 treatment inhibited human cell killing by *E. histolytica* (81). It is unclear if cysteine proteases play a specific role in degradation of material ingested during trogocytosis, or if trogocytosis is especially sensitive to cysteine protease inhibition as it appears to occur with faster kinetics than phagocytosis (20), and thus, ingested material may be trafficked to the lysosome more rapidly.

Another Layer to Trogocytosis: Membrane Protein Display

One characteristic of trogocytosis that has, until recently, only been described in immune cells is the transfer of membrane proteins from the donor cell membrane to the recipient cell membrane. This process modulates the immune response by allowing cells to take on and display new molecules. The mechanism of membrane protein transfer is still mostly unclear; however, in T cells it appears to be initiated at the immunological synapse.

Membrane protein display by immune cells

Dendritic cells can acquire intact peptide-MHC complexes from other cells *via* trogocytosis and present them to lymphocytes (82), in a process termed “cross-dressing” (83, 84). Dendritic cells that acquire peptide-MHC complexes through trogocytosis are able to present them and stimulate T cells (15, 31). Acquisition of membrane proteins *via* trogocytosis can also suppress the immune response in the

context of transplantation (85), and has also been well documented in regulatory T cells (86, 87). Acquisition of MHC-II molecules seems to enhance the suppressive activity of regulatory T cells through lymphocyte-activation gene 3 (88, 89). Finally, acquisition of membrane proteins *via* trogocytosis appears to be a driver of the T_H2 immune response. CD4+ T cells that performed trogocytosis were associated with a T_H2 phenotype (90). Similarly, basophils that acquired peptide-MHC-II complexes *via* trogocytosis were able to stimulate peptide-specific naïve CD4+ T cells *in vitro*, in a manner consistent with a T_H2 phenotype (4).

Membrane protein display and complement evasion by E. histolytica

Extending membrane protein display beyond immune cells, *E. histolytica* acquires and displays human cell membrane proteins after performing trogocytosis **(Fig. 1.2D)** (20). Amoebic display of human cell membrane proteins was quantitatively inhibited when amoebae were treated with cytochalasin D, consistent with a requirement for trogocytosis (20). This suggests that the acquisition and display of membrane proteins is potentially a conserved feature of trogocytosis.

The display of human cell membrane proteins by *E. histolytica* may impact many host-pathogen interactions. After performing trogocytosis, *E. histolytica* was protected from lysis by human serum (20). Protection was specific to trogocytosis, as it required actin and direct cell-cell contact, and amoebae were not protected after performing phagocytosis (20). The molecular mechanism by which amoebae become protected from complement by displaying human cell proteins is not yet clear. It is possible that

complement regulatory proteins are displayed by amoebae and directly provide protection. Multiple factors may act together to protect amoebae from complement. Amoebic cysteine proteases have a role in cleavage of complement components (91–93), and the heavy chain of the Gal/GalNAc lectin can act as a CD59 mimic (94). Since trogocytosis occurs in other microbes, this strategy, in which acquired membrane proteins contribute to immune evasion, could potentially apply to other infections.

Major Questions

Taking together the many diverse examples of trogocytosis in different organisms and scenarios, there are many outstanding questions. A central question is: what is the mechanism underlying trogocytosis? There are clearly shared features between trogocytosis and phagocytosis, but also emerging hints that aspects of the trogocytosis mechanism are distinct. How does a cell "decide" to initiate trogocytosis or phagocytosis? Many cells are capable of both trogocytosis and phagocytosis, such as *E. histolytica,* neutrophils, or mammalian macrophages. There may be roles for receptor-ligand interactions, since expression of engineered receptors can induce macrophages to perform trogocytosis of target cells that they would normally ingest *via* phagocytosis (57). Additionally, in some cases, trogocytosis and phagocytosis are differentially performed during the ingestion of live and dead cells (19, 21), which have different surface ligands.

What is (or isn't) ingested during trogocytosis? An overall theme is that cell membrane is transferred from one cell to another during trogocytosis. Additionally, in

many different scenarios, cytoplasm, mitochondria and other organelles are also transferred (9, 17, 21, 46). In immune cell trogocytosis, it is generally accepted that only cell membrane is transferred, but empirical evidence is likely insufficient to rule out the transfer of other cellular components. Conversely, in many cases, nuclei are not ingested during trogocytosis (11, 21). Is the acquisition and display of membrane proteins a universal feature of trogocytosis? While this occurs in immune cells and *E. histolytica,* it has not yet been investigated in other systems.

An almost totally unexplored area is the response of the cell that has been nibbled. Why does trogocytosis only sometimes result in cell death? This is especially relevant to cell types that are capable of nibbling with or without killing, such as macrophages and neutrophils. Are additional factors, such as toxins, needed to kill cells through trogocytosis? Since cell killing *via* trogocytosis requires direct contact, toxins would need to be specifically targeted to the cell that is being nibbled, or could be generally secreted but only result in the death of cells that have been nibbled. In *E. histolytica,* there is a very large amount of polymerized actin at the site of interaction between the amoeba and human cell (21), making secretion of toxins at this site less likely. When cells are killed by nibbling, why do they die? Is a cell death pathway activated, or do nibbled cells die due to the accumulation of physical damage? In some studies, it is clear that the nibbled cell initially retains membrane integrity, and eventually loses membrane integrity after many bites have been taken, potentially because the nibbled cells has become too damaged to be repaired (9, 21). Conversely, when cells are not killed by trogocytosis, how do they retain cellular integrity? Fitting with the idea

that cellular repair pathways might be activated in nibbled cells, influx of extracellular calcium occurs in human cells nibbled by *E. histolytica* (21), and calcium influx is a trigger of plasma membrane repair (95).

Summary

Trogocytosis is a broad, rapidly developing theme that is relevant to eukaryotic biology in general, and to human biology, from normal physiology to disease. Trogocytosis applies to host-pathogen interactions in many contexts, from pathogens that nibble host cells, pathogens that acquire and display host proteins, bacteria that subvert trogocytosis, and pathogens that are attacked and killed by host trogocytosis. Given its apparently fundamental nature and relevance to disease, eukaryotic trogocytosis demands further investigation. It seems probable that more new examples of trogocytosis will be uncovered in the future. Quite a few fundamental questions have arisen and many areas of trogocytosis are ready to be “chewed on” in future studies.

Acknowledgements

We thank the members of our laboratory for helpful discussions, and Anita Impagliazzo of Anita Impagliazzo Medical Illustration for the illustrations. A.B. was supported by a fellowship from the UC Davis Training Program in Biomolecular Technology. Work in our laboratory is supported by NIH grant 1R01AI146914 and a Pew Scholarship awarded to K.S.R.

References

1. Dance A. 2019. Core Concept: Cells nibble one another via the under-appreciated process of trogocytosis. Proc Natl Acad Sci USA 116:17608–17610.

2. Ralston KS. 2015. Taking a bite: Amoebic trogocytosis in Entamoeba histolytica and beyond. Current Opinion in Microbiology 28:26–35.

3. Batista FD, Iber D, Neuberger MS. 2001. B cells acquire antigen from target cells after synapse formation. Nature 411:489–494.

4. Miyake K, Shiozawa N, Nagao T, Yoshikawa S, Yamanishi Y, Karasuyama H. 2017. Trogocytosis of peptide–MHC class II complexes from dendritic cells confers antigen-presenting ability on basophils. PNAS 114:1111–1116.

5. Li K-J, Wu C-H, Shen C-Y, Kuo Y-M, Yu C-L, Hsieh S-C. 2016. Membrane Transfer from Mononuclear Cells to Polymorphonuclear Neutrophils Transduces Cell Survival and Activation Signals in the Recipient Cells via Anti-Extrinsic Apoptotic and MAP Kinase Signaling Pathways. PLoS One 11.

6. Hudrisier D, Riond J, Mazarguil H, Gairin JE, Joly E. 2001. Cutting edge: CTLs rapidly capture membrane fragments from target cells in a TCR signaling-dependent manner. J Immunol 166:3645–3649.

7. Wetzel SA, McKeithan TW, Parker DC. 2005. Peptide-Specific Intercellular Transfer of MHC Class II to CD4+ T Cells Directly from the Immunological Synapse upon Cellular Dissociation. The Journal of Immunology 174:80–89.

8. Vanherberghen B, Andersson K, Carlin LM, Nolte-`t Hoen ENM, Williams GS, Höglund P, Davis DM. 2004. Human and murine inhibitory natural killer cell receptors transfer from natural killer cells to target cells. Proc Natl Acad Sci U S A 101:16873–16878.

9. Brown T. 1979. Observations by immunofluorescence microscopy and electron microscopy on the cytopathogenicity of naegleria fowleri in mouse embryo-cell cultures. Journal of Medical Microbiology 12:363–371.

10. Waddell DR, Vogel G. 1985. Phagocytic behavior of the predatory slime mold, Dictyostelium caveatum. Cell nibbling. Exp Cell Res 159:323–334.

11. Culbertson CG. 1970. Pathogenic Naegleria and Hartmannella (Acenthamoeba). Ann N Y Acad Sci 174:1018–1022.

12. Culbertson CG. 1971. The pathogenicity of soil amebas. Annu Rev Microbiol 25:231–254.

13. Joly E, Hudrisier D. 2003. What is trogocytosis and what is its purpose? Nature Immunology 4:815.

14. Huang J-F, Yang Y, Sepulveda H, Shi W, Hwang I, Peterson PA, Jackson MR, Sprent J, Cai Z. 1999. TCR-Mediated Internalization of Peptide-MHC Complexes Acquired by T Cells. Science 286:952–954.

15. Wakim LM, Bevan MJ. 2011. Cross-dressed dendritic cells drive memory CD8+ T-cell activation after viral infection. Nature 471:629–632.

16. Weinhard L, di Bartolomei G, Bolasco G, Machado P, Schieber NL, Neniskyte U, Exiga M, Vadisiute A, Raggioli A, Schertel A, Schwab Y, Gross CT. 2018. Microglia remodel synapses by presynaptic trogocytosis and spine head filopodia induction. Nat Commun 9:1228.

17. Abdu Y, Maniscalco C, Heddleston JM, Chew T-L, Nance J. 2016. Developmentally programmed germ cell remodelling by endodermal cell cannibalism. Nat Cell Biol 18:1302–1310.

18. Steele S, Radlinski L, Taft-Benz S, Brunton J, Kawula TH. 2016. Trogocytosis-associated cell to cell spread of intracellular bacterial pathogens. eLife 5:e10625.

19. Mercer F, Ng SH, Brown TM, Boatman G, Johnson PJ. 2018. Neutrophils kill the parasite Trichomonas vaginalis using trogocytosis. PLoS Biol 16:e2003885.

20. Miller HW, Suleiman RL, Ralston KS. 2019. Trogocytosis by Entamoeba histolytica Mediates Acquisition and Display of Human Cell Membrane Proteins and Evasion of Lysis by Human Serum. mBio 10:e00068-19.

21. Ralston KS, Solga MD, Mackey-Lawrence NM, Somlata, Bhattacharya A, Petri Jr WA. 2014. Trogocytosis by *Entamoeba histolytica* contributes to cell killing and tissue invasion. Nature 508:526–530.

22. Cone RE, Sprent J, Marchalonis JJ. 1972. Antigen-Binding Specificity of Isolated Cell-Surface Immunoglobulin from Thymus Cells Activated to Histocompatibility Antigens. Proc Natl Acad Sci U S A 69:2556–2560.

23. Nakayama M. 2015. Antigen Presentation by MHC-Dressed Cells. Front Immunol 5.

24. Bona C, Robineaux R, Anteunis A, Heuclin C, Astesano A. 1973. Transfer of antigen from macrophages to lymphocytes. Immunology 24:831–840.

25. Bona C, Anteunis A, Robineaux R, Astesano A. 1972. Transfer of antigenic macromolecules from macrophages to lymphocytes. Immunology 23:799–816.

26. Hwang I, Huang J-F, Kishimoto H, Brunmark A, Peterson PA, Jackson MR, Surh CD, Cai Z, Sprent J. 2000. T Cells Can Use Either T Cell Receptor or Cd28 Receptors to Absorb and Internalize Cell Surface Molecules Derived from Antigen-Presenting Cells. Journal of Experimental Medicine 191:1137–1148.

27. Patel DM, Arnold PY, White GA, Nardella JP, Mannie MD. 1999. Class II MHC/Peptide Complexes Are Released from APC and Are Acquired by T Cell Responders During Specific Antigen Recognition. The Journal of Immunology 163:5201–5210.

28. Stinchcombe JC, Bossi G, Booth S, Griffiths GM. 2001. The Immunological Synapse of CTL Contains a Secretory Domain and Membrane Bridges. Immunity 15:751–761.

29. Hudrisier D, Aucher A, Puaux A-L, Bordier C, Joly E. 2007. Capture of Target Cell Membrane Components via Trogocytosis Is Triggered by a Selected Set of Surface Molecules on T or B Cells. The Journal of Immunology 178:3637–3647.

30. Nakayama M, Takeda K, Kawano M, Takai T, Ishii N, Ogasawara K. 2011. Natural killer (NK)-dendritic cell interactions generate MHC class II-dressed NK cells that regulate CD4+ T cells. Proc Natl Acad Sci USA 108:18360–18365.

31. Bonaccorsi I, Morandi B, Antsiferova O, Costa G, Oliveri D, Conte R, Pezzino G, Vermiglio G, Anastasi GP, Navarra G, Münz C, Carlo ED, Mingari MC, Ferlazzo G. 2014. Membrane Transfer from Tumor Cells Overcomes Deficient Phagocytic Ability of Plasmacytoid Dendritic Cells for the Acquisition and Presentation of Tumor Antigens. The Journal of Immunology 192:824–832.

32. Pham T, Mero P, Booth JW. 2011. Dynamics of Macrophage Trogocytosis of Rituximab-Coated B Cells. PLoS One 6.

33. Matlung HL, Babes L, Zhao XW, van Houdt M, Treffers LW, van Rees DJ, Franke K, Schornagel K, Verkuijlen P, Janssen H, Halonen P, Lieftink C, Beijersbergen RL, Leusen JHW, Boelens JJ, Kuhnle I, van der Werff Ten Bosch J, Seeger K, Rutella S, Pagliara D, Matozaki T, Suzuki E, Menke-van der Houven van Oordt CW, van Bruggen R, Roos D, van Lier RAW, Kuijpers TW, Kubes P, van den Berg TK. 2018. Neutrophils Kill Antibody-Opsonized Cancer Cells by Trogoptosis. Cell Rep 23:3946-3959.e6.

34. Megjugorac NJ, Jacobs ES, Izaguirre AG, George TC, Gupta G, Fitzgerald-Bocarsly P. 2007. Image-Based Study of Interferongenic Interactions between Plasmacytoid Dendritic Cells and HSV-Infected Monocyte-Derived Dendritic Cells. Immunological Investigations 36:739–761.

35. Kolaczkowska E, Kubes P. 2013. Neutrophil recruitment and function in health and inflammation. Nat Rev Immunol 13:159–175.

36. Gül N, Egmond M van. 2015. Antibody-Dependent Phagocytosis of Tumor Cells by Macrophages: A Potent Effector Mechanism of Monoclonal Antibody Therapy of Cancer. Cancer Res.

37. Beum PV, Peek EM, Lindorfer MA, Beurskens FJ, Engelberts PJ, Parren PWHI, van de Winkel JGJ, Taylor RP. 2011. Loss of CD20 and bound CD20 antibody from opsonized B cells occurs more rapidly because of trogocytosis mediated by Fc receptor-expressing effector cells than direct internalization by the B cells. J Immunol 187:3438–3447.

38. Beum PV, Kennedy AD, Williams ME, Lindorfer MA, Taylor RP. 2006. The Shaving Reaction: Rituximab/CD20 Complexes Are Removed from Mantle Cell Lymphoma and Chronic Lymphocytic Leukemia Cells by THP-1 Monocytes. The Journal of Immunology 176:2600–2609.

39. Taylor RP, Lindorfer MA. 2014. Analyses of CD20 monoclonal antibody-mediated tumor cell killing mechanisms: rational design of dosing strategies. Mol Pharmacol 86:485–491.

40. Boross P, Jansen JHM, Pastula A, van der Poel CE, Leusen JHW. 2012. Both activating and inhibitory Fc gamma receptors mediate rituximab-induced trogocytosis of CD20 in mice. Immunology Letters 143:44–52.

41. Velmurugan R, Challa DK, Ram S, Ober RJ, Ward ES. 2016. Macrophage-Mediated Trogocytosis Leads to Death of Antibody-Opsonized Tumor Cells. Mol Cancer Ther 15:1879–1889.

42. Liew PX, Kim JH, Lee W-Y, Kubes P. 2017. Antibody-dependent fragmentation is a newly identified mechanism of cell killing in vivo. Sci Rep 7:10515.

43. Fu R, Shen Q, Xu P, Luo JJ, Tang Y. 2014. Phagocytosis of Microglia in the Central Nervous System Diseases. Mol Neurobiol 49:1422–1434.

44. Sofroniew MV, Vinters HV. 2010. Astrocytes: biology and pathology. Acta Neuropathol 119:7–35.

45. Nguyen JV, Soto I, Kim K-Y, Bushong EA, Oglesby E, Valiente-Soriano FJ, Yang Z, Davis CO, Bedont JL, Son JL, Wei JO, Buchman VL, Zack DJ, Vidal-Sanz M, Ellisman MH, Marsh-Armstrong N. 2011. Myelination transition zone astrocytes are constitutively phagocytic and have synuclein dependent reactivity in glaucoma. PNAS 108:1176–1181.

46. Davis CO, Kim K-Y, Bushong EA, Mills EA, Boassa D, Shih T, Kinebuchi M, Phan S, Zhou Y, Bihlmeyer NA, Nguyen JV, Jin Y, Ellisman MH, Marsh-Armstrong N. 2014. Transcellular degradation of axonal mitochondria. Proc Natl Acad Sci USA 111:9633–9638.

47. Mills EA, Davis CO, Bushong EA, Boassa D, Kim K-Y, Ellisman MH, Marsh-Armstrong N. 2015. Astrocytes phagocytose focal dystrophies from shortening

myelin segments in the optic nerve of Xenopus laevis at metamorphosis. PNAS 112:10509–10514.

48. Chihara D, Nance J. 2012. An E-cadherin-mediated hitchhiking mechanism for C. elegans germ cell internalization during gastrulation. Development 139:2547–2556.

49. Sulston JE, Schierenberg E, White JG, Thomson JN. 1983. The embryonic cell lineage of the nematode Caenorhabditis elegans. Developmental Biology 100:64–119.

50. Wen JW, Winklbauer R. 2017. Ingression-type cell migration drives vegetal endoderm internalisation in the Xenopus gastrula. eLife 6:e27190.

51. Steele SP, Chamberlain Z, Park J, Kawula TH. 2019. Francisella tularensis enters a double membraned compartment following cell-cell transfer. eLife 8:e45252.

52. Jambou R, Combes V, Jambou M-J, Weksler BB, Couraud P-O, Grau GE. 2010. Plasmodium falciparum Adhesion on Human Brain Microvascular Endothelial Cells Involves Transmigration-Like Cup Formation and Induces Opening of Intercellular Junctions. PLOS Pathogens 6:e1001021.

53. Cannon GJ, Swanson JA. 1992. The macrophage capacity for phagocytosis. J Cell Sci 101 (Pt 4):907–913.

54. Takemura R, Stenberg PE, Bainton DF, Werb Z. 1986. Rapid redistribution of clathrin onto macrophage plasma membranes in response to Fc receptor-ligand interaction during frustrated phagocytosis. J Cell Biol 102:55–69.

55. Gong J, Gaitanos TN, Luu O, Huang Y, Gaitanos L, Lindner J, Winklbauer R, Klein R. 2019. Gulp1 controls Eph/ephrin trogocytosis and is important for cell rearrangements during developmentGulp1 regulates Eph/ephrin trogocytosis. J Cell Biol 218:3455–3471.

56. Martínez-Martin N, Fernández-Arenas E, Cemerski S, Delgado P, Turner M, Heuser J, Irvine DJ, Huang B, Bustelo XR, Shaw A, Alarcón B. 2011. T Cell Receptor Internalization from the Immunological Synapse is Mediated by TC21 and RhoG GTPase-Dependent Phagocytosis. Immunity 35:208–222.

57. Morrissey MA, Williamson AP, Steinbach AM, Roberts EW, Kern N, Headley MB, Vale RD. 2018. Chimeric antigen receptors that trigger phagocytosis. eLife 7:e36688.

58. Flannagan RS, Jaumouillé V, Grinstein S. 2012. The cell biology of phagocytosis. Annu Rev Pathol 7:61–98.

59. Swanson JA, Hoppe AD. 2004. The coordination of signaling during Fc receptor-mediated phagocytosis. J Leukoc Biol 76:1093–1103.

60. Fairn GD, Grinstein S. 2012. How nascent phagosomes mature to become phagolysosomes. Trends in Immunology 33:397–405.

61. Osborne DG, Wetzel SA. 2012. Trogocytosis Results in Sustained Intracellular Signaling in CD4+ T Cells. The Journal of Immunology 189:4728–4739.

62. Beum PV, Mack DA, Pawluczkowycz AW, Lindorfer MA, Taylor RP. 2008. Binding of Rituximab, Trastuzumab, Cetuximab, or mAb T101 to Cancer Cells Promotes Trogocytosis Mediated by THP-1 Cells and Monocytes. The Journal of Immunology 181:8120–8132.

63. Shin N, Ahn N, Chang-Ileto B, Park J, Takei K, Ahn S-G, Kim S-A, Di Paolo G, Chang S. 2008. SNX9 regulates tubular invagination of the plasma membrane through interaction with actin cytoskeleton and dynamin 2. J Cell Sci 121:1252–1263.

64. Bendris N, Schmid SL. 2017. Endocytosis, Metastasis and Beyond: Multiple Facets of SNX9. Trends Cell Biol 27:189–200.

65. Gold ES, Underhill DM, Morrissette NS, Guo J, McNiven MA, Aderem A. 1999. Dynamin 2 is required for phagocytosis in macrophages. J Exp Med 190:1849–1856.

66. Marie-Anaïs F, Mazzolini J, Herit F, Niedergang F. 2016. Dynamin-Actin Cross Talk Contributes to Phagosome Formation and Closure. Traffic 17:487–499.

67. Ventrella R, Kaplan N, Getsios S. 2017. Asymmetry at cell-cell interfaces direct cell sorting, boundary formation, and tissue morphogenesis. Experimental Cell Research 358:58–64.

68. Astin JW, Batson J, Kadir S, Charlet J, Persad RA, Gillatt D, Oxley JD, Nobes CD. 2010. Competition amongst Eph receptors regulates contact inhibition of locomotion and invasiveness in prostate cancer cells. Nat Cell Biol 12:1194–1204.

69. Zisch AH, Kalo MS, Chong LD, Pasquale EB. 1998. Complex formation between EphB2 and Src requires phosphorylation of tyrosine 611 in the EphB2 juxtamembrane region. Oncogene 16:2657–2670.

70. Gaitanos TN, Koerner J, Klein R. 2016. Tiam–Rac signaling mediates trans-endocytosis of ephrin receptor EphB2 and is important for cell repulsionRac-mediated ephrin receptor trans-endocytosis. J Cell Biol 214:735–752.

71. Liu QA, Hengartner MO. 1998. Candidate Adaptor Protein CED-6 Promotes the Engulfment of Apoptotic Cells in C. elegans. Cell 93:961–972.

72. Lanzetti L, Palamidessi A, Areces L, Scita G, Fiore PPD. 2004. Rab5 is a signalling GTPase involved in actin remodelling by receptor tyrosine kinases. Nature 429:309–314.

73. Schafer DP, Lehrman EK, Kautzman AG, Koyama R, Mardinly AR, Yamasaki R, Ransohoff RM, Greenberg ME, Barres BA, Stevens B. 2012. Microglia sculpt postnatal neural circuits in an activity and complement-dependent manner. Neuron 74:691–705.

74. Peng Y, Elkon KB. 2011. Autoimmunity in MFG-E8–deficient mice is associated with altered trafficking and enhanced cross-presentation of apoptotic cell antigens. J Clin Invest 121:2221–2241.

75. Somlata null, Nakada-Tsukui K, Nozaki T. 2017. AGC family kinase 1 participates in trogocytosis but not in phagocytosis in Entamoeba histolytica. Nat Commun 8:101.

76. Tillack M, Nowak N, Lotter H, Bracha R, Mirelman D, Tannich E, Bruchhaus I. 2006. Increased expression of the major cysteine proteinases by stable episomal transfection underlines the important role of EhCP5 for the pathogenicity of Entamoeba histolytica. Molecular and Biochemical Parasitology 149:58–64.

77. Bracha R, Nuchamowitz Y, Anbar M, Mirelman D. 2006. Transcriptional silencing of multiple genes in trophozoites of Entamoeba histolytica. PLoS Pathog 2:e48.

78. Watanabe N, Nakada-Tsukui K, Nozaki T. Two isotypes of phosphatidylinositol 3-phosphate-binding sorting nexins play distinct roles in trogocytosis in Entamoeba histolytica. Cellular Microbiology n/a:e13144.

79. Gilmartin AA, Ralston KS, Petri WA. 2017. Inhibition of Amebic Lysosomal Acidification Blocks Amebic Trogocytosis and Cell Killing. mBio 8.

80. Gilmartin AA, Ralston KS, Petri WA. 2020. Inhibition of Amebic Cysteine Proteases Blocks Amebic Trogocytosis but Not Phagocytosis. J Infect Dis.

81. Faust DM, Marquay Markiewicz J, Danckaert A, Soubigou G, Guillen N. 2011. Human liver sinusoidal endothelial cells respond to interaction with Entamoeba histolytica by changes in morphology, integrin signalling and cell death. Cell Microbiol 13:1091–1106.

82. Harshyne LA, Watkins SC, Gambotto A, Barratt-Boyes SM. 2001. Dendritic Cells Acquire Antigens from Live Cells for Cross-Presentation to CTL. The Journal of Immunology 166:3717–3723.

83. Yewdell JW, Haeryfar SMM. 2005. UNDERSTANDING PRESENTATION OF VIRAL ANTIGENS TO CD8+ T CELLS IN VIVO: The Key to Rational Vaccine Design. Annual Review of Immunology 23:651–682.

84. Campana S, De Pasquale C, Carrega P, Ferlazzo G, Bonaccorsi I. 2015. Cross-dressing: an alternative mechanism for antigen presentation. Immunology Letters 168:349–354.

85. Chow T, Whiteley J, Li M, Rogers IM. 2013. The transfer of host MHC class I protein protects donor cells from NK cell and macrophage-mediated rejection during hematopoietic stem cell transplantation and engraftment in mice. STEM CELLS 31:2242–2252.

86. McIntyre MSF, Young KJ, Gao J, Joe B, Zhang L. 2008. Cutting Edge: In Vivo Trogocytosis as a Mechanism of Double Negative Regulatory T Cell-Mediated Antigen-Specific Suppression. The Journal of Immunology 181:2271–2275.

87. Zhou G, Ding Z-C, Fu J, Levitsky HI. 2011. Presentation of Acquired Peptide-MHC Class II Ligands by CD4+ Regulatory T Cells or Helper Cells Differentially Regulates Antigen-Specific CD4+ T Cell Response. The Journal of Immunology 186:2148–2155.

88. Sega EI, Leveson-Gower DB, Florek M, Schneidawind D, Luong RH, Negrin RS. 2014. Role of Lymphocyte Activation Gene-3 (Lag-3) in Conventional and Regulatory T Cell Function in Allogeneic Transplantation. PLoS One 9.

89. Tian D, Yang L, Wang S, Zhu Y, Shi W, Zhang C, Jin H, Tian Y, Xu H, Sun G, Liu K, Zhang Z, Zhang D. 2019. Double negative T cells mediate Lag3-dependent antigen-specific protection in allergic asthma. Nat Commun 10.

90. Reed J, Wetzel SA. 2019. Trogocytosis-Mediated Intracellular Signaling in CD4+ T Cells Drives TH2-Associated Effector Cytokine Production and Differentiation. The Journal of Immunology 202:2873–2887.

91. Reed SL, Ember JA, Herdman DS, DiScipio RG, Hugli TE, Gigli I. 1995. The extracellular neutral cysteine proteinase of Entamoeba histolytica degrades anaphylatoxins C3a and C5a. J Immunol 155:266–274.

92. Reed SL, Gigli I. 1990. Lysis of complement-sensitive Entamoeba histolytica by activated terminal complement components. Initiation of complement activation by an extracellular neutral cysteine proteinase. J Clin Invest 86:1815–1822.

93. Reed SL, Keene WE, McKerrow JH, Gigli I. 1989. Cleavage of C3 by a neutral cysteine proteinase of Entamoeba histolytica. J Immunol 143:189–195.

94. Braga LL, Ninomiya H, McCoy JJ, Eacker S, Wiedmer T, Pham C, Wood S, Sims PJ, Petri WA. 1992. Inhibition of the complement membrane attack complex by the galactose-specific adhesion of Entamoeba histolytica. J Clin Invest 90:1131–1137.

95. Andrews NW, Corrotte M. 2018. Plasma membrane repair. Curr Biol 28:R392–R397.

96. Mercer F, Johnson PJ. 2018. Trichomonas vaginalis: Pathogenesis, Symbiont Interactions, and Host Cell Immune Responses. Trends Parasitol 34:683–693.

Chapter 2

Trogocytosis by *Entamoeba histolytica* Mediates Acquisition and Display of Human Cell Membrane Proteins and Evasion of Lysis by Human Serum

Hannah W. Miller, Rene L. Suleiman and Katherine S. Ralston

The content of this chapter is reprinted from *mBio*, Volume 10, Issue 2, e00068-19 https://doi.org/10.1128/mBio.00068-19.

Abstract

We previously showed that *Entamoeba histolytica* kills human cells through a mechanism that we termed trogocytosis (*trogo-:* nibble), due to its resemblance to trogocytosis in other organisms. In microbial eukaryotes like *E. histolytica,* trogocytosis is used to kill host cells. In multicellular eukaryotes, trogocytosis is used for cell-killing and cell-cell communication in a variety of contexts. Thus, nibbling is an emerging theme in cell-cell interactions both within and between species. When trogocytosis occurs between mammalian immune cells, cell membrane proteins from the nibbled cell are acquired and displayed by the recipient cell. In this study, we tested the hypothesis that through trogocytosis, amoebae acquire and display human cell membrane proteins. We demonstrate that *E. histolytica* acquires and displays human cell membrane proteins through trogocytosis and that this leads to protection from lysis by human serum. Protection from human serum only occurs after amoebae have undergone trogocytosis of live cells, but not phagocytosis of dead cells. Likewise, mutant amoebae defective in phagocytosis, but unaltered in their capacity to perform trogocytosis, are protected from human serum. Our studies are the first to reveal that amoebae can display human cell membrane proteins and suggest that acquisition and display of membrane proteins is a general feature of trogocytosis. These studies have major implications for interactions between *E. histolytica* and the immune system and also reveal a novel strategy for immune evasion by a pathogen. Since other microbial eukaryotes use trogocytosis for cell killing, our findings may apply to the pathogenesis of other infections.

Importance

Entamoeba histolytica causes amoebiasis, a potentially fatal diarrheal disease. Abscesses in organs such as the liver can occur when amoebae are able to breach the intestinal wall and travel through the bloodstream to other areas of the body. Therefore, understanding how *E. histolytica* evades immune detection is of great interest. Here we demonstrate for the first time that *E. histolytica* acquires and displays human cell membrane proteins by taking “bites” of human cell material in a process named trogocytosis (*trogo-:* nibble), and that this allows amoebae to survive in human serum. Display of acquired proteins through trogocytosis has only been previously characterized in mammalian immune cells. Our study suggests that this is a more general feature of trogocytosis not restricted to immune cells and broadens our knowledge of eukaryotic biology. These findings also reveal a novel strategy for immune evasion by a pathogen and may apply to the pathogenesis of other infections.

Introduction

Entamoeba histolytica is the protozoan parasite responsible for amoebiasis, a potentially fatal diarrheal disease. Amoebiasis is most prevalent in developing countries, in areas with poor sanitation (1–3). A recent study found that nearly 80% of infants living in an urban slum in Bangladesh had been infected with *E. histolytica* by two years of age (4). The infection has a wide range of clinical symptoms that include asymptomatic infection, diarrhea, bloody diarrhea, and fatal abscesses outside of the intestine. Bloody diarrhea arises when amoebic trophozoites (amoebae) invade and ulcerate the intestine. Amoebae that have invaded the intestine can disseminate and cause abscesses in other tissues, most commonly in the liver. Although amoebic liver abscesses are rare, they are fatal if untreated. Little is known about the mechanisms that allow *E. histolytica* to evade immune detection and disseminate upon entering the bloodstream.

The parasite was named “histolytica” for its ability to damage tissue (*histo-:* tissue; *lytic-:* dissolving) (5–7). Despite this name-giving property, precisely how amoebae invade and damage tissues is not clear. The most well-known virulence factor is the amoeba surface D-galactose and N-acetyl-D-galactosamine (Gal/GalNAc) lectin (8, 9), which mediates attachment to human cells and intestinal mucin (10–13). Surface-localized and secreted cysteine proteases contribute to proteolysis of substrates including mucin and extracellular matrix (10–13). The profound cell killing activity of amoebae is likely to drive tissue damage. Amoebae can kill almost any type of human cell within minutes. Direct contact with human cells is required for killing to occur (8, 9).

Until recently, the accepted model was that the pore-forming amoebapores act as secreted toxins (14–17). However, the contact-dependence of cell killing (8, 9), and the lack of killing activity in cell lysates and supernatants (6, 7, 18), are not consistent with the presence of secreted toxins. Furthermore, transfer of amoebapores to human cells has not been demonstrated.

We previously established a new paradigm by showing that *E. histolytica* kills human cells through a mechanism that we termed trogocytosis (*trogo*-: nibble), due to its resemblance to trogocytosis in other organisms (19). During trogocytosis, amoebae kill human cells by extracting and ingesting "bites" of human cell membrane and intracellular contents (19). We defined that trogocytosis requires amoebic actin rearrangements (19). It also requires signaling initiated by the Gal/GalNAc lectin, phosphatidylinositol 3-kinase (PI3K) signaling and an amoebic C2 domain-containing kinase (*Eh*C2PK) (19). By applying multiphoton imaging using explanted mouse intestinal tissue from fluorescent-membrane mice, we found that trogocytosis was required for tissue invasion, demonstrating relevance to pathogenesis (19).

Trogocytosis is not unique to *E. histolytica*, as it can be observed in other eukaryotes (20). Examples in microbes include reports of trogocytosis by *Naegleria fowleri* (21) and *Dictyostelium caveatum* (22). In multicellular eukaryotes, trogocytosis is used for a variety of cell-cell interactions in the immune system (23, 24), in the central nervous system (25, 26), and during development (27). It is not yet clear how trogocytosis can paradoxically be both a benign form of cell-cell interaction and a mechanism for cell-killing. The previous paradigm was that microbes engage

trogocytosis for cell-killing, and trogocytosis in multicellular organisms was believed to be a benign form of cell-cell interaction. However, recent reports have now shown that neutrophils can use trogocytosis to kill parasites (28), and neutrophils and macrophages can use trogocytosis to kill cancer cells in a form of antibody-dependent cell-mediated cytotoxicity (29, 30). Trogocytosis is therefore likely to be a conserved, fundamental form of eukaryotic cell-cell interaction that can be cytotoxic or benign, depending on the context.

One intriguing outcome of trogocytosis between mammalian immune cells is that it changes the makeup of cell surface proteins on both the donor and the recipient cell. The nibbling cell displays the acquired membrane proteins from the nibbled cell on its own surface (24, 31). Acquired membrane proteins appear as foci or patches on the recipient cell. This allows the recipient cell to take on new properties that impact its subsequent interactions with other cells (24, 31). For instance, uninfected dendritic cells can acquire and display pre-loaded major histocompatibility complex class II (MHC II) molecules by nibbling infected dendritic cells, and thus they can present peptides from microbes they have not directly encountered, which has been termed “cross-dressing” (24). Transferred molecules are not limited to MHC complexes as induced regulatory T cells can acquire cluster of differentiation (CD) molecules from mature dendritic cells including CD80 and CD86 (32). It has also been shown that monocytes, NK cells, and granulocytes can acquire CD22, CD19, CD21, and CD79b from antibody-opsonized B cells (33). In addition to allowing the nibbling cell to display newly acquired membrane

proteins, since membrane fragments are removed from the nibbled cell, trogocytosis also affects the nibbled cell by effectively downregulating surface proteins (34).

Since mammalian immune cells acquire and display membrane proteins through trogocytosis, we hypothesized that amoebae may acquire and display human cell membrane proteins. Amoebic display of human proteins would have significant implications for host-pathogen interactions. We predicted that one outcome of amoebic human cell protein display could be the inhibition of lysis by human complement. Previous studies have suggested that amoebae become more resistant to complement after interacting with host cells or tissues, and that complement resistance appears to involve proteins on the amoeba surface (35–37).

Here we show that *E. histolytica* acquires and displays human cell membrane proteins. Acquisition and display of human cell membrane proteins requires actin and direct contact, and is associated with subsequent protection from lysis by human serum. Protection from human serum occurs after amoebae have undergone trogocytosis, but not phagocytosis, suggesting protection is not generally associated with ingestion. Collectively, these findings support that amoebae acquire and display human cell membrane proteins through trogocytosis and that this leads to protection from lysis by human serum complement. These studies have major implications for interactions between *E. histolytica* and the immune system.

(This article was submitted to an online preprint archive (38).)

Results

Amoebae acquire and display human cell membrane proteins.

We first asked whether trogocytosis by *E. histolytica* could result in transfer of human cell membrane proteins to the cell membrane of the amoeba. Human Jurkat T cells were surface-biotinylated and then co-incubated with amoebae. After co-incubation, cells were fixed and labeled with fluorescently-conjugated streptavidin **(Fig. 2.1A)**. Since cells were not permeabilized, this approach required human cell proteins to be surface-exposed and to retain correct orientation for recognition by streptavidin. After five minutes of co-incubation, patches of streptavidin-labeled human cell proteins were detected on the surface of amoebae **(Fig. 2.1B – 2.1C, arrows)**. Similar to immune cell "cross-dressing" (24), the biotin-streptavidin label appeared as foci on the amoeba surface. To track an individual human cell membrane protein, immunofluorescence was used to detect human major histocompatibility complex class I (MHC I) **(Fig. 2.1D)**. Following co-incubation, cells were fixed without permeabilization, and MHC I was detected using a monoclonal antibody. Comparable to the biotin-streptavidin labeling experiments, MHC I was detected in foci on the surface of amoebae after five minutes of co-incubation **(Fig. 2.1E – 2.1F)**. Thus, human cell membrane proteins were acquired and displayed by amoebae.

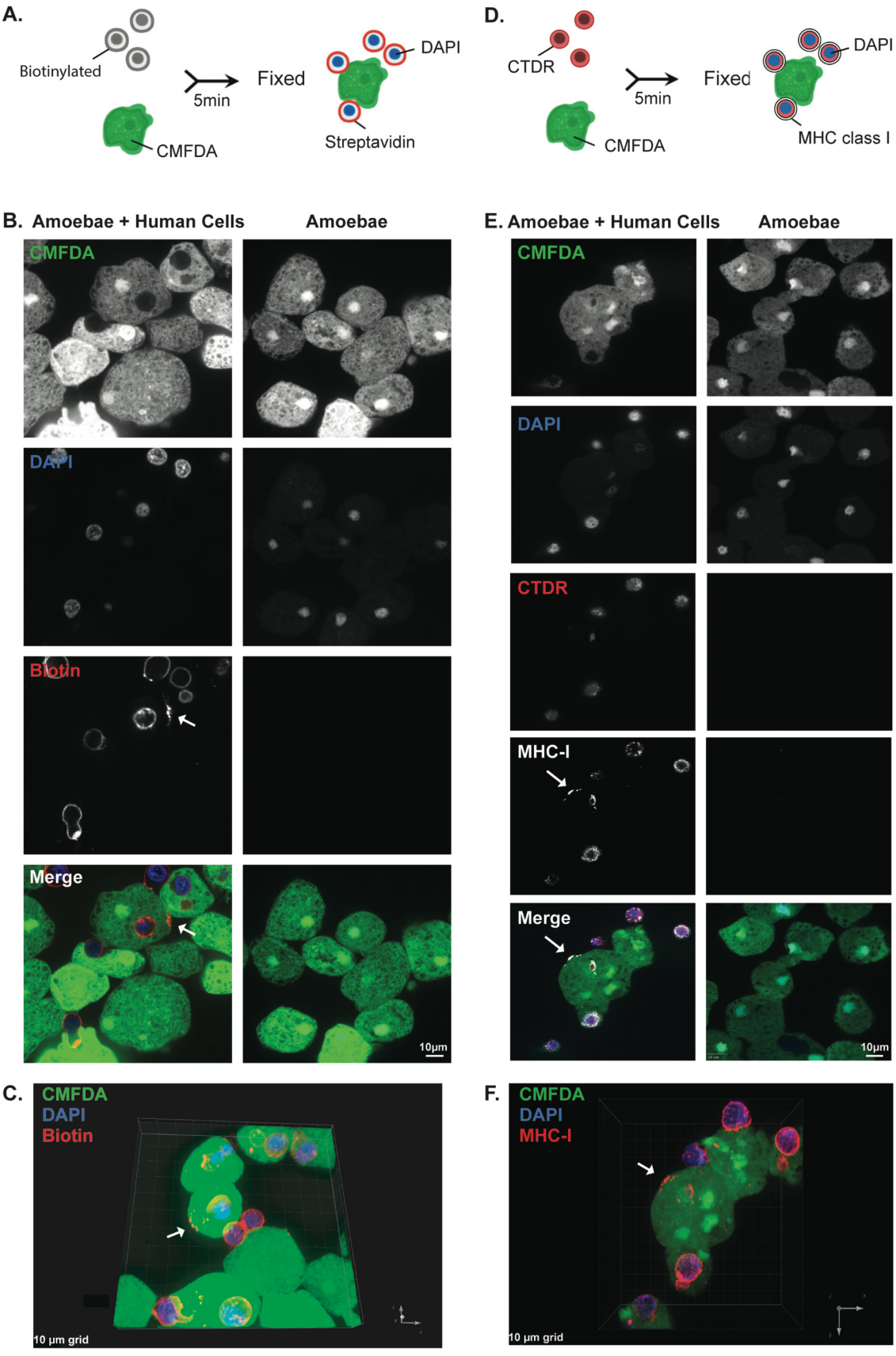
A.
Biotinylated
5min
Fixed
DAPI
CMFDA
Streptavidin
D.
CTDR
5min
Fixed
DAPI
CMFDA
MHC class I
B. Amoebae + Human Cells
Amoebae
CMFDA
DAPI
Biotin
Merge
10µm
E. Amoebae + Human Cells
Amoebae
CMFDA
DAPI
CTDR
MHC-I
Merge
10µm
C.
CMFDA
DAPI
Biotin
10 µm grid
F.
CMFDA
DAPI
MHC-I
10 µm grid

Fig. 2.1: Following interaction with human cells, human cell membrane proteins are displayed by amoebae
(A) Human cell membrane proteins were labeled with biotin prior to co-incubation with CMFDA-labeled amoebae. Cells were co-incubated for 5 minutes and immediately fixed. Following fixation, samples were labeled with fluorescently-conjugated streptavidin and DAPI. **(B)** Representative images of amoebae incubated alone or co-incubated with biotinylated human cells. Amoebae are shown in green and streptavidin is shown in red. Nuclei are shown in blue. Arrow indicates a patch of biotin-streptavidin localized to the amoeba surface. **(C)** 3D rendering of Z stack images taken from panel B. Arrow indicates transferred biotin. **(D)** Human cells were labeled with cell tracker deep red (CTDR) prior to co-incubation with CMFDA-labeled amoebae. Cells were co-incubated for 5 minutes and immediately fixed. Following fixation, samples were labeled with DAPI and MHC-I was detected using immunofluorescence. **(E)** Representative images of amoebae incubated alone or co-incubated with CTDR-labeled human cells. Amoebae are shown in green, human cell cytoplasm is shown in red, MHC-I is shown in yellow and nuclei are shown in blue. Arrow indicates MHC-I present on the amoeba surface. **(F)** 3D rendering of Z stack images taken from E. Arrow indicates transferred MHC-I. For panels B-F, images were collected from 4 independent experiments. For Biotin experiments, 76 images of amoebae with human cells and 21 images of amoebae alone were collected. For MHC-I experiments, 83 images of amoebae with human cells and 40 images of amoebae alone were collected.

Acquisition and display of human cell membrane proteins requires actin.

Trogocytosis by *E. histolytica* requires actin rearrangements and is inhibited by cytochalasin D (19). Therefore, we asked whether acquisition of human cell membrane proteins required actin. Imaging flow cytometry was used to quantify biotinylated human cell membrane proteins on the amoeba surface. It was important to distinguish between amoebae that displayed human cell membrane proteins and amoebae that were attached to intact, extracellular human cells. While the latter amoebae may also display human cell membrane proteins, we focused our analysis on images that lacked extracellular human cells as this allowed for the highest stringency in quantifying displayed human cell membrane proteins. Since human cell nuclei are not internalized by amoebae during trogocytosis (19), human cell nuclei were fluorescently labeled, and this was used to gate images that contained or lacked extracellular human cells.

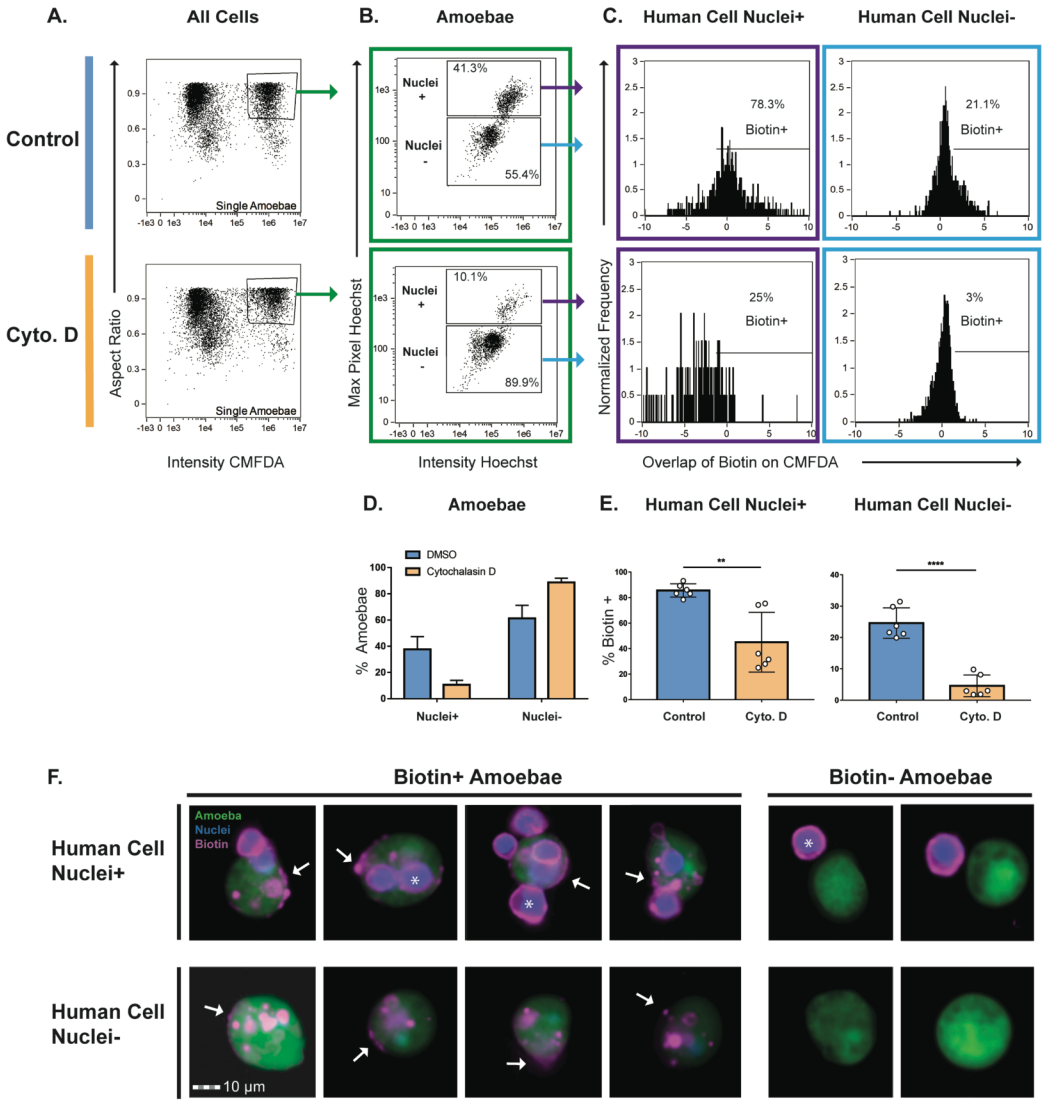

Fig. 2.2: Acquisition of human cell membrane proteins is inhibited with cytochalasin D treatment CMFDA-labeled amoebae were pre-treated with either cytochalasin D (Cyto. D) or DMSO (Control) and were then combined with Hoechst-labeled human cells. Immediately after co-incubation, cells were placed on ice to halt ingestion and stained with fluorescently-conjugated streptavidin. Samples were quantitatively analyzed using imaging flow cytometry, with 10,000 images collected for each sample. **(A)** Gate used to identify single amoebae from total cells. Focused cells were gated on single amoebae using aspect ratio and intensity of CMFDA fluorescence. **(B)** Representative plots of images with and without human cell nuclei (Hoechst high or low populations) are shown. The Hoechst high population contained images of amoebae with human cells and the Hoechst low population contained images of amoebae without human cells. **(C)** Overlap of biotin and CMFDA fluorescence was measured, and biotin positive images were gated. Representative plots of DMSO and cytochalasin D treated samples are shown. **(D)** Quantification of plots from panel B. DMSO treated samples are shown in blue and cytochalasin D treated samples are shown in orange. **(E)** Quantification of plots from panel C. **(F)** Representative images of the populations shown in panel C. Amoebae are shown in green, cell nuclei are shown in blue, and biotin is shown in magenta. Arrows indicate patches of transferred biotin. Whole human cells with stained nuclei are marked with asterisks. n=6 from 3 independent experiments.

Human cell nuclei were labeled with Hoechst, and human cell membrane proteins were biotinylated prior to co-incubation with amoebae. After gating on single amoebae out of total cells **(Fig. 2.2A, Fig. S2.1)**, Hoechst staining was used to gate on images of amoebae with and without extracellular human cells **(Fig. 2.2B, D, F)**. Next, the extent of overlap of fluorescent-streptavidin and individual amoebae was quantified **(Fig. 2.2C, E)**. In the dimethyl sulfoxide (DMSO) treated control amoebae, 25% of amoebae contained foci of biotin labeling (Human Cell Nuclei-/Biotin+), while in the cytochalasin D treated amoebae, 5% of amoebae contained foci of biotin labeling **(Fig. 2.2E)**. Thus, amoebae acquire and display human cell membrane proteins through an actin-dependent process, consistent with trogocytosis. Moreover, only 3% of biotin-positive amoebae had undergone phagocytosis **(Fig. S2.2)**, consistent with a predominant role for trogocytosis in acquisition and display of human cell membrane proteins.

Interaction with human cells leads to protection from lysis by human serum.

The acquisition and display of human cell membrane proteins has many potential implications for host-parasite interactions. One possible implication is in resistance to lysis by complement in human serum, particularly since it has been previously suggested that ingestion of human erythrocytes protects amoebae from lysis by human complement (35). Amoebae preferentially perform trogocytosis on live human cells (19), therefore amoebae were incubated in the presence or absence of live human cells and then exposed to human serum **(Fig. 2.3A, Fig. S2.3)**. Using imaging flow cytometry,

amoeba viability **(Fig. 2.3C – D)**, and trogocytosis were simultaneously measured **(Fig. 2.3B, Fig. S2.4)**. Amoebae that had interacted with live human cells, and had thus undergone trogocytosis and acquired human cell membrane proteins, were quantitatively protected from lysis by human serum **(Fig. 2.3C – 2.3D, Fig. S2.5)**. Among amoebae that had been incubated with human cells, amoebae that were lysed by human serum had undergone quantitatively less trogocytosis than amoebae that

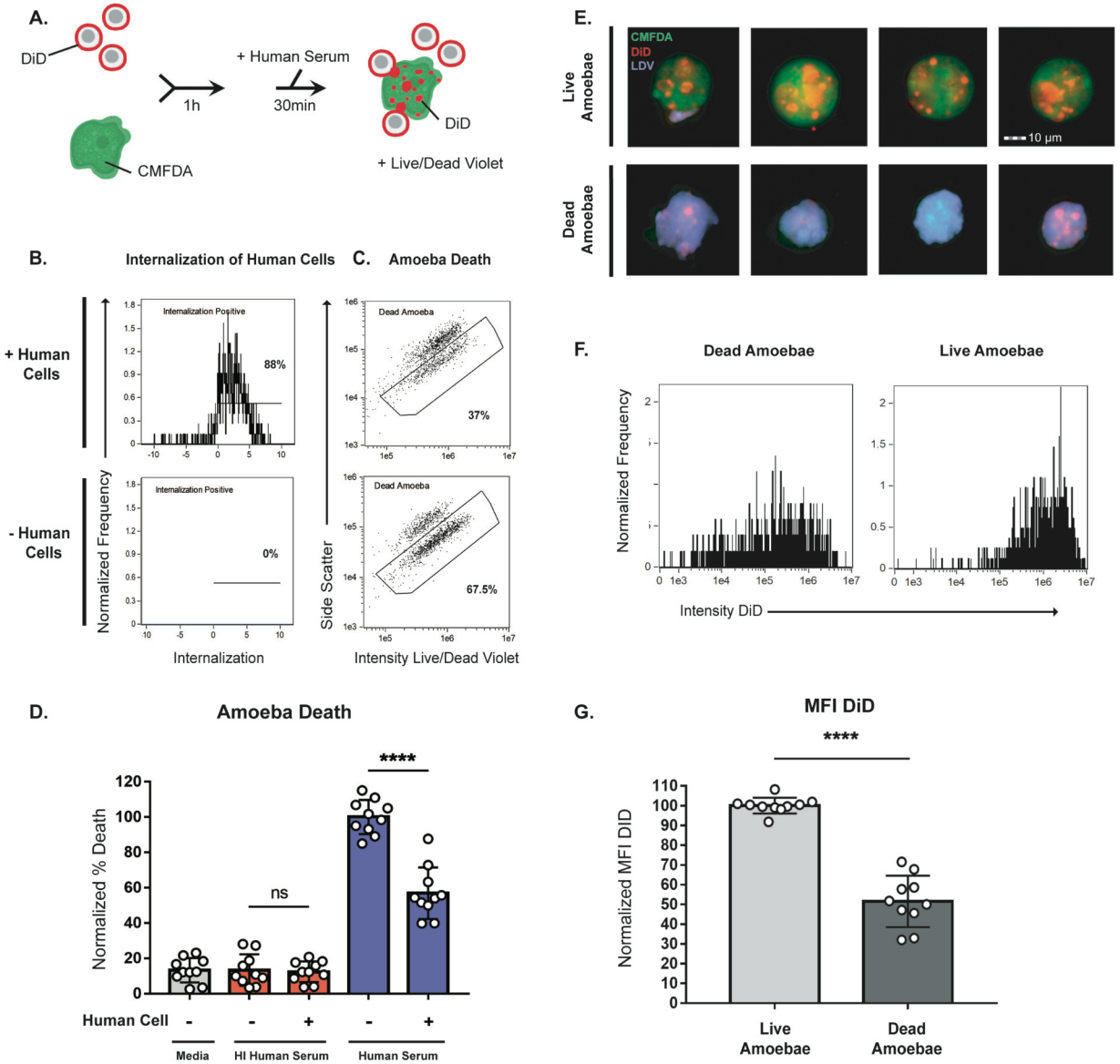

Fig. 2.3: Interaction with human cells leads to protection from lysis by human serum
(A) CMFDA-labeled amoebae were incubated alone or in the presence of DiD-labeled human cells for 1 hour. Cells were then exposed to either active human serum, heat-inactivated human serum, or M199s medium. Following exposure to serum, samples were stained with Live/Dead Violet and viability was quantified using imaging flow cytometry, with 10,000 images collected for each sample. **(B)** Representative plots showing internalization of human cells in each condition. **(C)** Representative plots comparing amoebic death in the active serum, and heat-inactivated serum conditions. **(D)** Quantification of amoebic death for all experimental conditions. Cells exposed to M199s medium are shown in grey, heat-inactivated human serum in red, and active human serum in blue. % Death was normalized to the amoeba alone samples that were treated with active human serum. **(E)** Representative images of live and dead amoebae from amoebae co-incubated with human cells and exposed to active human serum. Amoebae are shown in green, human cells in red, and dead cells in violet. **(F)** Representative histograms showing the mean fluorescence intensity (MFI) of DiD in live and dead amoebae from samples exposed to human serum. **(G)** Quantification of the DID MFI shown in panel F. n=10 from 5 independent experiments.

survived exposure to human serum **(Fig. 2.3E – 2.3G)**. Therefore, trogocytosis is associated with subsequent protection from lysis by human serum.

Protection from human serum lysis is dependent on contact with human cells.

We next asked if protection from serum lysis required direct contact between amoebae and human cells, in order to determine if protection is a consequence of trogocytosis, or if protection could be acquired through secreted human cell proteins or exosomes. Amoebae and human cells were co-incubated in transwell dishes, with or without direct contact **(Fig. 2.4A)**. Human cells were not able to pass through transwell membranes **(Fig. 2.4B)**. Protection from complement lysis occurred only when amoebae and human cells were incubated together in the same chamber of the transwell, but not when they were separated **(Fig. 2.4C)**. Protection from human serum thus required direct contact between amoebae and human cells, supporting a requirement for trogocytosis in the acquisition of protection.

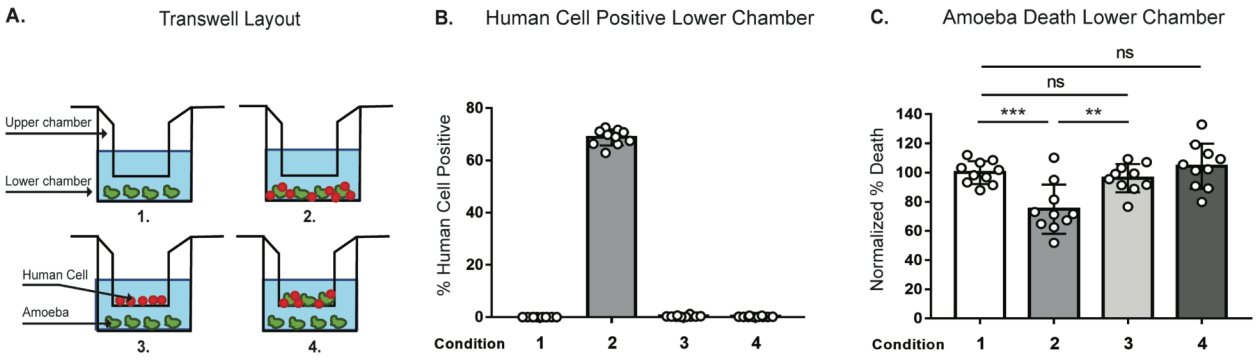

Fig. 2.4: Protection from human serum lysis is dependent on contact with human cells
(A) Depiction of each transwell condition used in panels B-C. CMFDA-labeled amoebae and DiD-labeled human cells were incubated alone, together or separately in four different transwell conditions. Condition 1: amoebae alone in the lower chamber; condition 2: amoebae and human cells together in the lower chamber; condition 3: human cells in the upper chamber and amoebae in the lower chamber; and condition 4: amoebae and human cells together in the upper chamber and amoebae in the lower chamber. Cells were co-incubated in transwells for 1 hour and then cells from the lower chambers were harvested, exposed to human serum and analyzed. Viability was assessed using Live/Dead Violet dye and imaging flow cytometry **(B)** Quantification of human cell positive amoebae in conditions 1-4. **(C)** Quantification of amoebic death in conditions 1-4 from panel A. % Death was normalized to amoebae alone (condition 1). n=10 from 5 independent experiments.

Protection from human serum requires actin.

Since acquisition and display of human cell membrane proteins requires actin **(Fig. 2.2)**, we next asked if treatment with cytochalasin D would also abrogate protection from human serum. Amoebae were treated with cytochalasin D, incubated in the presence or absence of human cells, and then exposed to human serum. Imaging flow cytometry was used to simultaneously measure trogocytosis **(Fig. 2.5A)** and amoeba viability **(Fig. 2.5B)**. Amoebae that were treated with cytochalasin D were impaired in their ability to undergo trogocytosis and were not protected from serum lysis after co-incubation with human cells. Since cytochalasin D inhibits cell motility, centrifugation was used to bring amoebae and human cells into contact **(Fig. S2.6)**. In these conditions, cytochalasin D-treated amoebae were still impaired in their ability to

undergo trogocytosis, and were not protected from subsequent serum lysis. Thus, centrifugation does not rescue the defect in cytochalasin D-treated amoebae. Actin rearrangements are therefore required for subsequent protection from lysis by human serum.

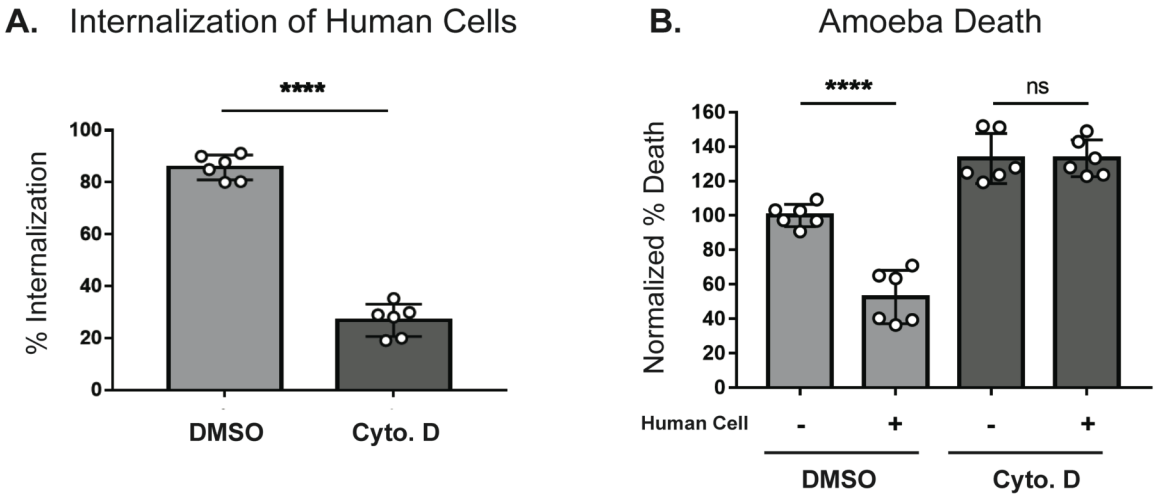

Fig. 2.5: Protection from human serum is actin-dependent.
CMFDA labeled amoebae were incubated alone or in the presence of DiD-labeled human cells for 1 hour and then exposed to active human serum. Samples were then stained with Live/Dead Violet viability dye and analyzed by imaging flow cytometry. **(A)** Amoebae were either pretreated with cytochalasin D (light grey) or DMSO (dark grey) for 1 hour. Quantification of internalization of human cells. **(B)** Quantification of amoebic death is shown. % Death has been normalized to the amoeba alone DMSO-treated samples. n=6 from 3 independent experiments.

Protection occurs after trogocytosis and does not occur after phagocytosis.

To ask if protection from human serum specifically occurs after trogocytosis, or if any form of ingestion leads to protection from serum, we compared amoebae that had undergone trogocytosis with those that had undergone phagocytosis. We previously showed that amoebae undergo trogocytosis of live human cells, and in contrast, undergo phagocytosis of pre-killed human cells (19). Therefore, we asked if

phagocytosis of pre-killed cells could also provide protection from complement lysis. Human cells were pre-killed by pre-treating with staurosporine to induce apoptosis **(Fig. 2.6A)**. Amoebae were co-incubated with live or pre-killed human cells or incubated in the absence of human cells. Amoebae that had undergone trogocytosis or phagocytosis ingested a similar amount of human cell material **(Fig. 2.6B)**, however, amoebae were only protected from lysis by human serum after undergoing trogocytosis **(Fig. 2.6C)**. Therefore, protection from lysis by human serum occurs specifically after trogocytosis of live cells.

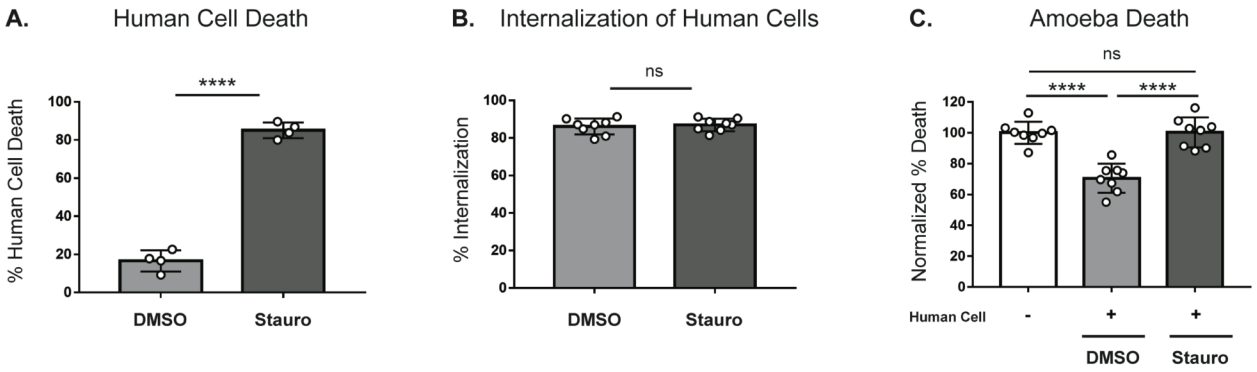

Fig. 2.6: Protection requires trogocytosis but not phagocytosis of human cells.
(A) Human cells were pretreated with staurosporine (dark grey) or DMSO (light grey). The human cell viability before co-incubation is shown. **(B)** Quantification of human cell internalization by amoebae. **(C)** Quantification of amoebic death. % Death was normalized to the amoebae alone samples. n=8 from 4 independent experiments.

To further distinguish between requirements for trogocytosis and phagocytosis, we tested mutants deficient in rhomboid protease 1 (*Eh*ROM1) (EHI_197460), a protease with roles in attachment and ingestion (39, 40). *Eh*ROM1 mutants have been shown to be deficient in phagocytosis and pinocytosis, and attachment to live cells (39, 40). Furthermore, silencing of *Eh*ROM1 does not change susceptibility to serum lysis,

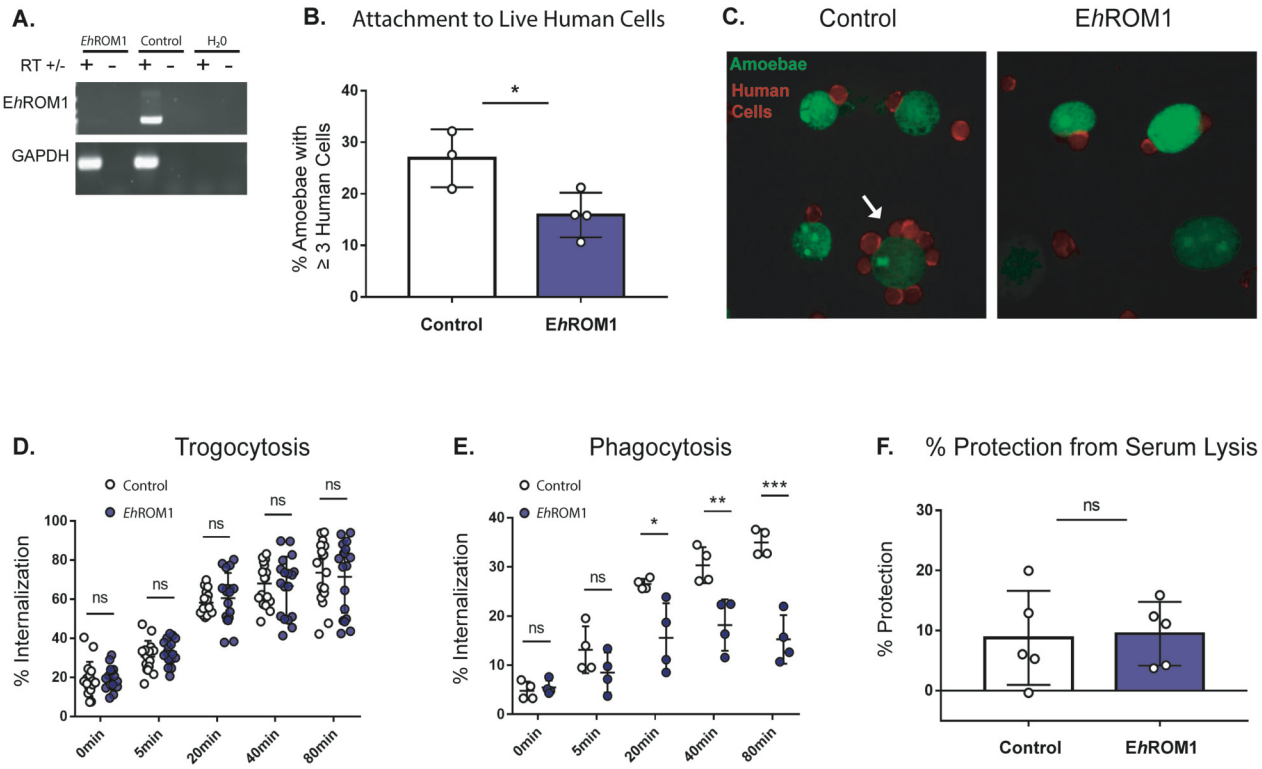

Fig.2.7: *Eh*ROM1 knockdown mutants defective in phagocytosis but not trogocytosis are protected from serum lysis.
Amoebae were stably transfected with an *Eh*ROM1 knockdown plasmid (EhROM1) or vector control plasmid (Control). **(A)** Silencing of *Eh*ROM1 was verified by using RT-PCR. Reverse transcriptase (RT) was included (+) or omitted (-) as a control. GAPDH was used to control for loading. **(B)** *Eh*ROM1 and vector control transfectants were incubated on ice with live human cells for 1 hour, then fixed and analyzed using confocal microscopy. The percentage of amoebae with 3 or more attached human cells for each condition is displayed; vector control is shown with open bars and the *Eh*ROM1 knockdown mutant is shown with blue bars. n=4 replicates from 2 independent experiments. 20 images were collected per slide and 195-252 individual amoebae were counted per condition. **(C)** Representative images from panel B. Amoebae are shown in green and human cells are shown in red. Arrow indicates an amoeba with a rosette of attached human cells. **(D)** CMFDA-labeled *Eh*ROM1 knockdown mutants (blue circles) or vector control (open circles) transfectants were incubated alone or in the presence of live DiD-labeled human cells for 0, 5, 20, 40 or 80 minutes. Internalization of human cell material was quantified using imaging flow cytometry. n=20 from 10 independent experiments. **(E)** CMFDA-labeled *Eh*ROM1 knockdown mutants (blue circles) or vector control (open circles) transfectants were incubated alone or in the presence of heat-killed CTDR-labeled human cells for 0, 5, 20, 40 or 80 minutes. Internalization of human cell material was quantified using imaging flow cytometry. n=4 from 2 independent experiments. **(F)** *Eh*ROM1 (blue bar) or vector control (open bar) amoebae were co-incubated with live human cells for 1 hour, and then exposed to human serum. Viability was assessed using Live/Dead Violet dye and imaging flow cytometry. % protection was calculated by subtracting the total lysis of amoebae co-incubated with human cells from the total lysis of amoebae incubated alone. n= 9-10 from 5 independent experiments. Protection data displays means of 2 replicates from all 5 experiments.

making these mutants an ideal tool for testing the effects conferred by ingestion of

human cells (39, 40). We generated stable *Eh*ROM1 knockdown mutants **(Fig. 2.7A)**, which were deficient in attachment to healthy human cells **(Fig. 2.7B-C)**, consistent with previous studies (40). Also consistent with previous studies, *Eh*ROM1 mutant amoebae incubated alone were not more susceptible to serum lysis then control amoebae **(Fig. S2.7B)**. *Eh*ROM1 mutants did not exhibit a trogocytosis defect **(Fig. 2.7D, Fig. S2.8)**. As expected, *Eh*ROM1 mutants were defective in phagocytosis **(Fig. 2.7E)**. After trogocytosis, *Eh*ROM1 mutants were no more or less protected from lysis by human serum than control amoebae **(Fig. 2.7F, Fig. S2.7)**. Therefore, a mutant deficient in phagocytosis does not exhibit a difference in protection from serum, further supporting that phagocytosis is not involved in resistance to lysis by human serum. Moreover, resistance to lysis by human serum is not associated with simple attachment to human cells, since *Eh*ROM1 mutants are impaired in binding to live human cells but still exhibit no difference in resistance to human serum. Together, these finding further underscore that protection from lysis by human serum is not associated with phagocytosis.

Collectively, these results support a new model of immune evasion in which amoebae perform trogocytosis on live human cells and through trogocytosis, acquire and display human cell membrane proteins. Display of human cell membrane proteins then leads to protection from human serum, most likely by inhibiting complement-mediated lysis **(Fig. 2.8)**.

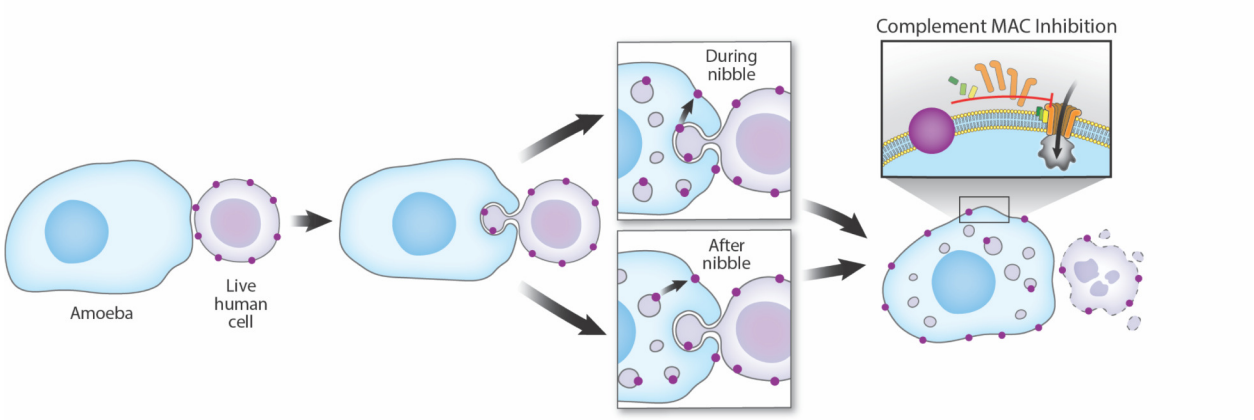

Fig. 2.8: Proposed model of protection from serum lysis.
Amoebae encounter live human cells while invading the intestine or disseminating in the blood stream and perform trogocytosis. Trogocytosis leads to acquisition and display of human cell membrane proteins on the amoebae surface. One potential mechanism for the acquisition and display of human cell membrane proteins could be through fusion of the amoebic and human cell plasma membranes during trogocytosis. Human cell proteins could be directly transferred to the amoeba surface through membrane fusion at the site of trogocytosis without being first internalized. Another potential mechanism could be through internalization of bites during trogocytosis. The ingested membrane proteins could then be trafficked to the amoeba surface. Display of human cell membrane proteins then protects the amoebae from lysis in the blood by inhibiting the complement cascade.

Discussion

Our studies revealed that amoebae acquire and display human cell membrane proteins. This process is actin-dependent and is associated with resistance to lysis by human serum. Protection from lysis by human serum requires direct contact between amoebae and human cells, is actin-dependent, and is specifically associated with trogocytosis, not phagocytosis. Collectively, these data suggest that amoebae acquire and display human cell membrane proteins through trogocytosis, and that this leads to protection from lysis by human serum complement.

Complement resistance by amoebae is relevant to invasive disease. Once amoebae have invaded intestinal tissue, they can spread from the intestine to the liver through the portal vein (41), and they can ingest erythrocytes (42), thus they are capable of surviving in the bloodstream. A study that depleted complement by using cobra venom factor in the hamster model of amoebic liver abscess, found that loss of complement was correlated with greater severity of liver lesions (43). Additionally, serum from women was more effective in killing amoebae then serum from men, and men are known to be more susceptible to invasive amoebiasis (44). Furthermore, pathogenic amoebae have been shown to resist complement. *E. histolytica* appears to evade complement deposition, while the closely related nonpathogenic species *Entamoeba dispar* does not (45). Similarly, amoebae isolated from patients with invasive infection resist complement, while strains isolated from asymptomatic patients are complement-sensitive (46).

Previous studies have hinted that amoebae become more resistant to complement after interacting with host cells or tissues, and that complement resistance involves proteins on the amoeba surface. It has previously been demonstrated that amoebae that were made resistant to complement lysis by hamster liver passage, lost resistance after treatment with trypsin (36), suggesting that complement-resistance is associated with proteins on the amoeba surface. It has also been shown that amoebae acquire serum resistance after ingestion of live human erythrocytes, and that resistant amoebae stained positive with antiserum directed to erythrocyte membrane antigens (35). Though this previous study described ingestion of erythrocytes as erythrophagocytosis, we now know that amoebae are also capable of performing trogocytosis on live erythrocytes (19). In older literature, amoebae were also seen to ingest bites of erythrocytes in a process that was termed microphagocytosis (47). Therefore, we propose a model in which invasive amoebae are able to evade complement detection in the blood by trogocytosis of human cells and display of human cell membrane proteins.

Other mechanisms of complement resistance in *E. histolytica* have been described such as mimicry of the complement regulatory protein CD59 (48, 49), an inhibitor of the membrane attack complex (MAC). Amoebic cysteine proteinases play a role in cleavage of complement components (50–52). Amoebae are also made temporarily resistant to complement lysis through treatment with increasing doses of heat-inactivated human serum, though the mechanism remains unclear (37, 53), and it was recently found that amoebae do not develop resistance to serum from rats by this

method (54). As the percentage of amoebae lysed after exposure to human serum in our assays never reached 100%, even in conditions where amoebae were incubated alone, it is likely that multiple factors contribute to complement resistance in *E. histolytica,* including display of human cell membrane proteins.

It will be of great interest to determine which human proteins are displayed by amoebae. It is possible that complement regulatory proteins such as CD55 or CD46 are displayed by amoebae and that this directly promotes resistance to complement lysis. Displayed human cell membrane proteins may also bind to soluble factors in human serum, such as factor H. It is notable that acquired human cell membrane proteins do not have an even distribution on the amoeba surface, and instead appear in foci. This was similar for both biotin-streptavidin and MHC-I staining. In mammalian immune cells, similar focal localization of acquired membrane proteins is seen, with biotin-streptavidin staining, fluorescently-tagged proteins, and immunofluorescence (24, 55). It is not clear if the acquired membrane proteins are present in lipid microdomains (*e.g.,* lipid rafts), or are in clusters. It is also possible that while patchy foci of acquired membrane proteins are clearly seen, these proteins may also be found throughout the membrane at lower concentrations below the limit of detection. In any case, the distribution of human cell proteins appears sufficient to confer protection from complement.

We used E*h*ROM1 knockdown mutants that were defective in phagocytosis but not trogocytosis to test whether protection was specifically associated with trogocytosis. Consistent with the original description of *Eh*ROM1 mutants (40), we found that they were still capable of attachment to human cells, but were defective in attaching to

multiple human cells at the same time. Amoebae attached to numerous human cells are termed “rosettes.” The phenotype of *Eh*ROM1 mutants is consistent with the *E. histolytica* literature in general, where attachment phenotypes do not manifest as abolishment of all attachment, but instead result in decreased rosette formation compared to control amoebae (40, 56, 57). Since most *Eh*ROM1 mutants still attached to at least one human cell, it appears that the lowered levels of attachment were sufficient to allow trogocytosis to proceed and to allow acquisition of human cell membrane proteins, since the mutants were still protected from lysis by human serum.

With the discoveries of amoebic trogocytosis and display of human cell membrane proteins, a new paradigm for amoeba-human cell interactions is emerging. We previously showed that when amoebae kill cells, they do not ingest dead cell corpses (19). Prior to this, amoebae were thought to fully ingest the corpses of the cells they had killed (5, 58, 59). Now, with the discovery of acquisition and display of human cell membrane proteins, together with the lack of ingestion of cell corpses, a different paradigm is emerging. It is possible that rather than acquiring nutrition by killing and ingesting entire cells, amoebae nibble and acquire membrane proteins that contribute to immune evasion. Invasive disease involves survival of amoebae in blood vessels. Since trogocytosis contributes to tissue invasion (19), it is possible that amoebae acquire human cell membrane proteins as they invade the intestine. Amoebae would then be equipped to survive in the bloodstream and to spread to other tissues. Moreover, since there is the potential for a variety of human cell proteins to be displayed, display of human cell proteins may impact host-amoeba interactions in many ways.

Display of human cell proteins acquired during trogocytosis is a novel strategy for immune evasion by a pathogen. Since other microbial eukaryotes use trogocytosis for cell killing, including *N. fowleri,* there is the potential for display of acquired membrane proteins to apply to the pathogenesis of other infections. Furthermore, our studies extend acquisition and display of membrane proteins beyond mammalian immune cells, suggesting that this may be a fundamental feature of eukaryotic trogocytosis. How membrane proteins are acquired and displayed by immune cells during trogocytosis is not well understood. Thus, ongoing studies in amoebae may shed light on acquisition and display of membrane proteins during trogocytosis in general.

In summary, amoebae display human cell membrane proteins on their surface and are protected from lysis by human serum after trogocytosis. We propose a new model of immune evasion by *E. histolytica,* whereby amoebae survive complement attack in the bloodstream through trogocytosis and display of human cell membrane proteins. This work broadens our understanding of trogocytosis as a conserved feature of eukaryotic biology, as well as our understanding of the pathogenesis of amoebiasis.

Materials and Methods

Cell culture.

HM1: IMSS (ATCC) *E. histolytica* trophozoites (amoebae) were cultured at 35°C in TYI-S-33 media supplemented with 80 Units/mL penicillin and 80 μg/mL streptomycin (Gibco), 2.3% Diamond Vitamin Tween 80 Solution 40x (Sigma-Aldrich) and 15% heat-inactivated adult bovine serum (Gemini Bio-Products). Amoebae were harvested when tissue culture flasks reached 80-100% confluency and then resuspended in M199s media (Gibco medium M199 with Earle's Salts, L-Glutamine, 2.2 g/L Sodium Bicarbonate and without Phenol Red) supplemented with 5.7 mM L-cysteine, 25 mM HEPES and 0.5% bovine serum albumin.

Human Jurkat T cells from ATCC (Clone E6-1) were cultured at 37°C and 5% CO_2 in RPMI Medium 1640 (Gibco RPMI with L-Glutamine and without Phenol Red) supplemented with 10 mM HEPES, 100 Units/mL penicillin and 100 μg/mL streptomycin and 10% heat-inactivated fetal bovine serum (Gibco). human cells were harvested between $5x10^5$ and $2x10^6$ cells/ml and resuspended in M199s media.

Generation of *Eh*ROM1 mutants.

The *Eh*ROM1 silencing construct, made from a pEhEx plasmid backbone, was generated by Morf *et al.* as described in (60). The construct contained 132 base pairs of the trigger gene EHI_048600 fused to the first 537 base pairs of *Eh*ROM1 (EHI_197460). Amoebae were transfected with 20 μg of the *Eh*ROM1 silencing construct using Attractene Transfection Reagent (QIAGEN). Transfectants were then

maintained under selection with Geneticin at 6 μg/ml. Clonal lines were generated by limiting dilution in a 96-well plate contained in a BD GasPak EZ Pouch System (BD Biosciences), and silencing was confirmed with RT-PCR. An individual clonal line was used for all experiments. A vector control line was generated by transfection with the pEhEx-trigger construct backbone, using the same approach.

Confocal immunofluorescence assays.

In the biotin transfer experiments, human cells were resuspended in 1X Dulbecco's Phosphate Buffered Saline (PBS: Sigma-Aldrich) and then biotinylated with EZ-Link Sulfo-NHS-SS-Biotin (Thermo Fisher Scientific) at 480 μg/ml in 1X PBS for 25 minutes at 4°C. 1M Tris-HCL pH 8 was added to the samples for a final concentration of 100 mM to quench the reaction. Cells were next washed in 1X PBS containing Tris-HCL pH 8 at 100 mM, and then resuspended in M199s. Amoebae were washed and labeled in M199s with CellTracker Green CMFDA (Invitrogen) at 310 ng/ml for 10 minutes at 35°C. Amoebae and human cells were combined at a 1:5 ratio in M199s and co-incubated for 5 minutes at 35°C. Following co-incubation, cells were fixed with 4% paraformaldehyde (Electron Microscopy Sciences) for 30 minutes at room temperature and stained with an Alexa Fluor 633 streptavidin conjugate (Invitrogen) at 20 μg/ml for 1 hour at 4°C. After fixation, samples were stained with DAPI (Sigma-Aldrich) for 10 minutes at room temperature. Samples were then incubated on coverslips pre-coated with collagen (Collagen I, Rat Tail: Gibco), according to the manufacturer's instructions, for 1 hour at room temperature and mounted on glass slides using VECTASHIELD

(Vector Laboratories). In some experiments, samples were incubated on Superfrost Plus Micro Slides (VWR) for 1 hour, and coverslips were then mounted with VECTASHIELD. Samples were imaged on an Olympus FV1000 laser point-scanning confocal microscope or on an Intelligent Imaging Innovations Hybrid Spinning Disk Confocal-TIRF-Widefield Microscope. Images were collected from 4 independent experiments, including 76 images of amoebae with human cells and 21 images of amoebae alone.

For the MHC class I immunofluorescence experiments, human cells and amoebae were separately washed and resuspended in M199s. Amoebae and human cells were then combined at a 1:5 ratio in M199s and co-incubated for 5 minutes at 35°C. Following co-incubation and fixation with 4% paraformaldehyde, samples were blocked for 1 hour in PBS-T (0.1% Tween 20 in 1X PBS) supplemented with 20% Goat Serum (Jackson Immunoresearch Labs Inc.) and 5% bovine serum albumin. Samples were then washed in PBS-T and incubated overnight with an MHC class I monoclonal primary antibody (Thermo Fisher Scientific HLA-ABC Monoclonal Antibody W6/32) at 10 μg/ul, followed by washing with PBS-T and incubation with an anti-mouse Cy3 secondary antibody (Jackson Immunoresearch Labs Inc.) at 3.5 ng/ml at room temperature for 1 hour. Samples were stained with DAPI and mounted on glass slides as above. Images were collected from 4 independent experiments, including 83 images of amoebae with human cells and 40 images of amoebae alone.

Imaging flow cytometry immunofluorescence assays.

Amoebae were resuspended in M199s media and pretreated with cytochalasin D (Sigma-Aldrich) at 20 μM or with the equivalent volume of dimethylsulfoxide (DMSO) for 1 hour at 35°C. Cytochalasin D and DMSO were kept in the media for the duration of the experiment. Following pre-treatment, amoebae were labeled with CellTracker Green CMFDA at 93 ng/ml for 10 minutes at 35°C. Human cells were labeled in culture with Hoechst 33342 (Invitrogen) at 5 μg/ml for 1 hour at 37°C and then resuspended in 1X PBS. Human cells were then biotinylated with EZ-Link Sulfo-NHS-SS-Biotin at 480 μg/ml in 1X PBS for 25 minutes at 4°C. 100 mM Tris-HCL pH 8 was used to quench the reaction, cells were washed in 100 mM Tris-HCL pH 8 and were resuspended in M199s. Amoebae and human cells were combined at a 1:5 ratio in M199s and co-incubated for 5 minutes at 35°C. After co-incubation, samples were immediately placed on ice to halt ingestion, stained with an Alexa Fluor 633 streptavidin conjugate at 20 μg/ml for 1 hour at 4°C and fixed with 4% paraformaldehyde for 30 minutes at room temperature. Fixed samples were resuspended in 1X PBS and run on an Amnis ImageStreamX Mark II. 10,000 events per sample were collected from 6 repeats across three independent experiments.

Serum lysis assays.

Amoebae were washed and labeled in M199s with CellTracker Green CMFDA at 93 ng/ml for 10 minutes at 35°C. Human cells were washed and labeled in M199s with Diic18(5)-Ds [1,1-Dioctadecyl-3,3,3,3-Tetramethylindodicarbocyanine-5,5-Disulfonic

Acid] (DiD: Assay Biotech) at 21 μg/ml for 5 minutes at 37°C and 10 minutes at 4°C. After washing with M199s, amoebae and human cells were combined at a 1:5 ratio in M199s and co-incubated for 1 hour at 35°C, or amoebae were incubated in the same conditions in the absence of human cells. Next, cells were pelleted at 400 x *g* for 8 minutes and were resuspended in 100% normal human serum (Pooled Normal Human Complement Serum, Innovative Research Inc.), heat-inactivated human serum (inactivated at 56°C for 30 minutes), or M199s. Serum/media was supplemented with 150 μM $CaCl_2$ and 150 μM $MgCl_2$ (Fig. S2). Next, cells were incubated for 30 minutes at 35°C. Cells were then washed and resuspended in M199s media and incubated with LIVE/DEAD Fixable Violet Dead Cell Stain (Invitrogen) that was prepared according to the manufacturer's instructions, at 4 μl/ml for 30 minutes on ice. Next, samples were fixed with 4% paraformaldehyde for 30 minutes at room temperature. Fixed samples were pelleted and resuspended in 1X PBS, then run on an Amnis ImageStreamX Mark II. 10,000 events per sample were collected.

In the cytochalasin D experiments, amoebae were pretreated with cytochalasin D at 20 μM or an equivalent volume of DMSO for 1 hour at 35°C. Cytochalasin D/DMSO was kept in the media for the duration of the experiment. In experiments where amoebae ingested live or pre-killed cells, human cells were pretreated in culture with staurosporine (Sigma-Aldrich) at 1 μM or with the equivalent volume of DMSO overnight at 37°C. Human cells were then washed and suspended in M199s media and labeled with CellTracker Deep Red (CTDR) (Invitrogen) at 1 μM for 30 minutes at 37°C. In transwell assays, amoebae and human cells were incubated together at a 1:5 ratio or

separately in 12 mm transwells with 3.0 µm pore, 10 µm thick polycarbonate membrane inserts (Corning). In experiments using EhROM1 knockdown, stably transfected *Eh*ROM1 clonal mutants were compared to mutants that contained a pEhEx-trigger backbone vector control construct.

Ingestion assays.

In trogocytosis assays, CMFDA labeled transfectants were incubated alone or in the presence of live DiD-labeled Jurkat cells for 0, 5, 20, 40 or 80 minutes. Samples were then labeled with Live/Dead Violet and fixed with 4% paraformaldehyde. Internalization of human cell material was quantified using imaging flow cytometry. In phagocytosis assays, human cells were heat-killed at 60°C for 40 minutes and were labeled with CTDR and Hoechst prior to incubation with CMFDA labeled amoebae.

Attachment assay.

CMFDA labeled amoebae were combined with CTDR labeled live human cells at a 1:5 ratio, centrifuged at 150 x g for 5 minutes 4°C, and incubated on ice for 1 hour. Samples were then fixed with 4% paraformaldehyde. Samples were incubated on Superfrost Plus Micro Slides (VWR) for 1 hour, coverslips were mounted with VECTASHIELD and slides were imaged on an Intelligent Imaging Innovations Hybrid Spinning Disk Confocal-TIRF-Widefield Microscope. 20 images were collected per slide. Amoebae with 3 or more attached human cells were scored as attachment positive. Image collection and scoring were performed in a blinded manner.

Imaging flow cytometry analysis.

Samples were run on an Amnis ImageStreamX Mark II and 10,000 events were collected per sample. Data were analyzed using Amnis IDEAS software. Samples were gated on focused cells, single amoebae, amoebae that had come in contact with human cells, and amoebae that had internalized human material. From the single amoebae gate, amoebic death was quantified by plotting intensity of LIVE/DEAD Violet against side scatter and gating on LIVE/DEAD Violet positive cells (see Fig. S3).

In the biotin transfer experiment, single amoebae were divided into Hoechst high and Hoechst low populations in order to isolate single amoebae with and without human cells. Overlap of biotin with CMFDA labeled amoebae was plotted and biotin positive cells were selected from both Hoechst high and low populations (see Fig. S1).

For calculation of the background level of phagocytosis, the imaging flow cytometry data from the experiments shown in Fig. 2 were used. The DMSO control-treated amoebae were used for this analysis. Single amoebae were gated from total cells. Next, biotin-positive amoebae were gated. Amoebae associated with human cell nuclei that were surrounded by a biotin/streptavidin ring were considered phagocytosis-negative, while amoebae associated with human cell nuclei that lacked a biotin ring were considered phagocytosis-positive. Amoebae that were not associated with human cell nuclei were considered phagocytosis-negative. Some amoebae were out of focus or were associated with too many human cells to reliably score; thus, these images were left unscored. The first 100 images in the biotin-positive amoeba gate that could be scored (300 total images from three independent experiments) were analyzed. Since

some images were unscored, more than 100 total images were analyzed per experiment, as indicated in the raw data table. Images were counted independently by two different researchers and the counts were averaged.

In the trogocytosis and phagocytosis assays, focused cells were gated from total collected events. Next, single cells were gated, and then single amoebae were gated. Amoebae positive for human cells were gated and internalization of human cells was measured. (see Fig. S5)

Statistical analysis.

All statistical analysis was performed using GraphPad Prism. All data plots display means and standard deviation values. Data were statistically analyzed using a student's unpaired t-test (ns = $P>0.05$, * = $P \leq 0.05$, ** = $P \leq 0.01$, *** = $P \leq 0.001$, **** = $P \leq 0.0001$).

Acknowledgements

We thank the MCB Light Microscopy Imaging Facility at UC Davis for technical assistance. We thank Dr. Stephen McSorley and the members of our laboratory for helpful discussions. We thank Anita Impagliazzo of Anita Impagliazzo Medical Illustration for the illustration in Fig. 8. This work was supported by a Pew Scholarship awarded to K.S.R. The funders had no role in study design, data collection and interpretation, or the decision to submit the work for publication. The authors declare no competing financial interests.

H.W.M and K.S.R conceived and designed the study. H.W.M performed the experiments and analyzed the data. R.L.S. performed and analyzed the ROM1 trogocytosis and phagocytosis experiments. H.W.M and K.S.R. interpreted the data. H.W.M and K.S.R. wrote the manuscript

References

1. Haque R, Mondal D, Kirkpatrick BD, Akther S, Farr BM, Sack RB, Petri WA. 2003. Epidemiologic and clinical characteristics of acute diarrhea with emphasis on Entamoeba histolytica infections in preschool children in an urban slum of Dhaka, Bangladesh. Am J Trop Med Hyg 69:398–405.

2. Speich B, Croll D, Fürst T, Utzinger J, Keiser J. 2016. Effect of sanitation and water treatment on intestinal protozoa infection: a systematic review and meta-analysis. The Lancet Infectious Diseases 16:87–99.

3. Petri WA, Mondal D, Peterson KM, Duggal P, Haque R. 2009. Association of malnutrition with amebiasis. Nutr Rev 67:S207–S215.

4. Gilchrist CA, Petri SE, Schneider BN, Reichman DJ, Jiang N, Begum S, Watanabe K, Jansen CS, Elliott KP, Burgess SL, Ma JZ, Alam M, Kabir M, Haque R, Petri WA. 2016. Role of the Gut Microbiota of Children in Diarrhea Due to the Protozoan Parasite Entamoeba histolytica. J Infect Dis 213:1579–1585.

5. Ralston KS, Petri WA. 2011. Tissue destruction and invasion by Entamoeba histolytica. Trends Parasitol 27:254–263.

6. Ravdin JI, Croft BY, Guerrant RL. 1980. Cytopathogenic mechanisms of Entamoeba histolytica. J Exp Med 152:377–390.

7. Ravdin JI, Guerrant RL. 1980. Studies on the cytopathogenicity of Entamoeba histolytica. Arch Invest Med (Mex) 11:123–128.

8. Ravdin JI, Guerrant RL. 1981. Role of Adherence in Cytopathogenic Mechanisms of Entamoeba Histolytica. J Clin Invest 68:1305–1313.

9. Saffer LD, Petri WA. 1991. Role of the galactose lectin of Entamoeba histolytica in adherence-dependent killing of mammalian cells. Infect Immun 59:4681–4683.

10. Thibeaux R, Dufour A, Roux P, Bernier M, Baglin A-C, Frileux P, Olivo-Marin JC, Guillén N, Labruyère E. 2012. Newly visualized fibrillar collagen scaffolds dictate Entamoeba histolytica invasion route in the human colon. Cell Microbiol 14:609–621.

11. Hellberg A, Nickel R, Lotter H, Tannich E, Bruchhaus I. 2001. Overexpression of cysteine proteinase 2 in Entamoeba histolytica or Entamoeba dispar increases amoeba-induced monolayer destruction in vitro but does not augment amoebic liver abscess formation in gerbils. Cell Microbiol 3:13–20.

12. Keene WE, Petitt MG, Allen S, McKerrow JH. 1986. The major neutral proteinase of Entamoeba histolytica. J Exp Med 163:536–549.

13. Lidell ME, Moncada DM, Chadee K, Hansson GC. 2006. Entamoeba histolytica cysteine proteases cleave the MUC2 mucin in its C-terminal domain and dissolve the protective colonic mucus gel. Proc Natl Acad Sci USA 103:9298–9303.

14. Bracha R, Nuchamowitz Y, Leippe M, Mirelman D. 1999. Antisense inhibition of amoebapore expression in Entamoeba histolytica causes a decrease in amoebic virulence. Mol Microbiol 34:463–472.

15. Bracha R, Nuchamowitz Y, Mirelman D. 2003. Transcriptional silencing of an amoebapore gene in Entamoeba histolytica: molecular analysis and effect on pathogenicity. Eukaryotic Cell 2:295–305.

16. Leippe M, Andrä J, Müller-Eberhard HJ. 1994. Cytolytic and antibacterial activity of synthetic peptides derived from amoebapore, the pore-forming peptide of Entamoeba histolytica. Proc Natl Acad Sci USA 91:2602–2606.

17. Leippe M, Andrä J, Nickel R, Tannich E, Müller-Eberhard HJ. 1994. Amoebapores, a family of membranolytic peptides from cytoplasmic granules of

Entamoeba histolytica: isolation, primary structure, and pore formation in bacterial cytoplasmic membranes. Mol Microbiol 14:895–904.

18. Ravdin JI, Moreau F, Sullivan JA, Petri WA, Mandell GL. 1988. Relationship of free intracellular calcium to the cytolytic activity of Entamoeba histolytica. Infect Immun 56:1505–1512.

19. Ralston KS, Solga MD, Mackey-Lawrence NM, Somlata, Bhattacharya A, Petri Jr WA. 2014. Trogocytosis by *Entamoeba histolytica* contributes to cell killing and tissue invasion. Nature 508:526–530.

20. Ralston KS. 2015. Taking a bite: Amoebic trogocytosis in Entamoeba histolytica and beyond. Current Opinion in Microbiology 28:26–35.

21. Brown T. 1979. Observations by immunofluorescence microscopy and electron microscopy on the cytopathogenicity of naegleria fowleri in mouse embryo-cell cultures. Journal of Medical Microbiology 12:363–371.

22. Waddell DR, Vogel G. 1985. Phagocytic behavior of the predatory slime mold, Dictyostelium caveatum. Cell nibbling. Exp Cell Res 159:323–334.

23. Batista FD, Iber D, Neuberger MS. 2001. B cells acquire antigen from target cells after synapse formation. Nature 411:489–494.

24. Wakim LM, Bevan MJ. 2011. Cross-dressed dendritic cells drive memory CD8+ T-cell activation after viral infection. Nature 471:629–632.

25. Davis CO, Kim K-Y, Bushong EA, Mills EA, Boassa D, Shih T, Kinebuchi M, Phan S, Zhou Y, Bihlmeyer NA, Nguyen JV, Jin Y, Ellisman MH, Marsh-Armstrong N. 2014. Transcellular degradation of axonal mitochondria. Proc Natl Acad Sci USA 111:9633–9638.

26. Weinhard L, di Bartolomei G, Bolasco G, Machado P, Schieber NL, Neniskyte U, Exiga M, Vadisiute A, Raggioli A, Schertel A, Schwab Y, Gross CT. 2018. Microglia remodel synapses by presynaptic trogocytosis and spine head filopodia induction. Nat Commun 9:1228.

27. Abdu Y, Maniscalco C, Heddleston JM, Chew T-L, Nance J. 2016. Developmentally programmed germ cell remodelling by endodermal cell cannibalism. Nat Cell Biol 18:1302–1310.

28. Mercer F, Ng SH, Brown TM, Boatman G, Johnson PJ. 2018. Neutrophils kill the parasite Trichomonas vaginalis using trogocytosis. PLoS Biol 16:e2003885.

29. Matlung HL, Babes L, Zhao XW, van Houdt M, Treffers LW, van Rees DJ, Franke K, Schornagel K, Verkuijlen P, Janssen H, Halonen P, Lieftink C, Beijersbergen RL, Leusen JHW, Boelens JJ, Kuhnle I, van der Werff Ten Bosch J, Seeger K, Rutella S, Pagliara D, Matozaki T, Suzuki E, Menke-van der Houven van Oordt CW, van Bruggen R, Roos D, van Lier RAW, Kuijpers TW, Kubes P, van den Berg TK. 2018. Neutrophils Kill Antibody-Opsonized Cancer Cells by Trogoptosis. Cell Rep 23:3946-3959.e6.

30. Velmurugan R, Challa DK, Ram S, Ober RJ, Ward ES. 2016. Macrophage-Mediated Trogocytosis Leads to Death of Antibody-Opsonized Tumor Cells. Mol Cancer Ther 15:1879–1889.

31. Miyake K, Shiozawa N, Nagao T, Yoshikawa S, Yamanishi Y, Karasuyama H. 2017. Trogocytosis of peptide-MHC class II complexes from dendritic cells confers antigen-presenting ability on basophils. Proc Natl Acad Sci USA 114:1111–1116.

32. Gu P, Gao JF, D'Souza CA, Kowalczyk A, Chou K-Y, Zhang L. 2012. Trogocytosis of CD80 and CD86 by induced regulatory T cells. Cell Mol Immunol 9:136–146.

33. Rossi EA, Goldenberg DM, Michel R, Rossi DL, Wallace DJ, Chang C-H. 2013. Trogocytosis of multiple B-cell surface markers by CD22 targeting with epratuzumab. Blood 122:3020–3029.

34. Martínez-Martín N, Fernández-Arenas E, Cemerski S, Delgado P, Turner M, Heuser J, Irvine DJ, Huang B, Bustelo XR, Shaw A, Alarcón B. 2011. T cell receptor internalization from the immunological synapse is mediated by TC21 and RhoG GTPase-dependent phagocytosis. Immunity 35:208–222.

35. Gutiérrez-Kobeh L, Cabrera N, Pérez-Montfort R. 1997. A Mechanism of Acquired Resistance to Complement-Mediated Lysis by Entamoeba histolytica. The Journal of Parasitology 83:234–241.

36. Hamelmann C, Urban B, Foerster B, Horstmann RD. 1993. Complement resistance of pathogenic Entamoeba histolytica mediated by trypsin-sensitive surface component(s). Infect Immun 61:1636–1640.

37. Hamelmann C, Foerster B, Burchard GD, Shetty N, Horstmann RD. 1993. Induction of complement resistance in cloned pathogenic Entamoeba histolytica. Parasite Immunol 15:223–228.

38. Miller HW, Suleiman RL, Ralston KS. 2018. Trogocytosis by Entamoeba histolytica mediates acquisition and display of human cell membrane proteins and evasion of lysis by human serum. bioRxiv 487314.

39. Rastew E, Morf L, Singh U. 2015. Entamoeba histolytica rhomboid protease 1 has a role in migration and motility as validated by two independent genetic approaches. Exp Parasitol 154:33–42.

40. Baxt LA, Rastew E, Bracha R, Mirelman D, Singh U. 2010. Downregulation of an Entamoeba histolytica Rhomboid Protease Reveals Roles in Regulating Parasite Adhesion and Phagocytosis. Eukaryot Cell 9:1283–1293.

41. Rigothier M-C, Khun H, Tavares P, Cardona A, Huerre M, Guillén N. 2002. Fate of Entamoeba histolytica during establishment of amoebic liver abscess analyzed by quantitative radioimaging and histology. Infect Immun 70:3208–3215.

42. González-Ruiz A, Haque R, Aguirre A, Castañón G, Hall A, Guhl F, Ruiz-Palacios G, Miles MA, Warhurst DC. 1994. Value of microscopy in the diagnosis of dysentery associated with invasive Entamoeba histolytica. J Clin Pathol 47:236–239.

43. Capin R, Capin NR, Carmona M, Ortíz-Ortíz L. 1980. Effect of complement depletion on the induction of amebic liver abscess in the hamster. Arch Invest Med (Mex) 11:173–180.

44. Snow M, Chen M, Guo J, Atkinson J, Stanley SL. 2008. Differences in complement-mediated killing of Entamoeba histolytica between men and women--an explanation for the increased susceptibility of men to invasive amebiasis? Am J Trop Med Hyg 78:922–923.

45. Costa CA, Nunes AC, Ferreira AJ, Gomes MA, Caliari MV. 2010. Entamoeba histolytica and E. dispar trophozoites in the liver of hamsters: in vivo binding of antibodies and complement. Parasit Vectors 3:23.

46. Reed SL, Curd JG, Gigli I, Gillin FD, Braude AI. 1986. Activation of complement by pathogenic and nonpathogenic Entamoeba histolytica. J Immunol 136:2265–2270.

47. Lejeune A, Gicquaud C. 1987. Evidence for two mechanisms of human erythrocyte endocytosis by Entamoeba histolytica-like amoebae (Laredo strain). Biol Cell 59:239–245.

48. Braga LL, Ninomiya H, McCoy JJ, Eacker S, Wiedmer T, Pham C, Wood S, Sims PJ, Petri WA. 1992. Inhibition of the complement membrane attack complex by the galactose-specific adhesion of Entamoeba histolytica. J Clin Invest 90:1131–1137.

49. Ventura-Juárez J, Campos-Rodríguez R, Jarillo-Luna RA, Muñoz-Fernández L, Escario-G-Trevijano JA, Pérez-Serrano J, Quintanar JL, Salinas E, Villalobos-Gómez FR. 2009. Trophozoites of Entamoeba histolytica express a CD59-like molecule in human colon. Parasitol Res 104:821–826.

50. Reed SL, Ember JA, Herdman DS, DiScipio RG, Hugli TE, Gigli I. 1995. The extracellular neutral cysteine proteinase of Entamoeba histolytica degrades anaphylatoxins C3a and C5a. J Immunol 155:266–274.

51. Reed SL, Gigli I. 1990. Lysis of complement-sensitive Entamoeba histolytica by activated terminal complement components. Initiation of complement activation by an extracellular neutral cysteine proteinase. J Clin Invest 86:1815–1822.

52. Reed SL, Keene WE, McKerrow JH, Gigli I. 1989. Cleavage of C3 by a neutral cysteine proteinase of Entamoeba histolytica. J Immunol 143:189–195.

53. Calderon J, Tovar R. 1986. Loss of susceptibility to complement lysis in Entamoeba histolytica HM1 by treatment with human serum. Immunology 58:467–471.

54. Olivos-García A, Nequiz M, Liceaga S, Mendoza E, Zúñiga P, Cortes A, López-Velázquez G, Enríquez-Flores S, Saavedra E, Pérez-Tamayo R. 2018. Complement is a rat natural resistance factor to amoebic liver infection. Biosci Rep 38.

55. Steele S, Radlinski L, Taft-Benz S, Brunton J, Kawula TH. 2016. Trogocytosis-associated cell to cell spread of intracellular bacterial pathogens. eLife 5:e10625.

56. Teixeira JE, Huston CD. 2008. Participation of the serine-rich Entamoeba histolytica protein in amebic phagocytosis of apoptotic host cells. Infect Immun 76:959–966.

57. Ravdin JI, Guerrant RL. 1981. Role of adherence in cytopathogenic mechanisms of Entamoeba histolytica. Study with mammalian tissue culture cells and human erythrocytes. J Clin Invest 68:1305–1313.

58. Huston CD, Boettner DR, Miller-Sims V, Petri, Jr. WA. 2003. Apoptotic Killing and Phagocytosis of Host Cells by the Parasite Entamoeba histolytica. Infect Immun 71:964–972.

59. Sateriale A, Huston CD. 2011. A Sequential Model of Host Cell Killing and Phagocytosis by Entamoeba histolytica. J Parasitol Res 2011.

60. Khalil MI, Foda BM, Suresh S, Singh U. 2016. Technical advances in trigger-induced RNA interference gene silencing in the parasite Entamoeba histolytica. Int J Parasitol 46:205–212.

Supplemental Material

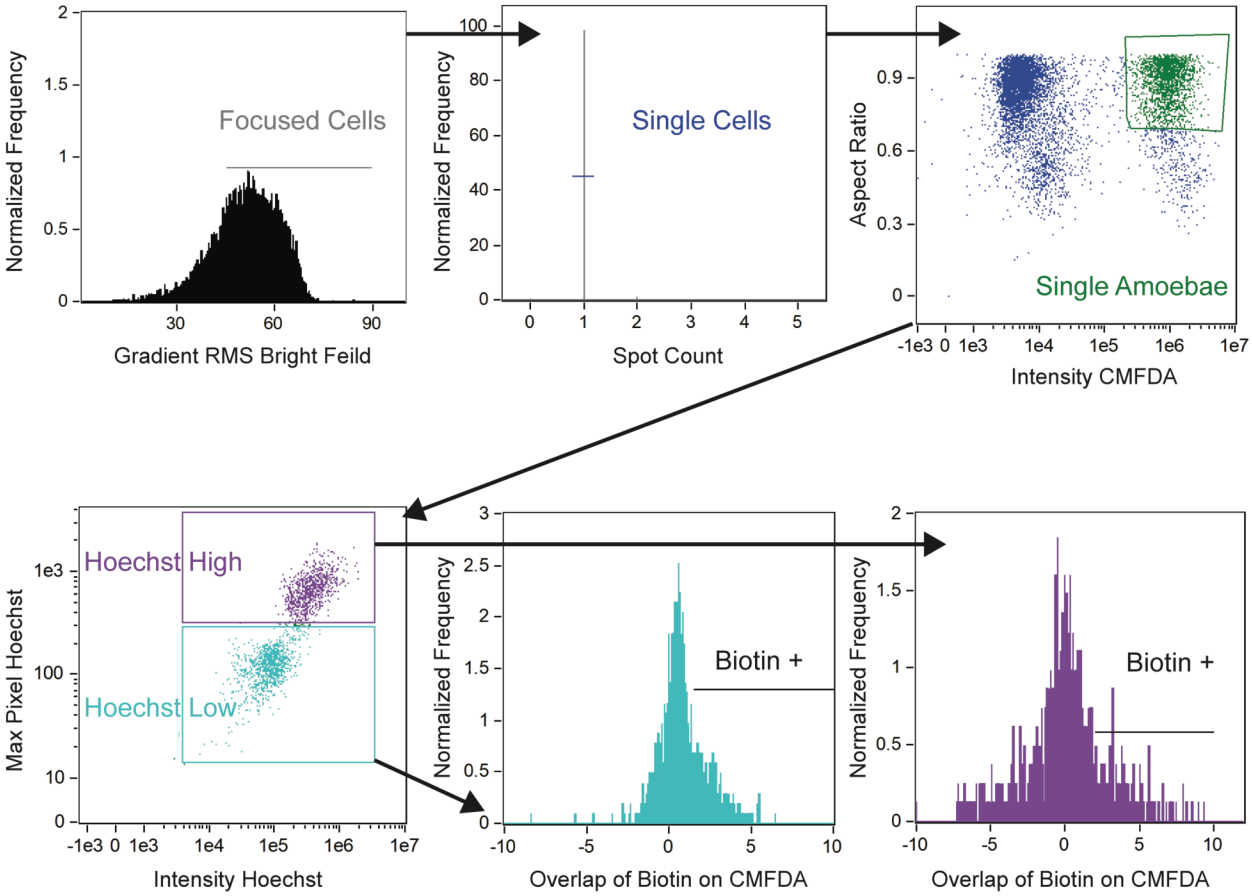

Fig. S2.1: Gating strategy used to quantify transferred biotin.
Gating strategy used to quantify biotin-positive amoebae. Focused cells were gated from total collected events. Next, single cells were gated, and then single amoebae were gated. Single amoebae were divided into Hoechst high and Hoechst low populations to identify images with and without human cell nuclei. Finally, biotin-positive amoebae were gated on from images with and without human cell nuclei.

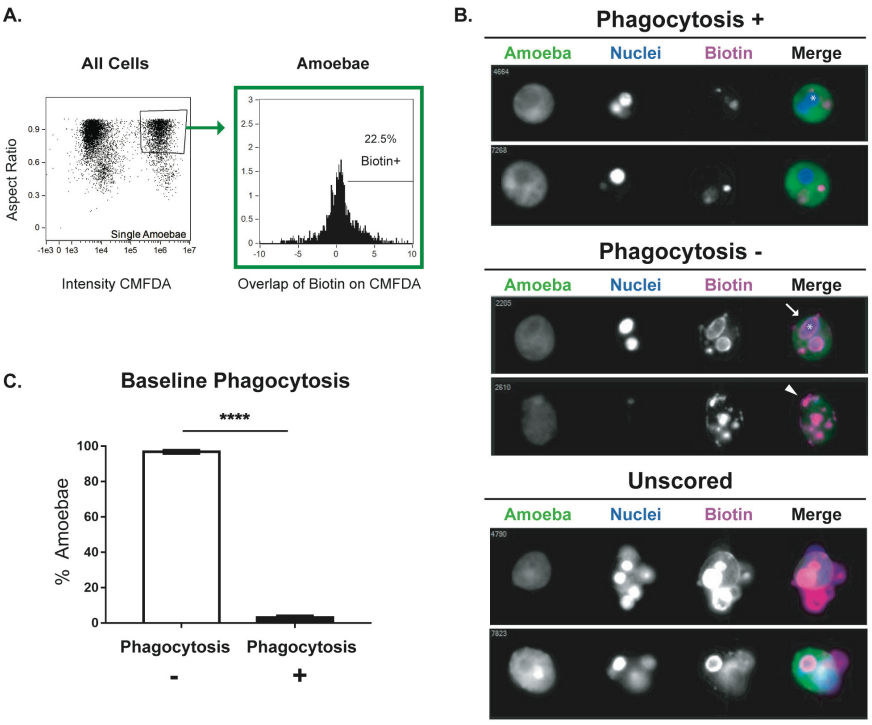

D.

Scorer 1	Experiment	# Phagocytosis +	# Phagocytosis -	# Unscored
	1	5	95	3
	2	4	96	9
	3	3	97	23
Scorer 2	**Experiment**	**# Phagocytosis +**	**# Phagocytosis -**	**# Unscored**
	1	2	98	19
	2	3	97	33
	3	2	98	41

Fig. S2.2: Analysis used to quantify the background level of phagocytosis in trogocytosis assays. The imaging flow cytometry data from the experiments shown in Fig. 2.2 were used to quantify the level of phagocytosis in trogocytosis assays. CMFDA-labeled DMSO control-treated amoebae were combined with Hoechst-labeled human cells. Immediately after co-incubation, cells were placed on ice to halt ingestion and stained with fluorescently-conjugated streptavidin. Samples were quantitatively analyzed using imaging flow cytometry, with 10,000 images collected for each sample. **(A)** Single amoebae were gated from total cells. Next, biotin-positive amoebae were gated. (**B)** Human cell nuclei (asterisks) that were surrounded by a biotin/streptavidin ring (arrow) were considered extracellular, while human cell nuclei that lacked a biotin ring were considered internalized. Thus, amoebae that were associated with extracellular human cells were considered phagocytosis-negative, while amoebae associated with internalized human cells were considered phagocytosis-positive. Amoebae that were biotin-positive (arrowhead) without associated human cell nuclei were considered phagocytosis-negative. Some amoebae were out of focus or were associated with too many human cells to reliably score; thus, these images were left unscored. Representative images of phagocytosis-positive, phagocytosis-negative, and unscored amoebae are shown. **(C)** Among three independent experiments, the average level of phagocytosis was 3% (range of 2-5%). **(D)** Table showing the raw data for the analysis in panel C. 100 images each from three separate experiments (300 total scored images, plus unscored images as indicated) were counted. Images were counted independently by two different researchers and the counts were averaged.

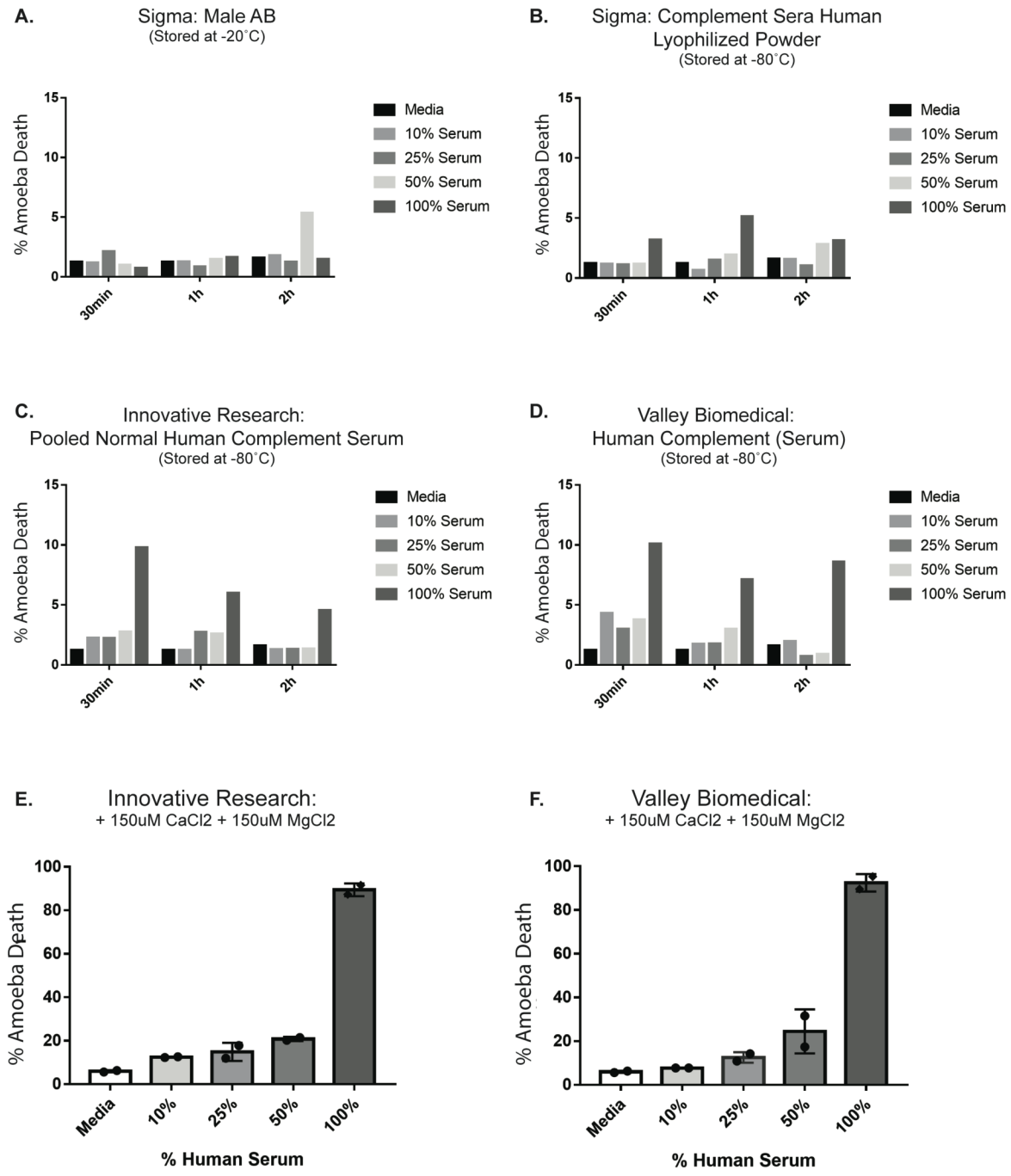

Fig. S2.3: Optimization of complement assay.
The ability of un-supplemented human serum from different vendors to lyse amoebae was tested at various concentrations for 30 minutes, 1 hour, and 2 hours at 35°C. Samples were labeled with the viability dye Live/Dead Violet and % amoeba death was quantified using imaging flow cytometry. % amoeba death was not normalized. **(A)** Sigma Male AB Serum. Note, serum was stored at -20°C instead of -80°C. **(B)** Sigma Complement Sera Human Lyophilized Powder. **(C)** Innovative Research Pooled Normal Human Complement Serum. **(D)** Valley Biomedical Human Complement (Serum). **(E-F)** Lysis of increasing concentration of serum from Innovative Research and Valley Biomedical was tested with the addition of 150 μM $CaCl_2$ and 150 μM $MgCl_2$ for 1 hour at 35°C.

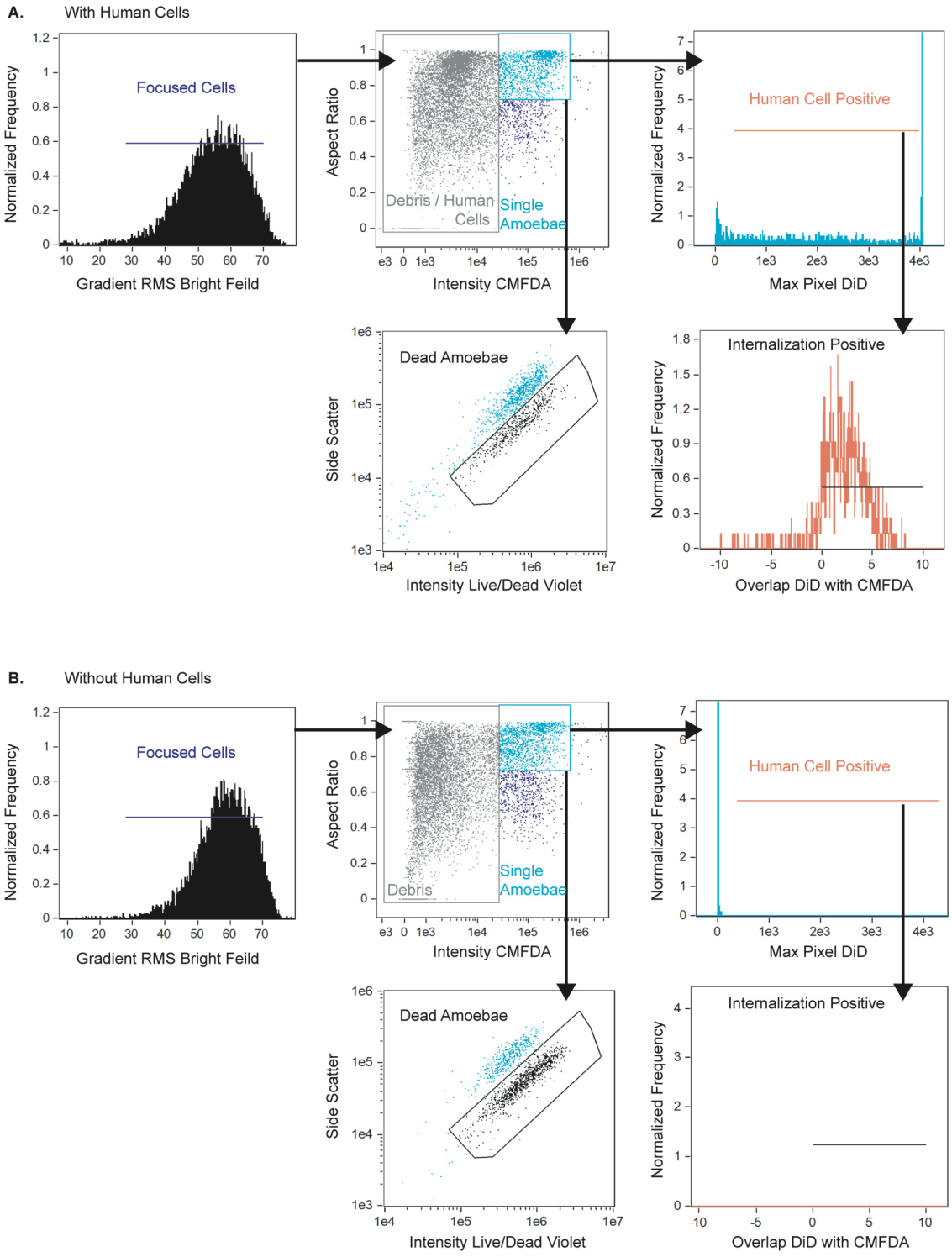

Fig. S2.4: Serum lysis assay gating strategy.
Gating strategy used in the serum lysis assay. Focused cells were gated from total collected events. Next, focused events were dived into gates that either contained debris and human cells, or single amoebae. Single amoebae positive for human cells were gated and then internalization of human cells was measured. % of dead amoebae was gated from single amoebae.

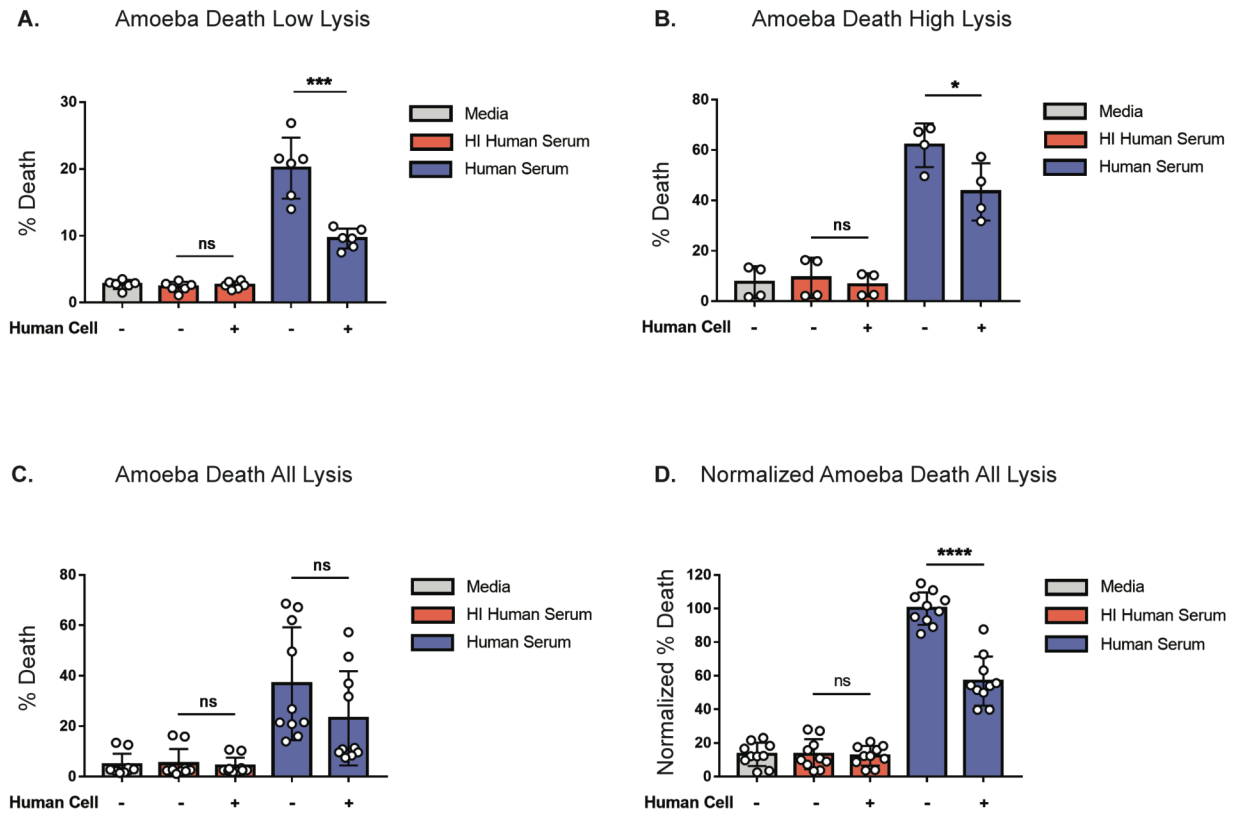

Fig. S2.5: Non-normalized data shown from Fig. 2.3.
Non-normalized data from the serum lysis assay shown in Fig. 2.3. Amoebic lysis was variable and fell in to two groups, Low lysis **(A)** and **(B)** high lysis. This variability in lysis was associated with how the human serum was stored and thawed. The highest lysis was achieved with serum stored at -80°C and rapidly thawed at 37 °C, leaving intact ice pellets, and then thawed to completion at room temperature. Lower lysis was achieved with serum stored at -20°C and thawed to completion at 37 °C. **(C)** Lysis from all data non- normalized. **(D)** Lysis from all data normalized to the amoeba incubated alone condition that was exposed to active human serum.

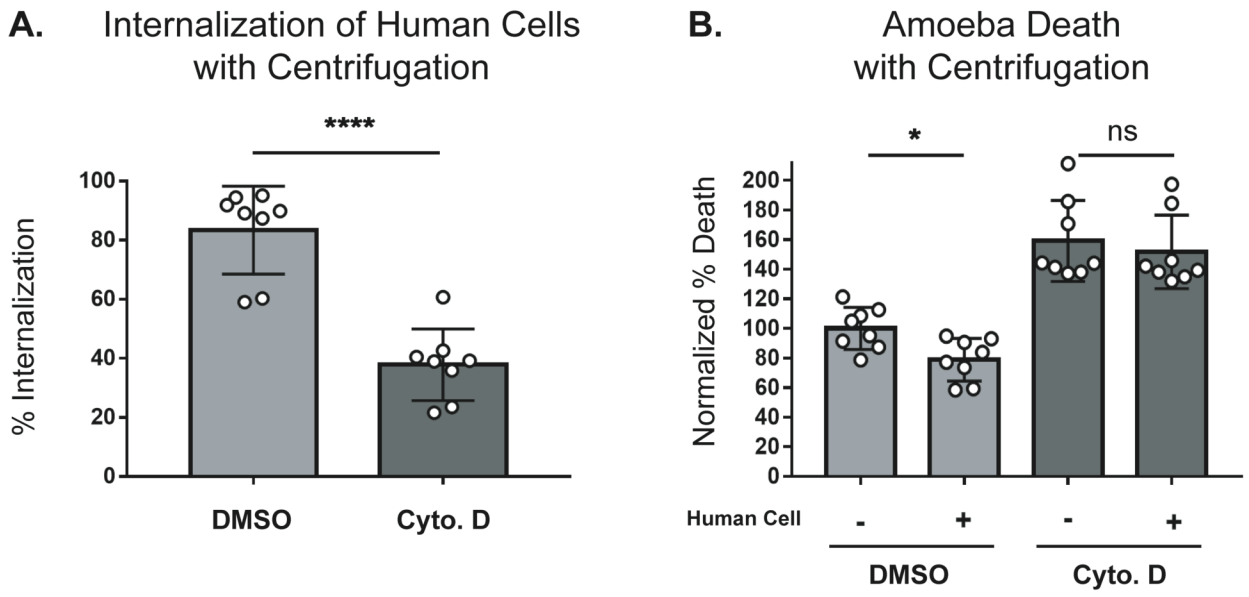

Fig. S2.6: Centrifugation does not rescue the defect in cytochalasin D-treated amoebae. The experiments shown in Fig. 2.5 were repeated with the addition of a centrifugation step to force contact between amoebae and human cells at the start of the co-incubation. CMFDA-labeled amoebae and DiD-labeled were centrifuged together at 400 x *g* for 8 min, and then co-incubated for 1 hour, or amoebae were centrifuged and incubated in the absence of human cells as a control. Samples were then exposed to active human serum for 1 hour, stained with Live/Dead Violet viability dye, and quantitatively analyzed using imaging flow cytometry. 10,000 images were collected for each sample. **(A)** Amoebae were either pretreated with cytochalasin D (light grey) or DMSO (dark grey) for 1 hour. Quantification of internalization of human cells. **(B)** Quantification of amoebic death is shown. % Death has been normalized to the amoeba alone DMSO-treated samples. n=8 from 4 independent

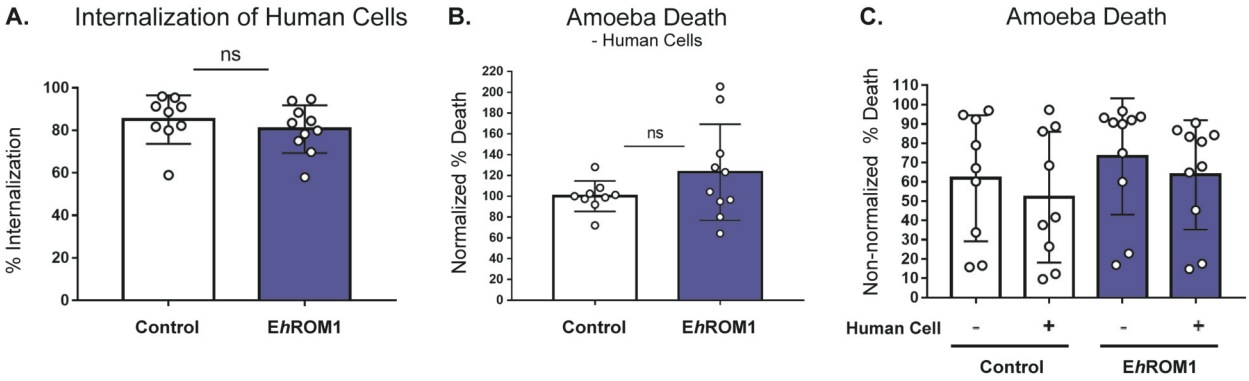

Fig. S2.7: Internalization of human cells and amoebic death from the serum lysis assay in Fig. 2.7. Additional data from the serum lysis assay used in Fig. 2.7. **(A**) Internalization of human cells by vector control transfectants (open bar) or *Eh*ROM1 (blue bar) knockdown mutants. **(B)** % of normalized amoeba death in the conditions where amoebae were incubated alone. **(C)** Non-normalized amoebic death from all conditions.

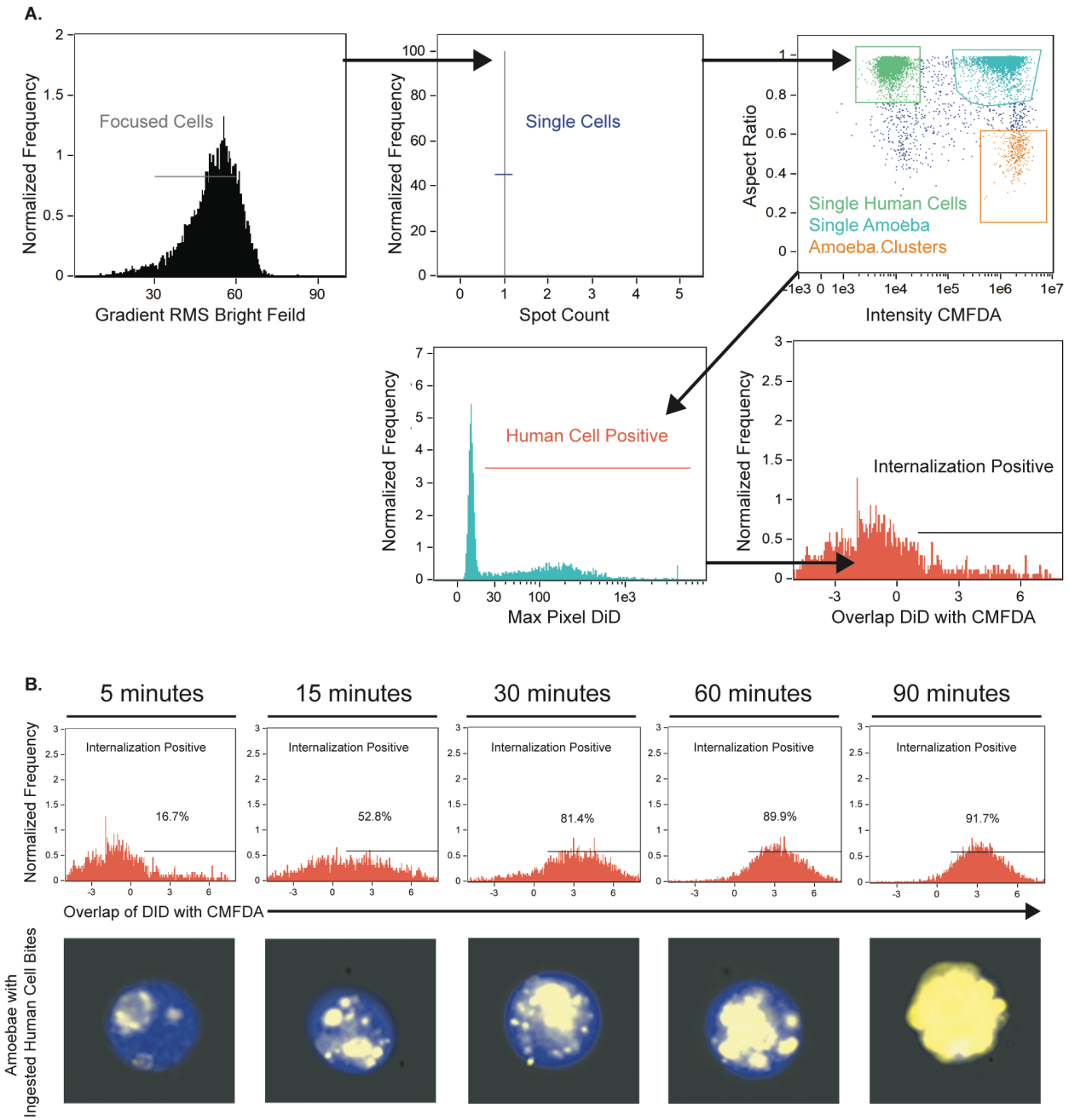

Fig. S2.8: Gating strategy used in trogocytosis and phagocytosis assays.
(A) Gating strategy used in the trogocytosis and phagocytosis assays shown in Fig. 2.7. Shown are example data from a trogocytosis assay, where CMFDA-labeled amoebae were incubated with live DiD-labeled human cells. For phagocytosis assays, CMFDA-labeled amoebae were incubated with CTDR-labeled heat-killed human cells. Focused cells were gated from total collected events. Next, single cells were gated, and then single amoebae were gated. Amoebae positive for human cells were gated and internalization of human cells was measured. **(B)** Example data from a trogocytosis assay, with representative plots from the vector control condition showing internalization of human cells over time as well as representative images collected at each time point.

Chapter 3

Entamoeba histolytica Develops Resistance to Complement Deposition and Lysis After Acquisition of Human Complement Regulatory Proteins through Trogocytosis

Hannah W. Miller, Tammie S.Y. Tam and Katherine S. Ralston

Abstract

Entamoeba histolytica is the cause of amoebiasis. The trophozoite (amoeba) form of this parasite is capable of invading the intestine, and can disseminate through the bloodstream to other organs. The mechanisms that allow amoebae to evade complement deposition during dissemination have not been well characterized. We previously discovered a novel complement-evasion mechanism employed by *E. histolytica*. *E. histolytica* ingests small bites of living human cells in a process termed trogocytosis. We demonstrated that amoebae were protected from lysis by human serum following trogocytosis of human cells, and that amoebae acquired and displayed human membrane proteins from the cells they ingested. Here, we aimed to define how amoebae are protected from complement lysis after performing trogocytosis. We found that amoebae were protected from complement lysis after ingestion of both human Jurkat T cells and red blood cells, and that the level of protection correlated with the amount of material ingested. Trogocytosis of human cells led to a reduction in deposition of C3b on the surface of amoebae. We asked whether display of human complement regulators is involved in amoebic protection, and found that CD59 was displayed by amoebae after trogocytosis. Deletion of a single complement regulatory protein, CD59 or CD46, from Jurkat cells was not sufficient to alter amoebic protection from lysis, suggesting that multiple, redundant complement regulators mediate amoebic protection. However, exogeneous expression of CD46 or CD55 in amoebae was sufficient to confer protection from lysis. These studies shed light on a novel strategy for immune evasion by a pathogen.

Importance

Entamoeba histolytica is the cause of amoebiasis, a diarrheal disease of global importance. While infection is often asymptomatic, the trophozoite (amoeba) form of this parasite is capable of invading and ulcerating the intestine, and can disseminate through the bloodstream to other organs. Understanding how *E. histolytica* evades the complement system during dissemination is of great interest. Here we demonstrate for the first time that amoebae that have performed trogocytosis (nibbling of human cells) resist deposition of the complement protein C3b. Amoebae that have performed trogocytosis display the complement regulatory protein CD59. Overall, our studies suggest that acquisition and display of multiple, redundant complement regulators is involved in amoebic protection from complement lysis. These findings shed light on a novel strategy for immune evasion by a pathogen. Since other parasites use trogocytosis for cell killing, our findings may apply to the pathogenesis of other infections.

Introduction

Amoebiasis remains a disease of global importance. The 2015 Global Burden of Disease Study estimated that it was responsible for 67,900 deaths worldwide that year (1). Its causative agent, *Entamoeba histolytica,* is prevalent in countries with poor sanitation and is spread through feces-contaminated food and water (2). In the rural area of Durango, Mexico, the seroprevalence of *E. histolytica* was found to be as high as 42% (3), and a longitudinal study of children living in an urban community of Dhaka, Bangladesh found that 80% were infected with the parasite by two years of age (4).

While infection with *E. histolytica* is often asymptomatic, it can result in diarrheal disease, colitis and extraintestinal abscesses (5). Following ingestion of the cyst form of the parasite, excystation occurs and the trophozoite stage (amoeba) colonizes the large intestine (6). Amoebae are capable of invading and ulcerating the intestine, causing tissue damage and bloody diarrhea. They can also disseminate through the bloodstream to other organs, most commonly the liver, where they form abscesses that are fatal if left untreated (5). The mechanisms that allow amoebae to evade complement deposition during dissemination have not been well characterized. Pathogenic strains of *E. histolytica* isolated from patients have been shown to be more resistant to complement lysis than nonpathogenic strains (7). It has also been found that the pathogenic amoeba species *E. histolytica* appears to be more resistant to complement than its nonpathogenic relative *E. dispar* (8). *E. histolytica* cysteine proteases can cleave complement components (9–11), and the Gal/GalNAc lectin has been described as a CD59 mimicry molecule (12). However, these mechanisms alone are not sufficient

to fully protect amoebae from complement lysis, as trophozoites are readily lysed by human serum *in vitro* (13).

We previously discovered a novel complement-evasion mechanism employed by *E. histolytica* (13). Trogocytosis, or “cell nibbling,” is present in many eukaryotes and occurs in a variety of contexts (14). In *E. histolytica*, trogocytosis is a process in which amoebae ingest small bites of living human cells (15). Our previous work has defined amoebic trogocytosis as both a mechanism for cell killing (15), and more recently, for immune evasion (13). We demonstrated that amoebae were protected from lysis by human serum following trogocytosis of human cells (13), and that amoebae acquired and displayed human membrane proteins from the cells they ingested (13). This work suggested a model in which amoebae incorporate proteins from human cells they eat on their surface, and these proteins in turn inhibit complement lysis.

In the present study, we aimed to define the mechanism by which amoebae are protected from complement lysis after performing trogocytosis. We found that trogocytosis of human cells reduced deposition of the complement protein C3b the surface of amoebae, and that amoebae were protected from complement lysis after ingestion of both human Jurkat T cells and primary red blood cells. We identified the human complement regulatory protein CD59 (protectin) as one of the proteins that is taken from ingested human cells and displayed on the amoebic surface. Deletion of a single complement regulatory protein, CD59 or CD46, from human Jurkat cells was not sufficient to alter conferred protection on amoebae. However, exogeneous expression of a single complement regulator, i.e., CD46 or CD55, in amoebae was sufficient to

confer protection from lysis. Overall, these studies suggest that multiple, redundant complement regulators are involved in amoebic protection.

Results

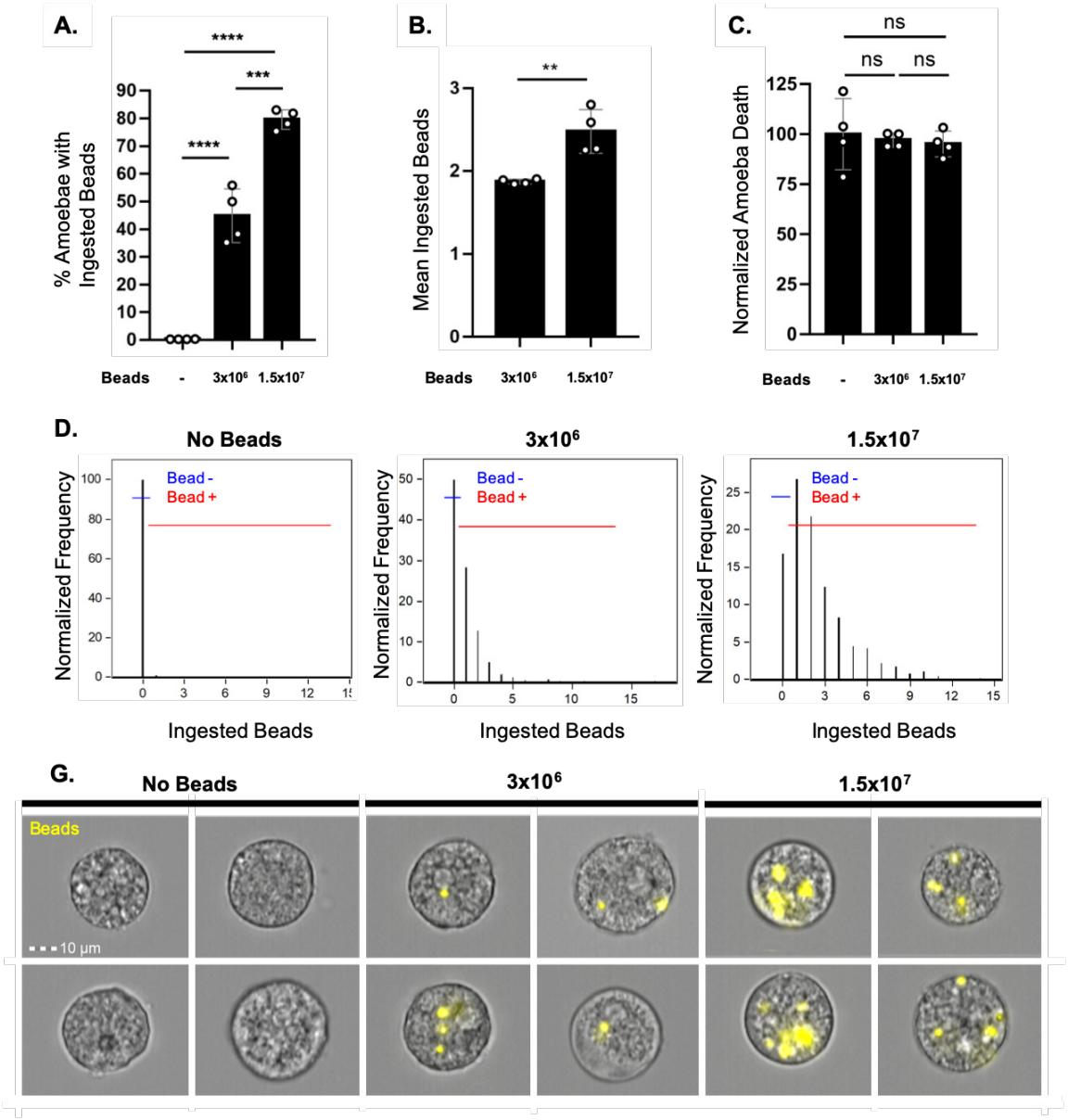

Fig. 3.1: Ingestion of latex beads does not protect amoebae from complement lysis
Amoebae were incubated with $3x10^6$ or $1.5x10^7$ fluorescent latex beads for 1 hour or were incubated without latex beads, and then exposed to human serum. Amoebic viability was determined with Zombie Violet viability dye. Imaging flow cytometry was used to quantify bead ingestion and amoebic viability. **(A)** The percentage of amoebae that had ingested any number of latex beads. **(B)** Mean number of ingested beads among amoebae that had ingested beads. **(C)** Normalized amoeba death following exposure to human serum. Values are normalized to the amoebae that were incubated without latex beads. **(D)** Quantification of the number of ingested beads per amoeba; shown are the data plots from one replicate per sample type. Amoebae that did not perform bead ingestion fall into the "Bead –" gate, while amoebae that ingested beads fall into the "Bead +" gate. **(G)** Representative images of amoebae that were incubated without beads, or in the presence of $3x10^6$ or $1.5x10^7$ beads. Ingested beads are shown in yellow. Data are from four replicates across two independent experiments.

Ingestion of beads does not confer protection from complement lysis.

We previously showed that protection from complement lysis occurred in amoebae that had performed trogocytosis on living human cells, and that known inhibitors of trogocytosis also inhibited protection from complement lysis (13). Amoebae that had performed phagocytosis of dead human cells did not become protected from complement. Likewise, amoebae that were capable of trogocytosis, but defective in phagocytosis, nonetheless became protected from complement (13). To extend these findings, and to examine the role of ingestion on protection in the absence of host proteins, we allowed amoebae to ingest increasing concentrations of latex beads. Amoebae that ingested beads were no more protected from lysis than control amoebae that did not perform ingestion **(Fig. 3.1, S3.1)**. Thus, trogocytosis confers protection from complement lysis, but phagocytosis of dead human cells or latex beads does not confer protection.

Amoebic protection from complement following trogocytosis is dose-dependent.

To determine if the amount of trogocytosed human cell material influenced protection, or if any level of trogocytosis was protective, we allowed amoebae to ingest incrementally larger amounts. Amoebae became increasingly protected from complement lysis **(Fig. 3.2B-C, S3.2A)** after ingesting higher quantities of live Jurkat cell material **(Fig. 3.2A, 3.2G)**. Thus, acquired protection from complement lysis correlates with the amount of human cell material ingested through trogocytosis.

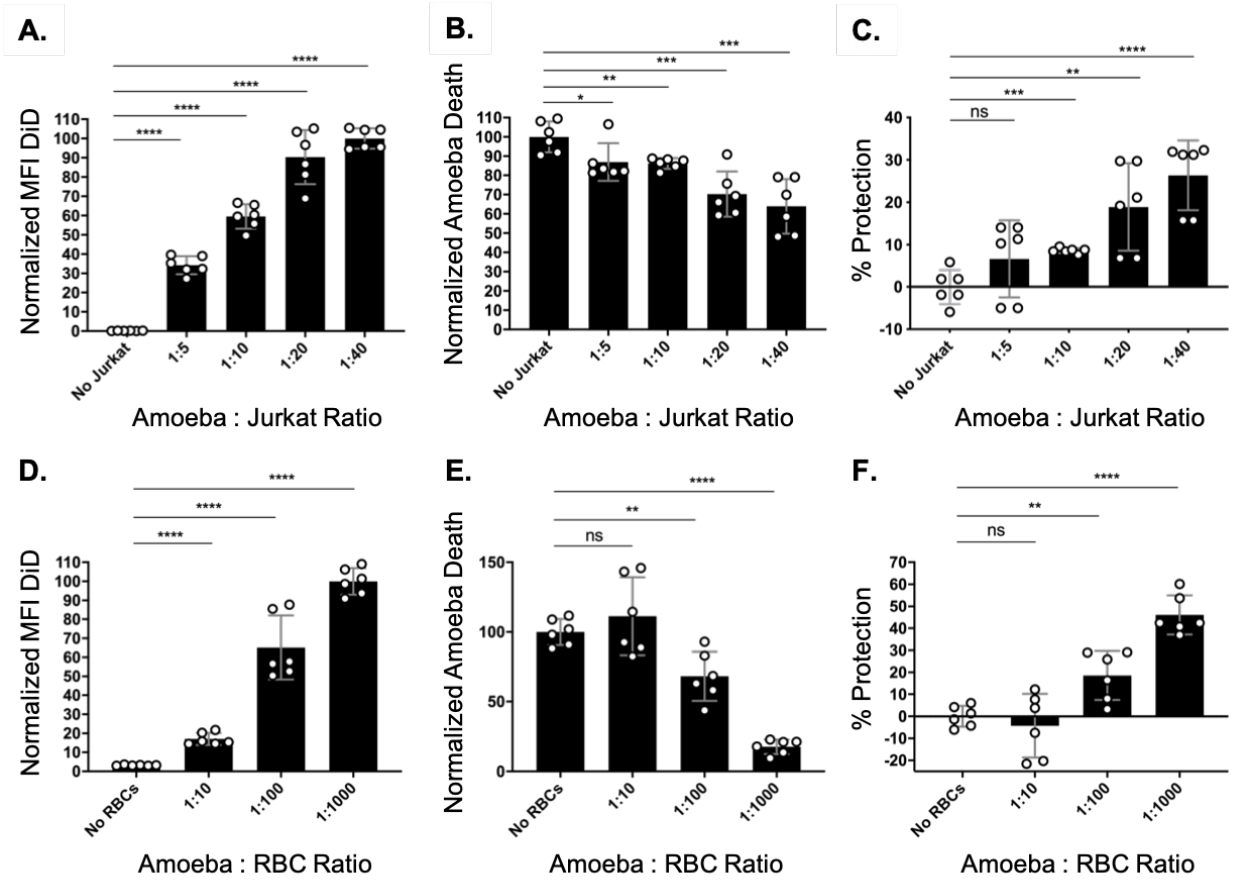
A.
Normalized MFI DiD
No Jurkat
1:5
1:10
1:20
1:40
Amoeba : Jurkat Ratio
B.
Normalized Amoeba Death
Amoeba : Jurkat Ratio
C.
% Protection
ns
Amoeba : Jurkat Ratio
D.
Normalized MFI DiD
No RBCs
1:10
1:100
1:1000
Amoeba : RBC Ratio
E.
Normalized Amoeba Death
Amoeba : RBC Ratio
F.
% Protection
Amoeba : RBC Ratio

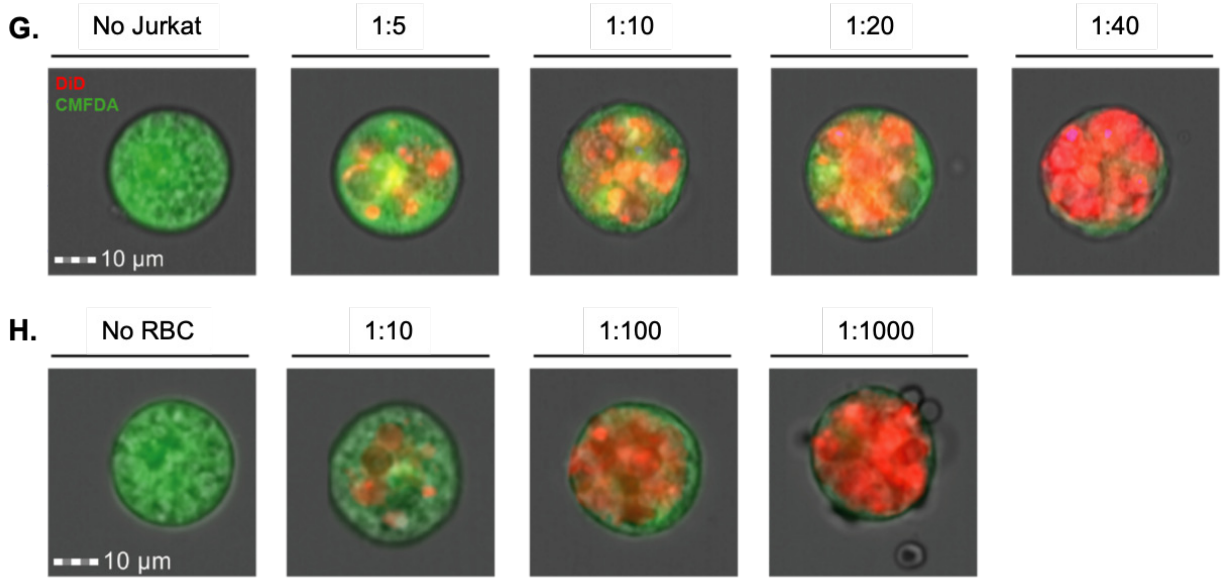
G.
No Jurkat
1:5
1:10
1:20
1:40
DiD
CMFDA
10 µm
H.
No RBC
1:10
1:100
1:1000
10 µm

Fig. 3.2: Amoebic protection from complement following trogocytosis is dose-dependent. Amoebae were labeled with CMFDA cytoplasm dye and incubated in the absence of human cells, or with increasing concentrations of human Jurkat cells or primary human red blood cells. Human cells were labeled with DiD membrane dye. Following exposure to human serum, amoeba death was assessed with Zombie Violet viability dye and ingested human cell material was determined by quantifying mean fluorescence intensity (MFI) of DiD present on amoebae. **(A)** Normalized MFI of DiD on amoebae incubated in the absence of Jurkat cells or with increasing concentrations of Jurkat cells. **(B)** Normalized death of amoebae from conditions in panel A. **(C)** Death of amoebae from conditions in panel A, expressed as percent protection. Percent protection was calculated by subtracting the total death of amoebae incubated with human cells from the total death of amoebae incubated in the absence of Jurkat cells. **(D)** Normalized MFI of DiD on amoebae incubated in the absence of red blood cells or with increasing concentrations of red blood cells. **(E)** Normalized death of amoebae from conditions in panel D. **(F)** Death of amoebae from conditions in panel D, expressed as percent protection. **(G)** Representative images of amoebae incubated with increasing concentrations of Jurkat cells. Amoebae are shown in green and ingested human cell material is shown in red. Data were analyzed by imaging flow cytometry and are from 6 replicates across 3 independent experiments. **(H)** Representative images of amoebae incubated with red blood cells. Data were analyzed by imaging flow cytometry and are from 6 replicates across 3 independent experiments.

We next asked if protection could be conferred through trogocytosis of primary human cells. During invasive infections, amoebae breach the intestinal wall and disseminate via the bloodstream. Detection of amoebae containing ingested red blood cells in the stool has previously been used as a diagnostic for invasive disease (16). Therefore, we asked if ingestion of human red blood cells would lead to protection. Amoebae were allowed to ingest increasing numbers of human red blood cells. Increased trogocytosis of red blood cells led to increased protection from complement lysis **(Fig. 3.2D-F, 3.2H, S3.2B)**. These results support a model where the level of protection from complement lysis is proportional to the amount of human cell material that was ingested during trogocytosis.

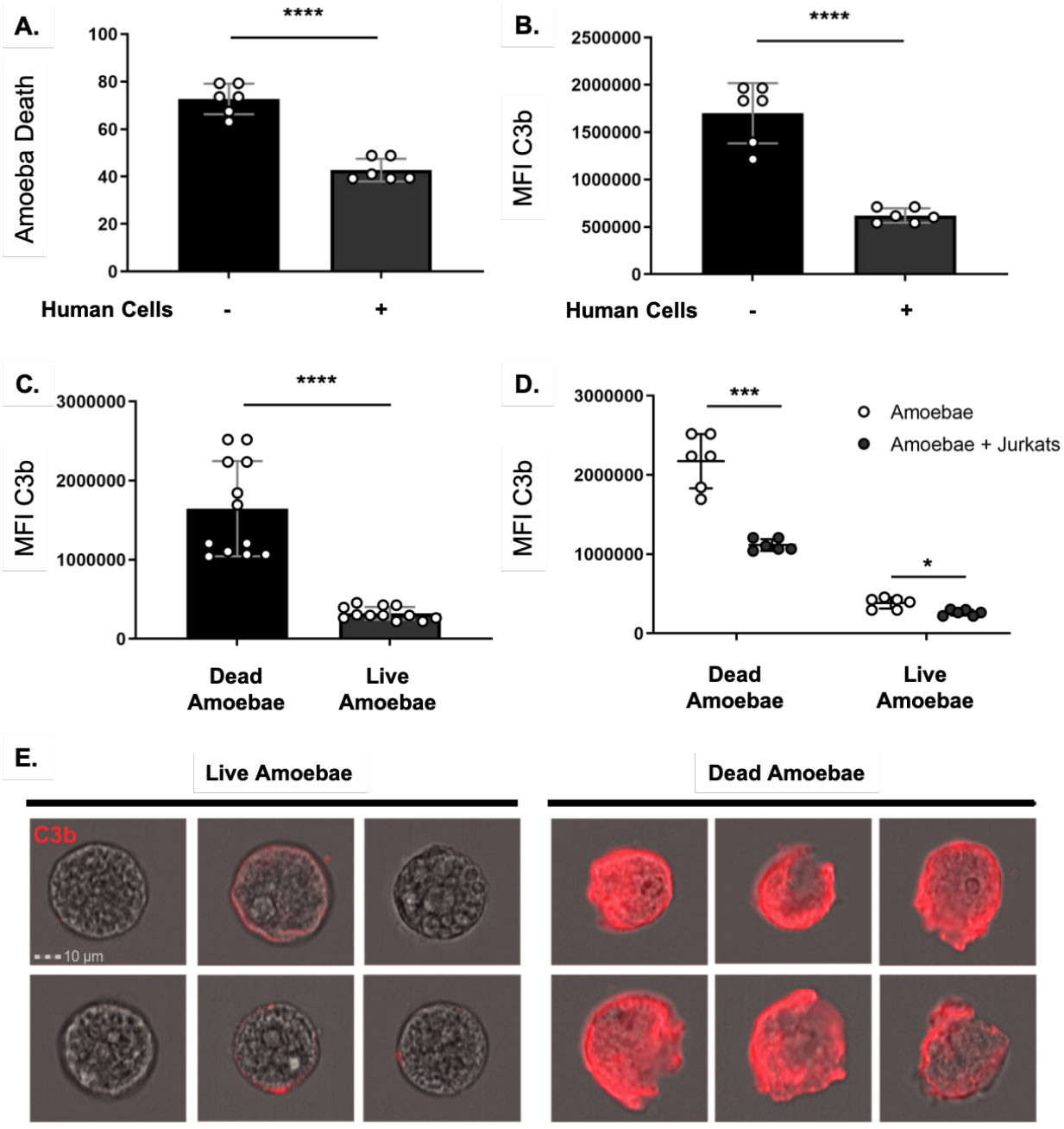

Fig. 3.3: Amoebic trogocytosis of human cells inhibits deposition of complement C3b. Amoebae were incubated in the absence of Jurkat T cells or in the presence of Jurkat cells, and subsequently exposed to human serum. Viability was assessed with Zombie Violet dye. The presence of C3b was detected using a mouse monoclonal antibody to C3b and iC3b. **(A)** Death of amoebae that were incubated in the absence of Jurkat cells or in the presence of Jurkat cells. **(B)** Mean fluorescence intensity of deposited C3b on amoebae. **(C)** Deposited C3b on dead or live amoebae. **(D)** Deposited C3b on dead or live amoebae that had been incubated in the absence of Jurkat cells (open circles) or in the presence of Jurkat cells (filled circles). **(E)** Representative images of C3b deposition (red) on live or dead amoebae. Data were analyzed by imaging flow cytometry and are from 6 replicates across 3 independent experiments.

Amoebic trogocytosis of human cells inhibits deposition of complement C3b.

It can be inferred that lysis of amoebae by human serum is due to complement activity because heat-inactivated serum does not lyse amoebae (13). Here, we formally tested if trogocytosis of human cells led to reduced deposition of complement on the amoebae surface. Amoebae that had been co-incubated with live human cells had less death and less deposited human C3b on their surface than amoebae that were incubated in the absence of Jurkat cells **(Fig. 3.3A-B, S3.3)**. Furthermore, live amoebae had less deposited C3b than dead amoebae **(Fig. 3.3C, 3.3e)**. Amoebae that had been co-incubated with human cells had less deposited C3b, compared to amoebae that were incubated in the absence of Jurkat cells **(Fig. 3.3D)**. Therefore, trogocytosis of human cells prevents complement lysis of amoebae and inhibits deposition of complement C3b.

Amoebae acquire the complement regulatory proteins CD59 and CD46 from human cells.

We hypothesized that protection from complement lysis was due to display of human complement regulatory proteins. We first chose to look at acquisition of the complement regulatory protein CD59 (protectin), a membrane protein that is expressed by both Jurkat cells and human red blood cells (17–19). CD59 inhibits terminal components of the complement cascade and formation of the membrane attack complex (17, 20–22). After amoebae had performed trogocytosis, patches of CD59 were detected on the amoeba surface within five minutes **(Fig. 3.4A)** and a larger

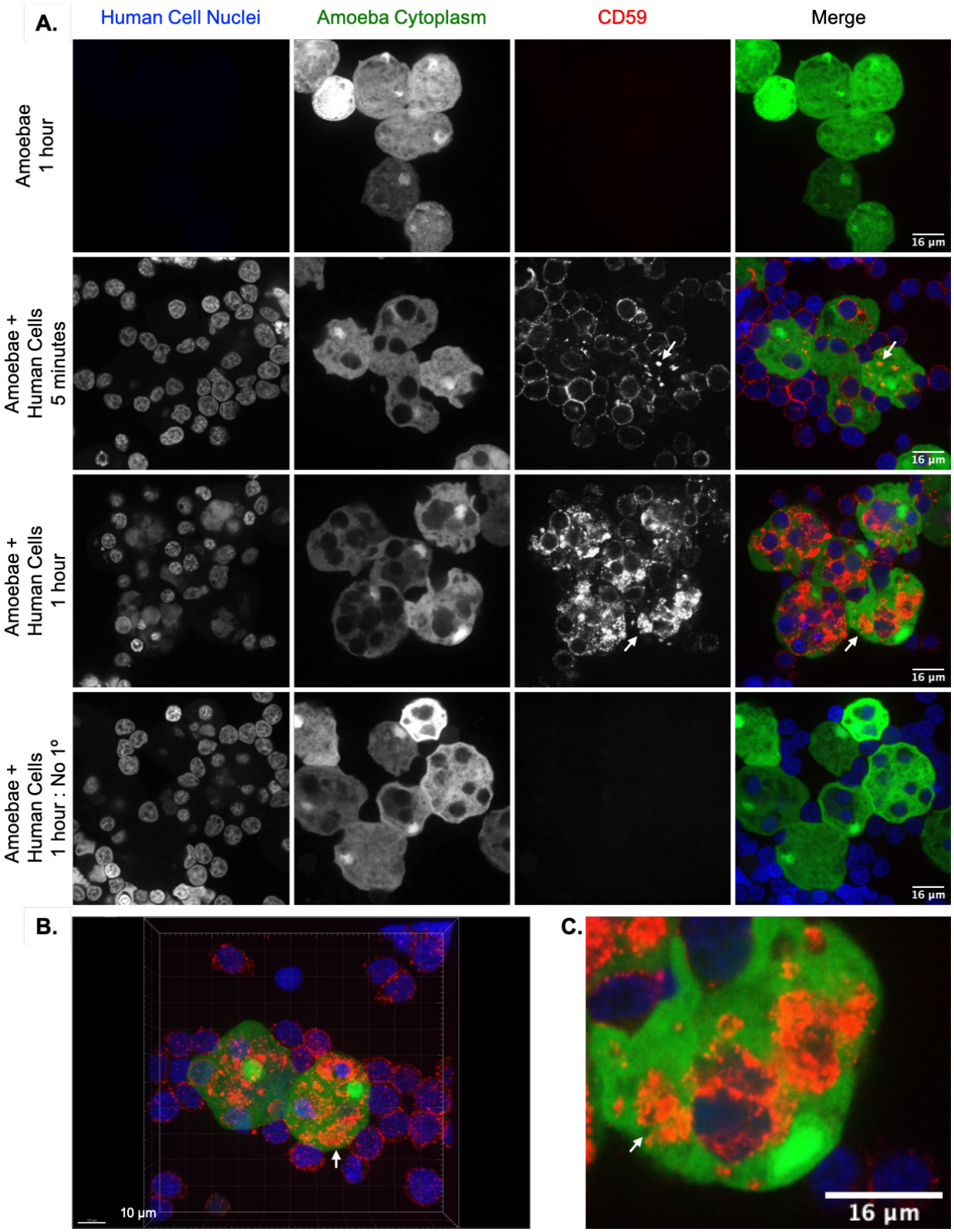
A.
Human Cell Nuclei
Amoeba Cytoplasm
CD59
Merge
Amoebae
1 hour
Amoebae +
Human Cells
5 minutes
Amoebae +
Human Cells
1 hour
Amoebae +
Human Cells
1 hour : No 1°
16 µm
B.
10 µm
C.
16 µm

Fig. 3.4: Amoebae acquire and display the complement regulatory protein CD59 from human cells. Amoebae were allowed to perform trogocytosis on human Jurkat T cells for 5 minutes or 1 hour, or were incubated in the absence of Jurkat cells. Human CD59 (red) was detected on the amoebae surface by monoclonal antibody staining. Amoebae were labeled with CMFDA (green) and human cell nuclei were labeled with Hoechst (blue). **(A)** Representative images from amoebae incubated in the absence of Jurkat cells or amoebae that performed trogocytosis on human Jurkat T cells for 5 minutes or 1 hour. Arrows indicate patches of displayed CD59 on the amoeba surface. **(B)** 3D rendering of Z stack images taken from amoebae that were incubated with human Jurkat T cells for 1 hour. **(C)** Zoomed in image of amoebae that were incubated with human Jurkat T cells for 1 hour. Data were analyzed by confocal microscopy. 136 Images were collected from 1 independent experiment.

quantity of CD59 patches were detected on the amoeba surface after one hour of trogocytosis **(Fig. 3.4A-C)**. The patchy/punctate localization pattern was similar to the localization pattern of other human proteins displayed by amoebae after trogocytosis (13). Importantly, the apparent display of human membrane proteins by amoebae was not an artifact of paraformaldehyde fixation, since the appearance of human membrane proteins displayed by amoebae was indistinguishable, whether staining was performed before or after fixation (**Fig. S3.4** and (13)). Since the heavy chain of the amoeba surface Gal/GalNAc lectin has been implicated as a CD59 mimicry molecule (12, 23), we asked if the CD59 antibody used in these assays cross-reacted with the Gal/GalNAc lectin. CD59 was not detected on control amoebae that had not performed trogocytosis **(Fig. 3.4A**), showing that the CD59 antibody did not cross-react with the Gal/GalNAc lectin.

Imaging flow cytometry analysis was used to quantify amoebic acquisition of CD59. Human cell nuclei are not ingested during trogocytosis (15). Therefore, labeling

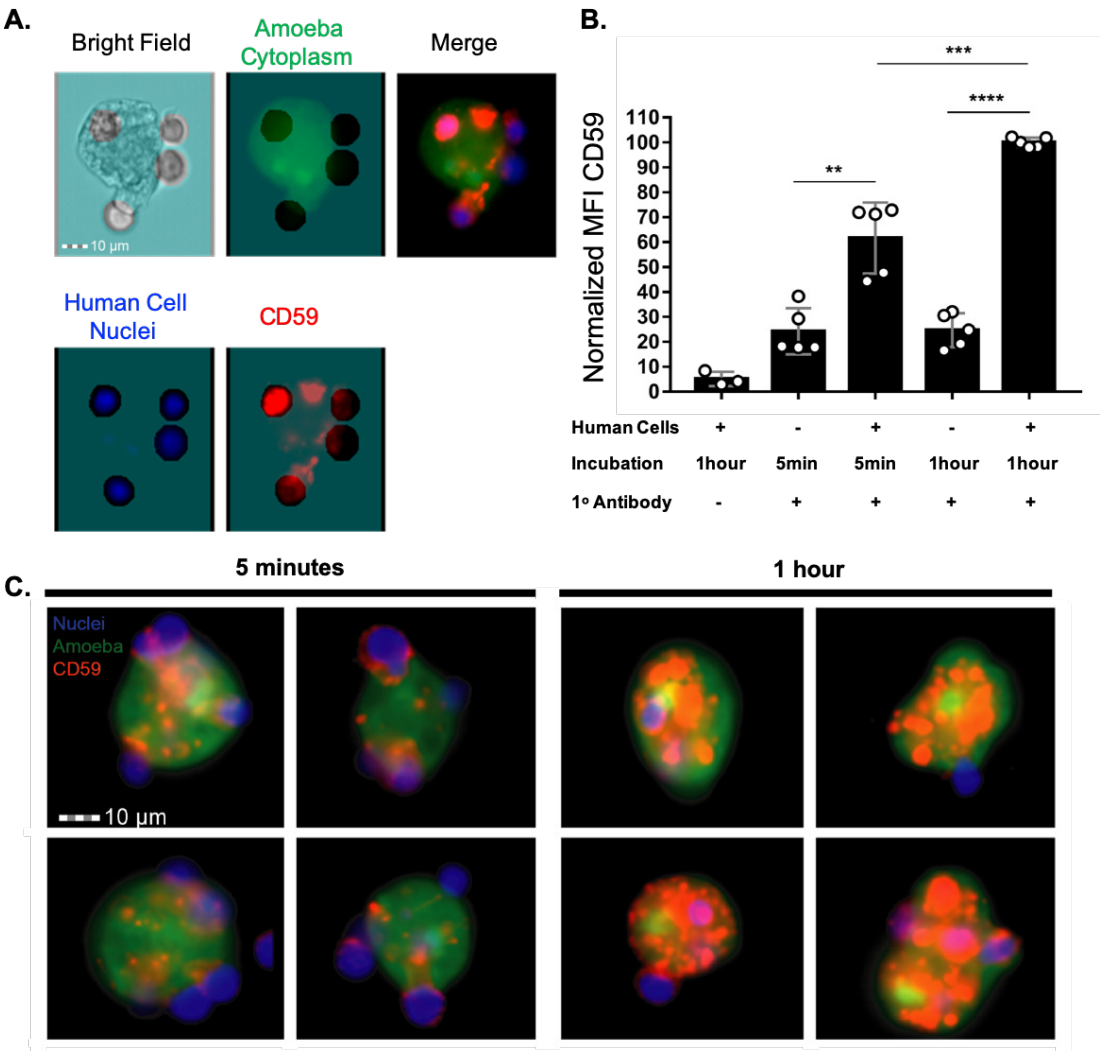

Fig. 3.5: The amount of displayed CD59 increases with increased trogocytosis of human cells. Acquired CD59 molecules were quantified on amoebae that were allowed to perform trogocytosis on human Jurkat T cells for 5 minutes or 1 hour, or were incubated in the absence of Jurkat cells. **(A)** Masking strategy for analysis of displayed CD59 on the amoeba surface. A mask was created in order to allow for the detection of CD59 that overlapped with amoebae, while excluding CD59 on intact human cells attached to amoebae. The mask is displayed in turquoise, as an overlay on the individual images. Amoebae were labeled with CMFDA (green), human cell nuclei were labeled with Hoechst (blue), and CD59 was detected with a monoclonal antibody (red). Extracellular human cell nuclei fluorescence was removed from the masked analysis area. The excluded area around human cell nuclei was then dilated by 4 pixels to include the entire diameter of the intact extra-cellular human cells and associated CD59. CD59 was analyzed in the remaining masked analysis area of each image to allow for analysis of displayed patches of acquired CD59 on amoebae. **(B)** The normalized mean fluorescence intensity of CD59 on amoebae after 5 minutes or 1 hour of trogocytosis or amoebae that were incubated in the absence of Jurkat cells. To normalize the data, samples were normalized to the 1 hour of trogocytosis condition. **(C)** Representative images of amoebae that had performed trogocytosis on human Jurkat T cells for 5 minutes or 1 hour. Arrows indicate displayed CD59. Data were analyzed by imaging flow cytometry and are from 5 replicates across 3 independent experiments. The no primary control condition was performed in 2 of 3 independent experiments and data are from 3 replicates.

of human cell nuclei was used to differentiate intact, extracellular human cells from patches of human proteins displayed on amoebae. Patches of displayed human CD59 were detected on amoebae that had performed trogocytosis, on amoebae that were incubated in the absence of Jurkat cells **(Fig. 3.5A-C, S3.5)**. Amoebae had ~38% more displayed CD59 after one hour of trogocytosis than after five minutes **(Fig. 3.5B)**. These findings indicate that amoebae acquired and displayed CD59 within five minutes of trogocytosis, and the quantity of displayed CD59 increased over time.

To determine if more than one complement regulatory protein was displayed by amoebae after trogocytosis, immunofluorescence was used to detect human CD46. CD46 (membrane cofactor protein) is expressed by human Jurkat cells (24) and acts as a co-factor for serum factor I, which cleaves and inactivates complement components C3b and C4b (25–27). After amoebae had performed trogocytosis, patches of CD46 were detected on the amoeba surface within five minutes **(Fig. S3.6).** Thus, amoebae acquire and display multiple complement regulatory proteins, after performing trogocytosis of human cells.

Removal of GPI-anchored surface proteins trends towards restoring complement lysis of amoebae.

We next sought to test the effect of removing complement regulatory proteins on conferred protection. CD59 is a glycosylphosphatidylinositol (GPI) anchored protein that can be cleaved with the enzyme phosphatidylinositol-specific phospholipase C (PI-PLC) (17, 18, 20, 22). In addition to removing CD59, treatment with PI-PLC also cleaves the

GPI-anchored complement regulatory protein CD55 (decay-accelerating factor) (28, 29). CD55 is expressed by both Jurkat cells and human red blood cells (19, 30) and accelerates the decay of C3 and C5 convertases of the classical and alternative complement pathways (30, 31). Amoebae were allowed to perform trogocytosis or incubated in the absence of Jurkat cells, and then treated with PI-PLC before exposure to human serum. Heat-inactivated PI-PLC was used as a control. PI-PLC treatment appeared to reduce amoebic protection from complement lysis **(Fig. S3.7, S3.8A)**. However, this difference was not statistically significant. This is likely to be due to the higher levels of variability in this assay, which were due to the prolonged incubation of amoebae on ice during PI-PLC treatment. Indeed, due to the incubation on ice, the background level of amoeba cell death was much higher than usual. These findings suggested that removal of all GPI-anchored proteins reduces amoebic protection from complement lysis, but did not prove a causal relationship.

Removal of CD59 and CD46 is not sufficient to sensitize amoebae to complement lysis.

Due to the higher levels of variability that we observed with PI-PLC treatment, we next used human cell mutants to test whether individual proteins were required for protection from complement lysis. We tested the requirements for CD59 and CD46. In order to determine if acquisition and display of human CD59 or CD46 molecules was required for protection from complement, we used CRISPR/Cas9 to create human cell knockout mutants that lacked these proteins. Sanger sequencing **(Fig. S3.9)** and

antibody staining of CD59 **(Fig. 3.6A-B)** and CD46 **(Fig. 3.6C-D)** showed that knockout mutants were successfully generated. Amoebae that were allowed to perform trogocytosis on control human cells or cells that lacked either CD59 or CD46 were equally protected from complement lysis **(Fig. 3.6E, S3.8)**. Additionally, there was no

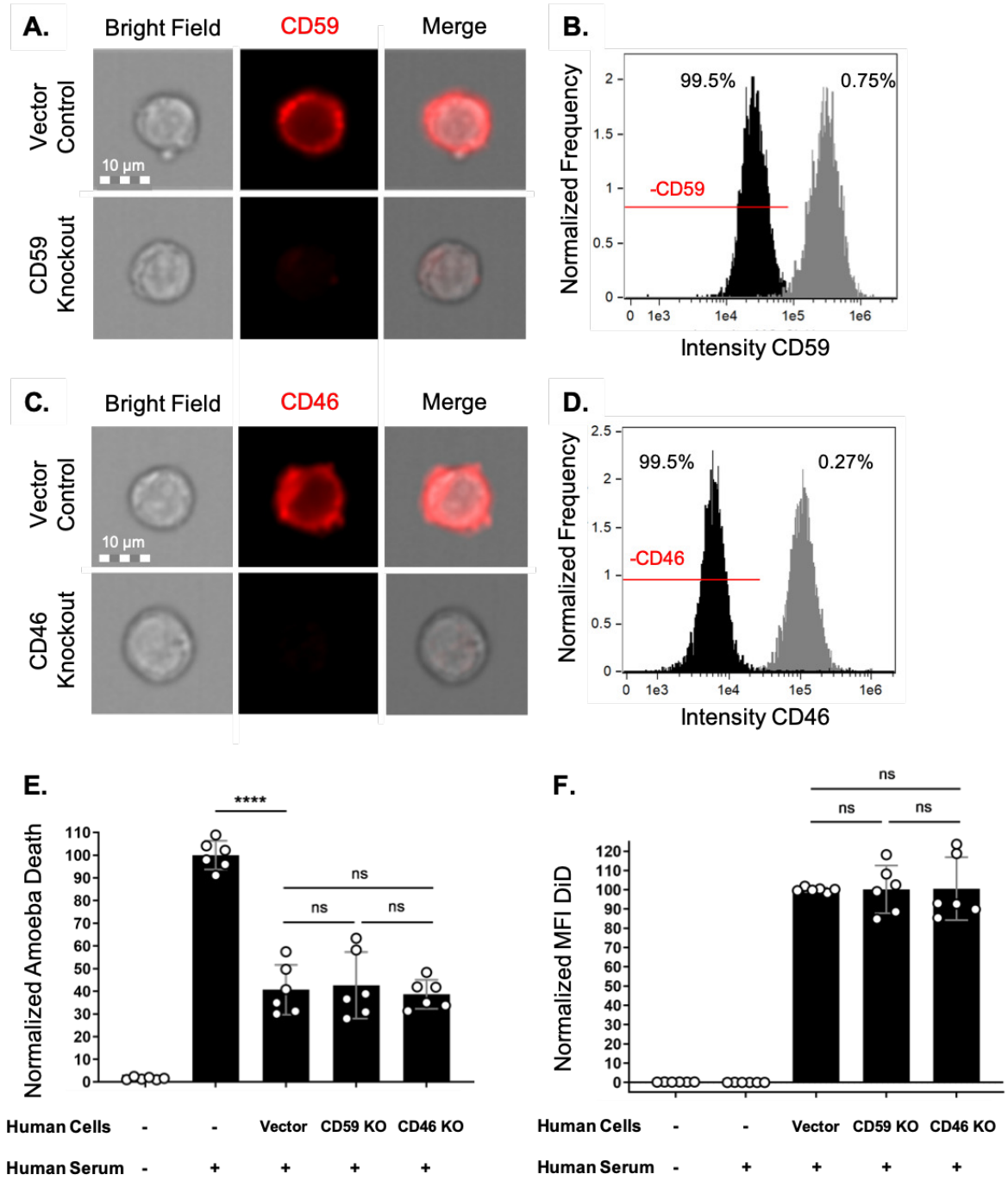

Fig. 3.6: Removal of CD59 and CD46 is not sufficient to sensitize amoebae to complement lysis. **(A-D)** Human Jurkat T cells deficient in CD59 or CD46 were constructed using CRISPR/Cas9. Immunofluorescence and imaging flow cytometry were used to quantify CD59 or CD46. **(A)** Representative images of CD59 antibody staining (red) in vector control human cells or CD59 mutants. **(B)** Intensity of CD59 antibody staining in vector control human cells (gray) or CD59 mutants (black). 99.5% of CD59 mutants were in the CD59-negative gate ("-CD59"), while 0.75% of vector control cells were in this gate. **(C)** Representative images of CD46 antibody staining (red) in vector control human cells or CD46 mutants. **(D)** Intensity of CD46 antibody staining in vector control human cells (gray) or CD46 mutants (black). 99.5% of CD46 mutants were in the CD46-negative gate ("-CD46"), while 0.27% of vector control cells were in this gate. **(E-F)** Amoebae were labeled with CMFDA cytoplasm dye and incubated in the absence of Jurkat cells or with Jurkat cells. Human cell lines were either vector control cells, CD59 KO mutants, or CD46 KO mutants. Human cells were labeled with DiD membrane dye. Following exposure to human serum, amoeba death was assessed with Zombie Violet viability dye and ingested human cell material was determined by quantifying mean fluorescence intensity (MFI) of DiD present on amoebae. **(E)** Normalized death of amoebae. **(F)** Normalized mean fluorescence intensity of DiD on amoebae. Data were analyzed by imaging flow cytometry and are from 6 replicates across 3 independent experiments.

difference in the amount of ingested human cell material **(Fig. 3.6F)**. These findings reveal that removal of either CD59 or CD46 individually is not sufficient to sensitize amoebae to complement lysis. Furthermore, they hint at redundancy in the mechanism of protection and that amoebae likely acquire and display multiple complement regulatory proteins from the cells they ingest.

Display of CD46 or CD55 is sufficient to protect amoebae from complement lysis.

To ask if display of human complement regulatory proteins was sufficient to protect amoebae from lysis, we created amoebae that exogenously expressed either human CD46 or CD55 **(Fig. 3.7, S3.2A).** Expression of CD46 or CD55 was detectable with RT-PCR analysis **(Fig. 3.7A).** Immunofluorescence analysis showed that CD46 or CD55 proteins were surface-localized in amoebae, as they were detected with antibody staining of non-permeabilized cells **(Fig. 3.7B-J, S3.2A).** Localization of the *E. histolytica* surface Gal/GalNAc lectin was used as a control **(Fig. 3.7D, 3.7G, 3.7J),** and

all transfected amoebae had equivalent amounts of Gal/GalNAc lectin. CD46 or CD55 expression was at a relatively low level **(Fig. 3.7B-C, 3.7E-F),** just above background

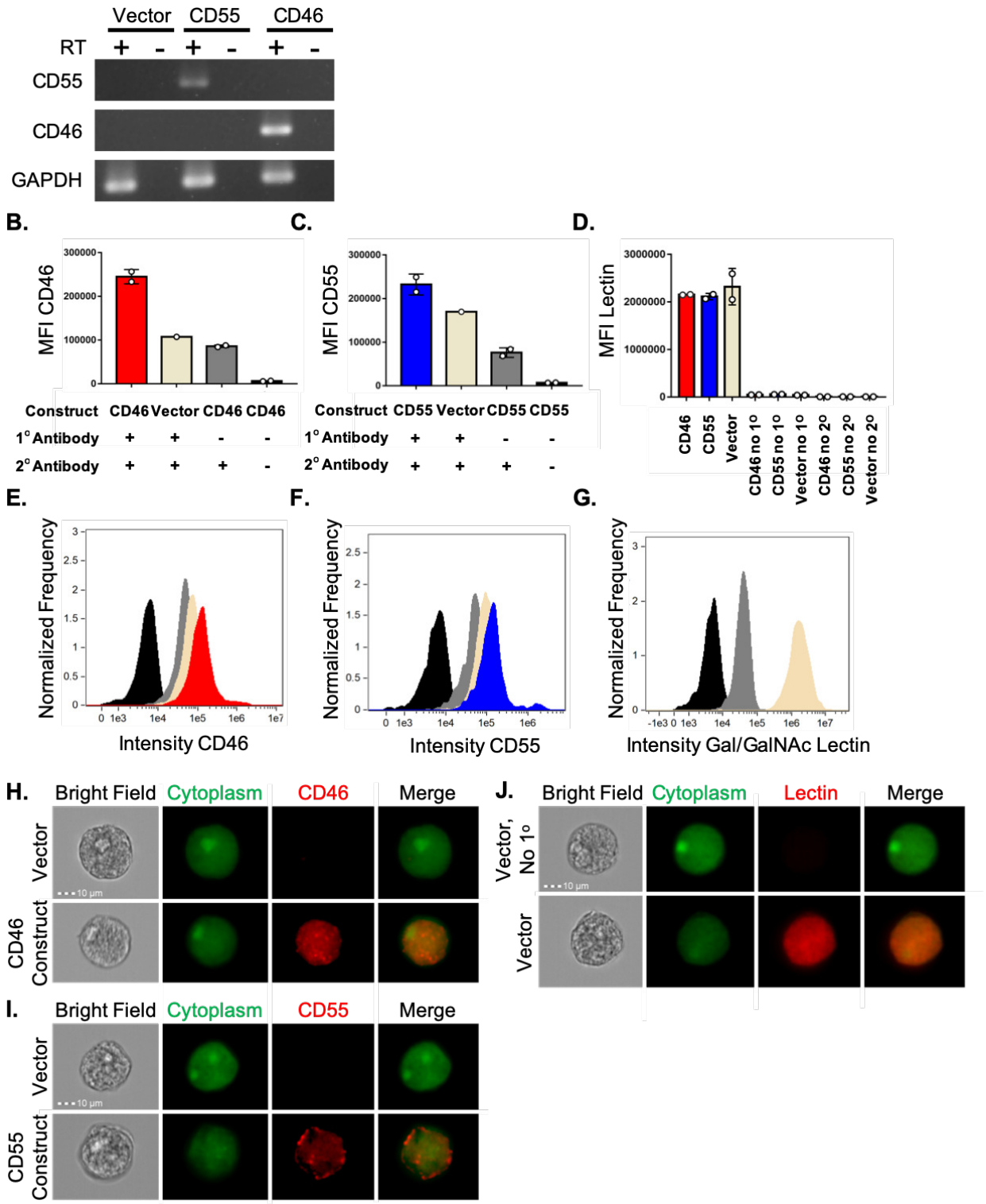

Figure 3.7: Amoebae transfected with expression plasmids display human CD46 or CD55. Amoebae were transfected with expression constructs for human CD46 or human CD55, or the expression plasmid backbone as a negative control. **(A)** RT-PCR analysis with primers specific for human CD46, human CD55, or amoebic GAPDH. Samples were incubated with or without reverse transcriptase (RT +/-), to control for DNA contamination. **(B-J)** Amoebae were labeled with a cytoplasmic dye (CMFDA) and immunofluorescence was performed without permeabilization. **(B)** Mean fluorescence intensity of human CD46 antibody staining. Amoebae were stably transfected with a plasmid for expression of human CD46 (red) or vector backbone (beige), and were stained using a CD46 primary antibody and a far red secondary antibody. Amoebae expressing human CD46 were also incubated without primary antibody (grey), or without any antibodies (black). **(C)** Mean fluorescence intensity of human CD55 antibody staining. Amoebae were stably transfected with a plasmid for expression of human CD55 (blue) or vector backbone (beige), and were stained using a CD46 primary antibody and a far red secondary antibody. Amoebae expressing human CD55 were also incubated without primary antibody (grey), or without any antibodies (black). **(D)** Mean fluorescence intensity of amoebic Gal/GalNAc lectin antibody staining. Amoebae were stably transfected with a plasmid for expression of human CD46 (red), or human CD55 (blue), or vector backbone (beige), and were stained using a Gal/GalNAc lectin primary antibody and a far red secondary antibody. Amoebae were also incubated without primary antibody, or without any antibodies. **(E-G)** Histograms corresponding to the mean fluorescence intensity data shown in panels B-D. Panel G shows antibody staining of vector control amoebae, stained with both antibodies (beige), without primary antibody (grey), or without any antibodies (black). (H-J) Representative images corresponding to the analysis shown in panels B-G. Data shown in panel A are representative of two replicates. Data shown in panels B-J were analyzed by imaging flow cytometry are from 3-4 replicates across 2 independent experiments; the data from one independent experiment are shown.

fluorescence of vector control amoebae. Additionally, CD46 or CD55 expression was markedly lower than the expression level of the Gal/GalNAc lectin **(Fig. 3.7D, 3.7G).** When exposed to human serum, amoebae that expressed human CD46 or CD55 were more protected from lysis than vector control amoebae **(Fig. 3.8, S3.8B)**. Therefore, display of a single complement regulatory protein is sufficient to protect amoebae from complement lysis.

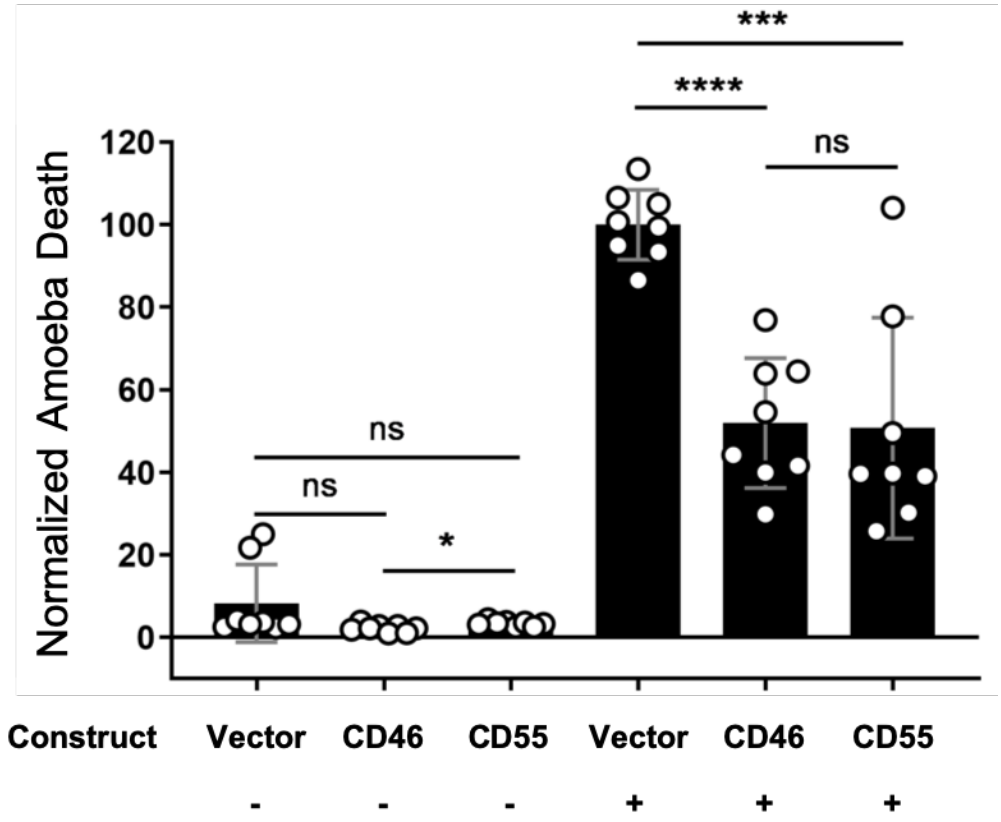

Figure 8: Display of human CD46 or CD55 is sufficient to protect amoebae from complement lysis. Amoebae were stably transfected with CD46 or CD55 expression constructs, or vector backbone. Following exposure to either media or human serum, amoeba viability was assessed using Zombie Violet viability dye and imaging flow cytometry. Amoebic death was normalized to vector control amoebae that were incubated with human serum. These data are from 8 replicates across 4 independent experiments.

Discussion

Our findings reveal that amoebae are protected from complement lysis through trogocytosis of human cells and that trogocytosis leads to less deposited C3b on the amoeba surface. Amoebae acquire protection from both human Jurkat cells as well as primary red blood cells and conferred protection is proportional to the amount of ingested human cell material. Trogocytosis of human cells results in the display of the complement regulatory protein CD59 on the amoebae surface. Finally, although removal of the individual complement regulatory proteins, CD59 or CD46 was not sufficient to sensitize amoebae to complement lysis, the display of an individual complement regulatory protein, CD46 or CD55, was sufficient to protect amoebae from complement lysis.

Many studies have shown that cancer cells overexpress complement regulatory molecules, allowing them to evade complement lysis. However, it should be noted that expression levels vary widely between cell types and between individual studies (32). Removal of GPI-anchored proteins, which include the complement regulatory proteins CD59 and CD55 but not CD46, with PI-PLC treatment resulted in enhanced susceptibility of cancer cells to complement lysis (28, 29). This is consistent with our finding that PI-PLC treated amoebae that had undergone trogocytosis of human cells, and been made resistant to complement, became more sensitive to complement lysis. Treatment with PI-PLC removes other GPI-anchored proteins in addition to CD59 and CD55, so we cannot rule out the possibility that loss of other membrane proteins contributed to the loss of complement resistance in our PI-PLC treated amoebae.

Amoebae that were engineered to express complement regulatory proteins became protected from lysis by human complement. We were unable to express human CD59 in amoebae, as although stably transfected amoebae with a CD59 expression construct were successfully recovered, these transfectants grew slowly and could not be maintained over time. While CD59 expression was detectable by RT-PCR, it is possible that the CD59 protein mis-localized in amoebae, or otherwise led to deleterious effects. CD46 and CD55 were each appropriately localized to the amoeba cell surface, as evidenced by immunofluorescence staining, and by the functional protection from complement lysis that they conferred. Notably, CD46 and CD55 were not greatly overexpressed in amoebae. When using immunofluorescence, CD46 and CD55 staining levels were just above the background levels of fluorescence seen in vector control amoebae. Thus, these proteins led to protection from complement lysis without dramatically high levels of expression. Only a single complement regulator at a low expression level was needed for protection from lysis by complement. These findings fit with the generally relatively low endogenous expression levels of complement regulatory proteins in human cells, in that low levels of these proteins are sufficient to inhibit the complement pathway.

There have been several studies that examined the efficacy of using blocking antibodies against complement regulatory proteins to enhance lysis of cancer cells. Results from blocking individual proteins have been highly variable in different cell types but blocking one or more proteins was effective in many cases. Using antibodies against CD46 was rarely effective, however antibodies against CD59 and CD55 often

were effective in enhancing complement lysis (32). Additionally, there appears to be an additive effect when multiple proteins are targeted at once. Cervical carcinoma cells were rendered more susceptible to complement after treatment with blocking antibodies to CD59 and CD55, and lysis was increased further when cells were treated with both antibodies (33). Similarly, breast carcinoma cells, were more easily lysed after treatment with anti-CD59 and anti-CD55 antibodies, but a much higher degree of lysis was achieved when a mixture of anti-CD59, anti-CD55, and anti-CD46 antibodies was used (34). Since neither removal of CD46 or CD59 was sufficient to sensitize amoebae to complement lysis, it is possible that amoebic display of multiple different complement regulators enables protection from lysis. In our assays, we used a 1:40 ratio of amoebae to Jurkat cells, a ratio that led to a high level of protection from complement lysis. It is possible that using fewer human cells, to lead to a suboptimal level of protection from complement lysis, might have more sensitively revealed differences in amoebic protection from complement lysis due to subtle perturbations like the loss of individual human complement regulators. While removal of CD46 or CD59 did not sensitize amoebae to complement lysis, these proteins could still contribute to amoebic complement protection, as part of a collection of multiple redundant, complement regulators that protect amoebae from lysis. Indeed, experiments in which amoebae were engineered to express complement regulators showed that display of CD46 or CD55 was sufficient to protect amoebae from lysis, supporting the relevance of these proteins in protecting amoebae that have performed trogocytosis.

Our results support a model whereby amoebae are protected from serum lysis in the blood through trogocytosis of red blood cells they encounter there, and potentially from other cells they encounter before reaching the bloodstream. Amoebae likely acquire and display multiple complement regulatory proteins from the human cells that they ingest, which then leads to less C3b deposition, and protection from complement lysis.

Materials and Methods

Cell culture

E. histolytica trophozoites (HM1:IMSS) from ATCC (amoebae) were cultured as described previously (13, 35). Amoebae were maintained in glass tissue culture tubes at 35°C in TYI-S-33 medium supplemented with 15% heat-inactivated adult bovine serum (Gemini Bio-Products), 2.3% Diamond vitamin Tween 80 solution (40×; Sigma-Aldrich), and 80 U/ml penicillin, 80 μg/ml streptomycin (Gibco). Amoebae were expanded in T25 un-vented tissue culture flasks and harvested when flasks reached 80% confluence. When used in serum lysis or immunofluorescence assays, amoebae were resuspended in M199s medium (Gibco; medium M199 with Earle's salts, L-glutamine, and 2.2 g/liter sodium bicarbonate, without phenol red) supplemented with 0.5% bovine serum albumin (BSA), 25 mM HEPES, and 5.7 mM L-cysteine.

Human Jurkat T cells (clone E6-1) from ATCC were grown in vented T25 tissue culture flasks at 37°C and 5% CO2 as previously described (13). Jurkat cells were cultured in RPMI 1640 medium (Gibco; RPMI 1640 with L-glutamine and without phenol red) supplemented with 10% heat-inactivated fetal bovine serum (Gibco), 100 U/ml penicillin, 100 μg/ml streptomycin, and 10 mM HEPES. Jurkat cells were expanded in T75 vented tissue culture flasks and harvested when cell density reached between 5×10^5 and 2×10^6 cells/ml. Jurkat cells were resuspended in M199s medium for use in serum lysis or immunofluorescence assays.

Single donor human red blood cells separated from whole blood by centrifugation and negative for the presence of human immunodeficiency virus-1 (HIV-1), HIV-2, HIV-1

antigen or HIV-1 nucleic acid test, hepatitis B surface antigen, hepatitis C virus , syphilis, and alanine aminotransferase test were purchased from Innovative Research (Cat# IWB3CPDA1UNIT). Red blood cells were stored at 4°C and resuspended in M199s medium prior to use in serum lysis assays.

DNA constructs

For creation of Jurkat cell CRISPR knockout mutants, guide RNAs (gRNA) to human CD59 or CD46 were cloned into a pX330-U6-Chimeric_BB-CBh-hSpCas9 plasmid backbone (pX330-U6-Chimeric_BB-CBh-hSpCas9 was a gift from Feng Zhang (Addgene plasmid # 42230; http://n2t.net/addgene:42230 ; RRID:Addgene_42230) (36)). Guide RNAs were created by using the sequences designed by Thielen et. al, 2018 (37). The gRNA oligos used are presented in Table 3.1 with BbsI restriction enzyme overhangs shown in bold. Guide RNAs were cloned into the pX330-U6-Chimeric_BB-CBh-hSpCas9 plasmid backbone using a modified version of the Zhang Lab General Cloning Protocol (Addgene http://www.addgene.org/crispr/zhang/). Briefly, the px330 plasmid backbone was digested with BbsI restriction enzyme (FastDigest BpiI: ThermoFisher Scientific). Guide RNA oligos containing BbsI overhangs were then phosphorylated and annealed. Next, annealed oligos were ligated into the pX330 plasmid backbone and NEB 5-alpha Competent *E. coli* were transformed (New England Biolabs). Positive colonies were screened by restriction digest. Plasmids with the correct inserts were confirmed by Sanger sequencing using the “U6” Universal Primer from GENEWIZ (LKO.1 5’) which is located in the human U6 promoter **(Table 3.1)**.

To generate amoebic expression constructs for exogeneous expression of human proteins, the coding regions of human CD46 or CD55 were amplified from human Jurkat cells. Briefly, RNA was extract from Jurat cells using the Direct-zol RNA MiniPrep Plus kit (Zymo Research) and cDNA was prepared. Next, the coding sequences for human CD46 or CD55 were amplified from Jurkat cDNA by PCR using primers described in Table 3.1. The amplified CD46 or CD55 inserts were then cloned into the *E. histolytica* expression plasmid pEhEx backbone (38) using the Gibson Assembly Ultra Kit (VWR). Primers used for Gibson cloning are described in Table 3.1. For creation of the CD46 expression plasmid, both the pEhEx backbone and the CD46 insert were PCR amplified with primers that added 20 base pairs corresponding to the ends of the insert or backbone, respectively. For creation of the CD55 expression plasmid, the pEhEx backbone was digested using XhoI (New England Biolabs) and the CD55 insert was PCR amplified with primers that added 20 base pairs corresponding to the ends of the backbone. NEB 5-alpha Competent *E. coli* were transformed, and positive colonies were screened by restriction digest analysis. Sanger sequencing was used to assess the sequences of the inserts and flanking vector sequences, using primers located in the Cysteine synthase A gene [EHI_024230] 5' and 3' UTR regions **(Table 3.1)**. The CD46 gene insert corresponds to the mRNA transcript variant d (GenBank accession number: NM_153826) and the CD55 gene insert corresponds to mRNA transcript variant 1 (GenBank accession number: NM_000574).

Jurkat T cell CRISPR/Cas9 mutants

Human Jurkat T cells were transfected with pX330 plasmids containing the CD59 gRNA, the CD46 gRNA, or the pX330 backbone as a control. Plasmid DNA was isolated in an endotoxin-free manner (GenElute™ HP Endotoxin-Free Plasmid Maxiprep Kit; Sigma-Aldrich) and concentrated using paramagnetic beads (HighPrep PCR Clean Up System; Magbio). Jurkat T cells were transfected using the Neon Transfection System (Invitrogen) with the 10 μl tip and 24 well plate format. Cells were prepared, and the Neon Transfection System was used according to the manufacturer's instructions. The transfection conditions used were as follows: volts = 1050, width = 30 and pulse # = 2.

When creating the CD59 and CD46 knockout mutants, 1.8 μg of plasmid DNA was used with 1 x 10^5 cells per transfection reaction and two reactions were performed for each plasmid and transferred to 1 well of a 24 well plate. Transfection efficiency was calculated by separately transfecting an enhanced green fluorescent protein (EGFP) expression plasmid pcDNA3-EGFP (pcDNA3-EGFP was a gift from Doug Golenbock (Addgene plasmid # 13031 ; http://n2t.net/addgene:13031 ; RRID:Addgene_13031)) in parallel. Percentage of EGFP expressing cells was calculated after 24 hours by fixing samples with 4% paraformaldehyde (Electron Microscopy Sciences) and analyzing with imaging flow cytometry. To generate CD59 expressing Jurkat cells, 2 μg of plasmid DNA was used with 2 x 10^5 cells per transfection reaction and two reactions were performed for each plasmid and transferred to 1 well of a 24 well plate.

Clonal lines of Jurkat cell mutants were obtained by limiting dilution in 96 well plates. Clonal lines were screened for knockout by labeling with primary mouse

monoclonal antibodies to CD59 (clone MEM-43/5; Abcam) or CD46 (clone C-10; Santa Cruz Biotechnology) and a Cy™5 AffiniPure Goat Anti-Mouse secondary antibody (Jackson ImmunoResearch Laboratories, Inc). Samples were analyzed by imaging flow cytometry. Knockout was confirmed in positive clones by isolating genomic DNA using the Quick-DNA Miniprep kit (Zymo Research) and polymerase chain reaction (PCR) amplifying regions of either CD59 or CD46. Primer sets had been identified in BLAST as specific to these genes **(Table 3.1)**. Next, purified PCR product was sequenced with primers upstream of the predicted CRISPR/Cas9 cut site **(Table 3.1)** and knockout was confirmed.

Characterization of amoebae exogenously expressing human CD46 or CD55

Amoebae were transfected as described previously (13). Briefly, amoebae were transfected with 20 μg of the human CD46 or CD55 expression construct, or the pEhEx plasmid backbone using Attractene transfection reagent (Qiagen). Stable transfectants were initially selected at 3 μg/ml Geneticin (ThermoFisher Scientific), and then maintained at 6 μg/ml Geneticin. Before use in immunofluorescence assays and serum lysis experiments, drug selection was gradually increased from 6 μg/ml to 48 μg/ml Geneticin, to increase plasmid copy number. Amoebae were maintained at 48 μg/ml Geneticin for 24 hours before experiments were performed.

Expression of human CD46 and CD55 was confirmed using RT-PCR analysis of amoebae maintained at 3 μg/ml Geneticin. RNA was extracted using the Direct-zol RNA MiniPrep Plus kit (Zymo Research) and cDNA was made. Primers used for RT-PCR are

shown in Table 3.1. RT-PCR was performed as described (35).

Imaging flow cytometry

To detect human CD59 displayed on amoebae following trogocytosis, Jurkat cells were with labeled Hoechst 33342 dye (Invitrogen) at 5 μg/ml for 30 minutes at 37°C. Amoebae were washed and resuspended in M199s medium and labeled with CellTracker green 5-chloromethylfluorescein diacetate (CMFDA; Invitrogen) at 186 ng/ml for 10 minutes at 35°C. Amoebae and Jurkat cells were then washed and resuspended in M199s medium. Amoebae were resuspended at 4 x 10^5 cells/ml and Jurkat cells were resuspended at 1.6 x 10^7 cells/ ml for a 1:40 amoeba: Jurkat cell ratio. Amoebae and Jurkat cells were co-incubated for either 5 minutes or 1 hour, or amoebae were incubated in the absence of Jurkat cells. Cells were fixed with 4% PFA for 30 minutes at room temperature. Samples were blocked in 1 x PBS containing 0.1% Tween20 (Sigma-Aldrich) (1 x PBST), 5% BSA and 20% Normal Goat Serum (Jackson ImmunoResearch Laboratories, Inc) for 1 hour at room temperature on a rocker. Next, samples were labeled with primary mouse monoclonal antibodies to CD59 (clone MEM-43/5; Abcam) diluted 1:50 in blocking solution at 4°C overnight on a rocker. Samples were washed with 1 x PBST and labeled with a Cy5 AffiniPure Goat Anti-Mouse secondary antibody (Jackson ImmunoResearch Laboratories, Inc) stored in 50% glycerol (Sigma-Aldrich). The secondary antibody was diluted 1:100 in blocking solution, for a final dilution of 1:200, and incubated for 3 hours at room temperature on a rocker. Lastly, samples were washed with 1 x PBST, resuspended in 50 μl 1 x PBS, and run on

an Amnis ImageStreamX Mark II. 10,000 events were collected for conditions where amoebae were incubated in the absence of Jurkat cells and 100,000 events were collected for conditions where amoebae were incubated with Jurkat cells. Data are from 5 replicates across 3 independent experiments. The no primary control condition was performed in 2 of 3 independent experiments and data are from 3 replicates. See Figure S3.5 for the analysis gating scheme.

To detect human CD46 displayed on amoebae following trogocytosis, amoebae and Jurkat cells were labeled in the same manner as for detection of CD59. Amoebae and Jurkat cells were co-incubated for 5 minutes or amoebae were incubated in the absence of Jurkat cells. Samples were labeled with a primary mouse monoclonal antibody to human CD46 (Clone C-10; Santa Cruz Biotechnology) at a 1:10 dilution, followed by a Cy5 AffiniPure Goat Anti-Mouse secondary antibody (Jackson ImmunoResearch Laboratories, Inc). Amoebae were gated on by size and 10,000 events were collected per sample. Data are from 2 replicates and 1 independent experiment.

For detection of CD46, CD55, or Gal/GalNAc lectin expression on amoebae exogenously expressing CD46 or CD55, amoebae were labeled with CMFDA and prepared in the same manner as for detection of displayed human CD59. Following fixation, samples were blocked overnight at 4°C on a rocker. Samples were then labeled with primary mouse monoclonal antibodies to human CD46 (Clone C-10; Santa Cruz Biotechnology) human CD55 (Clone NaM16-4D3; Santa Cruz Biotechnology) or the *E. histolytica* Gal/GalNAc lectin (Clone 7F4; the Gal/GalNAc lectin antibody was a gift from

William A. Petri, Jr., University of Virginia (39)) overnight at 4°C on a rocker. The CD46 and CD55 primary antibodies were diluted 1:10 and the Gal/GalNAc lectin primary antibody was diluted 1:50 in blocking solution. Samples were labeled with secondary antibody as described above. Amoebae were gated on by size and 10,000 events were collect per sample. Data are from 3-4 replicates from 2 independent experiments. See Figure S3.2a for the analysis gating scheme.

Confocal microscopy

To detect displayed CD59 on the amoeba surface after trogocytosis, cells were labeled for confocal microscopy as described previously (13). Amoebae were prepared in the same manner as the for the detection of displayed CD59 using imaging flow cytometry (above) with an approximate fourfold increased concentration of CMFDA. After labeling with antibodies, samples were mounted using Vectashield (Vector Laboratories) on Superfrost Plus microslides (VWR) with glass coverslips. Slides were imaged on an Intelligent Imaging Innovations hybrid Spinning Disk Confocal-TIRF-Widefield Microscope. 136 Images were collected from 1 independent experiment. FIJI software was used for image analysis (40).

For detection of displayed biotinylated human cell membrane proteins, amoebae were left unstained in some experiments or labeled with CMFDA as described above. Human Jurkat cells were biotinylated as described previously (13). Briefly, Jurkat cells were biotinylated with EZ-Link Sulfo-NHS-SS-Biotin (ThermoFisher Scientific) at 480 μg/ml in 1× PBS for 25 min at 4°C. The reaction was quenched using 100 mM Tris-

HCl (pH 8) and washed with washed in 100 mM Tris-HCl (pH 8) before being resuspending M199s medium. Amoebae were incubated with biotinylated Jurkat cells at a 1:5 ratio for 2 - 5 minutes and then immediately placed on ice. Next, samples were stained with Alexa Fluor 633 conjugated streptavidin (Invitrogen) at 20 μg/ml for 1 hour at 4°C, prior to fixation with 4% paraformaldehyde for 30 minutes at room temperature. In some experiments, samples were labeled with DAPI (4′,6-diamidino-2-phenylindole; Sigma-Aldrich) for 10 minutes at room temperature following fixation. Samples were mounted on either poly-lysine (Sigma-Aldrich) or collagen (collagen I, rat tail; Gibco) coated coverslips for 1 hour. Samples were mounted with Vectashield on glass slides, and slides were imaged on an Olympus FV1000 laser point-scanning confocal microscope.

Serum lysis assays

For experiments where amoebae were incubated with increasing numbers of Jurkat cells, amoebae were washed and resuspended in M199s medium and labeled with CMFDA at 186 ng/ml for 10 minutes at 35°C. Jurkat cells were washed and labeled in M199s with DiD at 21 μg/ml for 5 minutes at 37°C and 10 minutes at 4°C. Amoebae were washed and resuspended at 4 x 10^5 cells/ml. Jurkat cells were washed a resuspended at 2 x 10^6 cells/ml, 4 x 10^6 cells/ml, 8 x 10^6 cells/ml and 1.6 x 10^7 cells/ml. Amoebae were incubated in the absence of Jurkat cells or the presence of Jurkat cells at a 1:5, 1:10, 1:20, and 1:40 ratio for 1 hour at 35°C. Next, samples were resuspended in 100% normal human serum (pooled normal human complement serum; Innovative

Research Inc.) supplemented with 150 μM $CaCl_2$ and 150 μM $MgCl_2$ for 30 minutes at 35°C as described previously (13). Following exposure to human serum, samples were resuspended in M199s medium and labeled using Zombie Violet Fixable Viability dye (BioLegend), prepared according to the manufacturer's instructions, at a concentration of 4 μl/ml for 30 minutes on ice. Next, samples were fixed with 4% PFA at room temperature for 30 minutes. Samples were then resuspended in 50 μl 1 x PBS, and run on an Amnis ImageStreamX Mark II. 10,000 events were collected for samples where amoebae were incubated in the absence of Jurkat cells or with Jurkat cells at a 1:5 ratio. 10,00 – 20,000 events were collected for samples with Jurkat cells at a 1:10 ratio, 10,00 - 40,000 events were collected for samples with a 1:20 ratio, and 50,000 - 80,000 events for samples with a 1:40 ratio. Data are from 6 replicates across 3 independent experiments. See Figure S3.2 for the analysis gating scheme.

For experiments with CD59 and CD46 knockout mutants, the serum lysis assay used was the same as described above, except only a 1:40 ratio of amoebae to Jurkat cells was used, instead of multiple different ratios. Amoebae were incubated in the absence of Jurkat cells, in the presence of Jurkat cells transfected with the px330 vector control, or with either CD59 or CD46 knockout Jurkat cell mutants at a 1:40 ratio. Cells were gated on by size and 10,000 events from the amoebae that were incubated in the absence of Jurkat cells and 100,000 events from the amoebae incubated with Jurkat cells were collected. Data are from 6 replicates across 3 independent experiments. See Figure S3.8a for the analysis gating scheme.

In experiments where samples were treated with phospholipase C, the assay was performed as described above with the addition of a treatment step preceding exposure to serum. Only a 1:40 ratio of amoebae to Jurkat cells was used, instead of multiple different ratios. Following coincubation of amoebae and Jurkat cells, samples were immediately placed on ice and resuspended in ice-cold M199s medium. Samples were treated with either 500 mU of Phospholipase C (PI-PLC) (Phospholipase C, Phosphatidylinositol-specific from *Bacillus cereus*; Sigma-Aldrich) prepared according to the manufacturer's instructions, or 500 mU heat-inactivated PI-PLC. PI-PLC was heat-inactivated at 95°C for 30 minutes. PI-PLC was carried out on ice, on a rocker, in a 4°C cold room for 30 minutes. Cells were gated on by size and 10,000 events from the amoebae incubated in the absence of Jurkat cells and 100,000 events from the amoebae incubated with Jurkat cells were collected. Data are from 8 replicates across 4 independent experiments. The untreated control condition was performed 3 of 4 independent experiments and data are from 6 replicates. See Figure S3.8a for the analysis gating scheme.

For experiments where amoebae were incubated with increasing numbers of red blood cells, amoebae were incubated with red blood cells resuspended at 4×10^6 cells/ml, 4×10^7 cells/ml, and 4×10^8 cells/ml for a 1:10, 1:100, and 1:1000 amoebae to red blood cell ratio. The amoeba population was gated on by size and 10,000 amoeba events were collected for samples where amoebae were incubated in the absence of red blood cells or with red blood cells at a 1:10 ratio, a 1:100 ratio. 100,000 events were collected for amoebae incubated with red blood cells at a 1:1000 ratio. Data are from 6

replicates from 3 independent experiments. See Figure S3.2b for the analysis gating scheme.

For C3b experiments, amoebae were labeled with CMFDA and Jurkat cells were left unlabeled. Amoebae and Jurkats were incubated together at a 1:40 amoebae: Jurkat ratio. After fixation, samples were blocked in 1 x PBST containing 5% BSA and 20% Normal Goat Serum for 30 minutes at room temperature on a rocker. Samples were then labeled with a mouse monoclonal antibody to complement components C3b and iC3b (Clone 3E7; Sigma-Aldrich) diluted 1:100 in blocking solution at 4°C overnight on a rocker. Samples were washed in 1 x PBST and labeled with an Alexa Fluor 47 AffiniPure Fab Fragment Donkey Anti-Mouse secondary antibody (Jackson ImmunoResearch Laboratories, Inc) stored in 50% glycerol (Sigma-Aldrich). The secondary antibody was diluted 1:100 in blocking solution for a final dilution of 1:200, and samples were incubated for 3 hours at room temperature on a rocker. Samples were washed in 1 x PBST, resuspended in 50 μl 1 x PBS, and run on an Amnis ImageStreamX Mark II. 10,000 events were collected in samples where amoebae were incubated in the absence of Jurkat cells and 100,000 events were collected in samples where amoebae were incubated with Jurkat cells. Data are from 6 replicates across 3 independent experiments. See Figure S3.3 for the analysis gating scheme.

For latex bead ingestion experiments, amoebae were left unstained and incubated with either $3x10^6$ or $1.5x10^7$ fluorescent red carboxylate-modified polystyrene 2.0 µm latex beads (Sigma-Aldrich) or incubated in the absence of latex beads. Amoebae were gated on by size and 10,000 events were collected per sample. Data

are from 4 replicates across 2 independent experiments. See Figure S3.1 for the gating scheme used for analysis.

For experiments with amoebae exogenously expressing human CD46 or CD55, amoebae or vector control amoebae were labeled with CMFDA. Amoebae were either treated with M199s medium or exposed to human serum as described above. After gating on amoebae by size, 10,000 events were collected per sample. Data are from 8 replicates across 4 independent experiments. See Figure S3.8b for the gating scheme used for analysis.

Statistical analysis

GraphPad Prism software was used to perform all statistical analyses and the means and standard deviation values are displayed on all data plots. Analyses were done using a Student's unpaired t test (no significant difference was indicated by a P of >0.05; *, $P \leq 0.05$; **, $P \leq 0.01$; ***, $P \leq 0.001$; ****, $P \leq 0.0001$).

Acknowledgments

We thank Dr. Scott Dawson, Dr. Stephen McSorley, and the members of our laboratory for helpful discussions. All ImageStream and confocal data were acquired using shared instrumentation in the UC Davis MCB Light Microscopy Imaging Facility. We thank Dr. Michael Paddy for technical support in the use of these instruments. T.S.Y.T. was funded by the Khaira Family Experiential Learning Award through the UC Davis College of Biological Sciences. This work was funded by NIH grant AI146914 and a Pew Scholarship awarded to K.S.R.

Author Contributions

H.W.M. designed, performed, and analyzed the experiments. T.S.Y.T. created and characterized amoebae exogenously expressing complement regulatory proteins. K.S.R. conceived of the overall approach and oversaw the design and analysis of the experiments. H.W.M. and K.S.R. wrote the manuscript.

References

1. Wang H, Naghavi M, Allen C, Barber RM, Bhutta ZA, Carter A, Casey DC, Charlson FJ, Chen AZ, Coates MM, Coggeshall M, Dandona L, Dicker DJ, Erskine HE, Ferrari AJ, Fitzmaurice C, Foreman K, Forouzanfar MH, Fraser MS, Fullman N, Gething PW, Goldberg EM, Graetz N, Haagsma JA, Hay SI, Huynh C, Johnson CO, Kassebaum NJ, Kinfu Y, Kulikoff XR, Kutz M, Kyu HH, Larson HJ, Leung J, Liang X, Lim SS, Lind M, Lozano R, Marquez N, Mensah GA, Mikesell J, Mokdad AH, Mooney MD, Nguyen G, Nsoesie E, Pigott DM, Pinho C, Roth GA, Salomon JA, Sandar L, Silpakit N, Sligar A, Sorensen RJD, Stanaway J, Steiner C, Teeple S, Thomas BA, Troeger C, VanderZanden A, Vollset SE, Wanga V, Whiteford HA, Wolock T, Zoeckler L, Abate KH, Abbafati C, Abbas KM, Abd-Allah F, Abera SF, Abreu DMX, Abu-Raddad LJ, Abyu GY, Achoki T, Adelekan AL, Ademi Z, Adou AK, Adsuar JC, Afanvi KA, Afshin A, Agardh EE, Agarwal A, Agrawal A, Kiadaliri AA, Ajala ON, Akanda AS, Akinyemi RO, Akinyemiju TF, Akseer N, Lami FHA, Alabed S, Al-Aly Z, Alam K, Alam NKM, Alasfoor D, Aldhahri SF, Aldridge RW, Alegretti MA, Aleman AV, Alemu ZA, Alexander LT, Alhabib S, Ali R, Alkerwi A, Alla F, Allebeck P, Al-Raddadi R, Alsharif U, Altirkawi KA, Martin EA, Alvis-Guzman N, Amare AT, Amegah AK, Ameh EA, Amini H, Ammar W, Amrock SM, Andersen HH, Anderson BO, Anderson GM, Antonio CAT, Aregay AF, Ärnlöv J, Arsenijevic VSA, Artaman A, Asayesh H, Asghar RJ, Atique S, Avokpaho EFGA, Awasthi A, Azzopardi P, Bacha U, Badawi A, Bahit MC, Balakrishnan K, Banerjee A, Barac A, Barker-Collo SL, Bärnighausen T, Barregard L, Barrero LH, Basu A, Basu S, Bayou YT, Bazargan-Hejazi S, Beardsley J, Bedi N, Beghi E, Belay HA, Bell

B, Bell ML, Bello AK, Bennett DA, Bensenor IM, Berhane A, Bernabé E, Betsu BD, Beyene AS, Bhala N, Bhalla A, Biadgilign S, Bikbov B, Abdulhak AAB, Biroscak BJ, Biryukov S, Bjertness E, Blore JD, Blosser CD, Bohensky MA, Borschmann R, Bose D, Bourne RRA, Brainin M, Brayne CEG, Brazinova A, Breitborde NJK, Brenner H, Brewer JD, Brown A, Brown J, Brugha TS, Buckle GC, Butt ZA, Calabria B, Campos-Nonato IR, Campuzano JC, Carapetis JR, Cárdenas R, Carpenter DO, Carrero JJ, Castañeda-Orjuela CA, Rivas JC, Catalá-López F, Cavalleri F, Cercy K, Cerda J, Chen W, Chew A, Chiang PP-C, Chibalabala M, Chibueze CE, Chimed-Ochir O, Chisumpa VH, Choi J-YJ, Chowdhury R, Christensen H, Christopher DJ, Ciobanu LG, Cirillo M, Cohen AJ, Colistro V, Colomar M, Colquhoun SM, Cooper C, Cooper LT, Cortinovis M, Cowie BC, Crump JA, Damsere-Derry J, Danawi H, Dandona R, Daoud F, Darby SC, Dargan PI, das Neves J, Davey G, Davis AC, Davitoiu DV, de Castro EF, de Jager P, Leo DD, Degenhardt L, Dellavalle RP, Deribe K, Deribew A, Dharmaratne SD, Dhillon PK, Diaz-Torné C, Ding EL, dos Santos KPB, Dossou E, Driscoll TR, Duan L, Dubey M, Duncan BB, Ellenbogen RG, Ellingsen CL, Elyazar I, Endries AY, Ermakov SP, Eshrati B, Esteghamati A, Estep K, Faghmous IDA, Fahimi S, Faraon EJA, Farid TA, Farinha CS e S, Faro A, Farvid MS, Farzadfar F, Feigin VL, Fereshtehnejad S-M, Fernandes JG, Fernandes JC, Fischer F, Fitchett JRA, Flaxman A, Foigt N, Fowkes FGR, Franca EB, Franklin RC, Friedman J, Frostad J, Fürst T, Futran ND, Gall SL, Gambashidze K, Gamkrelidze A, Ganguly P, Gankpé FG, Gebre T, Gebrehiwot TT, Gebremedhin AT, Gebru AA, Geleijnse JM, Gessner BD, Ghoshal AG, Gibney KB, Gillum RF, Gilmour S, Giref AZ, Giroud M, Gishu MD, Giussani G, Glaser E, Godwin WW, Gomez-Dantes H,

Gona P, Goodridge A, Gopalani SV, Gosselin RA, Gotay CC, Goto A, Gouda HN, Greaves F, Gugnani HC, Gupta R, Gupta R, Gupta V, Gutiérrez RA, Hafezi-Nejad N, Haile D, Hailu AD, Hailu GB, Halasa YA, Hamadeh RR, Hamidi S, Hancock J, Handal AJ, Hankey GJ, Hao Y, Harb HL, Harikrishnan S, Haro JM, Havmoeller R, Heckbert SR, Heredia-Pi IB, Heydarpour P, Hilderink HBM, Hoek HW, Hogg RS, Horino M, Horita N, Hosgood HD, Hotez PJ, Hoy DG, Hsairi M, Htet AS, Htike MMT, Hu G, Huang C, Huang H, Huiart L, Husseini A, Huybrechts I, Huynh G, Iburg KM, Innos K, Inoue M, Iyer VJ, Jacobs TA, Jacobsen KH, Jahanmehr N, Jakovljevic MB, James P, Javanbakht M, Jayaraman SP, Jayatilleke AU, Jeemon P, Jensen PN, Jha V, Jiang G, Jiang Y, Jibat T, Jimenez-Corona A, Jonas JB, Joshi TK, Kabir Z, Kamal R, Kan H, Kant S, Karch A, Karema CK, Karimkhani C, Karletsos D, Karthikeyan G, Kasaeian A, Katibeh M, Kaul A, Kawakami N, Kayibanda JF, Keiyoro PN, Kemmer L, Kemp AH, Kengne AP, Keren A, Kereselidze M, Kesavachandran CN, Khader YS, Khalil IA, Khan AR, Khan EA, Khang Y-H, Khera S, Khoja TAM, Kieling C, Kim D, Kim YJ, Kissela BM, Kissoon N, Knibbs LD, Knudsen AK, Kokubo Y, Kolte D, Kopec JA, Kosen S, Koul PA, Koyanagi A, Krog NH, Defo BK, Bicer BK, Kudom AA, Kuipers EJ, Kulkarni VS, Kumar GA, Kwan GF, Lal A, Lal DK, Lalloo R, Lallukka T, Lam H, Lam JO, Langan SM, Lansingh VC, Larsson A, Laryea DO, Latif AA, Lawrynowicz AEB, Leigh J, Levi M, Li Y, Lindsay MP, Lipshultz SE, Liu PY, Liu S, Liu Y, Lo L-T, Logroscino G, Lotufo PA, Lucas RM, Lunevicius R, Lyons RA, Ma S, Machado VMP, Mackay MT, MacLachlan JH, Razek HMAE, Magdy M, Razek AE, Majdan M, Majeed A, Malekzadeh R, Manamo WAA, Mandisarisa J, Mangalam S, Mapoma CC, Marcenes W, Margolis DJ, Martin GR, Martinez-Raga J,

Marzan MB, Masiye F, Mason-Jones AJ, Massano J, Matzopoulos R, Mayosi BM, McGarvey ST, McGrath JJ, McKee M, McMahon BJ, Meaney PA, Mehari A, Mehndiratta MM, Mejia-Rodriguez F, Mekonnen AB, Melaku YA, Memiah P, Memish ZA, Mendoza W, Meretoja A, Meretoja TJ, Mhimbira FA, Micha R, Millear A, Miller TR, Mirarefin M, Misganaw A, Mock CN, Mohammad KA, Mohammadi A, Mohammed S, Mohan V, Mola GLD, Monasta L, Hernandez JCM, Montero P, Montico M, Montine TJ, Moradi-Lakeh M, Morawska L, Morgan K, Mori R, Mozaffarian D, Mueller UO, Murthy GVS, Murthy S, Musa KI, Nachega JB, Nagel G, Naidoo KS, Naik N, Naldi L, Nangia V, Nash D, Nejjari C, Neupane S, Newton CR, Newton JN, Ng M, Ngalesoni FN, de Dieu Ngirabega J, Nguyen QL, Nisar MI, Pete PMN, Nomura M, Norheim OF, Norman PE, Norrving B, Nyakarahuka L, Ogbo FA, Ohkubo T, Ojelabi FA, Olivares PR, Olusanya BO, Olusanya JO, Opio JN, Oren E, Ortiz A, Osman M, Ota E, Ozdemir R, Pa M, Pain A, Pandian JD, Pant PR, Papachristou C, Park E-K, Park J-H, Parry CD, Parsaeian M, Caicedo AJP, Patten SB, Patton GC, Paul VK, Pearce N, Pedro JM, Stokic LP, Pereira DM, Perico N, Pesudovs K, Petzold M, Phillips MR, Piel FB, Pillay JD, Plass D, Platts-Mills JA, Polinder S, Pope CA, Popova S, Poulton RG, Pourmalek F, Prabhakaran D, Qorbani M, Quame-Amaglo J, Quistberg DA, Rafay A, Rahimi K, Rahimi-Movaghar V, Rahman M, Rahman MHU, Rahman SU, Rai RK, Rajavi Z, Rajsic S, Raju M, Rakovac I, Rana SM, Ranabhat CL, Rangaswamy T, Rao P, Rao SR, Refaat AH, Rehm J, Reitsma MB, Remuzzi G, Resnikoff S, Ribeiro AL, Ricci S, Blancas MJR, Roberts B, Roca A, Rojas-Rueda D, Ronfani L, Roshandel G, Rothenbacher D, Roy A, Roy NK, Ruhago GM, Sagar R, Saha S, Sahathevan R, Saleh MM, Sanabria JR, Sanchez-Niño MD,

Sanchez-Riera L, Santos IS, Sarmiento-Suarez R, Sartorius B, Satpathy M, Savic M, Sawhney M, Schaub MP, Schmidt MI, Schneider IJC, Schöttker B, Schutte AE, Schwebel DC, Seedat S, Sepanlou SG, Servan-Mori EE, Shackelford KA, Shaddick G, Shaheen A, Shahraz S, Shaikh MA, Shakh-Nazarova M, Sharma R, She J, Sheikhbahaei S, Shen J, Shen Z, Shepard DS, Sheth KN, Shetty BP, Shi P, Shibuya K, Shin M-J, Shiri R, Shiue I, Shrime MG, Sigfusdottir ID, Silberberg DH, Silva DAS, Silveira DGA, Silverberg JI, Simard EP, Singh A, Singh GM, Singh JA, Singh OP, Singh PK, Singh V, Soneji S, Søreide K, Soriano JB, Sposato LA, Sreeramareddy CT, Stathopoulou V, Stein DJ, Stein MB, Stranges S, Stroumpoulis K, Sunguya BF, Sur P, Swaminathan S, Sykes BL, Szoeke CEI, Tabarés-Seisdedos R, Tabb KM, Takahashi K, Takala JS, Talongwa RT, Tandon N, Tavakkoli M, Taye B, Taylor HR, Ao BJT, Tedla BA, Tefera WM, Have MT, Terkawi AS, Tesfay FH, Tessema GA, Thomson AJ, Thorne-Lyman AL, Thrift AG, Thurston GD, Tillmann T, Tirschwell DL, Tonelli M, Topor-Madry R, Topouzis F, Towbin JA, Traebert J, Tran BX, Truelsen T, Trujillo U, Tura AK, Tuzcu EM, Uchendu US, Ukwaja KN, Undurraga EA, Uthman OA, Dingenen RV, van Donkelaar A, Vasankari T, Vasconcelos AMN, Venketasubramanian N, Vidavalur R, Vijayakumar L, Villalpando S, Violante FS, Vlassov VV, Wagner JA, Wagner GR, Wallin MT, Wang L, Watkins DA, Weichenthal S, Weiderpass E, Weintraub RG, Werdecker A, Westerman R, White RA, Wijeratne T, Wilkinson JD, Williams HC, Wiysonge CS, Woldeyohannes SM, Wolfe CDA, Won S, Wong JQ, Woolf AD, Xavier D, Xiao Q, Xu G, Yakob B, Yalew AZ, Yan LL, Yano Y, Yaseri M, Ye P, Yebyo HG, Yip P, Yirsaw BD, Yonemoto N, Yonga G, Younis MZ, Yu S, Zaidi Z, Zaki MES, Zannad F, Zavala DE,

Zeeb H, Zeleke BM, Zhang H, Zodpey S, Zonies D, Zuhlke LJ, Vos T, Lopez AD, Murray CJL. 2016. Global, regional, and national life expectancy, all-cause mortality, and cause-specific mortality for 249 causes of death, 1980–2015: a systematic analysis for the Global Burden of Disease Study 2015. The Lancet 388:1459–1544.

2. Marie C, Petri WA. 2013. Amoebic dysentery. BMJ Clin Evid 2013:0918.

3. Alvarado-Esquivel C, Hernandez-Tinoco J, Sanchez-Anguiano LF. 2015. Seroepidemiology of Entamoeba histolytica Infection in General Population in Rural Durango, Mexico. J Clin Med Res 7:435–439.

4. Gilchrist CA, Petri SE, Schneider BN, Reichman DJ, Jiang N, Begum S, Watanabe K, Jansen CS, Elliott KP, Burgess SL, Ma JZ, Alam M, Kabir M, Haque R, Petri WA. 2016. Role of the Gut Microbiota of Children in Diarrhea Due to the Protozoan Parasite Entamoeba histolytica. J Infect Dis 213:1579–1585.

5. Haque R, Huston CD, Hughes M, Houpt E, Petri WA. 2003. Amebiasis. New England Journal of Medicine 348:1565–1573.

6. Petri WA, Haque R, Mann BJ. 2002. The Bittersweet Interface of Parasite and Host: Lectin-Carbohydrate Interactions During Human Invasion by the Parasite Entamoeba histolytica. Annu Rev Microbiol 56:39–64.

7. Reed SL, Curd JG, Gigli I, Gillin FD, Braude AI. 1986. Activation of complement by pathogenic and nonpathogenic Entamoeba histolytica. J Immunol 136:2265–2270.

8. Costa CA, Nunes ÁC, Ferreira AJ, Gomes MA, Caliari MV. 2010. Entamoeba histolytica and E. dispar trophozoites in the liver of hamsters: in vivo binding of antibodies and complement. Parasites & Vectors 3:23.

9. Reed SL, Ember JA, Herdman DS, DiScipio RG, Hugli TE, Gigli I. 1995. The extracellular neutral cysteine proteinase of Entamoeba histolytica degrades anaphylatoxins C3a and C5a. J Immunol 155:266–274.

10. Reed SL, Gigli I. 1990. Lysis of complement-sensitive Entamoeba histolytica by activated terminal complement components. Initiation of complement activation by an extracellular neutral cysteine proteinase. J Clin Invest 86:1815–1822.

11. Reed SL, Keene WE, McKerrow JH, Gigli I. 1989. Cleavage of C3 by a neutral cysteine proteinase of Entamoeba histolytica. J Immunol 143:189–195.

12. Braga LL, Ninomiya H, McCoy JJ, Eacker S, Wiedmer T, Pham C, Wood S, Sims PJ, Petri WA. 1992. Inhibition of the complement membrane attack complex by the galactose-specific adhesion of Entamoeba histolytica. J Clin Invest 90:1131–1137.

13. Miller HW, Suleiman RL, Ralston KS. 2019. Trogocytosis by Entamoeba histolytica Mediates Acquisition and Display of Human Cell Membrane Proteins and Evasion of Lysis by Human Serum. mBio 10:e00068-19.

14. Bettadapur A, Miller HW, Ralston KS. 2020. Biting Off What Can Be Chewed: Trogocytosis in Health, Infection, and Disease. Infect Immun 88:e00930-19.

15. Ralston KS, Solga MD, Mackey-Lawrence NM, Somlata null, Bhattacharya A, Petri WA. 2014. Trogocytosis by Entamoeba histolytica contributes to cell killing and tissue invasion. Nature 508:526–530.

16. González-Ruiz A, Haque R, Aguirre A, Castañón G, Hall A, Guhl F, Ruiz-Palacios G, Miles MA, Warhurst DC. 1994. Value of microscopy in the diagnosis of dysentery associated with invasive Entamoeba histolytica. J Clin Pathol 47:236–239.

17. Davies A, Simmons DL, Hale G, Harrison RA, Tighe H, Lachmann PJ, Waldmann H. 1989. CD59, an LY-6-like protein expressed in human lymphoid cells, regulates the action of the complement membrane attack complex on homologous cells. Journal of Experimental Medicine 170:637–654.

18. Štefanová I, Hilgert I, Krištofová H, Brown R, Low MG, Hořejši V. 1989. Characterization of a broadly expressed human leucocyte surface antigen MEM-43

anchored in membrane through phosphatidylinositol. Molecular Immunology 26:153–161.

19. Cinek T, Horejsí V. 1992. The nature of large noncovalent complexes containing glycosyl-phosphatidylinositol-anchored membrane glycoproteins and protein tyrosine kinases. The Journal of Immunology 149:2262–2270.

20. Rollins SA, Sims PJ. 1990. The complement-inhibitory activity of CD59 resides in its capacity to block incorporation of C9 into membrane C5b-9. J Immunol 144:3478–3483.

21. Meri S, Morgan BP, Davies A, Daniels RH, Olavesen MG, Waldmann H, Lachmann PJ. 1990. Human protectin (CD59), an 18,000-20,000 MW complement lysis restricting factor, inhibits C5b-8 catalysed insertion of C9 into lipid bilayers. Immunology 71:1–9.

22. Zhao J, Rollins SA, Maher SE, Bothwell AL, Sims PJ. 1991. Amplified gene expression in CD59-transfected Chinese hamster ovary cells confers protection against the membrane attack complex of human complement. J Biol Chem 266:13418–13422.

23. Ventura-Juárez J, Campos-Rodríguez R, Jarillo-Luna RA, Muñoz-Fernández L, Escario-G-Trevijano JA, Pérez-Serrano J, Quintanar JL, Salinas E, Villalobos-Gómez

FR. 2009. Trophozoites of Entamoeba histolytica express a CD59-like molecule in human colon. Parasitol Res 104:821–826.

24. Wang G, Liszewski MK, Chan AC, Atkinson JP. 2000. Membrane Cofactor Protein (MCP; CD46): Isoform-Specific Tyrosine Phosphorylation. The Journal of Immunology 164:1839–1846.

25. Riley-Vargas RC, Gill DB, Kemper C, Liszewski MK, Atkinson JP. 2004. CD46: expanding beyond complement regulation. Trends in Immunology 25:496–503.

26. Liszewski MK, Atkinson JP. 2015. Complement regulator CD46: genetic variants and disease associations. Human Genomics 9:7.

27. Seya T, Turner JR, Atkinson JP. 1986. Purification and characterization of a membrane protein (gp45-70) that is a cofactor for cleavage of C3b and C4b. J Exp Med 163:837–855.

28. Goslings WR, Blom DJ, de Waard-Siebinga I, van Beelen E, Claas FH, Jager MJ, Gorter A. 1996. Membrane-bound regulators of complement activation in uveal melanomas. CD46, CD55, and CD59 in uveal melanomas. Invest Ophthalmol Vis Sci 37:1884–1891.

29. Varsano S, Rashkovsky L, Shapiro H, Ophir D, Mark-Bentankur T. 1998. Human lung cancer cell lines express cell membrane complement inhibitory proteins and are extremely resistant to complement-mediated lysis; a comparison with normal human respiratory epithelium in vitro, and an insight into mechanism(s) of resistance. Clin Exp Immunol 113:173–182.

30. Nicholson-Weller A, Burge J, Fearon DT, Weller PF, Austen KF. 1982. Isolation of a human erythrocyte membrane glycoprotein with decay-accelerating activity for C3 convertases of the complement system. The Journal of Immunology 129:184–189.

31. Medof ME, Kinoshita T, Nussenzweig V. 1984. Inhibition of complement activation on the surface of cells after incorporation of decay-accelerating factor (DAF) into their membranes. J Exp Med 160:1558–1578.

32. Fishelson Z, Donin N, Zell S, Schultz S, Kirschfink M. 2003. Obstacles to cancer immunotherapy: expression of membrane complement regulatory proteins (mCRPs) in tumors. Molecular Immunology 40:109–123.

33. Gelderman KA, Blok VT, Fleuren GJ, Gorter A. 2002. The Inhibitory Effect of CD46, CD55, and CD59 on Complement Activation After Immunotherapeutic Treatment of Cervical Carcinoma Cells with Monoclonal Antibodies or Bispecific Monoclonal

Antibodies. Lab Invest 82:483–493.

34. Jurianz K, Maslak S, Garcia-Schüler H, Fishelson Z, Kirschfink M. 1999. Neutralization of complement regulatory proteins augments lysis of breast carcinoma cells targeted with rhumAb anti-HER2. Immunopharmacology 42:209–218.

35. Suleiman RL, Ralston KS. Growth and genetic manipulation of Entamoeba histolytica. Current Protocols in Microbiology.

36. Cong L, Ran FA, Cox D, Lin S, Barretto R, Habib N, Hsu PD, Wu X, Jiang W, Marraffini LA, Zhang F. 2013. Multiplex genome engineering using CRISPR/Cas systems. Science 339:819–823.

37. Thielen AJF, van Baarsen IM, Jongsma ML, Zeerleder S, Spaapen RM, Wouters D. 2018. CRISPR/Cas9 generated human CD46, CD55 and CD59 knockout cell lines as a tool for complement research. Journal of Immunological Methods 456:15–22.

38. Saito-Nakano Y, Yasuda T, Nakada-Tsukui K, Leippe M, Nozaki T. 2004. Rab5-associated Vacuoles Play a Unique Role in Phagocytosis of the Enteric Protozoan Parasite Entamoeba histolytica*. Journal of Biological Chemistry 279:49497–49507.

39. Saffer LD, Petri WA. 1991. Role of the galactose lectin of Entamoeba histolytica in adherence-dependent killing of mammalian cells. Infect Immun 59:4681–4683.

40. Schindelin J, Arganda-Carreras I, Frise E, Kaynig V, Longair M, Pietzsch T, Preibisch S, Rueden C, Saalfeld S, Schmid B, Tinevez J-Y, White DJ, Hartenstein V, Eliceiri K, Tomancak P, Cardona A. 2012. Fiji: an open-source platform for biological-image analysis. Nat Methods 9:676–682.

Tables

Table 1: Primers used in these studies.

Purpose	Primer Name	F/R	Sequence
Cloning of guide RNAs into the pX330-U6-Chimeric_BB-CBh-hSpCas9 plasmid backbone	CD59 gRNA **(BbsI overhang)**	Forward	**CACC**GCAAGGAGGGTCTGTCCTGTT
	CD59 gRNA **(BbsI overhang)**	Reverse	**AAAC**AACAGGACAGACCCTCCTTGC
	CD46 gRNA **(BbsI overhang)**	Forward	**CACC**GAAAGGGACACTCGCGGCGGC
	CD46 gRNA **(BbsI overhang)**	Reverse	**AAAC**GCCGCCGCGAGTGTCCCTTTC
Sanger sequencing of CRISPR gRNA plasmids	GENEWIZ Universal Primer “U6”	Forward	GACTATCATATGCTTACCGT
BLAST-identified primer sets for specific PCR amplification of CD59 and CD46	CD59 PCR amplification	Forward	TTGACTCACTGACCCTGATGG
	CD59 PCR amplification	Reverse	TATCCATTGGTGTCCCCAAGC
	CD46 PCR amplification	Forward	ACAAATATGACGGCGAGCCA
	CD46 PCR amplification	Reverse	GGCTCAATCCCGAAAACACG
Sanger Sequencing of PCR product from CRISPR knockout clones	CD59 sequencing	Forward	GGGGCTTATAGGGACTGAGC
	CD46 sequencing	Forward	ACCTCTCGAAGGCCAAGG
Gibson cloning of	CD55 coding sequence	Forward	**AAACACATTAACAGATCTT**CATGACCGTCGCGCGGCCGAG

CD46 and CD55 coding sequences into a pEhEx plasmid backbone	**(homology to pEhEx)** CD55 coding sequence **(homology to pEhEx)**	Reverse	**GAAGAGTTCAACTCGAGTGG**CTAAGTCAGCAAGCCCATGG
	CD46 coding sequence **(homology to pEhEx)**	Forward	**AAACACATTAACAGATCTTC**ATGGAGCCTCCCGGCCGCCG
	CD46 coding sequence **(homology to pEhEx)**	Reverse	**GAAGAGTTCAACTCGAGTGG**TCAGCCTCTCTGCTCTGCTG
	pEhEx **(homology to CD46 coding sequence)**	Forward	CAGCAGAGCAGAGAGGCTGA**CCACTCGAGTTGAACTCTTC**
	pEhEx **(homology to CD46 coding sequence)**	Reverse	CGGCGGCCGGGAGGCTCCAT**GAAGATCTGTTAATGTGTTT**
Sequencing of CD59 and CD46 expression plasmids	pEhEx CS UTR Primer	Forward	TCAGTCTTACCACGTCATAAAGT
	pEhEx CS UTR Primer	Reverse	TGCAAGAAGATGTTACAAAGCA
RT-PCR of amoebae mutants	CD46 RT-PCR	Forward	TCCCTGCAAATGGGACTTAC
	CD46 RT-PCR	Reverse	GGGGGATCCCAAGTACTGTT
	CD55 RT-PCR	Forward	ATGAGTGCCGTCCAGGTTAC
	CD55 RT-PCR	Reverse	CTGAACTGTTGGTGGGACCT

Supplemental Material

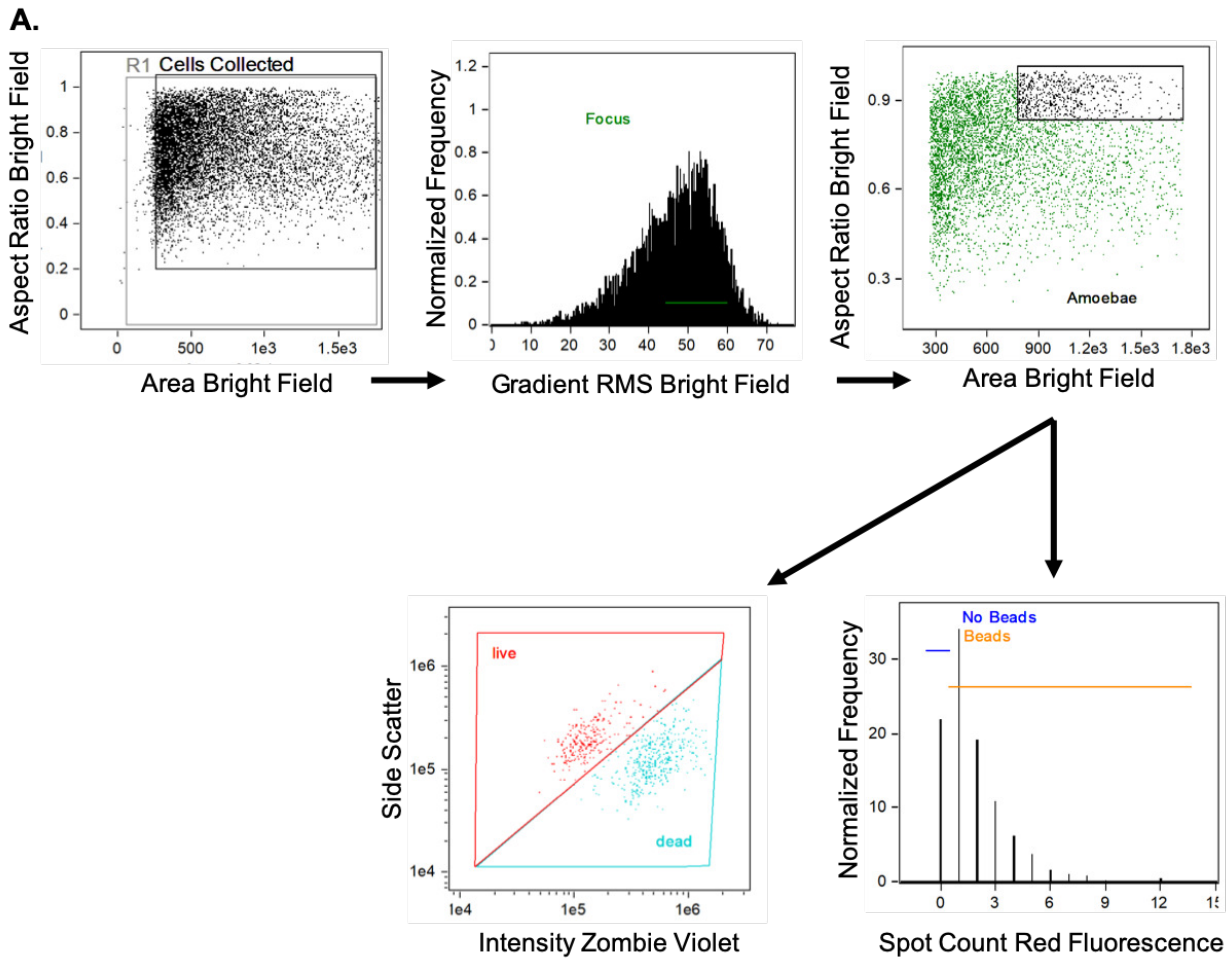

Fig. S3.1: Gating strategy used for analysis of bead ingestion experiments
Amoebae were gated on by brightfield area and aspect ratio during acquisition. Next, using Gradient RMS Bright Field, focused cells were gated on from total collected events. Because amoebae remained unstained in these experiments, single amoebae were then gated on using brightfield area and aspect ratio. From the single amoebae population, amoebae viability and bead ingestion were measured. Dead amoebae were gated on using fluorescence intensity of Zombie Violet dye and side scatter. Bead ingestion was quantified using the “spot count ” feature in Amnis IDEAS software and quantified spots of red bead fluorescence.

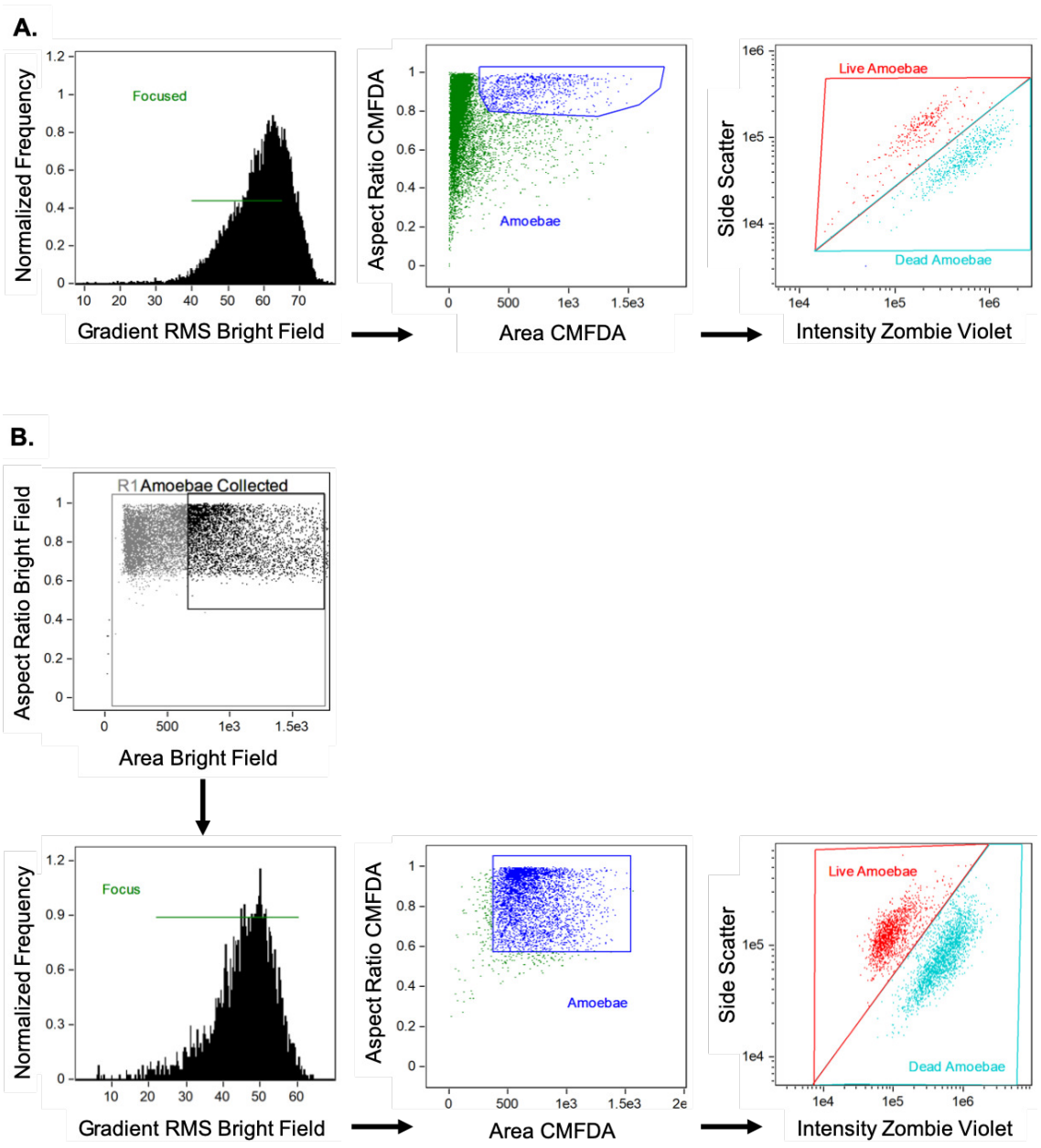

Fig. S3.2: Gating strategy used for analysis of experiments with increasing numbers of human cells, and for immunofluorescence analysis of amoebae exogenously expressing CD46 or CD55. (A) Gating strategy for experiments with increasing numbers of Jurkat cells, and for immunofluorescence analysis of amoebae exogenously expressing CD46 or CD55. Focused cells were gated on from total collected events, using Gradient RMS Bright Field. Single amoebae were gated using area and aspect ratio of CMFDA cytoplasm dye fluorescence. Dead amoebae were gated on using fluorescence intensity of Zombie Violet dye and side scatter. **(B)** Gating strategy for experiments with increasing numbers of red blood cells. Only amoeba events were collected for analysis and were gated on using bright field area and aspect ratio during data acquisition. Focused cells were gated on from total collected events, using Gradient RMS Bright Field. Single amoebae were gated using area and aspect ratio of CMFDA cytoplasm dye fluorescence. Dead amoebae were gated on using fluorescence intensity of Zombie Violet dye and side scatter.

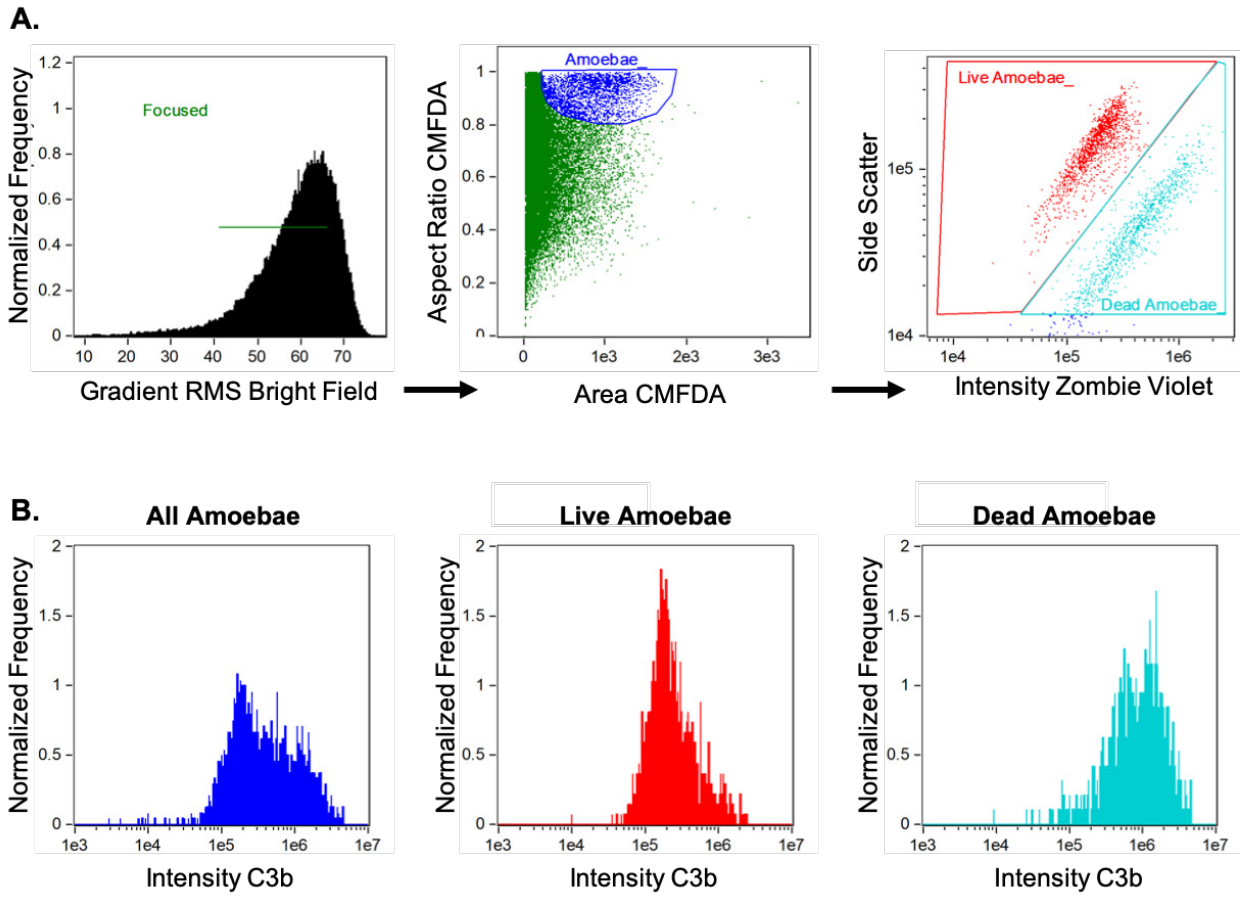

Fig. S3.3: Gating strategy used for analysis of C3b deposition experiments.
(A) Focused cells were gated on from total collected events, using Gradient RMS Bright Field. Single amoebae were gated using area and aspect ratio of CMFDA cytoplasm dye fluorescence. Dead amoebae were gated on using fluorescence intensity of Zombie Violet dye and side scatter. **(B)** Representative histograms of C3b fluorescence intensity of all single amoeba, live amoeba, or dead amoeba populations.

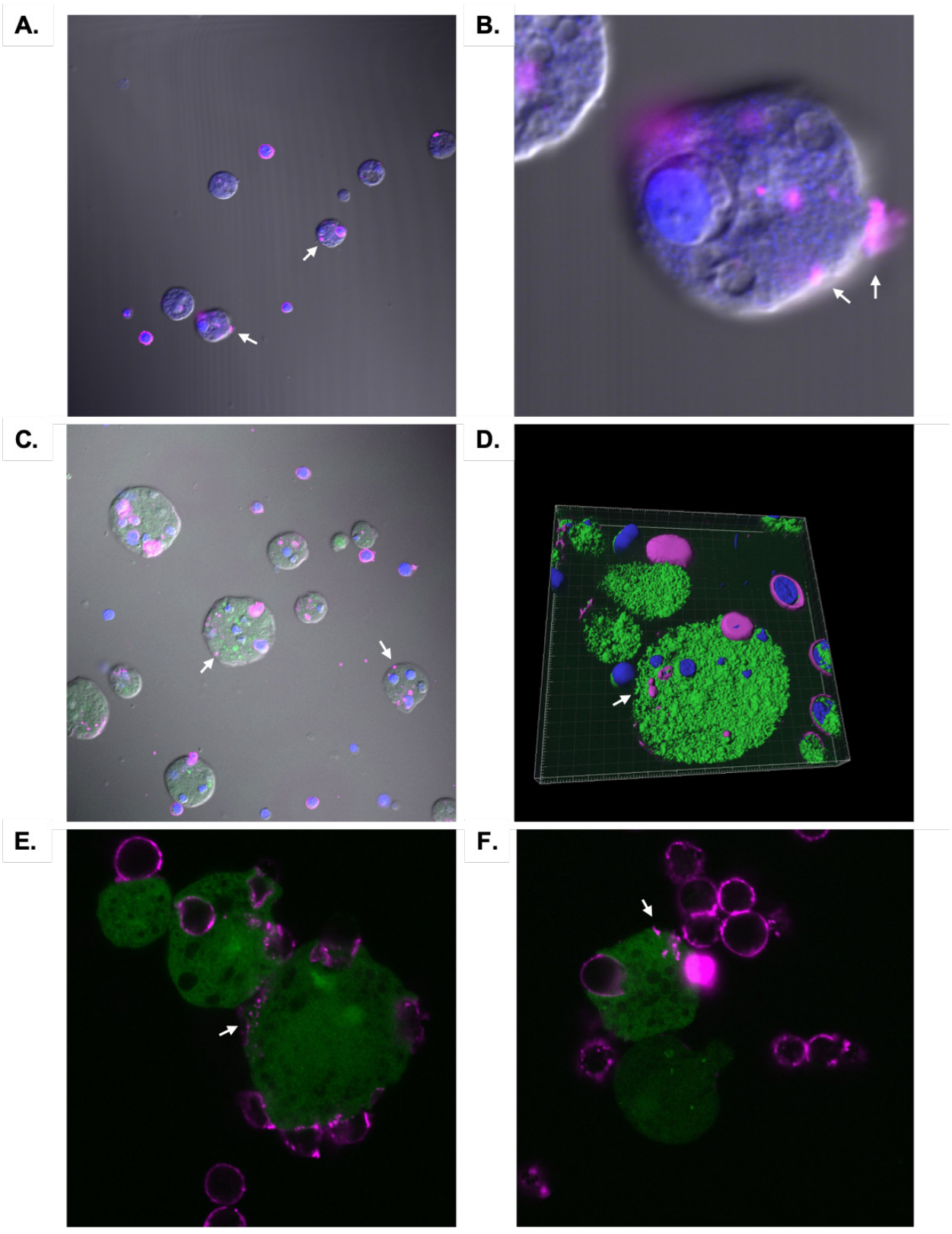
A.
B.
C.
D.
E.
F.

Fig. S3.4: Biotinylated human cell membrane proteins are detected on the surface of amoebae prior to fixation. The surface of human Jurkat cells was biotinylated prior to incubation with amoebae. Following incubation, samples were placed on ice to halt membrane turnover and fluorescently-conjugated streptavidin was used to detect biotinylated proteins on the surface on both human cells and amoebae (magenta) prior to fixation. DNA was labeled with DAPI nucleic acid stain following fixation. Arrows indicate transferred patches of human proteins on the surface of amoebae. **(A)** Amoebae and biotinylated human cells were incubated together for 2 minutes. **(B)** A closeup image of an amoebae from the panel shown in A with transferred human proteins on its surface. **(C)** Amoebae and human cells were incubated together for 5 minutes. Amoebic autofluorescence is shown in green. **(D)** 3-D reconstruction of Z stacks taken from the data in C. **(E-F)** Human cells and amoebae were incubated together for 5 minutes. Amoebae cytoplasm was labeled with CMFDA dye (green), and the nuclei of cells were left unstained. Data were analyzed by confocal microscopy. Images in A-F are representative of data collected from 4 independent experiments with incubation times of 2-5 minutes.

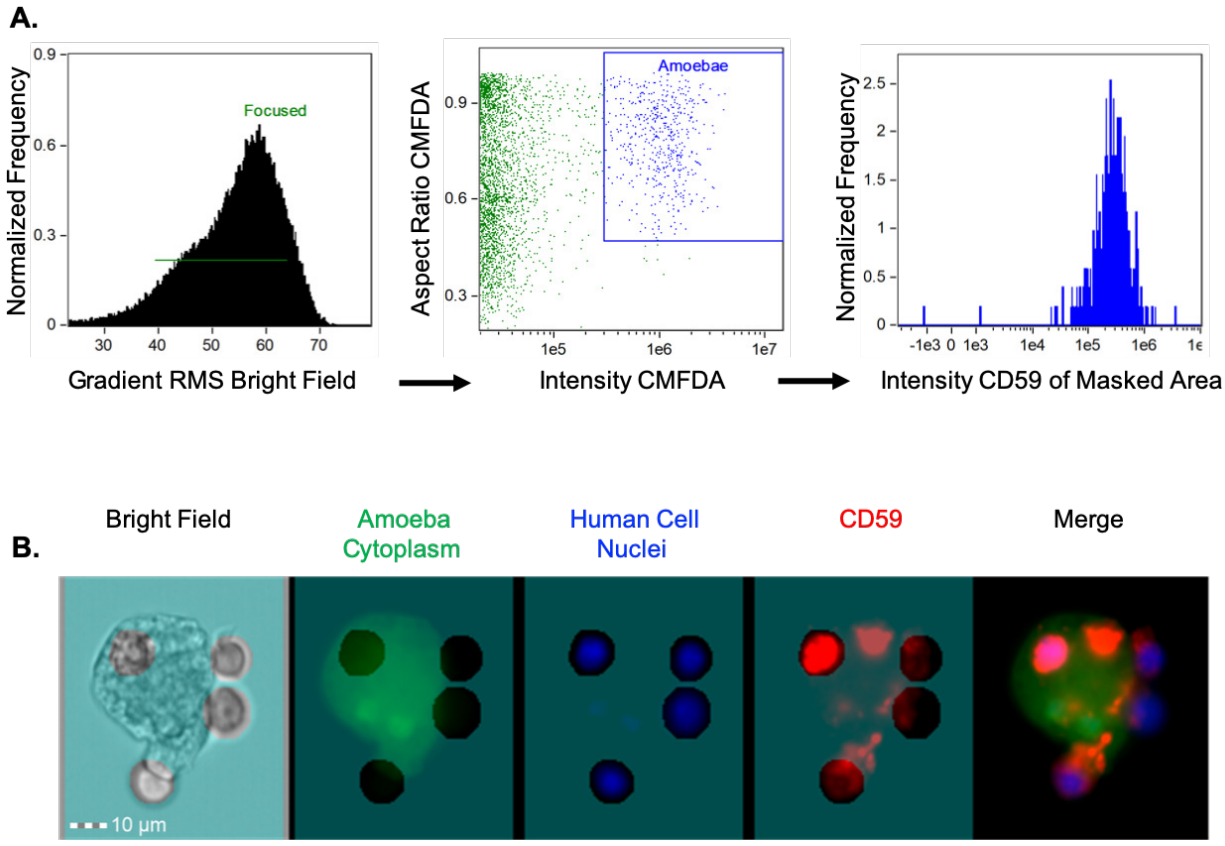

Fig. S3.5: Gating strategy used for analysis of CD59 displayed on amoebae after 5 minutes and 1 hour of trogocytosis. A masking strategy was developed to quantify only fluorescence of CD59 present on the amoebae, and not on extracellular human cells. **(A)** Focused cells were gated on from total collected events, using Gradient RMS Bright Field. Single amoebae were gated using area and aspect ratio of CMFDA cytoplasm dye fluorescence. Next, fluorescence intensity of CD59 inside of the masked area was measured. **(B)** Representative images of bright field, amoeba cytoplasm, human cell nuclei, and CD59 fluorescence with the masked area (turquoise) applied as an overlay.

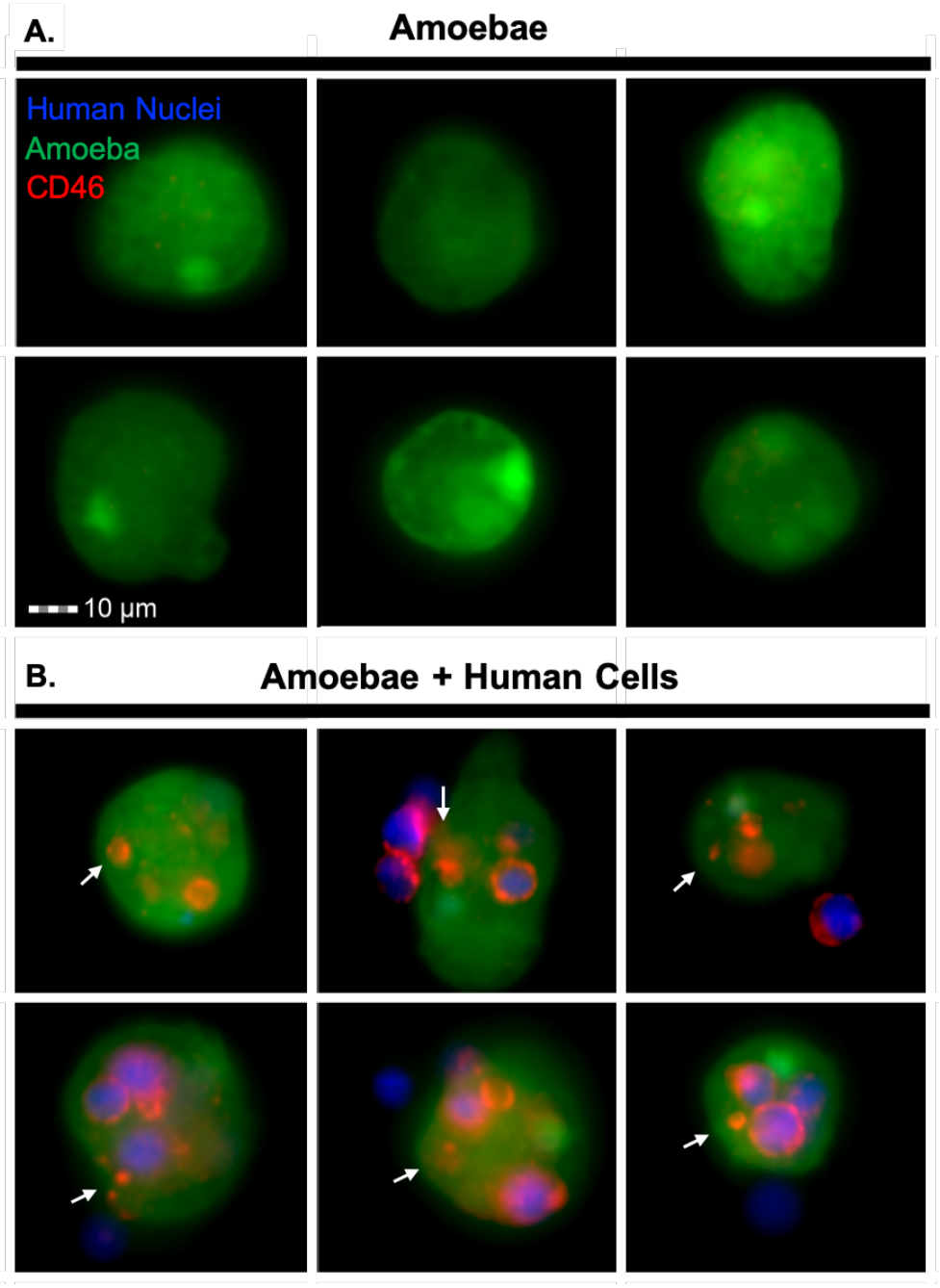

Fig. S3.6: Amoebae acquire and display the complement regulatory protein CD46 from human cells. Amoebae were incubated in the absence of Jurkat T cells, or were allowed to perform trogocytosis on human Jurkat cells for 5 minutes. Human cell nuclei were pre-labeled with Hoechst (blue), and amoebae were pre-labeled with CMFDA (green). Human CD46 (red) was detected on the amoebae surface by monoclonal antibody staining. (A) Representative images from amoebae that were incubated in the absence of Jurkat cells. (B) Representative images of amoebae that performed trogocytosis on human Jurkat cells for 5 minutes. Arrows indicate patches of displayed CD46 on the amoeba surface. Data were analyzed by imaging flow cytometry and are from 2 replicates and 1 independent experiment.

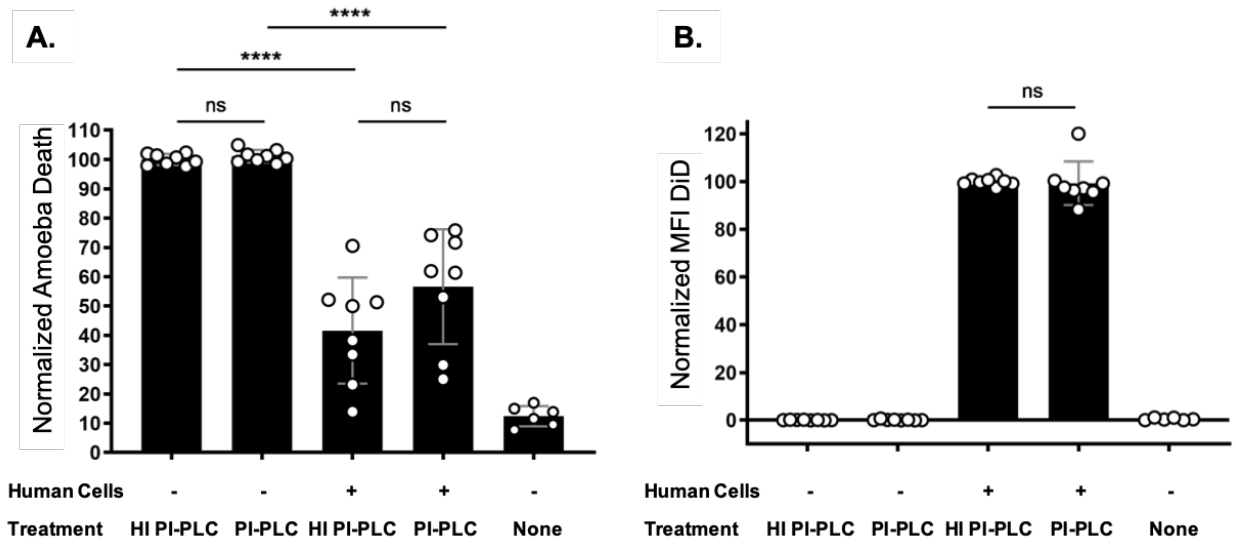

Fig. S3.7: Removal of GPI-anchored surface proteins using phosphatidylinositol-specific phospholipase C. Amoebae were labeled with CMFDA cytoplasm dye and incubated in the absence of Jurkat cells or with Jurkat cells. Human cells were labeled with DiD membrane dye. Samples were then treated with phosphatidylinositol-specific phospholipase C (PI-PLC) to remove GPI-anchored proteins, or heat-inactivated phosphatidylinositol-specific phospholipase C (HI-PI-PLC) as a control. Following exposure to human serum, amoeba death was assessed with Zombie Violet viability dye and ingested human cell material was determined by quantifying mean fluorescence intensity (MFI) of DiD present on amoebae. **(A)** Normalized death of amoebae. **(B)** Normalized mean fluorescence intensity of DiD on amoebae. Data were analyzed by imaging flow cytometry and are from 8 replicates across 4 independent experiments. The untreated control condition was performed 3 of 4 independent experiments and data are from 6 replicates.

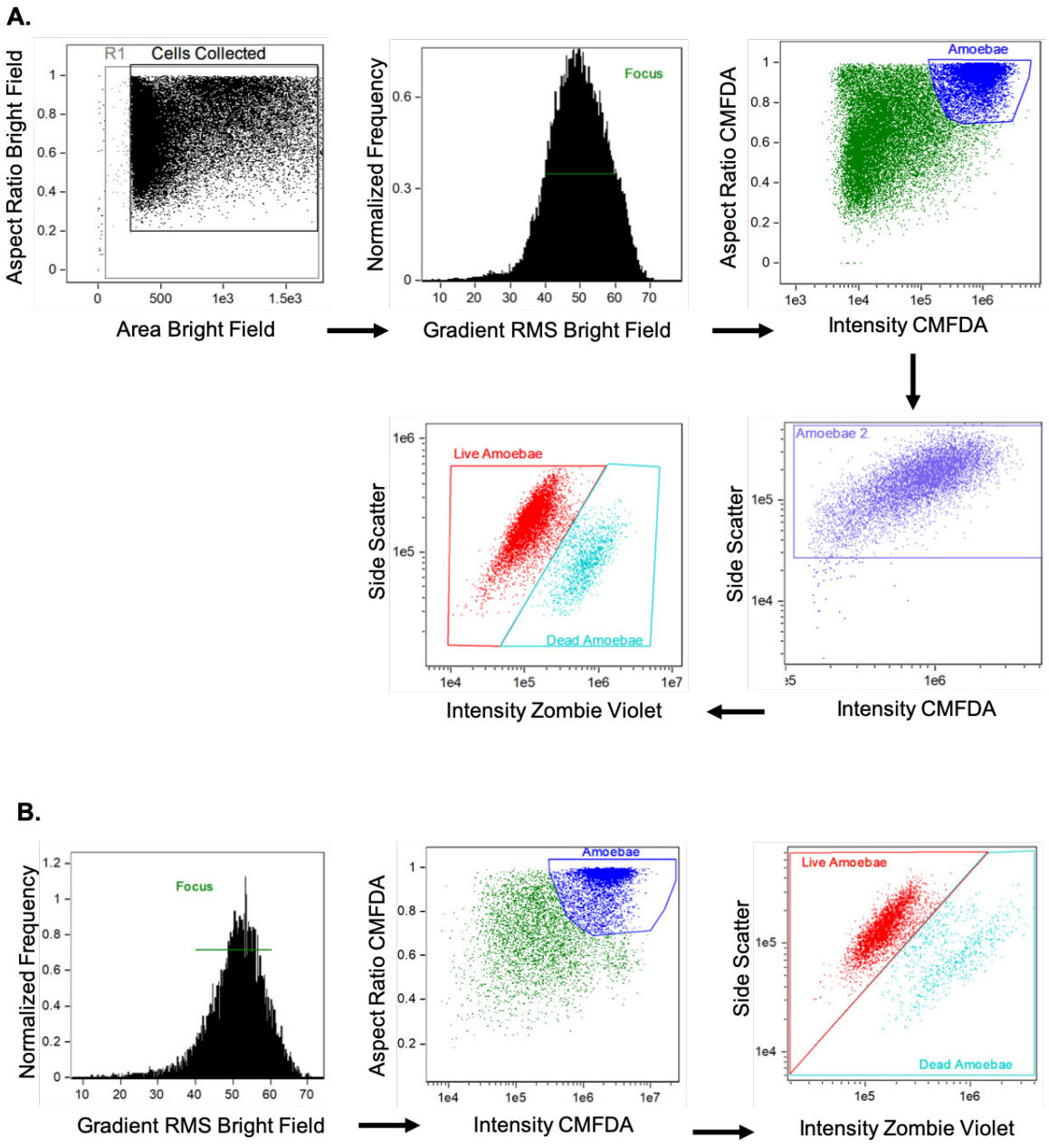

Fig. S3.8: Gating strategy used for analysis of experiments with CRISPR knockout mutants, PI-PLC treatment experiments, amoebae exogenously expressing CD46 or CD55.
Only cell events were collected for analysis (to minimize collection of debris) and were gated on using bright field area and aspect ratio during data acquisition. Focused cells were gated on from total collected events, using Gradient RMS Bright Field. Single amoebae were gated using intensity of and aspect ratio of CMFDA cytoplasm dye fluorescence. **(A)** In CRISPR knockout mutant and PI-PLC treatment experiments, amoebae were gated on a second time using CMFDA fluorescence intensity and side scatter to eliminate remaining clumps of human cells from the analysis. **(B)** In experiments with amoebae exogenously expressing CD46 or CD55, the second amoebae gate was not used. Finally, dead amoebae were gated on using fluorescence intensity of Zombie Violet dye and side scatter.

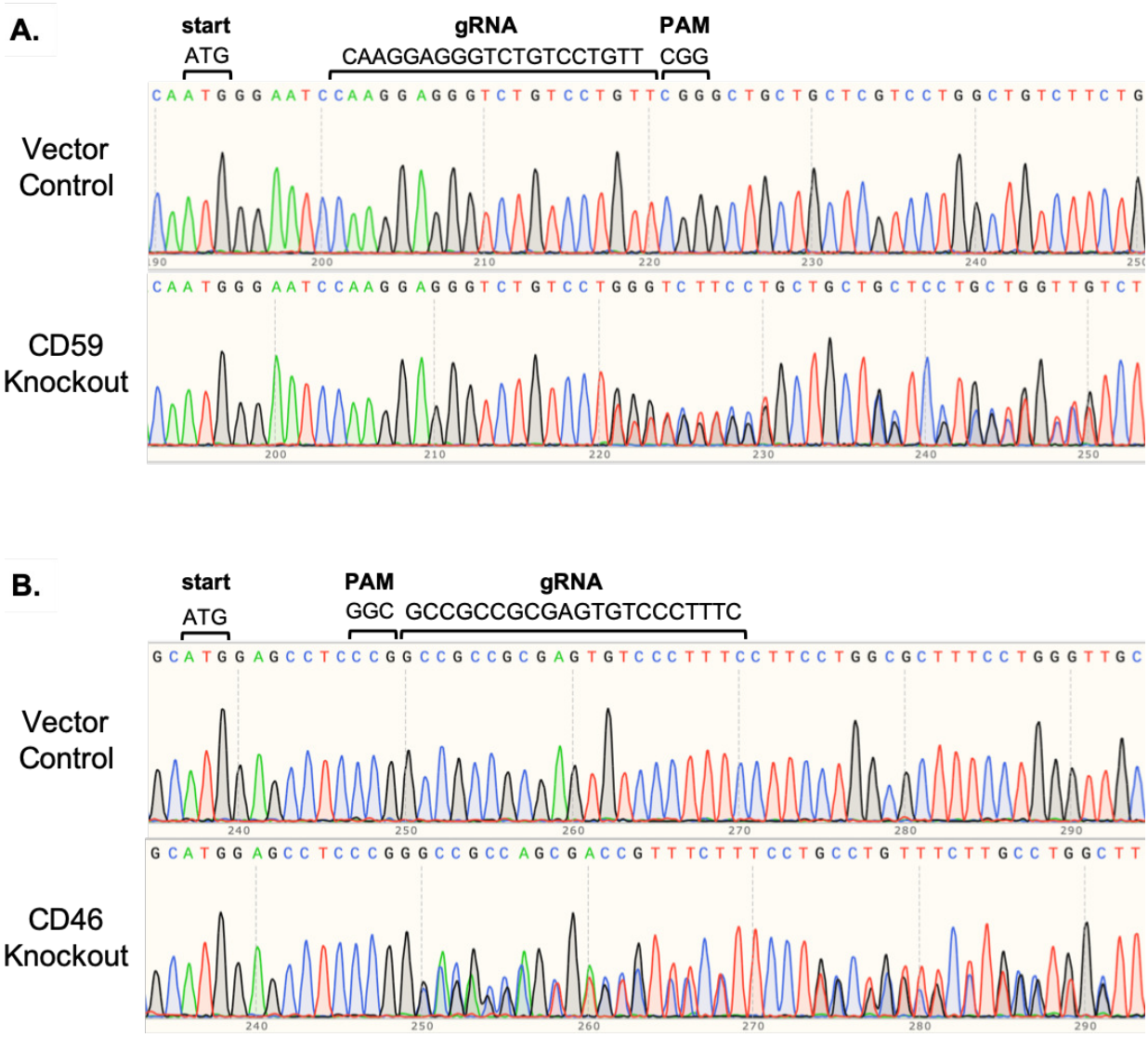

Fig. S3.9: Sequencing analysis of Jurkat CRISPR/Cas9 mutants.
Chromatograms from Sanger sequencing analysis of Jurkat T cell CRISPR/Cas9 mutants. Chromatograms from CD59 mutants **(A)** and CD46 mutants **(B)** show that the gene sequence of the mutants is different from the vector control cells downstream of the gRNA/PAM sites.

Chapter 4

Trogocytosis-Acquired Protection from Complement Lysis in *Entamoeba histolytica* is Not Altered by Knockdown of One or Two Complement Regulators in Human Cells

Hannah W. Miller, Tammie S.Y. Tam and Katherine S. Ralston

Abstract

Entamoeba histolytica is the parasite responsible for amoebiasis, a potentially fatal diarrheal disease. During severe infections, *E. histolytica* leaves the intestine and disseminates through the blood stream to other organs. While traveling via the blood, the trophozoite form of the parasite (amoeba) must contend with host immune factors present in the blood such as the complement system. We recently discovered a novel immune evasion mechanism employed by *E. histolytica*. We found that amoebae are capable of evading complement lysis through trogocytosis of human cells, which results in display of human membrane proteins by amoebae. The membrane proteins displayed by amoebae include negative regulators of the complement pathway, such as CD59 and CD46, suggesting that display of these regulatory proteins by amoebae leads to inhibition of complement lysis. However, knocking out a single complement regulatory protein using CRISPR/Cas9 was not sufficient to alter protection from lysis. In this present study, we employed CRIPSR interference to knockdown multiple complement regulatory proteins in human cells. Our findings revealed that human cell mutants altered for one or two complement regulators still conferred equivalent protection on amoebae as controls. Similarly, GPI-anchored protein knockdown mutants did not confer reduced protection from complement. These results suggest that multiple, redundant, proteins acquired from trogocytosis of human cells are involved in protecting amoebae from complement lysis.

Introduction

Amoebiasis is a potentially fatal diarrheal disease that is most prevalent in developing nations, in areas with poor sanitation (1–3). The disease is caused by *Entamoeba histolytica,* a protozoan parasite that is spread through feces-contaminated food and water (4). While infections are often mild or asymptomatic, the trophozoite form of the parasite (amoeba) is also capable of invading and ulcerating the intestine, or in rare cases, breaching the intestinal wall and disseminating via the blood stream (5). Once amoebae have disseminated, they can cause abscesses in extra-intestinal organs, mostly commonly the liver, that are fatal if left untreated (5).

We discovered a novel cell-killing mechanism employed by *E. histolytica* that we named trogocytosis or “cell nibbling” where amoebae ingest small pieces of living cells rather than engulfing them whole (6). Trogocytosis is present in a variety of eukaryotes and, in addition to cell killing, also results in benign interactions and can be used for cell to cell communication (7). Recently, we showed that amoebae acquire and display proteins from human cells they ingest via trogocytosis, and are protected from lysis by human serum (8)**(Ch3)**. We found that amoebae acquire and display the complement regulatory proteins human CD59 and CD46, which are known negative regulators of the complement pathway, and amoebae are protected from lysis by trogocytosis of both human Jurkat T cells and primary red blood cells **(Ch3)**. Additionally, amoebae that were made to exogenously express either CD46 or CD55 were protected from lysis **(Ch3)**, suggesting that display of these complement regulators can be protective. However, when we attempted to sensitize amoebae to human complement by knocking

out either CD59 or CD46 in Jurkat cells using CRISPR/Cas9, removal of a single complement regulatory protein was not sufficient to alter conferred protection **(Ch3)**.

In this present study, we utilized CRISPR interference (CRISPRi) in order to create multiple knockdown mutants, and we tested their ability to sensitize amoebae to complement lysis. We knocked down the complement regulatory proteins CD59, CD46 and CD55 in human Jurkat cells. Additionally, we created CD59/CD55 and CD46/CD55 double mutants. Finally, since the complement regulatory proteins CD59 and CD55 contain glycosylphosphatidylinositol (GPI) anchors, we knocked down phosphatidylinositol glycan anchor biosynthesis class A (PIGA), creating mutants that lacked all GPI anchored proteins. Jurkat cells that were mutated for a single complement regulatory protein, two complement regulatory proteins, or all GPI anchored proteins, were no less capable of conferring protection from complement on amoebae than controls. These findings suggest that amoebae acquire multiple, redundant complement regulators via trogocytosis from the human cells they ingest and that loss of one or two complement regulators is not sufficient to alter conferred protection.

Results

Knockdown of CD59, CD46, or CD55 is not sufficient to sensitize amoebae to complement lysis.

We recently demonstrated that removal of either CD59 or CD46 from human Jurkat T cells using CRISPR/Cas9 was not sufficient to sensitize amoebae to complement lysis **(Ch 3)**. Genetic compensation in response to gene knockout has been documented in a variety of organisms (9–11). It is possible that by creating knockout mutants, compensatory genetic changes may have taken place. For example, knocking out a complement regulatory protein may have led to compensatory increased expression of other complement regulatory proteins. The chances of compensatory genetic changes are also likely to increase in proportion to the length of time that it takes to generate a mutant. Creation of the CRISPR/Cas9 knockout mutants used in chapter 3, and characterization of clonal lines, happened over a relatively long timeframe. This could have provided an opportunity for changes to take place. Therefore, we wanted to test the effect of knocking down these proteins rather than knocking them out entirely. We utilized CRISPRi to knockdown CD59, CD49 and CD55 in human Jurkat cells **(Fig. 4.1A-E)**. Amoebae were incubated alone or allowed to perform trogocytosis on Jurkat mutants before being exposed to human serum. Jurkat mutants that expressed only dead Cas9 (dCas9), or dCas9 and a guide RNA to the unrelated human protein aminopeptidase (ANPEP), were used as controls. Following exposure to human serum, amoebic viability and the amount of ingested Jurkat cell material was measured **(Fig. 4.1F-G)**. There was no difference in acquired protection or

the amount of ingestion between amoebae that had been fed control Jurkat cells or knockdown mutants. These results indicate that knockdown of a single complement regulatory protein is not sufficient to sensitize amoebae to complement lysis.

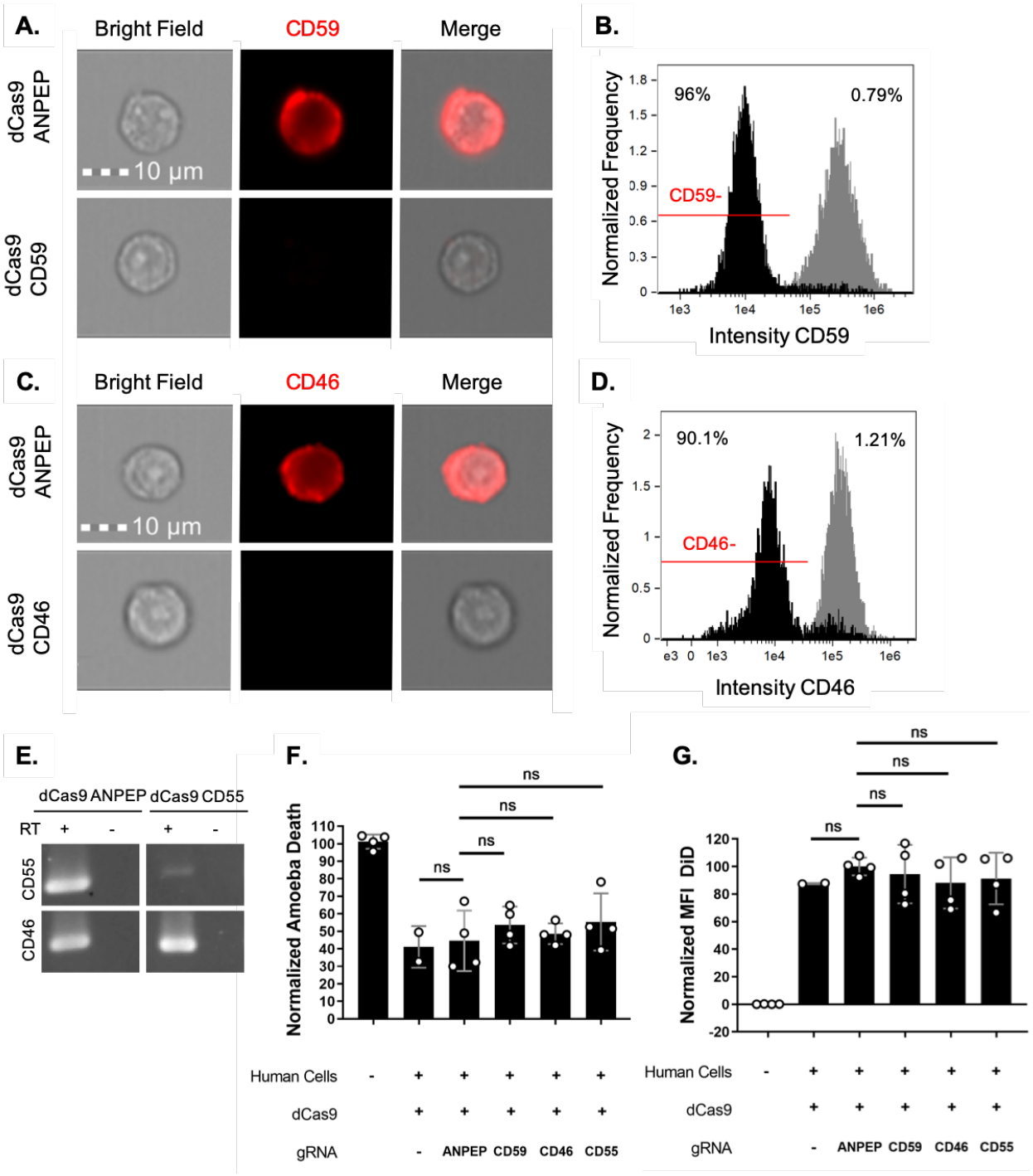

Fig. 4.1: Knockdown of CD59, CD46, or CD55 is not sufficient to sensitize amoebae to complement lysis. (A-E) Jurkat cells knocked down for CD59, CD46, or CD55 were generated using CRISPRi. Monoclonal antibodies and imaging flow cytometry was used to quantify CD59 or CD46, RT-PCR was used to evaluate CD55 mRNA expression. **(A)** Representative images of CD59 immunofluorescence (red) on ANPEP control or CD59 mutant Jurkat cells. **(B)** Intensity of CD59 antibody staining on vector control (gray) or CD59 mutants Jurkat cells (black). **(C)** Representative images of CD46 immunofluorescence (red) on ANPEP control or CD46 mutant Jurkat cells. **(D)** Intensity of CD46 antibody staining on ANPEP control (gray) or CD46 mutant Jurkat cells (black). **(E)** Expression of CD55 mRNA in CD55 mutant Jurkat cells or control cells mutated for the unrelated protein ANPEP. CD46 expression served as a control for the RT-PCR reaction. **(F-G)** Jurkat cells were stained with the membrane dye DiD. Amoebae were incubated alone or in the presence of CD59, CD46 and CD55 mutant Jurkat cells. Mutants expressing dCas9 but no gRNA or a gRNA to the unrelated protein ANPEP were used as controls. Samples were exposed to human serum and viability was assessed using zombie violet viability dye and imaging flow cytometry. **(F)** Normalized death of amoebae. **(G)** Normalized mean fluorescence intensity of DiD staining on amoebae. Data are from 2-4 replicates across 2 independent experiments.

Removal of two complement regulatory proteins is not adequate to sensitize amoebae to complement lysis.

As loss of one complement regulatory protein was no sufficient to alter acquired protection, we next sought to remove two complement regulators. We previously created Jurkat CD59 and CD46 knockout mutants using CRISPR/Cas9 **(Ch3)**. We knocked down CD55 in either our CD59 or CD46 knockout mutants using CRISPRi to create CD59/CD55 **(Fig. 4.2A-C)** and CD46/CD55 **(Fig. 4.3A-C)** double mutants. Amoebae were incubated alone or allowed to perform trogocytosis on Jurkat cells mutated for two complement regulatory proteins. As controls, Jurkat cells expressing dCas9, knocked down for CD55, or the parental CD59 and CD46 knockout cell lines were used.

Trogocytosis of the CD59/CD55 double mutant did not lead to less protection than trogocytosis of control cell lines **(Fig. 4.2D)**. Surprisingly, ingestion of the CD59 parental cell line and the CD59/CD55 double mutant led to slightly more ingested Jurkat

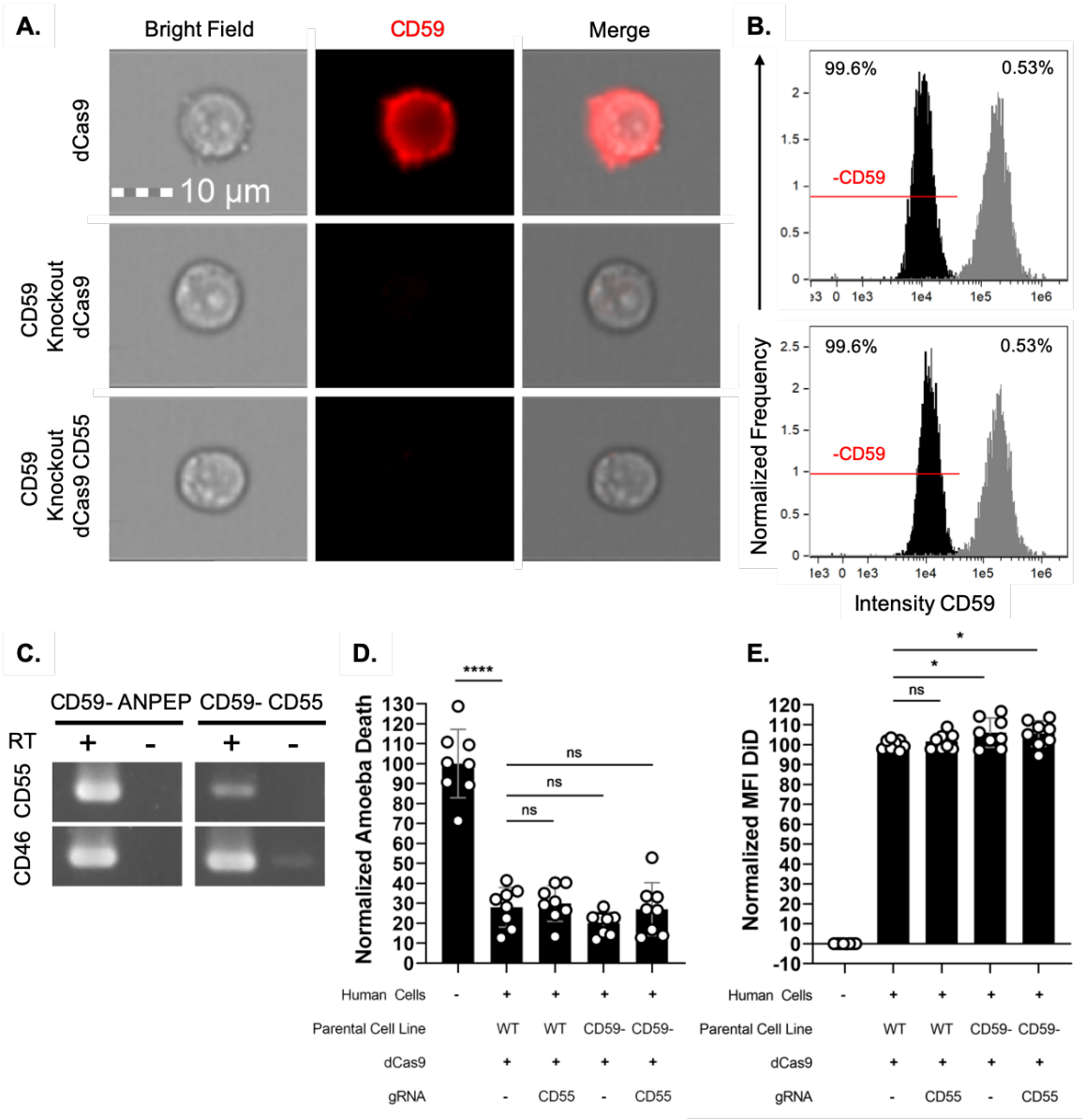

Fig. 4.2: Removal of CD59 and CD55 is not adequate to sensitize amoebae to complement lysis. **(A-E)** CD55 was knocked down in CD59 knockout Jurkat mutants using CRISPRi. A monoclonal antibody and imaging flow cytometry was used to quantify CD59, and RT-PCR was used to evaluate CD55 mRNA expression in Jurkat mutants. **(A)** Representative images of CD59 immunofluorescence (red) on dCa9 expressing control cells, CD59 knockout mutant cells, or CD59 knockout/ CD55 knockdown cells. **(B)** Intensity of CD59 antibody staining on dCas9 expressing control cells (gray), CD59 knockout mutant cells (black, top panel) or CD59 knockout/ CD55 knockdown mutants (black, bottom panel). **(C)** Expression of CD55 mRNA in CD59 knockout/ CD55 mutant Jurkat cells or control CD59 knockout cells mutated for the unrelated protein ANPEP. CD46 expression served as a control for the RT-PCR reaction. **(D-E)** Jurkat cells were stained with the membrane dye DiD. Amoebae were incubated alone or in the presence of mutant Jurkat cells. Mutants expressing dCas9 but no gRNA were used as controls. Samples were exposed to human serum and viability was assessed using zombie violet viability dye and imaging flow cytometry. **(D)** Normalized death of amoebae. **(E)** Normalized mean fluorescence intensity of DiD staining on amoebae. Data are from 8 replicates across 4 independent experiments.

cell material **(Fig. 4.2E)**. However, we did not observe this in previous assays using the CD59 knockout cell line **(Ch3)**. Similarly, trogocytosis of the CD46/CD55 double mutant did not lead to a difference in amoebic protection when compared to control cell lines **(Fig. 4.3D)**, and there was no difference in ingested Jurkat cell material **(Fig. 4.3E)**. Overall, these findings show that removal of two complement regulators is not adequate to reduce the protection amoebae acquire from performing trogocytosis on human cells.

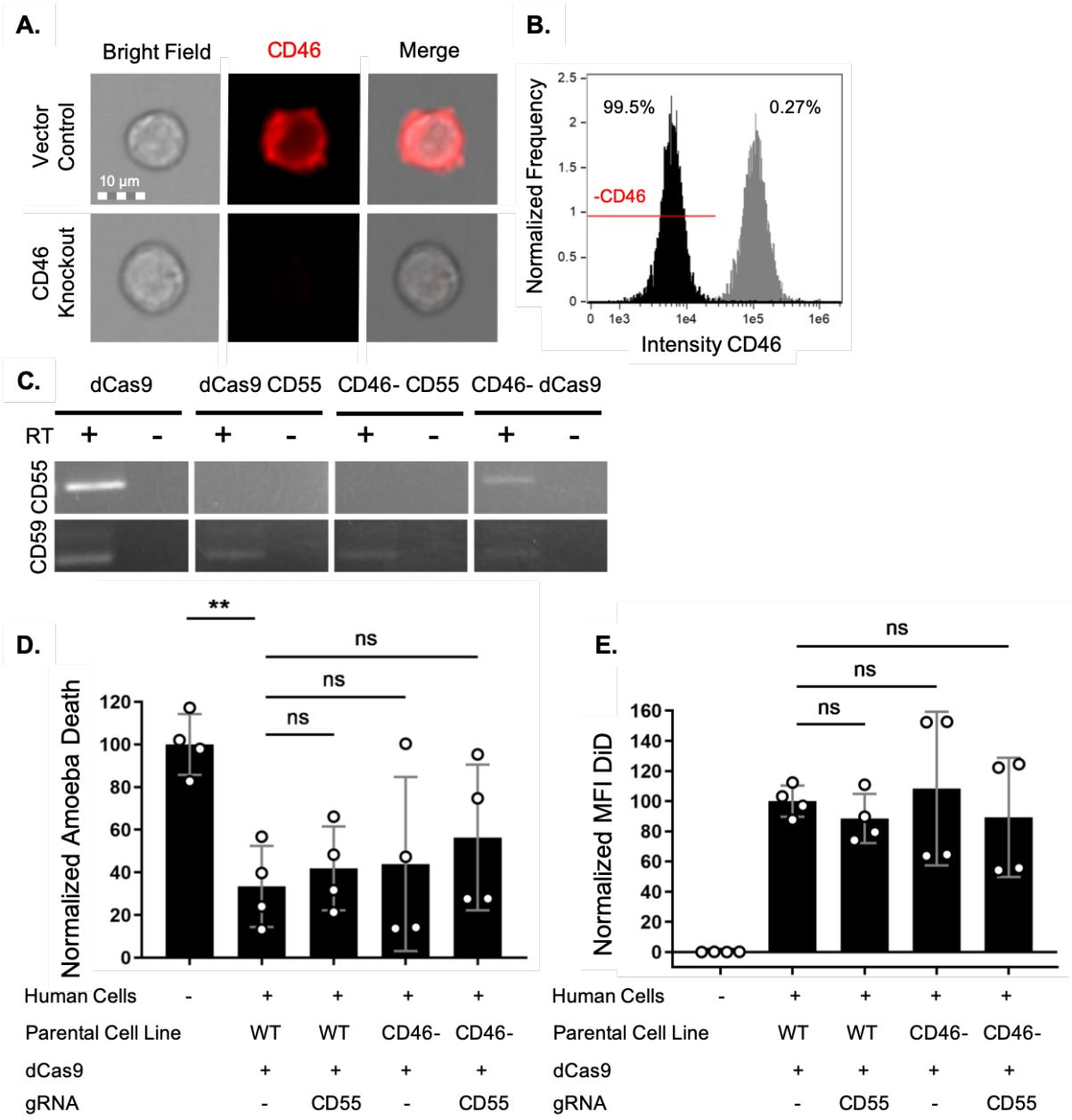

Fig. 4.3: Removal of CD46 and CD55 is not adequate to sensitize amoebae to complement lysis. **(A-C)** CD55 was knocked down in CD46 knockout Jurkat mutants using CRISPRi. RT-PCR was used to evaluate CD55 mRNA expression in Jurkat mutants. **(A-B)** This data was originally presented in Ch3 Fig. C-D. **(A)** Representative images of CD46 immunofluorescence (red) on vector control cells, or CD46 knockout Jurkat mutant cells. **(B)** Intensity of CD46 antibody staining on vector control cells (gray), or CD46 knockout mutant cells (black). **(C)** Expression of CD55 mRNA in dCas9 expressing control cells, CD55 mutants, CD46 knockout/ CD55 mutants, or CD46 knockout mutants. CD59 expression served as a control for the RT-PCR reaction. **(D-E)** Jurkat cells were stained with the membrane dye DiD. Amoebae were incubated alone or in the presence of mutant Jurkat cells. Mutants expressing dCas9 but no gRNA were used as controls. Samples were exposed to human serum and viability was assessed using zombie violet viability dye and imaging flow cytometry. **(D)** Normalized death of amoebae. **(E)** Normalized mean fluorescence intensity of DiD staining on amoebae. Data are from 4 replicates across 2 independent experiments.

Knockdown of GPI-anchored proteins does not sensitize amoebae to complement lysis.

We have previously demonstrated that treatment of amoebae with the enzyme phosphatidylinositol-specific phospholipase C (PI-PLC) following trogocytosis of human cells resulted in a non-significant reduction in protection from complement lysis **(Ch 3)**. PI-PLC cleaves GPI anchored proteins, including the complement regulatory proteins CD59 and CD55 (12–17). Therefore, we knocked down GPI anchored proteins in human Jurkat cells.

Phosphatidylinositol glycan anchor biosynthesis class A (PIGA) is involved in the biosynthesis of GPI anchored proteins (18). Paroxysmal nocturnal hemoglobinuria (PNH), is a life-threatening disease in humans characterized by hemolytic anemia (18). PNH is caused by mutations to the PIGA gene which results in lack of GPI-anchored proteins and the loss of expression of CD59 and CD55 on blood cells leading to their destruction by complement (18–20).

We thus knocked down PIGA in Jurkat cells to create mutants lacking GPI-anchored proteins. We isolated two different PIGA mutant clonal lines and validated

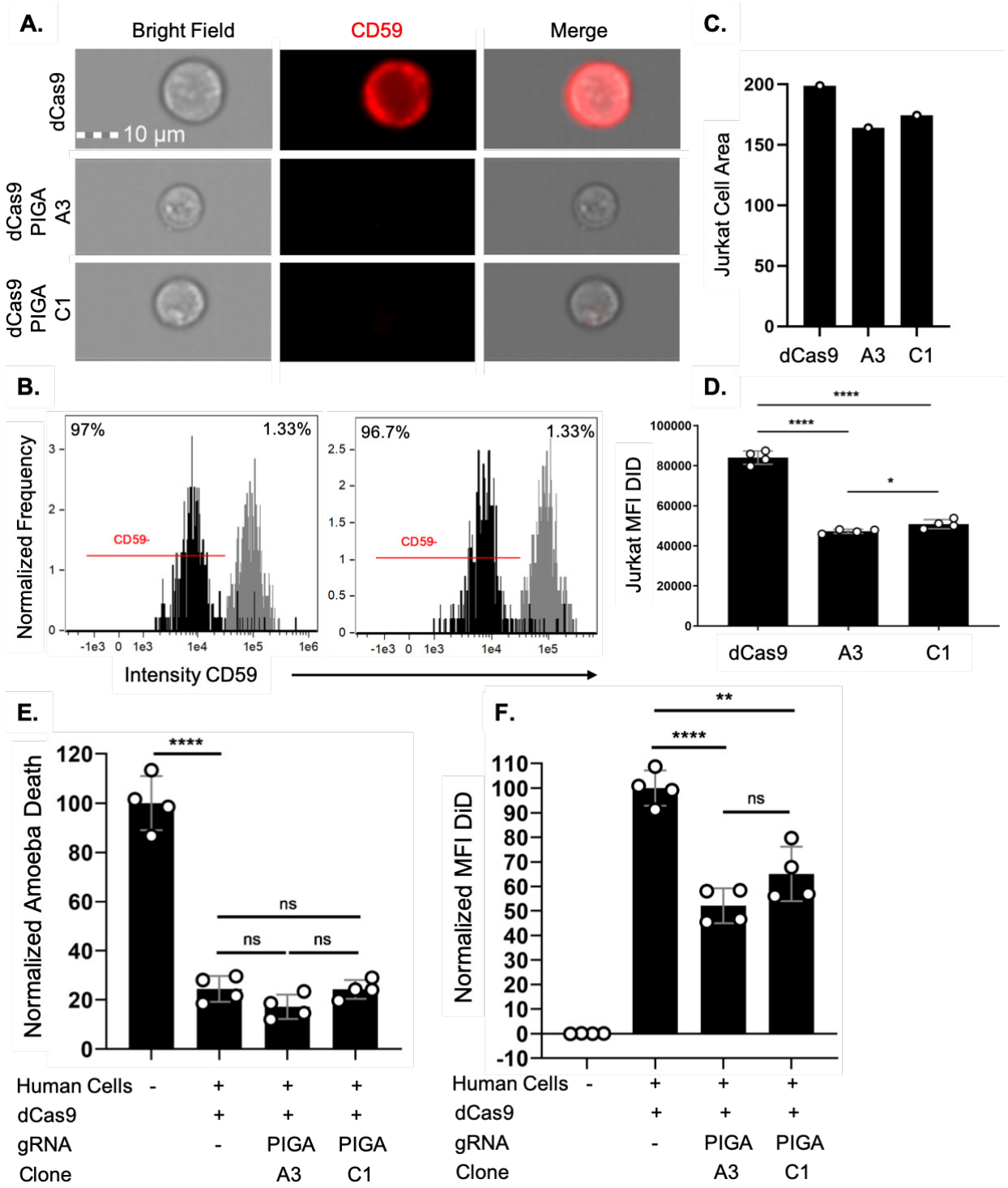

Fig. 4.4: Knockdown of GPI-anchored proteins does not sensitize amoebae to complement lysis. (A-D) PIGA knockdown Jurkat mutants were created using CRISPRi. A monoclonal antibody and imaging flow cytometry was used to quantify CD59 on PIGA mutants and area of Jurkat cells. **(A)** Representative images of CD59 immunofluorescence (red) on dCas9 expressing control cells, or PIGA Jurkat mutant clones. **(B)** Intensity of CD59 antibody staining on vector control cells (gray), or PIGA mutant clones (black) (left panel: A3 clone, and right panel: C1 clone). **(C)** Jurkat cell area of dCas9 control cells and PIGA mutant clones. **(D-F)** Jurkat cells were stained with the membrane dye DiD. **(D)** Mean fluorescence intensity of DiD staining on PIGA mutant clones and dCas9 expressing control cells. **(E-F)** Amoebae were incubated alone or in the presence of PIGA Jurkat mutant clones. Mutants expressing dCas9 but no gRNA were used as controls. Samples were exposed to human serum and viability was assessed using zombie violet viability dye and imaging flow cytometry. **(F)** Normalized death of amoebae. **(G)** Normalized mean fluorescence intensity of DiD staining on amoebae. Data are from 4 replicates across 2 independent experiments.

loss of GPI-anchored proteins through immunofluorescence staining for CD59 **(Fig. 4.4A-B)**. Interestingly, the average cell size was different between the two clonal lines and both were smaller in size than the control line **(Fig. 4.4A and C)**. When stained with the membrane dye DiD, the PIGA mutants stained less brightly then control cells and differed significantly in staining intensity from each other **(Fig. 4.4D)**. Amoebae were no less protected from human complement after performing trogocytosis on PIGA mutants than on control cells **(Fig. 4.4E)**. While ingested Jurkat cell material appeared to be less in amoebae that were incubated with PIGA mutants, this was expected due to the reduced staining intensity of membrane dye on the PIGA mutants compared to controls **(Fig. 4.4F)**, and therefore ingested material could not be accurately quantified. These results suggest that removal of Jurkat GPI-anchored proteins does not sensitize amoebae to complement lysis.

Discussion

Taken together with findings from our previous studies (8)**(Ch3)**, our results support the conclusion that amoebae acquire multiple, redundant, complement regulatory proteins from trogocytosis of human cells. We have previously shown that amoebae acquire and display membrane proteins from human cells following trogocytosis, and are protected from complement lysis (8)**(Ch3)**. Furthermore, we have shown that amoebae acquire and display the complement regulatory proteins CD59 and CD46, and amoebae made to exogenously express these proteins are protected from lysis **(Ch3)**. However, knockout of either CD59 or CD46 did not result in loss of conferred protection, hinting at redundancy in the mechanism of protection from complement. As we have demonstrated that amoebae also acquire MHC-I molecules **(Ch2)**, they likely acquire many different proteins from the cells they ingest. Therefore, loss of a single complement regulatory protein may be compensated for by the presence of other acquired complement regulators.

The findings of this study support our previous results. Knockdown of a single complement regulatory protein, CD59, CD46, or CD55 did not lead to loss in protection from complement. Likewise, mutants that lacked two complement regulatory proteins CD59/CD55 or CD46/CD55 were also equally capable of conferring protection on amoebae as controls. We have previously seen a slight decrease in protection following PI-PLC treatment that was not statistically significant **(Ch3)**. In line with this, Jurkat mutants that lacked all GPI-anchored proteins conferred equal levels of protection from complement on amoebae as controls. As CD59 and CD55 are both GPI-anchored

complement regulators, the data from our CD59/CD55 double mutant fits with this finding.

It should be noted that while we screened mutants for their expected phenotypes, we did not assay for overall genetic changes. Genetic compensation following gene knockout has been documented in different model organisms (9–11). Therefore, we cannot rule out the possibility of compensatory genetic changes that may have taken place due to loss of one or more complement regulatory proteins. There was a noticeable size difference in the PIGA clones compared to control cells, and consequently there could of have been other changes to these mutants we did not account for.

The high level of variability in these assays should also be taken into consideration. Perhaps, if differences between mutants and controls were especially small, then performance of additional replicates could have revealed minor changes.

Overall, the data from this study are consistent with our prior conclusions (8)**(Ch3)**. We conclude that amoebae acquire and display complement regulatory proteins via trogocytosis of human cells, and are protected from complement lysis through acquisition of multiple and redundant complement regulators.

Materials and Methods

Cell Culture

E. histolytica trophozoites (amoebae) were cultured as described previously (8, 21)**(Ch3)**. Amoebae (HM1:IMSS) from ATCC were grown in TYI-S-33 medium supplemented with 15% heat-inactivated adult bovine serum (Gemini Bio-Products), 2.3% Diamond vitamin Tween 80 solution (40×; Sigma-Aldrich), and 80 U/ml penicillin, 80 μg/ml streptomycin (Gibco) at 35°C in glass tissue culture tubes. For use in human serum lysis assays, amoebae were expanded in un-vented T25 tissue culture flasks that were allowed to reach 80% confluency. Amoebae were resuspended in M199s medium (Gibco medium M199 with Earle's salts, L-glutamine, and 2.2 g/liter sodium bicarbonate, without phenol red) supplemented with 0.5% bovine serum albumin (BSA), 25 mM HEPES, and 5.7 mM L-cysteine for use in serum lysis assays.

Human Jurkat T cells (clone E6-1) from ATCC were maintained as previously described (8, 21)**(Ch3)**. Jurkat cells were grown in RPMI 1640 medium (Gibco; RPMI 1640 with L-glutamine and without phenol red) supplemented with 10% heat-inactivated fetal bovine serum (Gibco), 100 U/ml penicillin, 100 μg/ml streptomycin, and 10 mM HEPES, and were cultured at 37°C and 5% CO2 in vented T25 tissue culture flasks. Prior to immunofluorescence and serum lysis assays, Jurkat cells were expanded in T75 vented tissue culture flasks and passaged when cultures reached a concentration of 5×10^5 and 2×10^6 cells/ml. For use in serum lysis or immunofluorescence assays, Jurkat cells were resuspended in M199s medium.

HEK 293T/17 cells from ATCC were maintained in Dulbecco's Modified Eagle Medium (DMEM) + GlutaMAX (Gibco; with D-Glucose and Sodium Pyruvate) supplemented with 10% heat-inactivated fetal bovine serum (Gibco), 100 U/ml penicillin, 100 μg/ml streptomycin, and 10 mM HEPES. HEK 293T/17 cells grown in vented T25 tissue culture flasks at 37°C and 5% CO2. Cells were passaged when flasks reached 80% -100% confluence using Trypsin-EDTA Solution (ATCC). For lentiviral production, cells were cultured in 6 well plates.

Jurkat T cell CRISPRi mutants

A lentiviral plasmid containing dCas9 (SC0575_phr-ucoe-ef1a-dcas9-ha-2xnls-xten80-krab-p2a-Bls) and packaging and envelope plasmids (SC0059-TEN pCMV delta R8.2 and Packaging and SC0058-TEN pMD2.G Envelope 2nd), were used for production of lentivirus and transduction of Jurkat T cells (SC0575, SC0059 and SC0058 were a gift from Sean R. Collins, University of California, Davis; SC0575 was modified from a plasmid created in the laboratory of Jonathan S. Weissman, University of California, San Francisco, Howard Hughes Medical Institute). Transduced Jurkat cells were kept under blasticidin (Blasticidin S HCl: Gibco) selection at 10μg/ml for two weeks. Next, guide RNA plasmids were generated. Guide RNAs to human CD59, CD46, CD55, and PIGA were cloned into a lentiviral plasmid backbone: SC0217_pU6-sgRNA ANPEP#1-puro (SC0217 was a gift from Sean R. Collins, University of California, Davis and created in the Collins Laboratory), to replace the ANPEP gRNA sequence already present. Guides were selected using the published sequences of

guides from the Human Genome-wide CRISPRi-v2 Libraries (Libraries were a gift from Sean R. Collins, University of California, Davis, and deposited by Jonathan S. Weissman, University of California, San Francisco; Addgene Pooled Libraries #83969, #1000000090, (22)). The mostly highly rated guide for each gene was used **(Table 4.1)**. Guide RNAs oligos containing BlpI and BstXI restriction enzyme overhangs were phosphorylated and annealed. Next, the lentiviral plasmid backbone was digested with BlpI and BstXI restriction enzymes (FastDigest Bpu1 102I and FastDigest BstXI: ThermoFisher Scientific) and oligos were ligated into the plasmid backbone. One Shot Stbl3 Competent *E. Coli* (Invitrogen) were transformed and positive colonies were screened by restriction digest. A primer located in the lentiviral plasmid backbone upstream of the inserted guide RNAs **(Table 4.1)** was used to confirm plasmids with correct inserts by sanger sequencing. Next, the gRNA plasmids were used to produce lentivirus and transduce dCas9 expressing Jurkat cells. Mutants were kept under puromycin (Puromycin dihydrochloride from Streptomyces alboniger: Sigma-Aldrich) selection at 2.5μg/ml for two weeks. The CD59 and CD46 CRISPR knockout mutants described in Chapter 3 were used to generate Jurkat cells lacking 2 complement regulatory proteins. The CD59/CD55 mutant and the CD46/CD55 mutant were obtained by transducing dCas9 expressing CD59 or CD46 knockout Jurkat cells with the CD55 lentiviral gRNA plasmid. Clonal lines of PIGA mutants were obtained by limiting dilution in 96 well plates. Other knockdown lines were heterogeneous. Mutants were screened for knockout by labeling with primary mouse monoclonal antibodies to CD59 (clone MEM-43/5 or MEM-43: Abcam) or CD46 (clone C-10; Santa Cruz Biotechnology) and a

Cy™5 AffiniPure Goat Anti-Mouse secondary antibody (Jackson ImmunoResearch Laboratories, Inc). Samples were analyzed by imaging flow cytometry. CD55 knockdown was verified through reverse transcription polymerase chain reaction (RT-PCR) using primers located within the coding region of human CD55 **(Table 4.1).**

Lentiviral transduction of Jurkat T cells

HEK 293T/17 cells (ATCC) were transfected in 6 well plates with the packaging and envelope plasmids SC0059-TEN pCMV delta R8.2 Packaging and SC0058-TEN pMD2.G Envelope 2nd G as well as either the dCas9 plasmid or a gRNA plasmid described above. Transfection was performed using Opti-MEM™ Reduced Serum Medium (Gibco) and TransIT®-2020 Transfection Reagent (Mirus). For each transfection, 0.77μg of Envelope, 1.51μg of Packaging, and 2.32μg of the dCas9 and gRNA plasmids was used. Transfected cells were incubated for 48 hours at 37°C and the lentiviral supernatant was harvested. Jurkat T cells at a concentration of 1 x 10^6 cells/ml in media containing polybrene (Millipore Sigma) at 8μg/ml were infected with lentiviral supernatant at a 1:1 volume to volume ratio for 24 hours. Jurkat cells were then washed and placed under antibiotic selection for 2 weeks as described above.

Serum lysis assays

Amoebae and Jurkat cells were washed and resuspended in M199s medium. Amoebae were labeled with CMFDA at 186 ng/ml for 10 minutes at 35°C, and Jurkat cells were labeled with DiD at 21 μg/ml for 5 minutes at 37°C followed by 10 minutes at

4°C. Next, amoebae were resuspended at a concentration of 4 x 10^5 cells/ml and Jurkat cells were resuspended at 1.6 x 10^7 cells/ml for a 1:40 amoeba: Jurkat cell ratio. Amoebae were then incubated alone or co-incubated with Jurkat cells for 1 hour at 35°C. Samples were then exposed to human serum as previously described **(Ch3)**. Samples were incubated in 100% normal human serum (pooled normal human complement serum; Innovative Research Inc.) supplemented with 150 μM $CaCl_2$ and 150 μM $MgCl_2$ for 30 minutes at 35°C. Next, samples were resuspended in M199s medium and labeled with Zombie Violet Fixable Viability dye (BioLegend) at a concentration of 4 μl/ml and incubated for 30 minutes on ice. Samples were fixed with 4% PFA at room temperature for 30 minutes and resuspended in 50 μl 1 x PBS.

ImageStream analysis

Samples were run on an Amnis ImageStreamX Mark II. Cells were gated on by size and 100,000 events were collected per sample. For assays where a single complement regulatory protein was knocked down, data are from 2-4 replicates across 2 independent experiments. In assays using the CD59/CD55 double mutant, data are from 8 replicates across 4 independent experiments. The data from assays with the CD46/CD55 double mutant or the PIGA mutant, are from 4 replicates across 2 independent experiments. Refer to chapter 3, figure S3.8 for the gating scheme used to analyze the experiments.

Statistical analysis

All statistical analyses were performed using GraphPad Prism software. Data was analyzed using a Student's unpaired t test (no significant difference was indicated by a P of >0.05; *, $P \leq 0.05$; **, $P \leq 0.01$; ***, $P \leq 0.001$; ****, $P \leq 0.0001$), and the means and standard deviations are displayed.

Acknowledgements

We thank Dr. Sean Collins and Stefan Lundgren for the plasmid constructs and advice on the lentiviral system for CRISPRi. We thank the members of our laboratory, Dr. Scott Dawson and Dr. Stephen McSorley, and for helpful discussions. All ImageStream data were acquired using shared instrumentation in the UC Davis MCB Light Microscopy Imaging Facility, and we thank Dr. Michael Paddy for technical assistance. T.S.Y.T. was funded by the Khaira Family Experiential Learning Award through the UC Davis College of Biological Sciences. This work was funded by NIH grant AI146914 and a Pew Scholarship awarded to K.S.R.

Author Contributions

H.W.M. designed, performed, and analyzed the experiments. T.S.Y.T. phenotyped the Jurkat mutants. K.S.R. conceived of the overall approach and oversaw the design and analysis of the experiments H.W.M wrote the chapter and it was edited by K.S.R.

References

1. Haque R, Mondal D, Kirkpatrick BD, Akther S, Farr BM, Sack RB, Petri WA. 2003. Epidemiologic and clinical characteristics of acute diarrhea with emphasis on Entamoeba histolytica infections in preschool children in an urban slum of Dhaka, Bangladesh. Am J Trop Med Hyg 69:398–405.

2. Speich B, Croll D, Fürst T, Utzinger J, Keiser J. 2016. Effect of sanitation and water treatment on intestinal protozoa infection: a systematic review and meta-analysis. The Lancet Infectious Diseases 16:87–99.

3. Petri WA, Mondal D, Peterson KM, Duggal P, Haque R. 2009. Association of malnutrition with amebiasis. Nutr Rev 67:S207–S215.

4. Marie C, Petri WA. 2013. Amoebic dysentery. BMJ Clin Evid 2013:0918.

5. Haque R, Huston CD, Hughes M, Houpt E, Petri WA. 2003. Amebiasis. New England Journal of Medicine 348:1565–1573.

6. Ralston KS, Solga MD, Mackey-Lawrence NM, Somlata, Bhattacharya A, Petri Jr WA. 2014. Trogocytosis by *Entamoeba histolytica* contributes to cell killing and tissue invasion. Nature 508:526–530.

7. Bettadapur A, Miller HW, Ralston KS. 2020. Biting Off What Can Be Chewed: Trogocytosis in Health, Infection, and Disease. Infect Immun 88:e00930-19.

8. Miller HW, Suleiman RL, Ralston KS. 2019. Trogocytosis by Entamoeba histolytica Mediates Acquisition and Display of Human Cell Membrane Proteins and Evasion of Lysis by Human Serum. mBio 10:e00068-19.

9. Mulligan GJ, Wong J, Jacks T. 1998. p130 Is Dispensable in Peripheral T Lymphocytes: Evidence for Functional Compensation by p107 and pRB. Mol Cell Biol 18:206–220.

10. El-Brolosy MA, Stainier DYR. 2017. Genetic compensation: A phenomenon in search of mechanisms. PLoS Genet 13:e1006780.

11. Salanga CM, Salanga MC. 2021. Genotype to Phenotype: CRISPR Gene Editing Reveals Genetic Compensation as a Mechanism for Phenotypic Disjunction of Morphants and Mutants. IJMS 22:3472.

12. Davies A, Simmons DL, Hale G, Harrison RA, Tighe H, Lachmann PJ, Waldmann H. 1989. CD59, an LY-6-like protein expressed in human lymphoid cells, regulates the action of the complement membrane attack complex on homologous cells. Journal of Experimental Medicine 170:637–654.

13. Rollins SA, Sims PJ. 1990. The complement-inhibitory activity of CD59 resides in its capacity to block incorporation of C9 into membrane C5b-9. J Immunol 144:3478–3483.

14. Zhao J, Rollins SA, Maher SE, Bothwell AL, Sims PJ. 1991. Amplified gene expression in CD59-transfected Chinese hamster ovary cells confers protection

against the membrane attack complex of human complement. J Biol Chem 266:13418–13422.

15. Štefanová I, Hilgert I, Krištofová H, Brown R, Low MG, Hořejši V. 1989. Characterization of a broadly expressed human leucocyte surface antigen MEM-43 anchored in membrane through phosphatidylinositol. Molecular Immunology 26:153–161.

16. Goslings WR, Blom DJ, de Waard-Siebinga I, van Beelen E, Claas FH, Jager MJ, Gorter A. 1996. Membrane-bound regulators of complement activation in uveal melanomas. CD46, CD55, and CD59 in uveal melanomas. Invest Ophthalmol Vis Sci 37:1884–1891.

17. Varsano S, Rashkovsky L, Shapiro H, Ophir D, Mark-Bentankur T. 1998. Human lung cancer cell lines express cell membrane complement inhibitory proteins and are extremely resistant to complement-mediated lysis; a comparison with normal human respiratory epithelium in vitro, and an insight into mechanism(s) of resistance. Clin Exp Immunol 113:173–182.

18. Brodsky RA. 2014. Paroxysmal nocturnal hemoglobinuria. Blood 124:2804–2811.

19. Takeda J, Miyata T, Kawagoe K, Iida Y, Endo Y, Fujita T, Takahashi M, Kitani T, Kinoshita T. 1993. Deficiency of the GPI anchor caused by a somatic mutation of the PIG-A gene in paroxysmal nocturnal hemoglobinuria. Cell 73:703–711.

20. Bessler M, Mason PJ, Hillmen P, Miyata T, Yamada N, Takeda J, Luzzatto L, Kinoshita T. 1994. Paroxysmal nocturnal haemoglobinuria (PNH) is caused by somatic mutations in the PIG-A gene. EMBO J 13:110–117.

21. Suleiman RL, Ralston KS. Growth and genetic manipulation of Entamoeba histolytica. Current Protocols in Microbiology.

22. Horlbeck MA, Gilbert LA, Villalta JE, Adamson B, Pak RA, Chen Y, Fields AP, Park CY, Corn JE, Kampmann M, Weissman JS. 2016. Compact and highly active next-generation libraries for CRISPR-mediated gene repression and activation. Elife 5:e19760.

Table 4.1: Primers used in these studies.

Purpose	Primer Name	F/R	Sequence
Cloning of guide RNAs into the SC0217_pU6-sgRNA ANPEP#1-puro lentiviral plasmid backbone	CD59 gRNA **(BstXI and BlpI overhangs)**	Forward	**TTG**GCGCAGAAGCGGCTCGAGGC**GTTTAAGAGC**
	CD59 gRNA **(BstXI and BlpI overhangs)**	Reverse	**TTAGCTCTTAAAC**GCCTCGAGCCGCTTCTGCGC**CAACAAG**
	CD46 gRNA **(BstXI and BlpI overhangs)**	Forward	**TTG**GCCCTTCTGGGTCCAGATAT**GTTTAAGAGC**
	CD46 gRNA **(BstXI and BlpI overhangs)**	Reverse	**TTAGCTCTTAAAC**ATATCTGGACCCAGAAGGGC**CAACAAG**
	CD55 gRNA **(BstXI and BlpI overhangs)**	Forward	**TTG**GGCTGGGCGTAGCTGCGACT**GTTTAAGAGC**
	CD55 gRNA **(BstXI and BlpI overhangs)**	Reverse	**TTAGCTCTTAAAC**AGTCGCAGCTACGCCCAGCC**CAACAAG**
	PIGA gRNA **(BstXI and BlpI overhangs)**	Forward	**TTG**GTGGCGGCCATGGAACTCAC**GTTTAAGAGC**
	PIGA gRNA **(BstXI and BlpI overhangs)**	Reverse	**TTAGCTCTTAAAC**GTGAGTTCCATGGCCGCCAC**CAACAAG**
Sanger sequencing of CRISPRi gRNA plasmids	Primer located upstream of inserted gRNAs	Forward	ACGGACTTGTGGGAGAAGC
RT-PCR for CD55 expression	CD55 RT-PCR	Forward	ATGAGTGCCGTCCAGGTTAC
	CD55 RT-PCR	Reverse	CTGAACTGTTGGTGGGACCT

Chapter 5

Establishing an Assay for Detection of Trogocytosis Between Mammalian Immune Cells

Hannah W. Miller, Akhila Bettadapur, Tina Truong and Katherine S. Ralston

Abstract

Trogocytosis is a process common to many eukaryotes from microbes to mammalian immune cells. Cells extract small pieces of target cells rather than eating them whole as in phagocytosis. It can be lethal or benign and is also characterized by the transfer of membrane proteins from one cell to another. Here we developed an assay that can be used to further study trogocytosis in mammalian macrophages. We found that the mouse macrophage lines J774A.1 and RAW 264.7 perform trogocytosis on human Raji B cells. Trogocytosis occurred with or without opsonization of B cells using an anti-CD20 monoclonal antibody and was increased with opsonization. We detected transfer of CD20 molecules, dyed membrane patches, and biotinylated proteins from target B cells to the recipient macrophages. Furthermore, transfer was inhibited by cytochalasin D treatment, a known inhibitor of trogocytosis. Therefore, the assay we developed can be used to quantify trogocytosis in macrophages and could be employed to study this process further.

Introduction

Trogocytosis or “cell-nibbling” is a endocytic process that occurs in a variety of eukaryotes (1). It occurs when one cell ingests small pieces of another cell, rather than ingesting it whole as in phagocytosis, and is also characterized by transfer of membrane proteins from donor to recipient cells (2). Trogocytosis has been shown in the microbes *Entamoebae histolytica (3, 4)*, *Naegleria fowleri* (5) and *Dictyostelium caveatum* (6). It is also found in multicellular eukaryotes where it serves functions in the immune system (7, 8), in the central nervous system (9, 10), and during development (11). Instances of trogocytosis can be benign, as form of cell-cell interaction, or can be lethal, as mechanism for cell-killing, pointing to its broad range of functions in eukaryotes. For example, in the mammalian immune system, uninfected dendritic cells are able to non-lethally acquire and display major histocompatibility complex class II (MHC II) molecules through trogocytosis of infected dendritic cells (8). By contrast, neutrophils and macrophages can both use trogocytosis to kill cancer cells (12, 13). Consequently, the process of trogocytosis appears to be fundamental to eukaryotes and demands further study.

Here, we developed an assay that could be employed for further investigation of immune cell trogocytosis. Trogocytosis can occur when phagocytes recognize antibody coated target cells through engagement of their Fcγ receptors (13, 14). For example, both macrophages and neutrophils kill anti-CD20 opsonized target cells through trogocytosis (13, 15). Therefore, we utilized an anti-CD20 antibody to induce trogocytosis of opsonized B cells in macrophages. We were able to successfully induce

trogocytosis in two separate mouse macrophage cell lines. We quantified transferred CD20 molecules from target B cells to effector macrophages using imaging flow cytometry. We were also able to quantify transfer of membrane patches labeled with the membrane dye DiD, as well as biotinylated membrane proteins. Finally, we found that cytochalasin D, a known inhibitor of trogocytosis, reduced transferred membrane material. Therefore, we have developed an assay that can be used to quantify trogocytosis in macrophages and further investigate this eukaryotic process.

Results

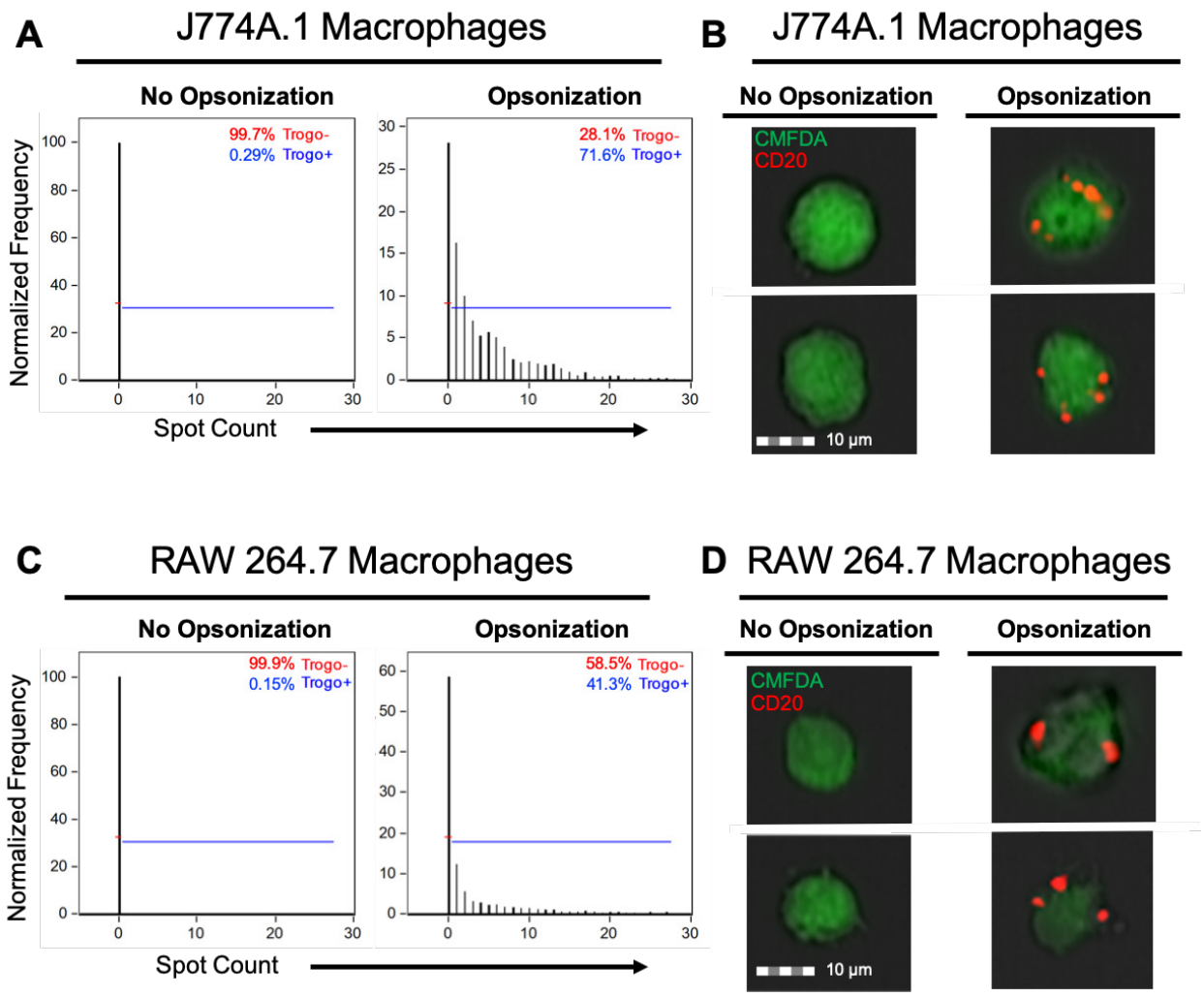

Fig. 5.1: **Trogocytosis and acquisition of CD20 was detected in mouse macrophages. (A-D)** J774A.1 or RAW 264.7 mouse macrophages were stained with the cytoplasm dye CMFD and allowed to perform trogocytosis on Raji B cells that had been opsonized with a monoclonal antibody to CD20 or left untreated. Displayed CD20 molecules were detected using immunofluorescence and imaging flow cytometry. CD20 was quantified using the "spot count" feature and Amnis IDEAS software. **(A)** % trogocytosis positive and negative J774A.1 macrophages. **(B)** Representative images of displayed CD20 on J774.1 macrophages. **(C)** % trogocytosis positive and % negative RAW 264.7 macrophages. **(B)** Representative images of displayed CD20 on RAW 264.7 macrophages. Data are from one independent experiment.

Trogocytosis and acquisition of CD20 was detected in mouse macrophages.

In order to study trogocytosis in phagocytes, we utilized two mouse macrophage lines and human Raji B cells. CD20 is a B cell marker that has been used extensively as

a target for monoclonal antibody treatment of B cell malignancies (16). We opsonized the B cells with a monoclonal mouse IgG1 antibody specific to human CD20 and co-incubated them with either J774A.1 or RAW 264.7 fluorescently labeled macrophages. As a control, we co-incubated macrophages with B cells that were left untreated. Next, we detected transferred CD20 molecules from B cells to macrophages that had undergone trogocytosis with a fluorescently conjugated anti-mouse secondary antibody. Using imaging flow cytometry, and the "spot count" feature in Amnis IDEAS software, we were able to quantify transferred CD20 **(Fig. 5.1A and C)**. No staining was detected on negative control cells that did not receive anti-CD20 antibody. Both J774A.1 and RAW 264.7 macrophages performed trogocytosis and transferred CD20 molecules appeared as small patches. **(Fig. 5.1B and D)**. Hence, macrophages acquire CD20 molecules from target cells through trogocytosis.

Trogocytosis and transfer of target cell membrane occurs both in the presence and absence of opsonization.

Next, we wanted to detect trogocytosis using a method independent of the anti-CD20 antibody used for opsonization. Use of the same primary CD20 antibody for both opsonization and to detect transferred CD20 molecules meant that we were unable to test for trogocytosis in non-opsonized samples, as they did not receive any CD20 antibody. We therefore chose to assay for the transfer of cell membrane patches using a membrane dye. This would allow us to look at baseline trogocytosis in the non-opsonized samples as well. We labeled B cells with a membrane dye that labels lipids

and quantified transfer of membrane patches in samples that had been opsonized or left untreated. For comparison to previous data, we also detected transferred CD20 molecules. As before, CD20 molecules from opsonized B cells were transferred to macrophages that had undergone trogocytosis **(Fig. 5.2A-B)**. Surprisingly, transfer of dye labeled membrane patches revealed that trogocytosis occurred in macrophages co-incubated with both opsonized and untreated B cells, though to a greater degree with opsonization **(Fig. 5.2C-D)**. While opsonization only increased the percentage of amoebae in the trogocytosis positive group by 8.8%, these amoebae also had a greater

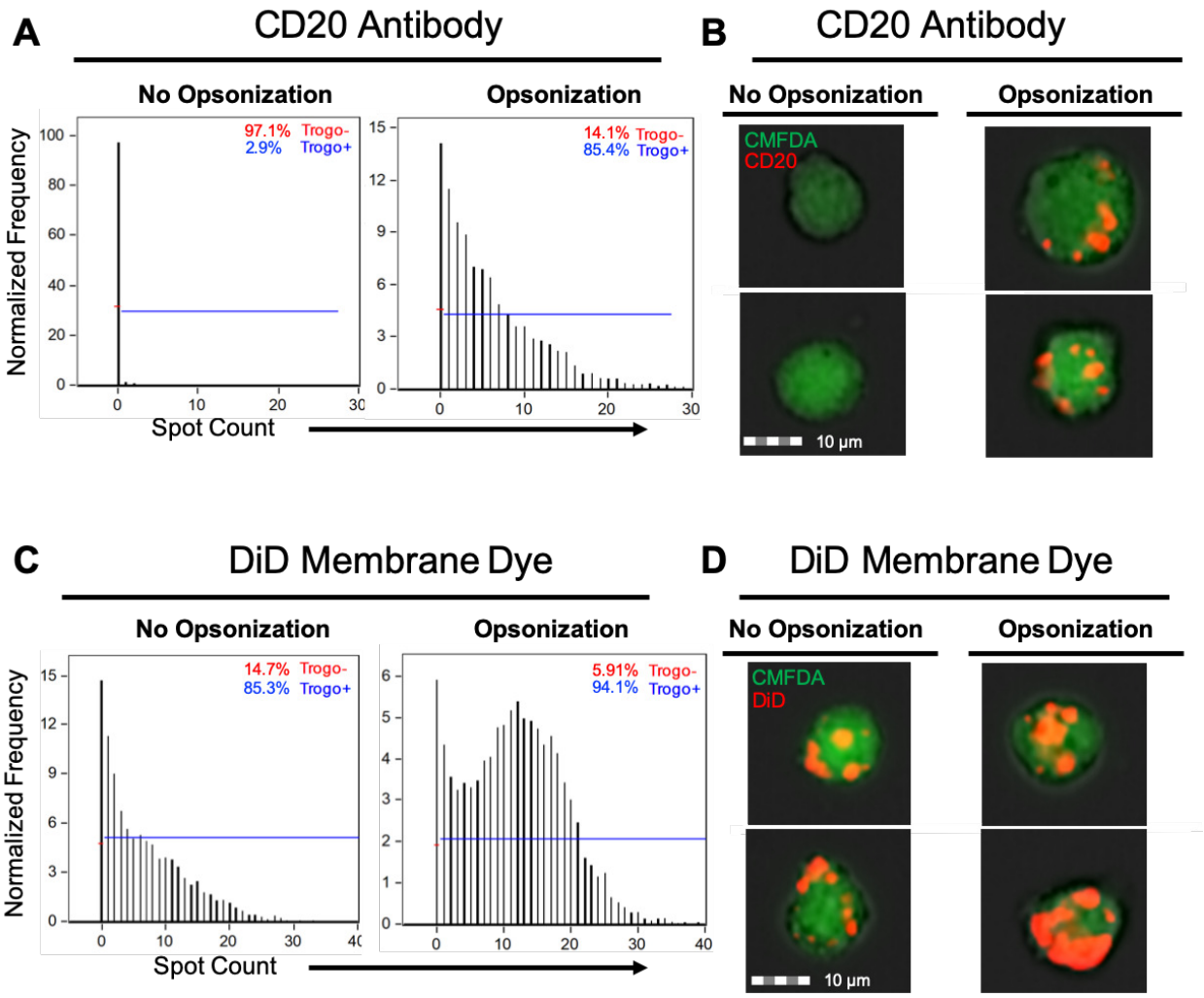

Fig. 5.2: **Trogocytosis and transfer of target cell membrane occurs both the presence and absence of opsonization. (A-D)** J774A.1 mouse macrophages were stained with the cytoplasm dye CMFD and allowed to perform trogocytosis on Raji B cells that had been opsonized with a monoclonal antibody to CD20 or left untreated. **(A-B)** Displayed CD20 molecules were detected using immunofluorescence and imaging flow cytometry. **(A)** % trogocytosis positive and negative J774A.1 macrophages. **(B)** Representative images of displayed CD20 on J774.1 macrophages. **(C-D)** Raji cells were labeled with the membrane dye DiD prior to co-incubation with macrophages. Displayed membrane patches were quantified using imaging flow cytometry **(C)** % trogocytosis positive and % negative J774A.1macrophages. **(B)** Representative images of displayed DiD membrane on J774A.1 macrophages. Data are from one independent experiment.

number of transferred membrane patches **(Fig. 5.2C-D)**. The dyed membrane patches were similar in appearance to the transferred CD20 molecules, but brighter overall **(Fig. 5.2D)**. Therefore, macrophages perform trogocytosis both in the presence and absence of opsonization of target cells.

CD20 molecules are transferred via trogocytosis without opsonization.

We next wanted to assay for the presence of whole B cells contamination or phagocytosis in these samples. By pre-labeling B cells with the nucleic acid dye Hoechst, we were able to detect macrophages with the presence of whole B cell nuclei in both the CD20 and DiD assays, and these cells contributed somewhat to the "trogocytosis positive" population (data not shown). Detection of B cell nuclei is more consistent with phagocytosis than trogocytosis, since nuclei are not nibbled during trogocytosis. The presence of B cell nuclei could also indicate that some whole B cells remained attached to macrophages, even though attempts were made to wash and remove non-ingested B cells. This should be taken into consideration when interpreting CD20 or membrane transfer results.

In previous assays that examined transfer of CD20 molecules, only samples with opsonized target cells received the primary CD20 antibody. We attempted to opsonize target cells with CD20 and quantify trogocytosis by examining transfer of CD19, however the CD19 antibody used proved to be non-specific (Data not shown). Since we had observed trogocytosis of non-opsonized target cells when we assayed for transferred membrane patches, we labeled macrophages with the CD20 antibody following trogocytosis of non-opsonized B cells. This allowed us to observe transfer of CD20 to macrophages that had performed trogocytosis on non-opsonized cells. We compared J774A.1 and RAW 264.7 mouse macrophage lines. We also used the human monocyte line THP-1. CD20 staining was compared to samples that did not received any antibody as a negative control. Samples that did not received any primary antibody did not show any CD20 fluorescence verifying the specificity of our antibody staining

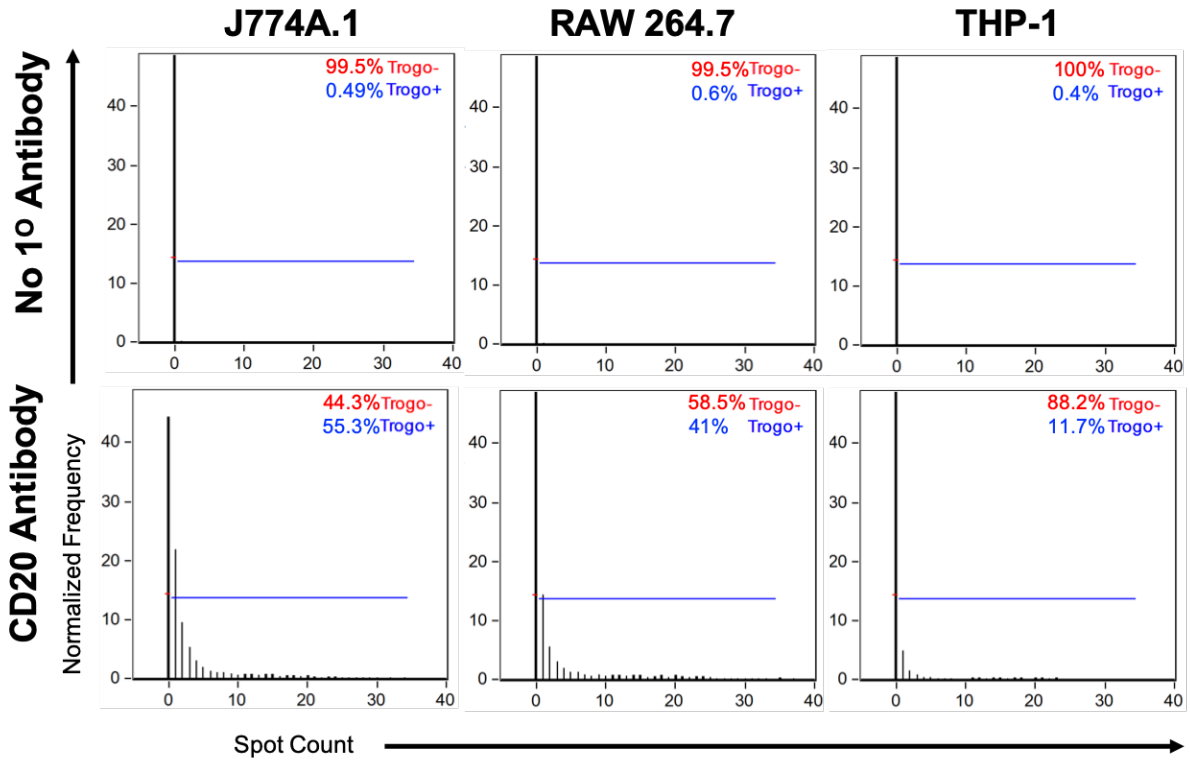

Fig. 5.3: **CD20 molecules are transferred via trogocytosis without opsonization.** J774.1, RAW 264.7 or THP-1 macrophages were incubated with non-opsonized Raji B cells. Following trogocytosis, displayed CD20 was quantified using a monoclonal CD20 antibody and imaging flow cytometry. Samples that did not receive primary antibody served as negative controls. % trogocytosis positive and % trogocytosis negative macrophages are displayed for each cell line. Data are from one independent experiment.

(Fig. 5.3.) We detected CD20 transfer in all three cell lines, though to a lesser degree than we had observed previously with opsonized target cells **(Fig. 5.3)**. Additionally, the mouse macrophage lines performed more trogocytosis than the human THP-1 monocytes **(Fig. 5.3)**. These results were consistence with our previous observation of trogocytosis in samples that did not receive opsonization when we assayed for transferred membrane patches.

Cytochalasin D inhibits macrophage trogocytosis.

Trogocytosis requires actin rearrangements. Cytochalasin D, a drug that inhibits actin polymerization, is a known inhibitor of trogocytosis (17). In *E. histolytica*, cytochalasin D treatment blocks the ingestion of host cells as well as the transfer of host proteins by trogocytosis (3, 18). We asked if cytochalasin D treatment would prevent the transfer of CD20 molecules and membrane patches in macrophages. We compared trogocytosis in J774A.1 macrophages treated with cytochalasin D to dimethyl sulfoxide (DMSO) treated controls in samples that received opsonized or non-opsonized target cells. We detected transferred CD20 molecules in samples that received opsonized B cells and cytochalasin D treatment decreased the amount of transferred CD20 **(Fig. 5.4A)**. When we analyzed transferred membrane patches, macrophages co-incubated with both opsonized and non-opsonized target cells acquired dye labeled membrane.

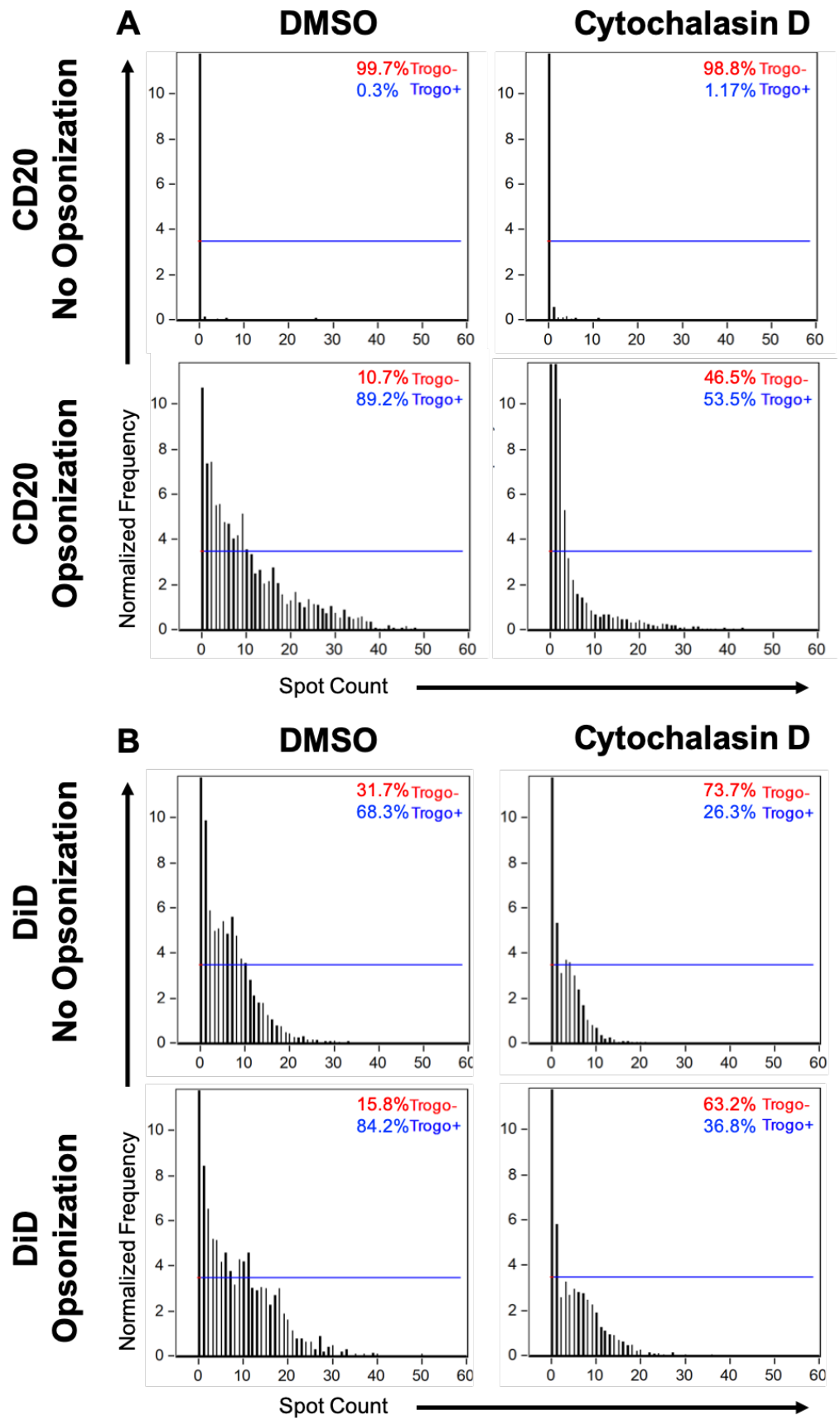
A
DMSO
Cytochalasin D
CD20
No Opsonization
CD20
Opsonization
99.7% Trogo-
0.3% Trogo+
98.8% Trogo-
1.17% Trogo+
10.7% Trogo-
89.2% Trogo+
46.5% Trogo-
53.5% Trogo+
Normalized Frequency
Spot Count
B
DMSO
Cytochalasin D
DiD
No Opsonization
DiD
Opsonization
31.7% Trogo-
68.3% Trogo+
73.7% Trogo-
26.3% Trogo+
15.8% Trogo-
84.2% Trogo+
63.2% Trogo-
36.8% Trogo+
Normalized Frequency
Spot Count

Fig. 5.4: **Cytochalasin D inhibits transfer of CD20 molecules and membrane patches. (A-B)** J774A.1, macrophages were pre-treated with cytochalasin D and allowed to perform trogocytosis on Raji B cells that had been opsonized with a CD20 antibody or left untreated. Macrophages were treated with DMSO as a control. Trogocytosis was quantified using immunofluorescence and imaging flow cytometry. **(A)** Displayed CD20 was used as readout for trogocytosis. % trogocytosis positive and % trogocytosis negative macrophages in each condition. **(B)** Raji cells were prelabeled with DiD membrane dye prior to co-incubation with macrophages. Transferred DiD membrane patches were used as readout for trogocytosis. % trogocytosis positive and % trogocytosis negative macrophages in each condition. Data are from one independent experiment.

Opsonized samples acquired more membrane patches and cytochalasin D treatment decreased trogocytosis in both groups **(Fig. 5.4B)**.

Next, we asked if the same would be true of trogocytosis in RAW 264.7 macrophages. We compared the effect of cytochalasin D treatment on trogocytosis in J774A.1 and RAW 264.7 macrophages of opsonized and non-opsonized B cells. We chose to examine acquired dye labeled membrane as a readout for trogocytosis because it did not rely on the CD20 antibody used for opsonization. Consistent with our previous results, macrophages acquired more membrane from opsonized target cells, though still acquired some from non-opsonized cells **(Fig. 5.5A-B)**. Trogocytosis was inhibited in both mouse macrophage lines following cytochalasin D treatment **(Fig. 5.5.A-B)**. Therefore, cytochalasin D treatment inhibits trogocytosis in mouse macrophages.

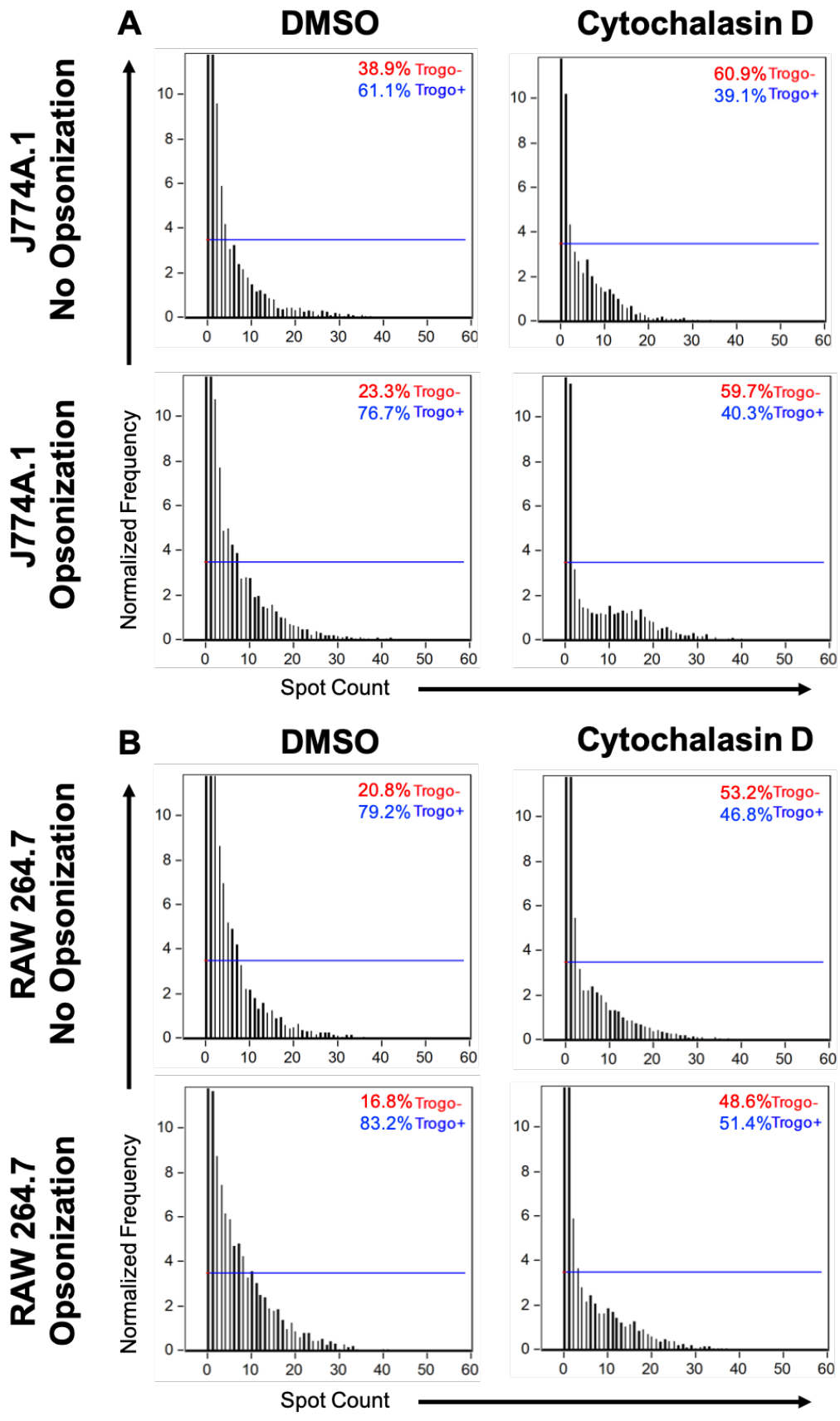
A
DMSO
Cytochalasin D
J774A.1
No Opsonization
38.9% Trogo-
61.1% Trogo+
60.9% Trogo-
39.1% Trogo+
J774A.1
Opsonization
23.3% Trogo-
76.7% Trogo+
59.7% Trogo-
40.3% Trogo+
Normalized Frequency
Spot Count
B
DMSO
Cytochalasin D
RAW 264.7
No Opsonization
20.8% Trogo-
79.2% Trogo+
53.2% Trogo-
46.8% Trogo+
RAW 264.7
Opsonization
16.8% Trogo-
83.2% Trogo+
48.6% Trogo-
51.4% Trogo+
Normalized Frequency
Spot Count

Fig. 5.5: **Cytochalasin D inhibits trogocytosis in both J774A.1 and RAW 264.7 macrophages. (A-B)** J774A.1 or RAW macrophages were pre-treated with cytochalasin D and allowed to perform trogocytosis on Raji B cells that had been opsonized with a CD20 antibody or left untreated. Macrophages were treated with DMSO as a control. Raji cells were prelabeled with DiD membrane dye prior to co-incubation with macrophages. Transferred DiD membrane patches were used as readout for trogocytosis and were quantified using immunofluorescence and imaging flow cytometry. **(A)** % trogocytosis positive and % trogocytosis negative J774A.1 macrophages in each condition. **(B)** % trogocytosis positive and % trogocytosis negative RAW 264.7 macrophages in each condition. Data are from one independent experiment.

Biotinylated membrane proteins are transferred via trogocytosis and transfer is inhibited by cytochalasin D treatment.

Having observed transfer of CD20 molecules and patches of membrane from target B cells to macrophages, we wanted to examine the transfer of biotinylated membrane proteins. Additionally, since the previous two methods for detecting trogocytosis included whole B cell contamination in the analysis, we were interested looking at transferred proteins in a more accurate way. Raji B cells were biotinylated and co-incubated with RAW264.1 macrophages. Since we had detected trogocytosis without opsonization, B cells were not opsonized. Following trogocytosis, fluorescently-conjugated streptavidin was used to detect transferred B cell proteins. Samples that did not receive B cells were used a negative control for the biotin/streptavidin staining. Additionally, cytochalasin D treated samples were compared to DMSO controls. No biotin/streptavidin fluorescence was detected in samples that did not receive biotinylated B cells **(Fig. 5.6A-B)**. Biotinylated target cell proteins were detected on macrophages that had undergone trogocytosis, and cytochalasin D treatment inhibited trogocytosis **(Fig. 5.6A)**. Patches of transferred biotinylated proteins were similar in appearance to transferred CD20 and dyed membrane **(Fig. 5.6B)**. In this assay,

because whole B cells fluoresced much more brightly then the transferred biotinylated proteins, we were able to exclude them from the analysis. Thus, we were able to more accurately measure transferred proteins. Therefore, examining transfer of biotinylated proteins from target to recipient cells was the most accurate method tested for quantifying trogocytosis.

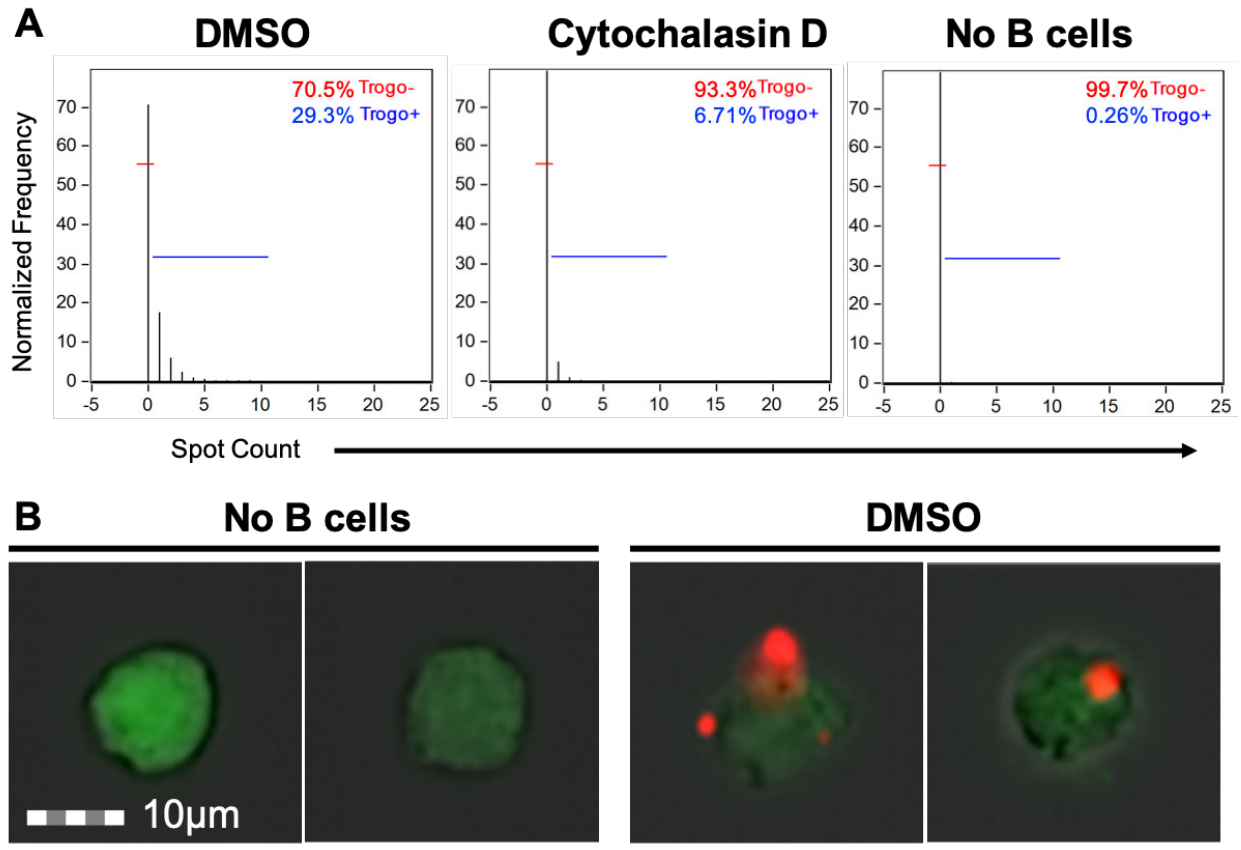

Fig. 5.6: **Biotinylated membrane proteins are transferred via trogocytosis and transfer is inhibited by cytochalasin D treatment. (A-B)** Raji B cells were biotinylated and then co-incubated with RAW264.1 macrophages without opsonization. Following co-incubation biotinylated proteins were detected with fluorescently conjugated streptavidin and quantified using imaging flow cytometry. **(A)** % trogocytosis positive macrophages in DMSO or cytochalasin D treated samples or controls. **(B)** Representative images of displayed biotinylated proteins. Data are from one independent experiment.

Discussion

We developed an assay that we used to quantify trogocytosis-dependent transfer of membrane proteins from target to recipient cells in the mouse macrophage lines J774A.1 and RAW 264.7. We were able to use it to detect transfer of CD20 molecules, fluorescently labeled membrane, and biotinylated membrane proteins from target B cells to recipient macrophages. One surprising discovery was the trogocytosis of non-opsonized B cells as previous data in the literate has indicated the need for Fcγ receptor engagement. Further study will be needed to elucidate the mechanism of trogocytosis in macrophages outside of Fcγ receptor engagement.

While our results from this preliminary study are promising, there are several caveats that should be taken into consideration. Each assay was performed only once, and the data shown in each figure are from one independent experiment. Our goal in this study was to optimize an assay that could reliably detect trogocytosis in macrophages. Further replicates would need to be performed if any of the methods reported in this chapter were to be used to interrogate hypotheses experimentally.

In experiments utilizing CD20 or the membrane dye DiD as a readout for trogocytosis, we did not remove any remaining whole B cells from the analysis. While B cells were washed off of the macrophages before they were collected, the data shown include minimal contamination of whole B cells still present. This could either be due to phagocytosis of B cells or attached extracellular B cells. We pre-labeled B cells with the nucleic acid dye Hoechst prior to co-incubation with macrophages in some experiments

and identified that there were indeed Hoechst labeled B cells still present in these samples.

There are several limitations to the use of these assays for quantifying trogocytosis. One major problem is an excessive amount of cell loss from start to finish. While we improved the number of cells that we were able to collect for imaging by coating our sample tubes with 1% BSA, we still only recovered a few thousand cells per sample. Additionally, the protocols presented require a lengthy amount of time to perform. Due to the large amount of cell loss, they are also very dilute and require additional time to image.

A further limitation is the inability to quantify both ingestion and transfer of surface proteins. Use of antibodies or biotin for labeling extracellular proteins allowed for quantification of displayed proteins but did not measure ingested cellular material. The use of a membrane dye allowed for visualization of membrane patches, however, could not distinguish between surface localized patches and ingested material. As trogocytosis results in both ingestion of pieces of target cells as well as transfer of surface proteins it would be useful to detect both of these outcomes.

In the assay that looked at transfer of biotinylated membrane proteins, we were able to gate out whole B cells by excluding cells that fluoresced most brightly for streptavidin from the analysis. Therefore, using biotin as a readout for trogocytosis was the most accurate method we tested. Furthermore, cytochalasin D treatment inhibited biotinylated protein transfer consistent with trogocytosis.

We have developed an assay for use in quantifying macrophage trogocytosis that detects transfer of biotinylated membrane proteins from target to recipient cells. This assay can be used for further study of macrophage trogocytosis and further elucidate this important aspect of eukaryote biology.

Materials and Methods

Cell Culture

J774A.1 (ATCC) and RAW 264.7 (ATCC) mouse macrophages were cultured in Dulbecco's Modified Eagle Medium (DMEM) (ThermoFisher Scientific; with High Glucose, L-glutamine, Phenol Red, Sodium Pyruvate) supplemented with supplemented with 10% heat-inactivated fetal bovine serum (Gibco), 100 U/ml penicillin and 100 μg/ml streptomycin. Cells were grown in vented T25 or T75 tissue culture flasks at 37°C and 5% CO_2. Cells were harvested when flasks reached ~80% confluency by scraping cells from the bottom of the flasks using a cell scraper. Macrophages were harvested and transferred into 6 well plates for use in experimental assays. Macrophages were resuspended in RPMI 1640 medium (Gibco; RPMI 1640 with L-glutamine and without phenol red) supplemented with 0.5% bovine serum albumin (BSA) for use in trogocytosis assays.

THP-1 (ATCC) human monocytes were cultured in RPMI 1640 medium (Gibco; RPMI 1640 with L-glutamine and without phenol red) supplemented with 10% heat-inactivated fetal bovine serum (Gibco), 100 U/ml penicillin, 100 μg/ml streptomycin and 0.05mM 2-mercaptoethanol.THP-1 monocytes were grown in T25 or T75 vented tissue culture flasks at 37°C and 5% CO_2 and kept at a concentration of $8x10^5$ cell/ml - $1x10^6$ cells/ml. THP-1 cells were resuspended in RPMI medium supplemented with 0.5% bovine serum albumin (BSA) for use in trogocytosis assays.

Human Raji B cells (ATCC) were cultured in RPMI 1640 medium (Gibco; RPMI 1640 with L-glutamine and without phenol red) supplemented with 10% heat-inactivated

fetal bovine serum (Gibco), 100 U/ml penicillin and 100 μg/ml streptomycin. Raji cells were grown in vented T25 or T75 culture flasks and kept at a concentration of $4x10^5$ cells/ml - $3x10^6$ cells/ml. Cells were grown at 37°C and 5% CO_2. Raji cells were resuspended in RPMI medium supplemented with 0.5% bovine serum albumin (BSA) for use in trogocytosis assays.

Trogocytosis Assays

Approximately 1.5 x 10^6 macrophages per sample were plated in 6 well plates and were labeled with CellTracker green 5-chloromethylfluorescein diacetate (CMFDA; Invitrogen) membrane dye at a concentration of ~370ng/ml for 15min at 37°C. Macrophages washed and then placed in RPMI medium. Raji B cells were left untreated or opsonized with 1ug/ml of a monoclonal mouse IgG1 antibody against human CD20 (InvivioGen; Anti-hCD20-mIgG1) for 30 minutes at 4°C. Media was removed from the plated macrophages, and ~7.5 x 10^6 Raji B cells in RPMI medium were added to each sample. Samples were incubated at 37°C. In some experiments Raji cells and macrophages were co-incubated for 80 minutes and in others they were co-incubated for 30 minutes. Following co-incubation Raji cells were washed off of macrophages and ice cold EDTA at concentration of 2mM was added to the sample wells. Macrophages were then collected using a cell scraper and placed in 1.5ml microtubes that had been pre-coated with 1% BSA. Samples were fixed with 4% paraformaldehyde (PFA) for 30 minutes at room temperature. Samples were washed and blocked in 1x phosphate-buffered saline (PBS) with 5% normal goat serum (Jackson ImmunoResearch

Laboratories, Inc) for 30 minutes at 4°C. Next, samples were labeled with an anti-mouse Alexa Fluor 647 secondary antibody (Jackson Immunoresearch Labs Inc.) at a 1:200 dilution for 30 minutes at room temperature. Samples were washed and resuspended in 1xPBS for imaging.

Prior to opsonization, Raji B cells were labeled with DiD membrane dye (AAT Bioquest; DiIC18(5)-DS) at 21 μg/ml for 5 minutes at 37°C and 10 minutes at 4°C, or left unstained in some experiments. These samples did not receive secondary antibody. Additionally, in some assays, Raji B cells were labeled with 1ug/ml of Hoechst 33342 (ThermoFisher Scientific).

In assays with cytochalasin D, Raji B cells and macrophages were pretreated with DMSO at μl/ml or cytochalasin D at a final concentration of 20mM for 1 hour prior to co-incubation. Additional, cytochalasin D and DMSO were present in sample media throughout the assay.

For the biotinylating experiment, Raji B cells were biotinylated with EZ-Link Sulfo-NHS-SS-Biotin (ThermoFisher Scientific) at 480 μg/ml in 1× PBS for 25 min at 4°C. Following fixation, samples were labeled with Alexa Fluor 633 conjugated streptavidin (Invitrogen) at 20 μg/ml for 1 hour at room temperature.

Imaging Flow Cytometry

Samples were run on an Amnis ImageStreamX Mark II, and the CMFDA positive macrophage population was collected. For analysis refer to figure S5.1.

Acknowledgments

We thank the members of our laboratory for helpful discussions. All ImageStream data were acquired using shared instrumentation in the UC Davis MCB Light Microscopy Imaging Facility. We thank Dr. Michael Paddy for technical support on this instrument. This work was funded by start-up funding and a UCD early career award to K.S.R.

Author Contributions

H.W.M and A.B. designed, performed, and analyzed the experiments. H.W.M. performed additional analyses for use in this chapter. T.T. developed the original protocol that was used and modified for the experiments. K.S.R. conceived of the overall approach and oversaw the design and analysis of the experiments. H.W.M wrote the chapter and it was edited by K.S.R.

References

1. Bettadapur A, Miller HW, Ralston KS. 2020. Biting Off What Can Be Chewed: Trogocytosis in Health, Infection, and Disease. Infect Immun 88:e00930-19.

2. Joly E, Hudrisier D. 2003. What is trogocytosis and what is its purpose? Nature Immunology 4:815.

3. Ralston KS, Solga MD, Mackey-Lawrence NM, Somlata null, Bhattacharya A, Petri WA. 2014. Trogocytosis by Entamoeba histolytica contributes to cell killing and tissue invasion. Nature 508:526–530.

4. Somlata null, Nakada-Tsukui K, Nozaki T. 2017. AGC family kinase 1 participates in trogocytosis but not in phagocytosis in Entamoeba histolytica. Nat Commun 8:101.

5. Brown T. 1979. Observations by immunofluorescence microscopy and electron microscopy on the cytopathogenicity of naegleria fowleri in mouse embryo-cell cultures. Journal of Medical Microbiology 12:363–371.

6. Waddell DR, Vogel G. 1985. Phagocytic behavior of the predatory slime mold, Dictyostelium caveatum. Cell nibbling. Exp Cell Res 159:323–334.

7. Batista FD, Iber D, Neuberger MS. 2001. B cells acquire antigen from target cells after synapse formation. Nature 411:489–494.

8. Wakim LM, Bevan MJ. 2011. Cross-dressed dendritic cells drive memory CD8+ T-cell activation after viral infection. Nature 471:629–632.

9. Davis CO, Kim K-Y, Bushong EA, Mills EA, Boassa D, Shih T, Kinebuchi M, Phan S, Zhou Y, Bihlmeyer NA, Nguyen JV, Jin Y, Ellisman MH, Marsh-Armstrong N. 2014. Transcellular degradation of axonal mitochondria. Proc Natl Acad Sci USA 111:9633–9638.

10. Weinhard L, di Bartolomei G, Bolasco G, Machado P, Schieber NL, Neniskyte U, Exiga M, Vadisiute A, Raggioli A, Schertel A, Schwab Y, Gross CT. 2018. Microglia remodel synapses by presynaptic trogocytosis and spine head filopodia induction. Nat Commun 9:1228.

11. Abdu Y, Maniscalco C, Heddleston JM, Chew T-L, Nance J. 2016. Developmentally programmed germ cell remodelling by endodermal cell cannibalism. Nat Cell Biol 18:1302–1310.

12. Matlung HL, Babes L, Zhao XW, van Houdt M, Treffers LW, van Rees DJ, Franke K, Schornagel K, Verkuijlen P, Janssen H, Halonen P, Lieftink C, Beijersbergen RL, Leusen JHW, Boelens JJ, Kuhnle I, van der Werff Ten Bosch J, Seeger K, Rutella S, Pagliara D, Matozaki T, Suzuki E, Menke-van der Houven van Oordt CW, van Bruggen R, Roos D, van Lier RAW, Kuijpers TW, Kubes P, van den Berg TK. 2018. Neutrophils Kill Antibody-Opsonized Cancer Cells by Trogoptosis. Cell Rep 23:3946-3959.e6.

13. Velmurugan R, Challa DK, Ram S, Ober RJ, Ward ES. 2016. Macrophage-Mediated Trogocytosis Leads to Death of Antibody-Opsonized Tumor Cells. Mol Cancer Ther 15:1879–1889.

14. Beum PV, Mack DA, Pawluczkowycz AW, Lindorfer MA, Taylor RP. 2008. Binding of Rituximab, Trastuzumab, Cetuximab, or mAb T101 to Cancer Cells Promotes Trogocytosis Mediated by THP-1 Cells and Monocytes. The Journal of Immunology 181:8120–8132.

15. Valgardsdottir R, Cattaneo I, Klein C, Introna M, Figliuzzi M, Golay J. 2017. Human neutrophils mediate trogocytosis rather than phagocytosis of CLL B cells opsonized with anti-CD20 antibodies. Blood 129:2636–2644.

16. Casan JML, Wong J, Northcott MJ, Opat S. 2018. Anti-CD20 monoclonal antibodies: reviewing a revolution. Hum Vaccin Immunother 14:2820–2841.

17. Ralston KS, Solga MD, Mackey-Lawrence NM, Somlata, Bhattacharya A, Petri Jr WA. 2014. Trogocytosis by *Entamoeba histolytica* contributes to cell killing and tissue invasion. Nature 508:526–530.

18. Miller HW, Suleiman RL, Ralston KS. 2019. Trogocytosis by Entamoeba histolytica Mediates Acquisition and Display of Human Cell Membrane Proteins and Evasion of Lysis by Human Serum. mBio 10:e00068-19.

Supplemental Material

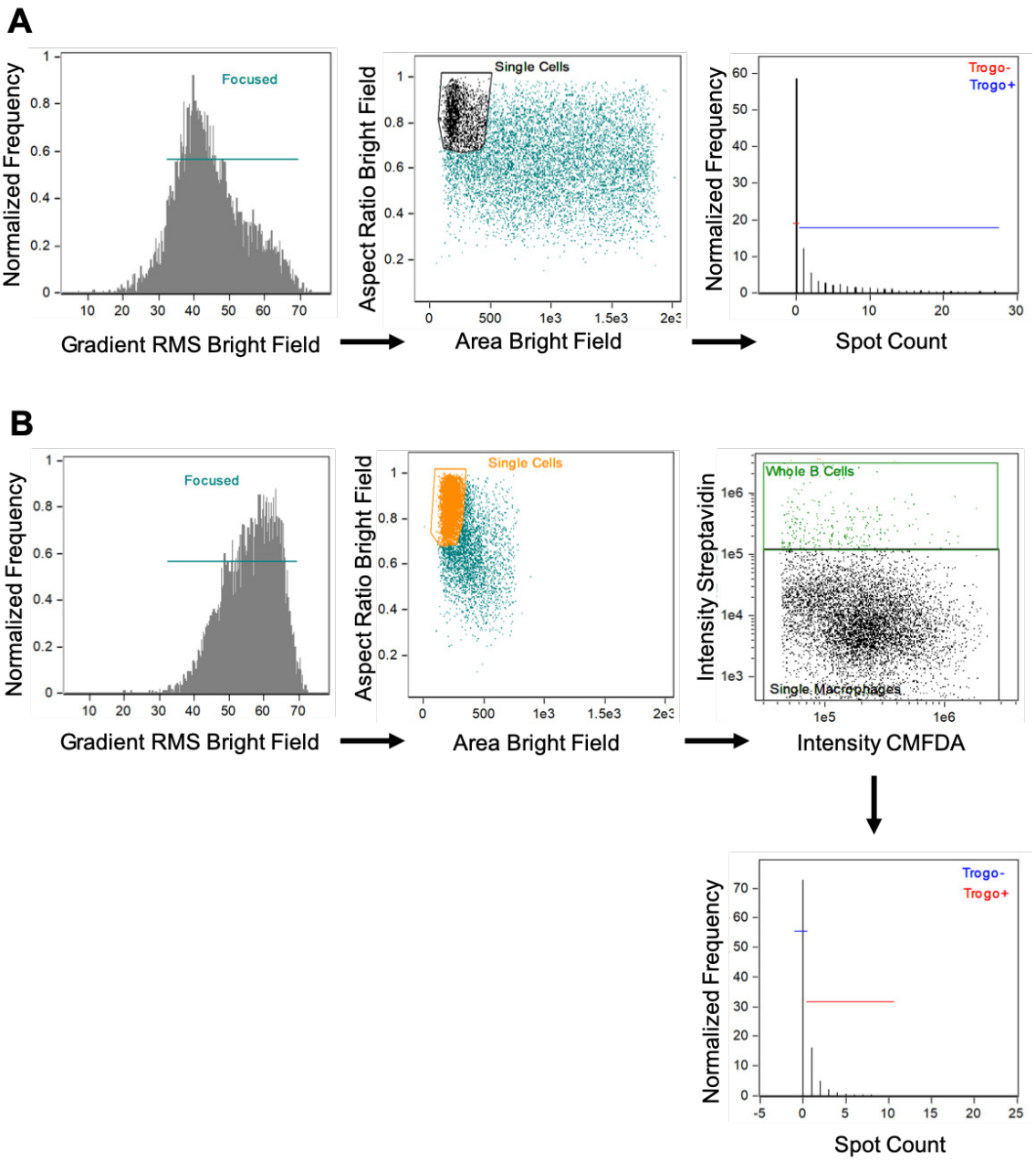

Fig. S5.1: Gating schemes used to analyze experiments. (A) Gates used to analyze CD20 and DiD membrane transfer experiments. After gating on focused cells, single cells were identified by brightfield area and aspect ratio. The “spot count” feature in Amnis IDEAS software was then used to quantify patches CD20 or DiD on macrophages. **(B)** Gates used to analyze transfer of biotinylated proteins. After gating on focused cells, single cells were identified by brightfield area and aspect ratio. Next, whole B cells were excluded from the analysis by gating on the streptavidin population that fluoresced less brightly. The “spot count” feature in Amnis IDEAS software was then used to quantify patches of biotin/streptavidin on macrophages.

Chapter 6

Generation of *Eh*C2PK, *Eh*AGCK1 and *Eh*AGCK2 Mutants in *Entamoeba histolytica* and Characterization of the Resulting Ingestion Phenotypes

Hannah W. Miller, Valeria Wang and Katherine S. Ralston

Abstract

Entamoeba histolytica is responsible for the diarrheal disease amoebiasis. Amoebic trogocytosis is a major virulence factor that contributes to human cell killing and immune evasion. A mutant defective in trogocytosis would therefore be a valuable tool for future study of *E. histolytica* infection and for further characterizing the contribution of trogocytosis to tissue damage and immune evasion. We used RNAi to generate *Eh*C2PK, *Eh*AGCK1 and *Eh*AGCK2 knockdown mutants as these genes have been reported to be involved in *E. histolytica* phagocytosis and trogocytosis. A mutant silenced for *Eh*C2PK displayed a trogocytosis defect at two of the time points tested and was deficient in phagocytosis. Silencing of *Eh*AGCK1 resulted in a clonal line lacking trogocytosis defects and another with a trogocytosis defect at one time point tested. Silencing of *Eh*AGCK2 did not result in a trogocytosis defect compared to control amoebae. While further research is required for creation of a mutant with a robust trogocytosis phenotype, we have generated a mutant deficient in both trogocytosis and phagocytosis and a mutant deficient in trogocytosis. These mutants could be used in future studies to gain insights into the roles these forms of ingestion play in *E. histolytica* biology such as acquisition of host membrane proteins or evasion from complement lysis.

Introduction

The parasite *Entamoeba histolytica* is responsible for diarrheal disease, colitis and potentially fatal extraintestinal abscesses (1). Trogocytosis, or “cell nibbling”, is an important virulence factor in this organism. Trophozoites (amoebae) are able to kill living human cells by ingesting small bites, which leads to membrane disruption and cell death (2). Furthermore, trogocytosis of human cells protects amoebae from complement lysis, a critical function of host immunity (3) (chapter 3). It would therefore be of great interest to generate an amoeba mutant defective in trogocytosis. Such a mutant would be a valuable tool in better understanding the contribution of amoebic trogocytosis to pathogenesis during amoebiasis.

The molecular mechanism of amoebic trogocytosis is not well defined (4). Molecules that are known to be involved include: the Gal/GalNAc lectin, the C2-domain-containing protein kinase *Eh*C2PK, actin, phosphatidylinositol 3-kinase (PI3K), and *Entamoeba* AGC family kinase 1 (*Eh*AGCK1) (4, 5). All of these with the exception of *Eh*AGCK1 are also involved in amoebic phagocytosis (4). Here, we attempted to create trogocytosis mutants by using RNAi to silence *Eh*C2PK, *Eh*AGCK1 and *Eh*AGCK2.

*Eh*C2PK has been shown to be involved in the initial stages of phagocytosis. It localizes to the phagocytic cups, where it binds to the calcium-binding protein *Eh*CaBP1, which then binds actin (6, 7). We have demonstrated that *Eh*C2PK is also involved in trogocytosis. An over-expression tetracycline-inducible kinase-dead point mutant of *Eh*C2PK displayed a reduced ability to perform trogocytosis on human cells than control amoebae (2).

*Eh*AGCK1 and *Eh*AGCK2 have been found to have roles in phagocytosis and trogocytosis. Knockdown mutants silenced for *Eh*AGCK2 were defective in both phagocytosis and trogocytosis, while mutants silenced for *Eh*AGCK1 exhibited only a trogocytosis defect (5). *Eh*AGCK2 localizes to both the phagocytic and "trogocytic" cups, however, *Eh*AGCK1 only localizes to the trogocytic cups (5).

We used a modern approach to RNAi silencing in *E. histolytica* to generate *Eh*C2PK, *Eh*AGCK1 and *Eh*AGCK2 mutants. This method takes advantage of an endogenously silent "trigger gene" and generates small RNAs that interfere with the gene of interest (8). We found that silencing of *Eh*C2PK resulted in a slight trogocytosis defect and impaired phagocytosis. Silencing of *Eh*AGCK1 resulted in a trogocytosis defect in one clone, at one time point tested, but did not alter trogocytosis in another. Finally, silencing of *Eh*AGCK2 did not result in a trogocytosis phenotype. While silencing of these genes did not result in strong ingestion phenotypes, the mutants that we have generated could be used for further study of trogocytosis and phagocytosis in *E. histolytica.*

Results

Knock down of *Eh*C2PK results in trogocytosis and phagocytosis phenotypes.

We have previously created a trogocytosis defect in *E. histolytica* by over-expression of tetracycline-inducible kinase-dead *Eh*C2PK (2). We asked if knockdown of wild type *Eh*C2PK would result in a similar phenotype. We created an RNAi silencing construct for *Eh*C2PK and generated mutant amoebae **(Fig. 6.1A-B)**. Both heterogenous and clonal lines were generated. Mutants transfected with the silencing construct backbone served as a control. We verified silencing of *Eh*C2PK at both the mRNA and protein level **(Fig. 6.1A-B)**.

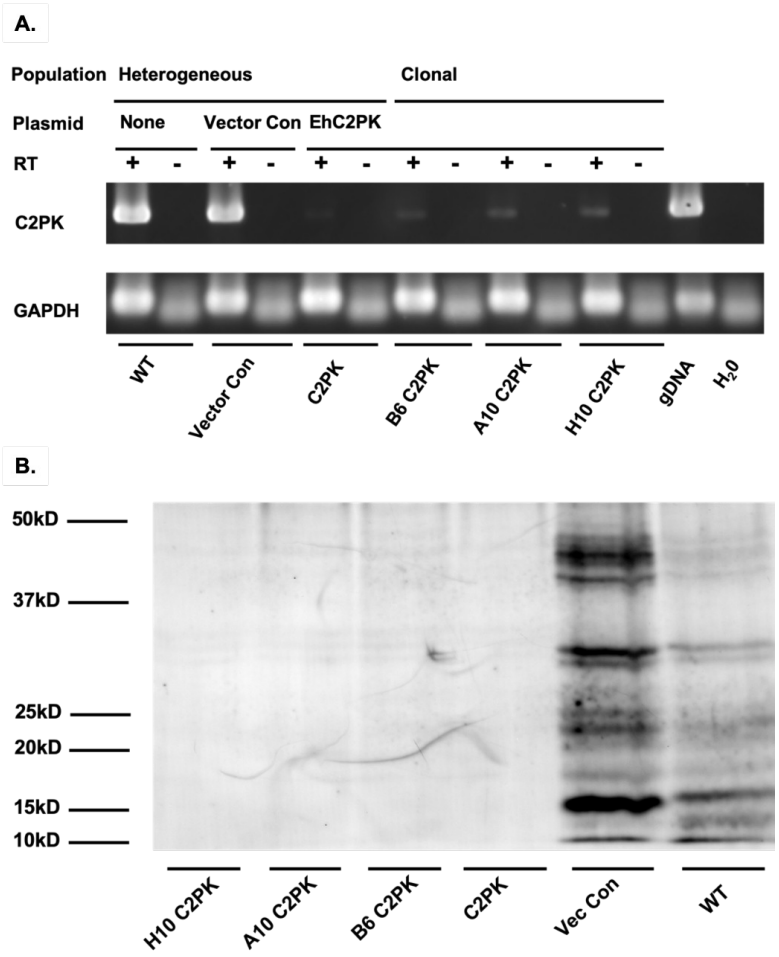

Fig. 6.1: Silencing of *Eh*C2PK. (A-B) Amoebae were transfected with a silencing construct to *Eh*C2PK and clonal lines were generated. **(A)** *Eh*C2PK mRNA expression was measured by RT-PCR. *Eh*GAPDH served as a control for the RT-PCR reaction. **(B)** Protein expression was determined by fluorescent western blot and a polyclonal antibody to *Eh*C2PK.

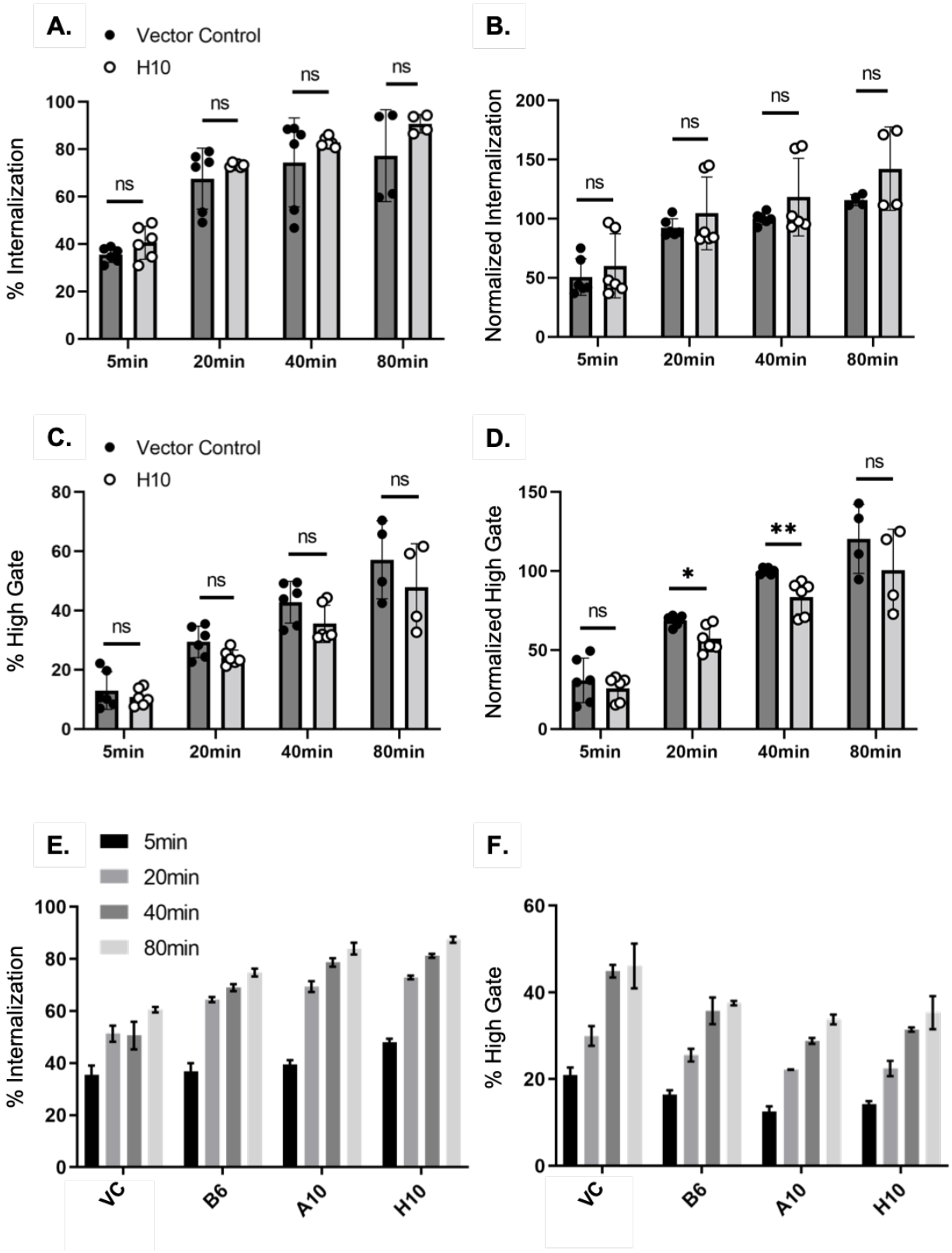
A.
Vector Control
H10
% Internalization
ns
5min
20min
40min
80min
B.
Normalized Internalization
C.
% High Gate
D.
Normalized High Gate
*
**
E.
5min
20min
40min
80min
% Internalization
VC
B6
A10
H10
F.
% High Gate

Fig. 6.2: Knock down of EhC2PK results in a trogocytosis phenotype. (A-B) Fluorescently labeled amoebae silenced for *Eh*C2PK or control amoebae were allowed to perform trogocytosis on membrane labeled human Jurkat cells for 5 minutes, 20 minutes, 40 minutes, or 80 minutes. Ingested human cell membrane was quantified by imaging flow cytometry. **(A)** % internalization of human cell membrane. **(B)** Internalization data normalized to control amoebae. **(C) %** amoebae that fell into the "trogocytosis high" gate. **(D)** Data from C normalized to control amoebae. **(E)** Internalization in mutant clonal lines. **(F) %** amoebae that fell into the "trogocytosis high" gate in mutant clonal lines. **(A-D)** Data are from 4-6 replicates from 3 independent experiments. **(E-F)** Data are from 2 replicates from one independent experiment.

We allowed fluorescently labeled mutant and control amoebae to perform trogocytosis on human Jurkat cells for increasing increments of time. Jurkat cells were labeled with a membrane dye and ingested membrane material was quantified using imaging flow cytometry **(Fig. S6.1)**. We chose to quantify percent of amoebae that had ingested human cell membrane as well as percent of amoebae that had performed a high level of trogocytosis. Amoebic trogocytosis is highly variable between individual experiments, so we also examined data normalized to the control amoebae. There was no difference in overall internalization of human cell membrane between the H10 clone and control amoebae **(Fig. 6.2 A-B)**. However, when we examined the percentage of amoebae that had performed a high level of trogocytosis, normalized data revealed a slight trogocytosis defect after 20 minutes and 40 minutes of ingestion **(Fig. 6.2 D)**. In an initial experiment, other clonal lines performed similarly to the H10 clone **(Fig. 6.2 E-F)**.

Since *Eh*C2PK is also involved in phagocytosis, we tested the H10 mutant for a phagocytosis phenotype. Our initial findings revealed a significant defect for phagocytosis of dead cytoplasm labeled Jurkat cells when we examined overall ingestion **(Fig. 6.3)**. However, these data are from one independent experiment and more replicates are needed to verify these findings. Taken together, these data indicate

that silencing of *Eh*C2PK results in a slight trogocytosis defect and a more significant phagocytosis defect. However, the resulting trogocytosis phenotype was not large, and the phagocytosis data require additional independent replicates.

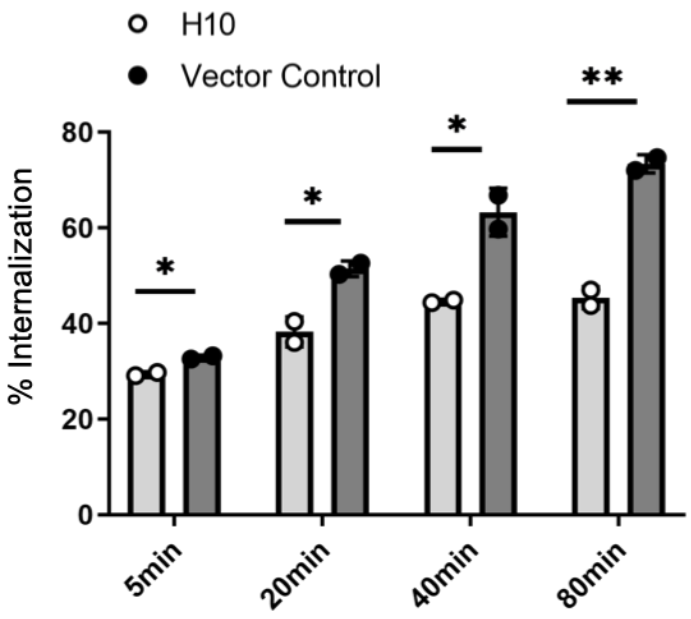

Fig. 6.3: Knock down of EhC2PK results in a phagocytosis phenotype. Fluorescently labeled amoebae silenced for *Eh*C2PK or control amoebae were allowed to perform trogocytosis on cytoplasm labeled human Jurkat cells for 5 minutes, 20 minutes, 40 minutes, or 80 minutes. Human cell ingestion was quantified by imaging flow cytometry. **(A)** % internalization of cytoplasm dye. **(B)** Internalization data normalized to control amoebae. Data are from 2 replicates from 1 independent experiment.

Knock down of *Eh*AGCK1 but not *Eh*AGCK2 impairs trogocytosis.

We next sought to create mutants for *Eh*AGCK1 and *Eh*AGCK2 as *Eh*AGCK1 is reported to be involved in trogocytosis and *Eh*AGCK2 in both trogocytosis and phagocytosis (5). We attempted to use the RNAi "trigger gene" silencing construct method to knock down these genes. We created silencing constructs that contained portions of either *Eh*AGCK1 or *Eh*AGCK2 fused to a portion of the endogenously silent "trigger gene" in order to generate small RNAs targeting the chromosomal copies of *Eh*AGCK1 or *Eh*AGCK2. Transfection with the *Eh*AGCK2 silencing construct resulted in silencing of *Eh*AGCK2 in the clonal line G7 **(Fig. 6.4A)**. Interestingly, in a different clonal line, C7, *Eh*AGCK2 was expressed and EhAGCK1 appeared to be overexpressed by

RT-PCR, though this method is not quantitative **(Fig. 6.4A)**. As a control, we checked for silencing of the related gene *Eh*AGCK3 but found it to be expressed in both clones **(Fig. 6.4A)**. In a subsequent transfection we generated additional *Eh*AGCK2 clonal lines and identified the clone F9 as being silent for *Eh*AGCK2 but expressing *Eh*AGCK1 at a level comparable to wild type amoebae **(Fig. 6.4B)**. Lastly, we generated clonal lines that were silent for *Eh*AGCK1 but expressed wildtype levels of *Eh*AGCK2 **(Fig. 6.4B)**.

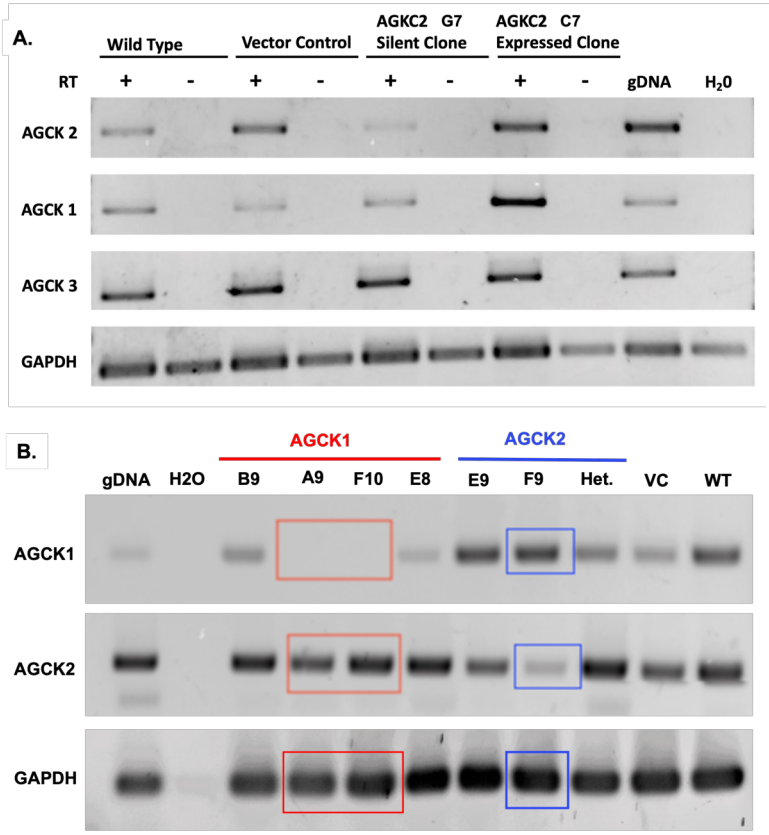

Fig. 6.4: Silencing of *Eh*AGCK2. **(A)** Amoebae were transfected with a silencing construct to *Eh*AGCK2 and clonal lines were generated. *Eh*AGCK1, *Eh*AGCK2 and *Eh*AGCK3 mRNA expression was measured by RT-PCR. *Eh*GAPDH served as a control for the RT-PCR reaction. **(B)** In a subsequent transfection, amoebae were transfected with silencing constructs to *Eh*AGCK1 and *Eh*AGCK2. Expression of *Eh*AGCK1 and *Eh*AGCK2 mRNA was measured by RT-PCR. *Eh*GAPDH served as a control for the RT-PCR reaction.

When allowed to perform trogocytosis on Jurkat cells, the G7 *Eh*AGCK2 mutant did not display a trogocytosis defect when compared to control amoebae **(Fig. 6.5A-B).** In contrast to previous assays, only approximately 1-6% of amoebae fell into the "trogocytosis high" population (data not shown). Therefore, we solely quantified overall internalization of Jurkat membrane. The C7 clone also did not display a trogocytosis

phenotype when compared to the G7 clone and control amoebae **(Fig. 6.5C-D)**. The F9 *Eh*AGCK2 knockdown clone generated independently a subsequent transfection also did not display a trogocytosis defect **(Fig. 6.6A-D)**. These results indicate that silencing of *Eh*AGCK2 using the RNAi "trigger gene" method does not result in a trogocytosis phenotype.

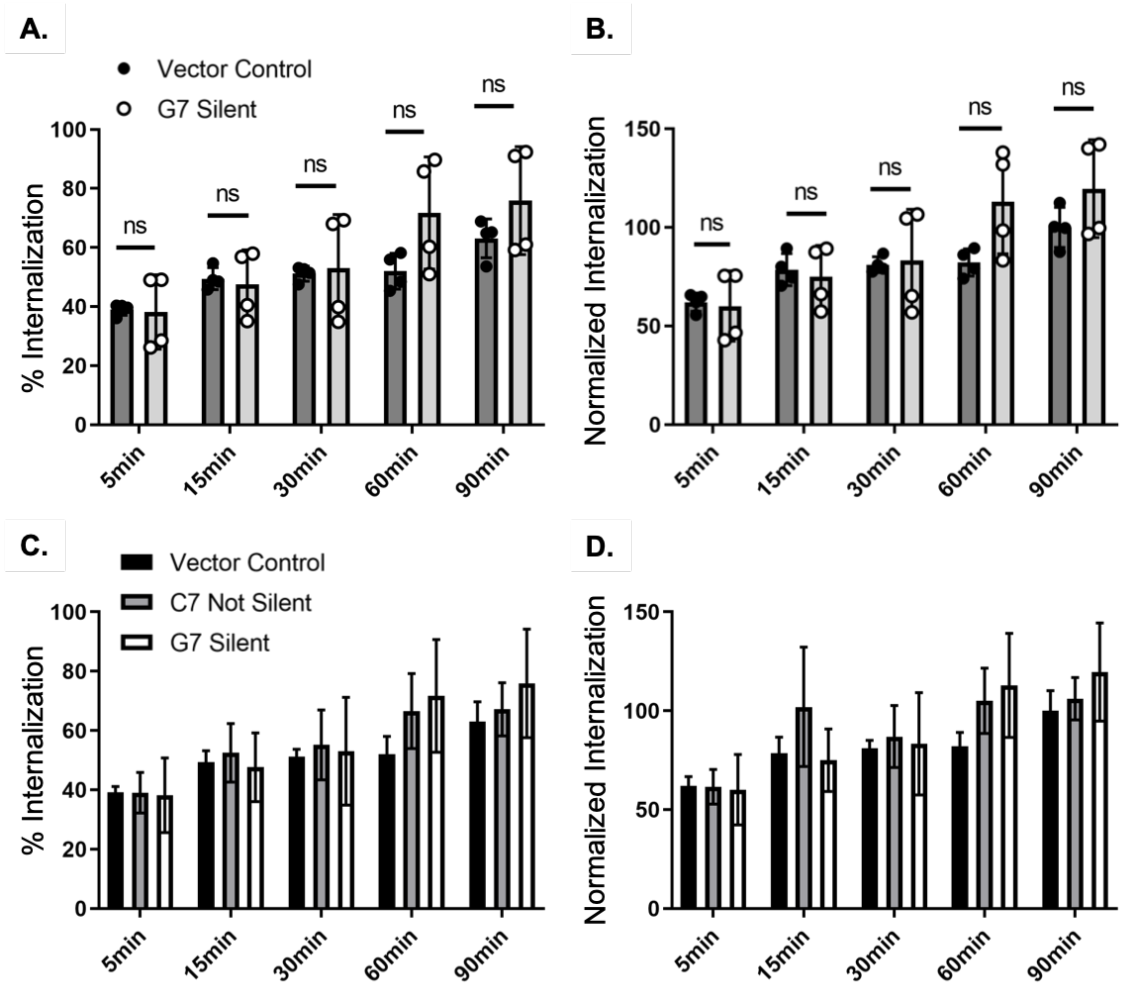

Fig. 6.5: Knock down of *Eh*AGCK2 does not result in a trogocytosis phenotype. (A-D) Fluorescently labeled amoebae silenced for *Eh*AGCK2 or control amoebae were allowed to perform trogocytosis on membrane labeled human Jurkat cells for 5 minutes, 15 minutes, 30 minutes, 60 minutes, or 90 minutes. Ingested human cell membrane was quantified by imaging flow cytometry. **(A)** % internalization of human cell membrane in the G7 *Eh*AGCK2 silent clonal line and control amoebae. **(B)** Internalization data from A normalized to control amoebae. **(C)** % internalization of human cell membrane in the G7 *Eh*AGCK2 silent and C7 non-silent clonal lines and control amoebae. **(D)** Data from C normalized to control amoebae. **(A-D)** Data are from 4 replicates from 2 independent experiments.

We next assayed mutants silenced for *Eh*AGCK1 for a trogocytosis defect. Notably, all amoebae mutants, including the vector control, performed less trogocytosis than wildtype amoebae **(Fig. 6.6A-B)**. The A9 clone performed an equivalent amount of trogocytosis as the vector control **(Fig. 6.6A-B, E-F)**. However, the F10 clone exhibited a small trogocytosis defect after 40 minutes of trogocytosis, though this was not significant in the normalization data **(Fig. 6.6G-H)**. These findings suggest that silencing of *Eh*AGCK1 leads to a weak impairment of trogocytosis.

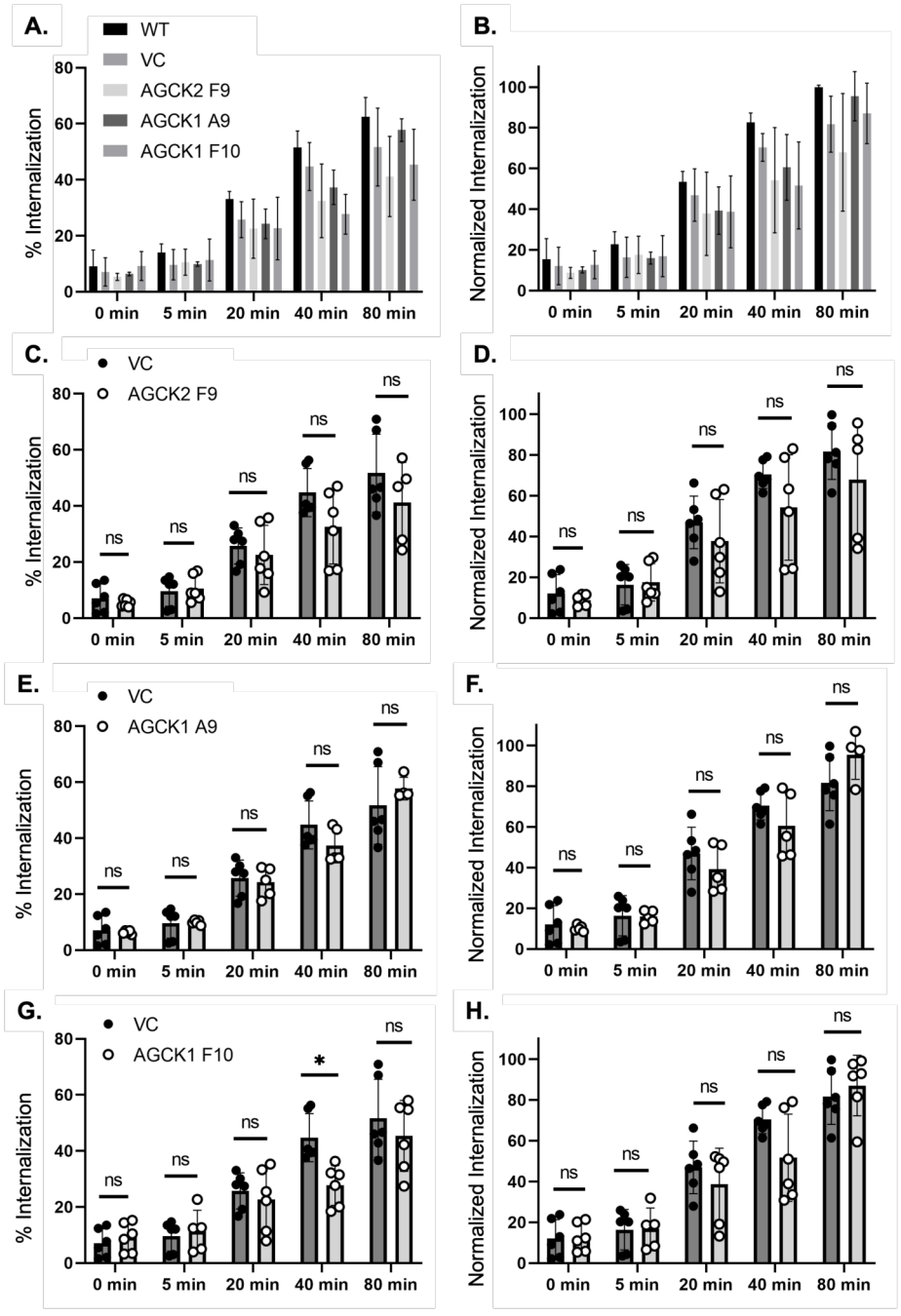

Fig. 6.6: Knock down of *Eh*AGCK1 results in a weak trogocytosis defect. (A-H) Fluorescently labeled amoebae mutants or control amoebae were allowed to perform trogocytosis on membrane labeled human Jurkat cells for 0 minutes, 5 minutes, 20 minutes, 40 minutes, or 80 minutes. Ingested human cell membrane was quantified by imaging flow cytometry. **(A)** % internalization of human cell membrane in wildtype, mutants and control amoebae. **(B)** Internalization data from A normalized to wildtype amoebae. **(C)** % internalization in the F9 *Eh*AGCK2 clone and control amoebae. **(D)** Data from C normalized to wildtype amoebae. **(E)** % internalization in the A9 *Eh*AGCK1 clone and control amoebae. **(F)** Data from E normalized to wildtype amoebae. **(G)** % internalization in the F10 *Eh*AGCK1 clone and control amoebae. **(H)** Data from G normalized to wildtype amoebae. **(A-H)** Data are from 3-6 replicates across 3 independent experiments.

Discussion

The pathogen *E. histolytica* uses trogocytosis for cell-killing as well as for immune evasion (2, 3). It is therefore likely that trogocytosis aids in invasion, dissemination, and tissue damage in the host during amoebiasis. A trogocytosis mutant would be a valuable tool in studying its contribution to pathogenesis during *E. histolytica* infection. *Eh*C2PK and *Eh*AGCK2 are kinases that have reported roles in both amoebic phagocytosis and trogocytosis (2, 5, 6). Mutants defective in these forms of ingestion could be used to study varied aspects of *E. histolytica* survival *in vitro.* For example, they could be used to study interactions with host immune cells, or acquisition of nutrients by phagocytosis of bacteria. We therefore attempted to create ingestion mutants by silencing these genes through RNAi.

Knockdown of *Eh*C2PK resulted in a trogocytosis defect at two time points tested and a phagocytosis defect at all timepoints tested. However, as we only assayed for trogocytosis performed, it is possible that we could have missed other changes at the molecular level. It is possible that there is redundancy in the mechanism of amoebic trogocytosis and therefore we can't rule out a greater involvement of *Eh*C2PK. Previous use of an over-expression tetracycline-inducible kinase-dead *Eh*C2PK point mutant resulted in a more pronounced trogocytosis deficit than with RNAi (2). However, both mutants displayed trogocytosis phenotypes after 20 minutes and 40 minutes of ingestion (2). The high variability of ingestion *in vitro* of the RNAi *Eh*C2PK mutants combined with their slight trogocytosis phenotype makes them unsuitable for *in vivo* studies. However, these mutants could be useful in studying these forms of ingestion in

a more controlled environment such as in *in vitro* experiments. For example, the *Eh*C2PK mutant could be used to examine the contribution of phagocytosis of dead human cells or trogocytosis of live human cells on complement resistance compared with control amoebae.

Silencing of *Eh*AGCK2 did not result in an ingestion phenotype in contrast to what others have found (5). Our data was highly variable, and a low percentage of amoebae fell into the “trogocytosis high” gate compared with previous assays. In assays with the *Eh*C2PK mutants roughly 10-50% of amoebae fell into the “trogocytosis high” gate, while only approximately 1-6% did so in the *Eh*AGCK2 experiments. Due to this variability the lack of observed phenotype could simply be due to nonoptimal experimental conditions. Likewise, though silencing of *Eh*AGCK1 resulted in a weak trogocytosis defect in one clone, it did not impair trogocytosis in another. It should also be noted that the mutant amoebae generated in these assays performed less trogocytosis than wild type amoebae. This is likely due that fact that they were maintained under drug selection which we have observed can cause amoebae to grow more slowly and appear less healthy in culture (data not shown).

Experiments that reported phenotypes in *Eh*AGCK1 and *Eh*AGCK2 mutants relied on a different method of RNAi gene silencing. They utilized the clonal G3 strain of *Entamoeba* which has been permanently silenced for amoebapore-A, and can be further silenced for addition genes (5, 9). Ingestion was also quantified in different ways. Absorbance of haem was measured in mutant amoebae that had performed erythrophagocytosis. Furthermore, trogocytosis was assessed indirectly by measuring

host cell monolayer destruction (5). These methods differ greatly from ours which utilized imaging flow cytometry. Consequently, further study is needed to determine the involvement of these genes in ingestion. However, our methods of quantifying trogocytosis measured ingestion directly, while the previous experiments discussed did so through indirect means. Therefore, our findings likely give a better understanding of their involvement.

The *Eh*C2PK, *Eh*AGCK1 and *Eh*AGCK2 RNAi knockdown mutants that we have generated did not display trogocytosis defects at all time points tested. However, a variety of factors such as high experimental variability, lack of replicates, or quantification methods could have contributed to our results. Additionally, there could be redundancy in the mechanism of amoebic trogocytosis. It is possible that mutated genes could be compensated for by the presence of other molecular pathways involve in trogocytosis. It is also possible that other forms of genetic manipulation of these genes may lead to more pronounced ingestion phenotypes. Additional work is needed to generate an *E. histolytica* mutant with a robust trogocytosis defect. However, the mutants we generated in this study could be useful *in vitro* for further examining the roles of trogocytosis and phagocytosis in *E. histolytica*.

Materials and Methods

Cell culture

E. histolytica trophozoites (HM1: IMSS (ATCC)) were grown as described previously (3, 10). Amoebae were cultured at 35°C in TYI-S-33 media supplemented with 15% heat-inactivated adult bovine serum (Gemini Bio-Products), 80 Units/mL penicillin and 80 μg/mL streptomycin (Gibco), and 2.3% Diamond Vitamin Tween 80 Solution 40x (Sigma-Aldrich). Amoebae were cultured in unvented T25 tissue culture flasks. When flasks reached 80-100% confluency, amoebae were harvested and resuspended in M199s media (Gibco medium M199 with Earle's Salts, L-Glutamine, 2.2 g/L Sodium Bicarbonate and without Phenol Red) supplemented with 5.7 mM L-cysteine, 25 mM HEPES and 0.5% bovine serum albumin.

Human Jurkat T cells (ATCC; Clone E6-1) were grown were grown as described previously (3, 10). Jurkat cells were cultured at 37°C and 5% CO_2 in RPMI Medium 1640 (Gibco RPMI with L-Glutamine and without Phenol Red) supplemented with 10% heat-inactivated fetal bovine serum (Gibco), 10 mM HEPES, 100 Units/mL penicillin and 100 μg/mL streptomycin. Jurkat cells were grown in vented T25 tissue culture flasks and harvested between $5x10^5$ and $2x10^6$ cells/ml. Cells were resuspended in M199s media for experiments.

Generation of *Eh*C2PK silencing construct

Genomic DNA was isolated from amoebae grown to %80 confluency and purified using the QIAquick PCR Purification Kit (QIAGEN). The first 533 base pairs of *Eh*C2PK

(Amoeba DB: EHI_053060) were then amplified with 6 additional nucleotides and XmaI and XhoI restriction sites using the following primers: Forward: TAA GCA **CCC GGG** ATG AGC CAT ATT AGT GCT AAA A, Reverse: TGC TTA **CTC GAG** ACT GCA ACA CTA ACT CCA TCC). Restriction sites are shown in bold. Next, the *Eh*ROM1 silencing construct, made from a pEhEx plasmid backbone, and generated by Morf *et al.* as described in (8) was modified to create the *Eh*C2PK silencing construct. *Eh*ROM1 was cut out of the *Eh*ROM1 silencing construct by XmaI and XhoI restriction enzyme digest. The amplified *Eh*C2PK PCR product was digested with the same enzymes and ligated into the silencing construct, generating a plasmid with 132 base pairs of the trigger gene EHI_048600 fused to the first 533 base pairs of *Eh*C2PK. One Shot TOP10 Competent *E. coli* were transformed, and positive colonies were screened by colony PCR. Primers used were the same as those for amplification of *Eh*C2PK. Plasmids with the correct inserts were verified using Sanger sequencing.

Generation of *Eh*AGCK1 and *Eh*AGCK2 silencing constructs

In order to generate *Eh*AGCK2 mutants, a trigger gene silencing construct to *Eh*AGCK2 was created. 514 base pairs of E*h*AGCK2 (5) at the 5' end of the gene were amplified from genomic DNA. 30 base pairs of homology to the silencing construct backbone were added at either end of the PCR product during amplification. The *Eh*AGCK2 insert was amplified with the following primers: Forward: **TTA AAA ACA AAA ATT GCA GCA TCA ACG CCC** TCA GTT AAA ACA GGA TGG GGA, Reverse: **GTT TAA AAA AGA AGA GTT CAA CTC GAG CCC** TTT GTG ATA ATA CTA CTT

TTT CGG ATA ATA. Homology to the construct backbone is shown in bold. Next, the silencing construct backbone was linearized by digest with the restriction enzyme SmaI and the amplified portion of *Eh*AGCK2 was inserted using Gibson cloning using the Gibson Assembly Ultra Kit (VWR).

The *Eh*AGCK1 silencing construct was generated in the same manner. 512 base pairs of E*h*AGCK1 (5) at the 5' end of the gene were amplified from genomic DNA with 30 base pairs of homology to the silencing construct and cloned into the silencing construct backbone. The *Eh*AGCK1 insert was amplified with the following primers: Forward: **TTA AAA ACA AAA ATT GCA GCA TCA ACG CCC** GAA GAG AAA ACA CAA GGA TGG CTT, Reverse: **GTT TAA AAA AGA AGA GTT CAA CTC GAG CCC** TTA GAG AGG ATA CGT CTT TCA GAC ATA G. Homology to the construct backbone is shown in bold.

NEB 5-alpha Competent *E. coli* were then transformed with the silencing constructs and positive colonies were screened by restriction digest. Correct plasmids were confirmed by Sanger Sequencing.

Transfection of amoebae and mutant phenotyping

Amoebae were transfected with 20 μg of the silencing constructs using Attractene Transfection Reagent (QIAGEN) as described previously ((3, 10)). Vector control lines were generated by transfection the pEhEx-trigger construct backbone. Transfectants were selected and maintained under selection with Geneticin (ThermoFisher Scientific) at 6 μg/ml. Clonal lines were generated by limiting dilution in a

96-well plate contained in a BD GasPak EZ Pouch System (BD Biosciences). Silencing was confirmed with RT-PCR. For expression of *Eh*C2PK the following primers were used: Forward: GTC AAA AGA AAG GTG TTA GTC GA, Reverse: TGT GGA TCA ACA ACA AGA CAC T. To check expression of *Eh*AGCK1, *Eh*AGCK2, and *Eh*AGCK3, the following primers were used: *Eh*AGCK1 Forward: AAC CAA GAA TAA GTA GTG TAC, *Eh*AGCK1 Reverse: TTC TAA TAA CAT AAC AAT ACA TTC, *Eh*AGCK2 Forward: TAG TAA TGA AGT AGA ACA TAT, *Eh*AGCK2 Reverse: CAA CTC CTG TTT TTA AAT CAA, *Eh*AGCK3 Forward: TTA TAA GTC TAA AAT TAC TAC AGA AA, *Eh*AGCK3 Reverse: AAC TAA TAA CTC TTG AAT ACA ACG. Silencing of *Eh*C2PK was also validated by fluorescent western blot. Protein was extracted from mutant and vector control amoebae and blots were blocked in 5% bovine serum albumin (BSA) and 5% non-fat dry milk. *Eh*C2PK was visualized using a rabbit polyclonal antibody to *Eh*C2PK (6) and an Alexa Fluor 680 rabbit secondary antibody (Invitrogen). Samples were imaged on an Odyssey western blot scanner.

Ingestion assays

Trogocytosis assays were performed as described previously (2). Amoebae and human Jurkat cells were washed and resuspended in M199 medium. Amoebae were labeled with CellTracker Green (CMFDA; Life Technologies) at 93 ng/ml for 10 minutes at 35°C. Jurkat cells were labeled with Diic18(5)-Ds [1,1-Dioctadecyl-3,3,3,3-Tetramethylindodicarbocyanine-5,5-Disulfonic Acid] (DiD: Assay Biotech) at 21 μg/ml for 5 minutes at 37°C and 10 minutes at 4°C. Amoebae were washed and resuspended at

4 x 10^5 cells/ml and Jurkat cells were washed and resuspended at 2 x 10^6 cells/ml for a 1:5 amoebae to Jurkat cell ratio. Next, amoebae and Jurkat cells were co-incubated for 5 minutes, 20 minutes, 40 minutes, or 80 minutes at 35°C. Samples were immediately placed on ice after incubation and labeled with LIVE/DEAD Fixable Violet Dead Cell Stain (Invitrogen) at 4 μl/ml for 30 minutes on ice. Samples were fixed with 4% paraformaldehyde (PFA) for 30 minutes at room temperature and resuspended in 1 x phosphate buffered saline (PBS).

In the phagocytosis assay, Jurkat cells were labeled with CellTracker Deep Red (CTDR: Invitrogen) at a 1:1000 dilution for 30 minutes at 37°C. Next, Jurkat cells were washed and resuspended at 2 x 10^6 cells/ml and heat-killed at 55°C for 15 minutes. Heat-killed Jurkat cells and CMFDA labeled amoebae were treated in the same manner as in trogocytosis assays.

Imaging flow cytometry

Samples were run on an Amnis ImageStreamX Mark II and 10,000 events were collected per sample. See figure S6.1 for the gating scheme used in analysis.

Statistical analysis

GraphPad Prism software was used to perform all statistical analyses and the means and standard deviation values are displayed on all data plots. Analyses were done using a Student's unpaired t test (no significant difference was indicated by a P of >0.05; *, $P \leq 0.05$; **, $P \leq 0.01$; ***, $P \leq 0.001$; ****, $P \leq 0.0001$).

Acknowledgments

We thank the members of our laboratory for helpful discussions. All ImageStream data were acquired using shared instrumentation in the UC Davis MCB Light Microscopy Imaging Facility, and we thank Dr. Michael Paddy for technical assistance. This work was funded by start-up funds and a K22 award to K.S.R.

Author Contributions

H.W.M. designed, performed, and analyzed the experiments. V.W. aided in generation and phenotyping of *Eh*AGCK1 and *Eh*AGCK2 mutants. K.S.R. conceived of the overall approach and oversaw the design and analysis of the experiments H.W.M wrote the chapter, and it was edited by K.S.R.

References

1. Haque R, Huston CD, Hughes M, Houpt E, Petri WA. 2003. Amebiasis. New England Journal of Medicine 348:1565–1573.

2. Ralston KS, Solga MD, Mackey-Lawrence NM, Somlata, Bhattacharya A, Petri Jr WA. 2014. Trogocytosis by *Entamoeba histolytica* contributes to cell killing and tissue invasion. Nature 508:526–530.

3. Miller HW, Suleiman RL, Ralston KS. 2019. Trogocytosis by Entamoeba histolytica Mediates Acquisition and Display of Human Cell Membrane Proteins and Evasion of Lysis by Human Serum. mBio 10:e00068-19.

4. Ralston KS. 2015. Chew on this: amoebic trogocytosis and host cell killing by Entamoeba histolytica. Trends in Parasitology 31:442–452.

5. Somlata null, Nakada-Tsukui K, Nozaki T. 2017. AGC family kinase 1 participates in trogocytosis but not in phagocytosis in Entamoeba histolytica. Nat Commun 8:101.

6. Somlata, Bhattacharya S, Bhattacharya A. 2011. A C2 domain protein kinase initiates phagocytosis in the protozoan parasite Entamoeba histolytica. Nat Commun 2:230.

7. Sahoo N, Labruyère E, Bhattacharya S, Sen P, Guillén N, Bhattacharya A. 2004. Calcium binding protein 1 of the protozoan parasite Entamoeba histolytica interacts with actin and is involved in cytoskeleton dynamics. Journal of Cell Science 117:3625–3634.

8. Khalil MI, Foda BM, Suresh S, Singh U. 2016. Technical advances in trigger-induced RNA interference gene silencing in the parasite Entamoeba histolytica. Int J Parasitol 46:205–212.

9. Bracha R, Nuchamowitz Y, Mirelman D. 2003. Transcriptional silencing of an amoebapore gene in Entamoeba histolytica: molecular analysis and effect on pathogenicity. Eukaryotic Cell 2:295–305.

10. Suleiman RL, Ralston KS. Growth and genetic manipulation of Entamoeba histolytica. Current Protocols in Microbiology.

Supplemental Material

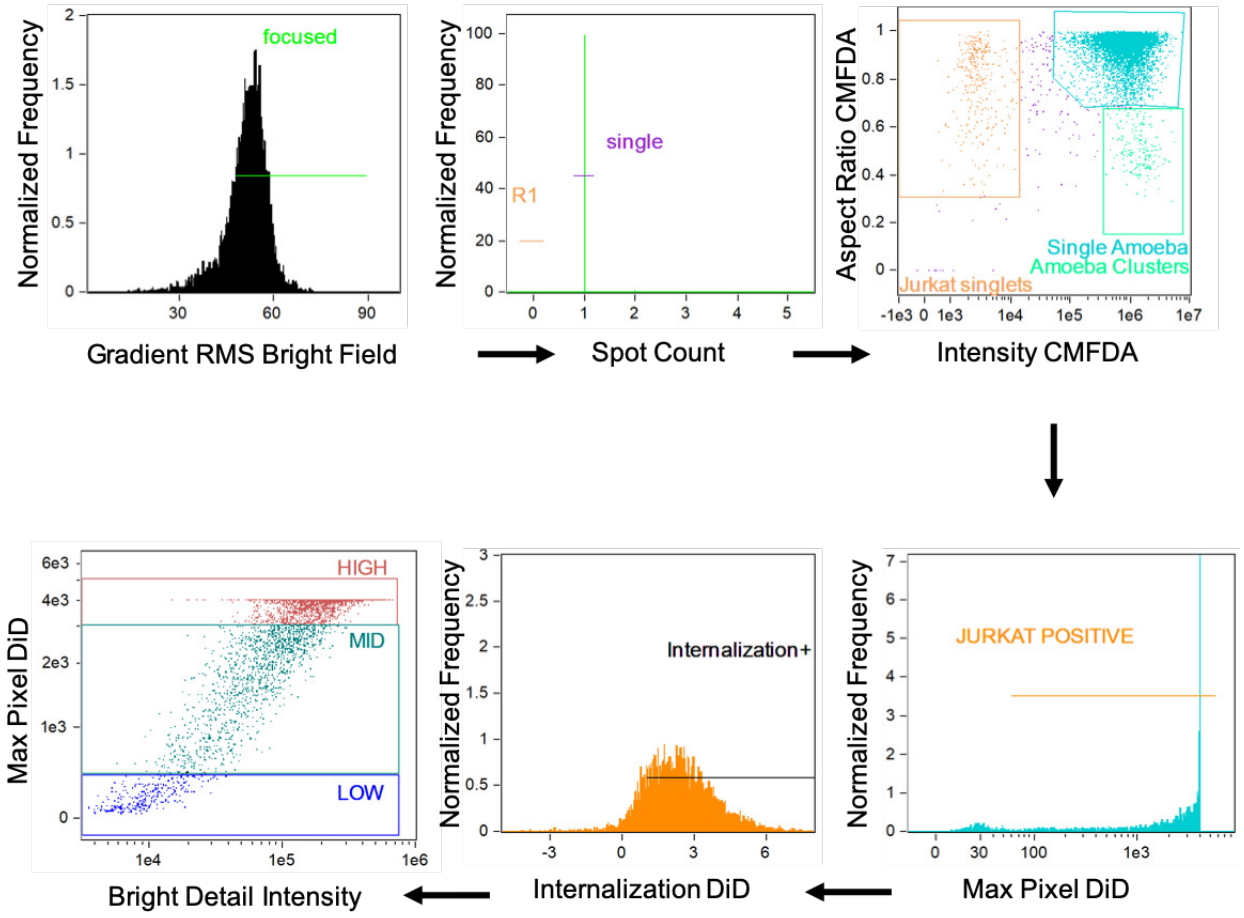

Fig. 6.5: Gates used for quantifying ingestion in RNAi mutants. Focused cells were gated on form total collected events. Next, cells were further separated from other events using the "spot count" feature in Amnsi IDEAS software. Single amoebae were identified by aspect ratio and intensity of CMFDA cytoplasm dye. Amoebae that had ingested Jurkat cells were then identified by max pixel intensity of DiD membrane dye. Internalization of membrane material was quantified. Amoebae were then identified as trogocytosis "high", "medium" or "low" by examining bright detail intensity and max pixel intensity of DiD membrane dye.

Chapter 7

Concluding Remarks

Trogocytosis is an important eukaryotic process that serves many functions. It occurs in both multicellular organisms as well as single celled microbes, though its molecular mechanism has not been well defined. It is characterized by extraction and ingestion of small pieces of living cells rather than whole cell engulfment as in phagocytosis. Trogocytosis requires direct cell to cell contact, happens in a fast time frame, and results in the transfer of proteins from one cell to another. Interestingly, it has many functions, including a form of cell killing, a normal process during development, a mechanism of cell to cell communication, and, in *Entamoeba histolytica*, a tool for immune evasion.

The major studies presented in this dissertation show that the pathogen *E. histolytica* acquires and displays human proteins through trogocytosis, establish amoebic trogocytosis as a tool for evasion of human complement, and develop tools to further study the trogocytic process in the future.

We have shown that *E. histolytica* acquires and displays biotinylated membrane proteins through trogocytosis of human cells. Additionally, we demonstrate that amoebae acquire MHC-I, CD59, and CD46 molecules. While we have demonstrated the transfer of these specific proteins to amoebae via trogocytosis of human cells, likely, amoebae acquire many additional membrane proteins that we did not assay for.

We establish that amoebae are protected from complement lysis by trogocytosis of human cells, including human Jurkat T cells and primary red blood cells. Importantly,

amoebae are only protected from lysis by trogocytosis of live cells but not phagocytosis of dead cells. Trogocytosis inhibits deposition of the complement protein C3b. Amoebic protection from complement by trogocytosis appears to involve the acquisition of multiple redundant complement regulators as loss of one or two complement regulatory proteins does not decrease conferred protection. In further support of this hypothesis, amoebae made to exogenously express human CD46 or CD55 are protected from complement.

Finally, we developed tools to further study trogocytosis in the future. We optimized a protocol for quantification of trogocytosis in mammalian macrophages that could be used to test unanswered questions about trogocytosis between immune cells. We also generated *E. histolytica* mutants with trogocytosis and phagocytosis defects that could be used to further study these processes in amoebae. One mutant was deficient in both forms of ingestion. This highlights the large overlap between trogocytosis and phagocytosis genes in *E. histolytica*. Relatively little is known about the molecular mechanisms of phagocytosis and trogocytosis in *E. histolytica*. It is therefore of great interest to continue to identify genes involved in these two forms of amoebic ingestion.

In conclusion, our work has shed light on aspects of trogocytosis that were previously unknown. While protein transfer via trogocytosis has been well documented in mammalian immune cells, we are the first to demonstrate it in a eukaryotic pathogen. We are also the first to establish trogocytosis as a mechanism for evasion of complement lysis, thus uncovering a novel mechanism by which a pathogen evades

complement. Our findings further the knowledge of this eukaryotic process and open up additional avenues for future research.